Role of Inflammation in Metabolism and Hepatotoxicity of Prototypical Drugs

A Dissertation Presented to the

Faculty of the Department of Pharmacological and Pharmaceutical Sciences

College of Pharmacy, University of Houston

In Partial Fulfillment of

the Requirements for the Degree of

Doctor of Philosophy

By

Adarsh Gandhi

May, 2012

Dedicated to my late Grandmother, my Parents and my wife, Gunjan

ACKNOWLEDGEMENTS

There are many people I would like to sincerely thank because this thesis would not have been possible without their support. Although I cannot thank all of them individually, I express my deepest gratitude to all of them who are connected in making this happen.

First and foremost, I would like to thank my primary advisor, Dr. Romi Ghose. It has been an honor to be her first Ph.D. student. I am very appreciative of her generosity with her time, advice, patience, and motivation, to name a few of her contributions. After doing my lab rotation in her lab, I was very much attracted with her research ideas and the more I was involved in her lab, I think I made the best decision. Dr. Ghose's words of encouragement and enthusiasm were important for the completion of this project. I have enjoyed each and every moment I spent in her lab which I will cherish for my entire life. Without her unmatched support, this project would not have been possible.

I consider myself fortunate to have Drs. Diana Chow, Ming Hu, Bhagavatula Moorthy and Michael Johnson to serve as my committee members. I am short of words to describe Dr. Chow's greatness as a scientist and a human being. But I would like just mention one thing about her- She is like a second mother to me. Dr. Hu has always inspired and supported me by giving invaluable ideas and suggestions in the project, which I will benefit from in my whole career. I appreciate the kindness of Dr. Moorthy for writing recommendation letters for me during my job search. My sincere thanks to Dr.

Johnson because of whom I was able to learn and apply all the new concepts in Biostatistics.

I would also like to thank Dr. Robert Edwards, Imperial College of Medicine for providing the anti-mouse Cyp3a11 antibody. Thanks for Dr. Gerard Fabre, Sanofi-Aventis (France) for his kind gift of 1'-hysroxymidazolam-glucuronide. I would also like to thank Dr. Milton Finegold at the Texas Children's Hospital for his advice on analysis of liver tissue sections.

I would like to thank all the Tao Guo (senior lab technician), Ozozoma Omoluabi (postdoctoral fellow), Pranav Shah and Pankajini Mallick (fellow graduate students), and Gaurav Dhar, Phuong Ha, Phuong Ly, Manasa Kodali, Lincy Varghese and Christina Kind (rotating undergraduate students) for all their help in my research. My time at University of Houston was made enjoyable in large part due to the many friends, staff and department faculties.

Last, but not the least, many thanks to my beloved family, who although thousands of miles away from me, have always encouraged, inspired and supported me in all my pursuits. And most of all for my loving, supportive, encouraging, and patient wife Gunjan whose faithful support during the final stages of this Ph.D. is so appreciated.

Adarsh Gandhi
University of Houston

ABSTRACT

Inflammation leads to altered drug metabolism and augments drug-induced hepatotoxicity. However, the mechanisms are not fully understood. Inflammation is known to alter the gene expression and activity of several key drug metabolizing enzymes (DMEs) further compromising the safety and efficacy of drugs. Inflammatory responses in the liver are primarily mediated by the Toll-like receptors (TLRs), found on the cell surface of hepatocytes and immune cells, such as Kupffer cells. TLR2 and TLR4, upon activation recruit the first adaptor molecule, the Toll-interleukin 1 receptor adaptor protein (TIRAP). TIRAP was shown to play a differential role in regulating gene expression of Cyp3a11 in lipopolysaccharide- (LPS, TLR4 agonist) or lipoteichoic acid- (LTA, TLR2 agonist) induced inflammation in mice. In this project, we studied the role of the TLR signaling pathway in regulating inflammation-mediated altered drug metabolism and hepatotoxicity of prototypical drugs in mice. **Aim 1**: We observed significant down-regulation of Cyp3a11 protein expression and activity (measured by midazolam (MDZ) metabolism) in LPS- or LTA-induced inflammation. This further correlated with reduced clearance and increased pharmacological action of MDZ in both, LPS- or LTA-treated mice. In contrast to LPS, TIRAP was involved only in LTA-mediated down regulation of Cyp3a11 and metabolism of MDZ. **Aim 2:** We studied the effects of inflammation and the TLR signaling pathway in regulating hepatotoxicity of chlorpromazine (CPZ). We selected CPZ due to its idiosyncratic hepatotoxicity reported in humans and animals. Sustained activation of the kinase, c-Jun-N-terminal kinase

(JNK) is associated with cell death. However, the roles of JNK and TIRAP in regulating CPZ-induced hepatotoxicity in presence of inflammation are unknown. In our *in vivo* study, LPS or LTA treatment led to significant induction of CPZ hepatotoxicity with increase in serum tumor necrosis factor (TNF)-α and sustained activation of JNK upto 4 h. Histopathological analysis revealed marked depletion of hepatic glycogen in LPS/CPZ or LTA/CPZ groups. Also, CPZ-induced hepatotoxicity, increase in serum TNF-α and activation of JNK in presence of LPS or LTA were dependent on TIRAP. In our *in vitro* study, we observed significant induction of alanine aminotransferase (ALT) in CPZ-treated primary mouse hepatocytes in presence of LPS or LTA. We observed prolonged activation of JNK in presence TNF-α and TNF-α-mediated increase in ALT in presence of CPZ was attenuated by the JNK inhibitor. Overall, by focusing on the TLR signaling pathway, this dissertation provides novel insights in the underlying mechanisms involved in regulating drug metabolism and hepatotoxicity of prototypical drugs in inflammation.

TABLE OF CONTENTS

LIST OF FIGURES

LIST OF TABLES

CHAPTER 1

General Introduction

1.1. Changes in metabolism and pharmacokinetics/pharmacodynamics (PK/PD) of drugs in infections and inflammation

1.1.1. Drug metabolism and PK/PD

Drug metabolism can either lead to detoxification, bio-inactivation and/or elimination of drugs from the body. Of all the cytochrome P450 (CYP), enzymes, CYP3A4 is the most common isoform expressed in human liver and intestine accounting for ~30-60% of CYPs (Nebert and Russell, 2002). More than 50% of the currently marketed drugs are metabolized by CYP3A4 in humans (Guengerich, 1999). However, a large inter-subject variability has been demonstrated with drugs. This can be accounted for various factors including, but not limited to, age, sex, diet, underlying disease condition or genetic polymorphisms. In simple terms, the term pharmacokinetics means what the body does to the drug and pharmacodynamics means what the drug does to the body. Thus, changes in PK/PD of drugs can depend on various factors such as physicochemical properties of the drug such as pKa or lipophilicity; or biological factors such as gastric emptying time or absorption from the site of administration. Monitoring the PK of drugs is critical in terms of safe and effective clinical pharmacotherapy.

1.1.2. Statement of the problem

Altered drug metabolism can lead to adverse drug reactions which account for ~10% of hospitalized cases (Deng *et al.*, 2009). However, due to underreporting, the actual incidences may be much higher (Pirmohamed *et al.*, 2004). As early as 1960s, variations in drug metabolism were reported in patients or animals with diabetes (Dixon

et al., 1961), cancer (Kato *et al.*, 1963), hepatitis (Klotz *et al.*, 1974) or influenza (Kraemer *et al.*, 1982) along with a corresponding change in the PD of drugs (Dixon *et al.*, 1961; Kato *et al.*, 1968). One of the most dramatic examples demonstrating the role of infection and loss of CYP450 activity occurred during the 1980 influenza epidemic (Kraemer *et al.*, 1982). The authors reported that, theophylline metabolism was severely altered in asthmatic children suffering from influenza. These early studies prompted researchers to further elucidate drug metabolizing enzymes (DME) gene expression and PK/PD of clinically-relevant drugs in inflammation.

The liver is an important site of host-microbe interaction. Inflammation-mediated down regulatory effects on drug metabolism are largely ascribed to the stimulation of cellular immune responses (Aitken *et al.*, 2006; Kato, 1977). The challenges in this field are identifying the DMEs whose activity or expression is significantly altered by inflammatory conditions and using this information in predicting drug interactions in disease conditions and medications. The major focus for these investigations is based on identification of individual DMEs involved in drug metabolism of these specific agents, their regulation in different models of inflammation, identifying the relevant biomarkers mediating this effect and extrapolating the preclinical data to clinical studies for early drug development. These problems can be addressed by knowledge of the differences and similarities in regulation of DMEs in animals and humans in inflammatory conditions. As already discussed, CYP enzymes are the major DMEs involved in deciding the metabolic fate of several xenobiotics. Therefore this discussion will primarily, but not limited to,

focus on changes in CYP-mediated drug metabolism in infections and underlying inflammation.

1.1.3. Significance of these findings

Studies in humans and experimental animals have shown that infections or inflammatory stimuli can lead to changes in the activities and/or gene expression of various isoforms of DMEs in the liver, kidney, intestine or brain. Therefore, changes in DME activities in inflammation/infections can modulate the therapeutic efficacy or toxicity of drugs, especially those with a narrow therapeutic index. However, the mechanisms involved in inflammation-mediated altered drug metabolism are not completely known.

The data presented in this dissertation will allow the readers to gain valuable insights in the novel role of the immune receptors in regulation of Cyp3a11 (analog of human CYP3A4) gene expression and metabolism of the Cyp3a substrate, midazolam. This study provides novel mechanisms involved in regulation of inflammation-mediated altered drug metabolism. This study also provides the rationale for monitoring dosage regimen in patients with underlying inflammation or infections.

1.2. Regulation of DMEs and PK/PD of drugs in infections and inflammation

1.2.1. Bacterial infections

Most of the studies on regulation of DMEs have been documented with gram-negative bacteria. Clinically relevant cecal ligation and puncture (CLP) or inflammatory bowel disease (IBD) induced by *Citrobacter rodentium* (gram-negative pathogen) are the

most frequently used models owing to their close resemblances in the progression and characteristics of human sepsis (Higgins *et al.*, 1999; Wichterman *et al.*, 1980). Although, an estimated population of more than 1 million North Americans is susceptible to IBD, very little is known about its effect on expression and activity of DMEs in humans (Aitken *et al.*, 2006). Alterations in total hepatic microsomal CYP content and activities were reported in CLP rat or IBD mouse models (Chaluvadi *et al.*, 2009; Godellas *et al.*, 1995). Specifically, these studies showed that rats in the CLP group exhibited significant decreases in the enzymatic activities of mixed function oxidases (MFOs), with greater effect on down-regulation of CYP2B1/2B2 activity compared to CYP1A1/1A2, when compared to rats in the sham-operated or control groups (Godellas *et al.*, 1995). The effects in the CLP-rats worsened with increasing time of sepsis and were partially prevented by increased oxygen treatment (hyperoxia) suggesting that these effects are not related to the production of oxygen-derived free radicals. Similarly, in the IBD mouse model, significant induction in hepatic CYP4F18 and CYP2D9 and significant down-regulation of CYP4A was observed after *C. rodentium* infection in mice (Chaluvadi *et al.*, 2009) .There was a strong correlation in the regulation of CYP450s and colonic inflammation and bacterial colonization which peaked at 7-10 days after infection and returned to normal levels at 15-24 days. The rapid down-regulation of CYP2Cs and CYP3As after intraperitoneal (i.p) injection and CYP4As after oral injection of *C. rodentium* was quantitatively and qualitatively different, suggesting that the effects of oral infection are not due to bacterial translocation to the liver (Chaluvadi *et al.*, 2009).

Infection of pigs with the gram-negative respiratory pathogen, *Actinobacillus pleuropneumoniae,* led to decreased microsomal metabolism of several CYP-dependent substrates 24 h after inoculation (Monshouwer *et al.*, 1995). Similarly, gram-positive bacterial infections account for more than 50% of the total community acquired infections (Martin *et al.*, 2003). Listeriosis, caused by *Listeria monocytogenes,* is one of the most critical food-borne diseases in humans. *L. monocytogenes* induced CNS infection in rodents significantly down-regulated mRNA, protein and activity of hepatic CYPs (Garcia Del Busto Cano and Renton, 2003).

The gram-negative and gram-positive bacterial components, lipopolysaccharide (LPS), and lipoteichoic acid (LTA), serve as sterile infection models by inducing inflammatory responses in animals (Ginsburg, 2002; Leemans *et al.*, 2002). LPS injections down-regulate expression and activity of key hepatic, intestinal and renal DMEs in several animal species such as mice, rats or rabbits (Ghose *et al.*, 2008; Sewer *et al.*, 1996). The effect of LPS on CYP expression and activity is dependent on the route of administration at same dose of LPS (Shimamoto *et al.*, 1998). We recently showed that LTA significantly down-regulated the gene expressions of several phase I and phase II DMEs in mice (Ghose *et al.*, 2009).

As early as 1980's, reduced clearances of clinically relevant drugs have been reported in humans infected with BCG vaccine, *Streptococcus pneumoniae* or *Mycoplasma pulmonis* (Gray *et al.*, 1983; Modric *et al.*, 1998; Sonne *et al.*, 1985). LPS injections in animals and humans altered PK parameters such as maximum plasma

concentration (C_{max}, increase), area under the curve (AUC, increase), half-life ($T_{1/2}$), volume of distribution (V_d) and clearance (CL, deccrease) of various drugs including cisplatin, antipyrine, theophylline, hexobarbital, gentamicin and vancomycin (Gous *et al.*, 1995; Hasegawa *et al.*, 1994; Ishikawa *et al.*, 1990a; Shedlofsky *et al.*, 1994). Humans infected with gram-positive bacteria such as *Pseudomonas* or *Staphylococcus*, showed an increase in V_d and dilution of antimicrobial agents in plasma and extracellular fluids, requiring careful monitoring of the dosage regimen (Pinder *et al.*, 2002). PD changes were observed in turpentine oil-injected mice which showed high anti-tumor activity of gimatecan compared to the controls (Frapolli *et al.*, 2010). On the other hand, despite of very high plasma concentrations of the calcium channel blocker, verapamil, or potassium channel antagonists, sotalol or propranolol; no change in the PD was observed in inflamed animals (Guirguis and Jamali, 2003; Mayo *et al.*, 2000). This discrepancy may be related to altered receptor-functioning or receptor-ligand binding in inflammation. Nevertheless, the above studies need further evaluations to delineate the disparities in altered drug metabolism caused by different bacterial infections or inflammation which has significant clinical implications for drug therapy in disease states.

1.2.2. Viral infections

Viral infections result in the release of various inflammatory mediators from the immune cells (Mannering and Deloria, 1986). Several studies have shown deleterious effects of viral infections such as mouse-adapted influenza virus (Corbett and Nettesheim, 1973), Newcastle disease virus (Singh and Renton, 1981),

encephalomyocarditis virus (Renton, 1981), chronic active hepatitis and cirrhosis (Schoene *et al.*, 1972; Wilkinson, 1997) and HIV infection (Lee *et al.*, 1993) on alteration of expression and activity of DMEs and oxidative pathways in animals and humans. Decreased levels of hepatic CYP1A2 were detected in children suffering from upper respiratory tract viral infections during an influenza outbreak (Kraemer *et al.*, 1982). With exceptions of CYP2D6 mRNA and CYP1A2 activity, other major CYPs such as CYP2C9, 2C19, and 3A4 in hepatitis C virus (HCV) infected PXB mice (mouse model with human hepatocytes) were comparable to the non-infected controls (Kikuchi *et al.*, 2010). Recombinant adenovirus injections in Sprague-Dawley rats led to a significant down-regulation of renal CYP2E1 and hepatic CYP3A2 and CYP2C11 expression and activity, and induction of CYP4A protein expression (Callahan *et al.*, 2005; Le *et al.*, 2006). Recently, compared to age and sex matched healthy subjects, in a clinical study with 10 men and 7 women with HIV infection, the hepatic enzyme activity of CYP3A4 was reduced by 18%, CYP2D6 reduced by 90%, N-acetyltransferase 2 (NAT2) reduced by 53%, xanthine oxidase (XO) activity increased by 22% whereas no change was reported with CYP1A2 activity (Jones *et al.*, 2010).

During the 1982 influenza B outbreak in King County, Washington, 11 children whose asthma had previously been controlled with a stable theophylline dose, developed theophylline toxicity at this same dose (Kraemer *et al.*, 1982). These children had a significant decrease in CL and increase in $T_{1/2}$ of theophylline. HIV infections could also lead to altered PK of levofloxacin and fluconazole (Goodwin *et al.*, 1994; Tett *et al.*,

1995). End-stage liver disease, which is largely the result of HCV infection, now accounts for up to 50% of deaths among persons with HIV-1 infection (Bica *et al.*, 2001). A clinical study in HIV-HCV-coinfected patients showed significantly lower nelfinavir oral clearances in HIV+ and HCV+ patients with and without cirrhosis compared to HIV+ and HCV-negative patients (Regazzi *et al.*, 2005). This begs the need for therapeutic drug monitoring in individualizing nelfinavir dosage in HIV-HCV-coinfected patients. In addition, an increase in AUC and C_{max} of several anti-retrovirals is reported in HCV-infected patients with moderate liver impairment (Veronese *et al.*, 2000; Wyles and Gerber, 2005). Other studies also showed significantly higher AUC of docetaxel and reduced glomerular filtration rate, suggesting changes in renal CYP in rats injected with the recombinant adenovirus expressing β-galactosidase (Le *et al.*, 2006; Wonganan *et al.*, 2009).

1.3. Molecular mechanism of regulation of CYP gene expression

It is known that down-regulation of DMEs and transporters during inflammation are associated with reduced expression of the regulatory nuclear receptors (Ghose *et al.*, 2009; Ghose *et al.*, 2008; Ghose *et al.*, 2004; Synold *et al.*, 2001). Various nuclear receptors including pregnane X receptor (PXR), constitutive androstane receptor (CAR), liver X receptor (LXR), and aryl hydrocarbon receptor (AhR) and peroxisome proliferator activated receptor (PPAR) are involved in regulating the gene expression of DMEs (Chen *et al.*, 2012). PXR and CAR heterodiemrize with another nuclear receptor retinoid X receptor alpha (RXRα) and are translocated in the nucleus for their

functioning. Cytokines such as IL-1 or TNF-α regulate the gene transcription by activating the cytokine-activated basal transcription factor such as nuclear factor-κB (NF-κB) (Aggarwal, 2004; Xiao and Ghosh, 2005), which has pleiotropic functions and plays an important role in down-regulating the transcriptional activity of multiple steroid/nuclear receptors (McKay and Cidlowski, 1999). It was shown that NF-κB activation by LPS and TNF-α played a pivotal role in the suppression of CYP3A4 through interactions of NF-κB with the PXR/RXR complex in primary human hepatocytes and HepG2 cell line (Gu *et al.*, 2006). The authors further showed that, inhibition of NF-κB by NF-κB-specific suppressor SRIκBα reversed the suppressive effects of LPS and TNF-α on CYP3A4 gene regulation. This study leads us to think that the mechanism of suppression by NF-κB activation may be extended to other nuclear receptor-regulated systems utilizing RXRα as a heterodimer.

Most of the times, the loss of mRNA precedes the enzyme loss and the magnitude in this decrease is proportional to the amount of enzyme activity observed. However measuring the relating the transcriptional changes to loss of enzyme activity become often difficult. For e.g. the transcription of CYP2C11 gene was suppressed in male rats treated with endotoxin or turpentine (Wright and Morgan, 1990). On the other hand, the authors showed that, transcription of CYP2C12 gene was not changed as much as the CYP2C12 mRNA in endotoxin-treated female rats. This discrepancy can be accounted by several factors such as lack of measurement of transcription at early time points or post-transcriptional changes.

In addition to the nuclear receptors, PXR and CAR, C/EBPβ isoforms could also mediate the down-regulation of drug metabolism in mice bearing extrahepatic tumors as observed in a murine Engelbreth-Holm-Swarm sarcoma mouse model (Kacevska *et al.*, 2011). This was also accompanied with reduced accumulation of the RXRα in hepatocytes implying an impaired functioning of nuclear receptors which rely primarily on RXRα dimerization. Detailed analysis revealed reduced hepatic expression levels of other nuclear receptors such as Car, Trβ, Lxβ, Pparα, Errα/β, Reverbα/β, and Shp only in tumor-bearing mice compared with the controls. Another study also showed that down-regulation PXR and CAR in livers of chronic hepatitis C patients with stage 3 fibrosis significantly correlated with the down-regulation observed in hepatic mRNA levels of CYP1A2, 2E1, 2D6 and UGT1A (Hanada *et al.*, 2011). The authors also concluded that down-regulation of mRNA of AhR during the progression of liver fibrosis was also associated with down-regulation of various DMEs studied. IL-6 mediated down-regulation of CYP3A4 mRNA in human hepatoma BC2 cells was linked with induction of translational activation of C/EBPβ-LIP (liver-enriched transcriptional inhibitory protein) along with 2 folds increase in C/EBPβ mRNA (Jover *et al.*, 2002). On the other hand, the amount of C/EBPβ-LAP (liver-enriched transcriptional activating protein), the major C/EBPβ form in nonstimulated cells, remained unchanged after IL-6 treatment (Jover *et al.*, 2002). The same group confirmed these observations in primary human hepatocytes also. In addition, the effects of LIP induction were shown by dose-dependent decrease in CYP3A4 mRNA levels upon adenovirus-mediated overexpression of

C/EBPβ-LIP while overexpression of C/EBPα and C/EBPβ-LAP caused a significant induction of CYP3A4 mRNA (Jover *et al.*, 2002). Thus, involvement of nuclear receptors in inflammation-mediated regulation of DMEs may depend on the nature of the inflammatory stimuli.

1.4. Role of Toll-like receptor signaling pathway and cytokines in regulation of expression of DMEs

Bacterial or viral infections activate Toll-like receptor (TLR) signaling pathway, which leads to the induction of pro-inflammatory cytokines such as IL-1β, IL-6 and TNF-α in the immune cells. In the liver, TLRs are present on the cell surface of various immune cells such as Kupffer cells, hepatic stellate cells, biliary epithelial cells, liver sinusoidal endothelial cells and hepatic dendritic cells as well as on the hepatocytes (Scott *et al.*, 2009; Seki and Brenner, 2008). The discovery of mammalian homologues of the *Drosophila* Toll receptor protein elicited a wide interest in the role of these proteins in innate immunity (Medzhitov and Janeway, 1997). A total of 13 TLRs have been identified in mammals. A detailed schematic of all the TLRs with their respective ligands can be found in Fig. 1.1 as shown below.

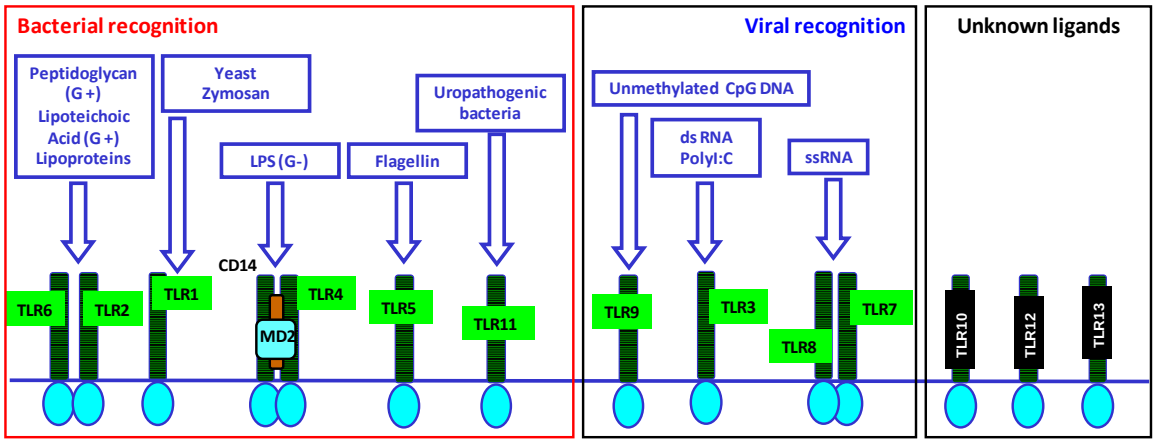

Figure 1.1 Mammalian TLRs and their ligands (Lee et al., 2012)

The TLRs are also called as pathogen recognition receptors as they recognize specific pathogen associated molecular patterns (PAMPs) which are not observed in mammals. Out of the 13 TLRs, this dissertation will focus primarily on TLR4 as it is activated by the gram-negative bacterial endotoxin, LPS, and TLR2 as it is activated by the gram-positive bacterial endotoxin, LTA (Aliprantis *et al.*, 1999; Takeuchi *et al.*, 1999). Gram-negative and gram-positive bacterial infections are among the highly prevalent microbial infections worldwide. Increasing recognition is observed in development of drug targets against TLRs in chronic liver diseases.

Here we will review the functioning of the TLR signaling pathway upon activation by microbial components. A schematic overview of TLR2 and TLR4 signaling pathways is shown in Fig. 1.2. Mammalian TLR, as well as *Drosophila* Toll, is characterized by extracellular leucine-rich repeat motifs and a cytoplasmic Toll

interleukin 1 receptor (TIR) homology domain. TLR4 requires the association with LPS-binding protein (LBP), CD14, and MD2 to recognize LPS. Upon TLR4 ligation, the intracellular domain of TLR4 recruits Toll-interleukin 1 receptor adaptor protein (TIRAP) and MyD88 for MyD88-dependent signaling and TRAM bridges TRIF for MyD88-independent signaling. MyD88 serves as a common adaptor to all the TLRs except for TLR3 which operates through the TRIF pathway and TLR4 has an additional secondary pathway in addition to MyD88. It was shown that MyD88 *knockout* mice were unresponsive to LPS and did not secrete TNF-α, IL-6 and NO (Kawai *et al.*, 1999). Ligand binding to TLRs triggers association of MyD88 with TIR domain and assembly of IL-1R-associated kinase (IRAK) 1/IRAK4 complex. IRAK4 prosphorylates IRAK1 creating a binding site for tumor necrosis receptor-associated factor (TRAF) 6. The IRAK1-TRAF6 complex dissociates and activates the transforming growth factor-β-activated kinase 1 (TAK1). The active TAK1 activates two distinct signal transduction proteins: (a) TAK1 phosphorylates the inhibitor of NF-κB kinase (IKK) consisting of two catalytic kinase subunits (IKKa and/or IKKb) which further activate the NF-κB pathway. IKK then phosphorylates IκB causing it to release NF-κB which then translocates from the cytoplasm to the nucleus and activates transcription of cytokine genes. (b) TAK1 also phosphorylates and activates the upstream mitogen activated protein kinase (MAPK) cascade which regulates the downstream kinases such as p38, extracellular signal regulated kinase (ERK1/2) and JNK and activates transcription of MAPK genes such as c-Jun, activator protein (AP-1), etc.

In the MyD88-independent TLR4 and TRIF-dependent TLR3 pathway, TRIF associates with TRAF family member associated NF-κB activator binding kinase 1 (TBK1) and IKKϵ with subsequent phosphorylation and nuclear translocation of IRF3 leading to IFN-β transcription as shown in Fig. 1.2.

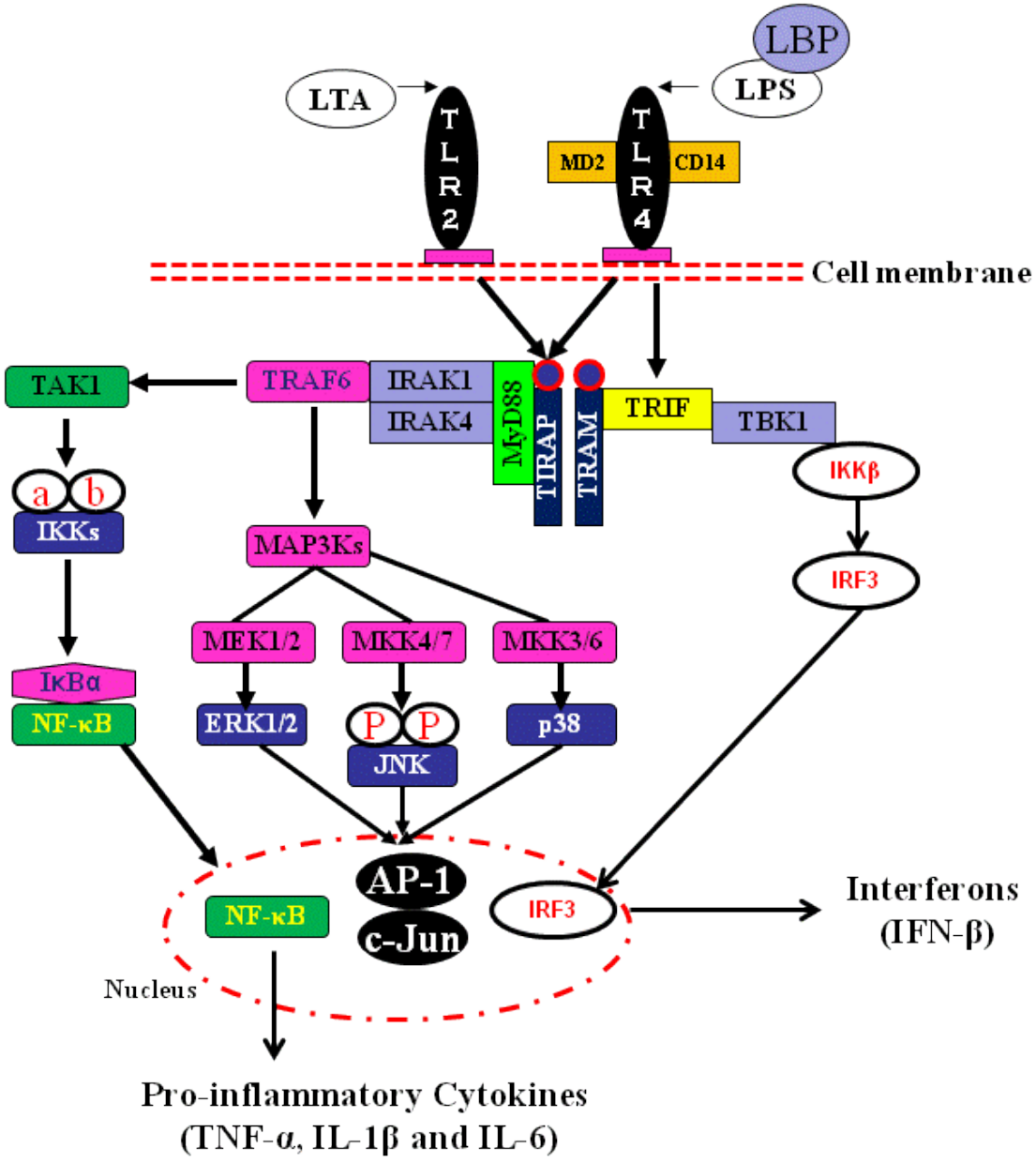

Figure 1.2 TLR2 and TLR4 signaling pathways

Various dissimilarities among the different members of the TLR family play an important role in deciding the inflammatory actions of the ligands. For e.g. although MyD88 is required for cytokine production induced by both TLR4 and TLR9 ligands (Schnare *et al.*, 2000), only TLR4, but not TLR9, activates NF-κB and MAPK such as the c-Jun-N-terminal kinase (JNK), as well as dendritic cell maturation independent of MyD88 (Kaisho *et al.*, 2001; Kawai *et al.*, 1999; Schnare *et al.*, 2000). Unlike TLR4, activation of NF-κB and MAPK by the TLR2 ligands and IL-1β was shown to be dependent on MyD88 (Adachi *et al.*, 1998; Takeuchi *et al.*, 2000). These data therefore suggest that only TLR4, but not TLR9 or TLR2 can mediate the immune responses independent of MyD88. Thus, later studies identified that TLR4-mediated signaling could be initiated by an additional down-stream adaptor protein, TIRAP, in 293T HEK (293T) and RAW264.7 (RAW) cell lines (Horng *et al.*, 2001; Kagan and Medzhitov, 2006).

We have shown that down-regulation of Cyp3a11 in LPS-sensitive TLR4 *wild type* (C3HeB/FeJ) mice could not be detected in TLR4-mutant (C3H/HeJ) mice (Ghose *et al.*, 2008). Recent data from our group showed that down-regulation of gene expression of key hepatic phase I and phase II DMEs in $TLR2^{+/+}$ mice by LTA was blocked in $TLR2^{-/-}$ mice (Ghose *et al.*, 2011a). Although, most of the studies have cited the role of Kupffer cell-derived TLRs in hepatic drug metabolism, we and others have also shown that LPS or LTA treatment of primary mouse hepatocytes can directly affect the DMEs via TLRs present on the hepatocytes, independent of cytokines (Ferrari *et al.*, 2001; Ghose *et al.*, 2011a). We showed that TIRAP was involved only in TLR2-mediated

regulation of DME genes (Ghose *et al.*, 2011a), and not by TLR4 (Ghose *et al.*, 2008). TLR-mediated down-regulation of DMEs was also shown to be associated with down-regulation of nuclear receptors. We showed that down-regulation of nuclear receptors by LPS in $TLR4^{+/+}$ or by LTA in $TLR2^{+/+}$ mice was blocked in TLR4 mutant or $TLR2^{-/-}$ mice (Ghose *et al.*, 2009; Ghose *et al.*, 2011a; Ghose *et al.*, 2008). However, mRNA and protein expression of several CYPs did not differ in $PXR^{-/-}$ or $PPAR^{-/-}$ mice treated with LPS (Richardson and Morgan, 2005).

Cytokines are involved in alteration of DMEs *in vitro* (Barker *et al.*, 1992; Muntane-Relat *et al.*, 1995). LPS-treatment of primary rat cocultures of hepatocytes and Kupffer cells significantly suppressed phenobarbital-mediated induction of CYP2B1 (Milosevic *et al.*, 1999). This decrease was associated with a 5-fold induction in TNF-α released from the Kupffer cells in cocultures.

In contrast to the above studies, recent evidence suggests that cytokines may not be playing a major role in regulation of DMEs. Earlier studies in TNF-$\alpha^{-/-}$ and IL-$6^{-/-}$ knockout mice revealed that DMEs were still down-regulated (Warren *et al.*, 1999; Warren *et al.*, 2001). A recent study by *Kinloch et al* in $TNFR1^{-/-}$, $IL1R1^{-/-}$ and Kupffer cell-depleted mice showed that only TNF-α, but not IL-1β or Kupffer cells, was involved in regulation of CYP3A11 and 3A25 in oral *C. rodentium* infected mice (Kinloch *et al.*, 2011). In addition, we showed that although down-regulation of DMEs was blocked in LTA-treated $TIRAP^{-/-}$ mice, hepatic cytokine gene expression remained unchanged (Ghose *et al.*, 2011a). Cytokine specific effects on repressing the major DMEs were

studied in primary human hepatocytes in which only IL-1β, TNF-α, and IL-6, but not IFN-γ, were involved in down-regulation of CYP3A4 mRNA expression (Abdel-Razzak *et al.*, 1993), whereas IFN-γ and also IL-6, unlike TNF-α or IL-1β, repressed CYP2B6 mRNA expression (Aitken and Morgan, 2007).

Nitric oxide (NO), released from macrophages and hepatocytes during inflammation is also known to regulate DMEs (Morris and Billiar, 1994). However, contrasting results have been reported for the role of NO in regulation of DMEs in cytokine-treated primary rat hepatocytes (Carlson and Billings, 1996; Sewer and Morgan, 1997). IL-1β and TNF-α-mediated down-regulation of CYP protein was NO dependent, but not in IL-6 mediated down-regulation (Carlson and Billings, 1996). NO was also shown to regulate the suppression of UGT activities in cytokine-treated hepatocytes (Monshouwer *et al.*, 1996b).

Activation of TLRs in the Kupffer cells releases cytokines which can act on cytokine receptors present on the hepatocytes. LPS or LTA can activate TLRs which are also present on the hepatocyte cell surface to down-regulate CYP450 genes (Galloway *et al.*, 2008; Ghose *et al.*, 2011a). Although, there is a direct link between cytokines and down-regulation of hepatic CYP450s, LPS-induced down-regulation of CYP3A was not completely blocked in Kupffer cell inactivated mouse livers (Xu *et al.*, 2004). LPS or LTA can activate TLR4 or TLR2 on the hepatocytes and regulate the activity of the cell signaling components, NF-κB and JNK. Inflammation-mediated activation of NF-κB plays a significant role in down-regulation of DMEs (Abdulla *et al.*, 2005; Gilmore,

2006). NF-κB can either indirectly regulate CYP gene expression through mutual repression between NF-κB and nuclear receptors, or can directly regulate CYP gene expression through binding to NF-κB response element in the promoter region of CYP genes (Pascussi *et al.*, 2003). Interaction of NF-κB with nuclear receptors during pathophysiological conditions can alter expression of DMEs (Gu *et al.*, 2006). Inflammation activates the MAPK, JNK, which also regulates nuclear receptors and DMEs (Adam-Stitah *et al.*, 1999; Yu *et al.*, 1999). Recent experiments in primary cultures of human hepatocytes microtubules-interfering agents restricted aryl hydrocarbon receptor-mediated CYP1A2 induction via interaction of JNK and probably aryl hydrocarbon receptor (Vrzal *et al.*, 2008). This suggests a prominent role of JNK in regulation of CYP1A2 expression. On the contrary, another study showed that inhibition of JNK activation by docosahexaenoic acid played a significant role at least in regulating docosahexaenoic acid-mediated down-regulation of CYP 2B1 expression induced by phenobarbital in primary mouse hepatocytes (Lu *et al.*, 2009). However, further detailed studies using *in vitro* models such as cell lines or primary hepatocytes, and specific inhibitors of these cell signaling components will significantly contribute in understanding the mechanistic regulation of DMEs during inflammation.

1.5. Post-transcriptional and post-translational regulation of DMEs in infection and inflammation

1.5.1. RNA turnover

To determine the effect of inflammatory conditions on mRNA degradation, studies on measuring the mRNA half-lives of various CYP isoforms are necessary. For e.g. in matrigel-cultured hepatocytes, the mRNA half-life for CYP2C12 is ~ 10 h and it was observed that CYP2C12 was degraded to 5% of its control levels within 12 h in LPS-treated rats suggesting a posttranscriptional modification (Morgan, 1989). Similarly, studies have shown that mRNA degradation is accelerated in rats treated with IFN in presence of actinomycin D (transcriptional deactivator) (Delaporte and Renton, 1997). IFN display their antiviral actions by cleaving the double stranded viral RNAs but it also has some effects on cellular RNAs. However, when activated, a latent endonuclease, RNase L, which cleaves single-stranded mRNA after UA, UG, UC, and UU residues at the 3 end could degrade mRNAs coding for CYP, accounting for the increased mRNA turnover (Floyd-Smith *et al.*, 1981).

1.5.2. Protein synthesis and turnover

Early studies showed that CYP down-regulation by IFN inducers can be due a decrease in protein synthesis. For e.g. In animals treated with Poly I:C decreased CYP content was shown to decrease CYP protein synthesis as a result of decrease in mRNA levels rather than to a change in translation or protein degradation (Singh and Renton, 1984). Subsequent studies showed that changes in turnover of a CYP gene product by IL-

6 in rat hepatocytes did not alter the CYP2B1/2 protein or activity upon inhibition of protein synthesis (Clark *et al.*, 1996). Similarly, in LPS-treated rats, CYP2C12 mRNA and protein levels declined simultaneously suggesting that attenuation in mRNA levels did not account for the change in protein (Morgan, 1989). Contrary to the above study where protein degradation was responsible for decrease in CYP content, it was also shown that LPS-induced suppression of CYP2C11 mRNA in rats was achieved in 48 h where as the protein levels were not suppressed to the same extent (Morgan, 1989).

1.5.3. Enzyme inhibition

It is mostly believed that changes in a specific CYP protein and its activity is due to decreased enzyme activity thought due to reduced amount of enzyme. However, studies have shown contradicting results where although protein levels of CYP3A2 in rat hepatocytes treated with IFN-γ were reduced to 30% of control where as CYP3A2 activity as demonstrated by testosterone hydroxylation was 3% of control (Tapner *et al.*, 1996). Further studies will be needed to gain better understanding of these differences in changes in CYP protein and enzyme activity.

1.6. Drug-induced hepatotoxicity in infections and inflammation

1.6.1. Drug-induced hepatotoxicity

Liver, apart from being the major site of drug metabolism, also regulates the immune responses in the body. Drug-induced hepatotoxicity is a subject of intense discussion among clinicians involved in liver pathology, pharmaceutical scientists, epidemiologists, biostatisticians and regulatory agencies such as the Food and Drug Administration (FDA). Over the last two decades, drug-induced hepatotoxicity has been the leading cause of approved drug withdrawal from the market (McBurney *et al.*, 2009). It can be primarily classified into two groups: 1) Drugs that directly affect the liver (intrinsic hepatotoxicity) and 2) Drugs that mediate an immune response (hypersensitivity) or idiosyncratic hepatotoxicity. Intrinsic or direct hepatotoxicity is usually dose-dependent, reproducible in different animal models and has a consistent period of onset. For e.g. the APAP-induced hepatotoxicity (Larson *et al.*, 2005). Idiosyncratic drug-induced hepatotoxicity comprises of several factors including, but not limited to, lack of reproducible animal models, dose-independent and host-dependent, immune system or genetic variability (Chalasani and Bjornsson, 2010; Ikeda, 2011). Examples of idiosyncratic hepatotoxins are troglitazone and CPZ (Buchweitz *et al.*, 2002; Kohlroser *et al.*, 2000). Some distinct features of intrinsic and idiosyncratic hepatotoxicity are shown in the table below.

Table 1.1 Characteristics of intrinsic and idiosyncratic drug-induced hepatotoxicity

Intrinsic	Idiosyncratic
Dose dependent (predictable)	Dose independent (non-predictable)
Host independent	Host dependent
Reproducible in animal models	Lack of animal models exist
Predictable latent period after exposure	Variable onset relative to exposure
Distinctive liver lesion	Variable liver pathology

1.6.2. Statement of the problem

Despite innovations and early assessment of biomarkers of liver toxicity in drug development, there is a wide array of drugs which exhibit hepatotoxicity, eventually sliding them into the "death valley of drugs". Several widely used drugs such as APAP (Tylenol®, analgesic), valproic acid (an anticonvulsant), isoniazid (used in the management of tuberculosis), zafirlukast (antiasthmatic agent) and many more have been shown to be associated with liver injury and thus carry a warning label.

Several reports documented in the literature provide enormous evidences suggesting drug-induced hepatotoxicity is prevalent for more than 50 years. Table 1.2 provides a list of drugs withdrawn from the market or those which carry a warning after being declared as life-threatening hepatotoxins. Of particular attention is the fact that, antibiotics and nonsteroidal anti-inflammatory drugs (NSAIDs) used clinically in patients with underlying inflammation top the list of the most common causes of hepatic idiosyncratic ADRs (Chalasani *et al.*, 2008; Hussaini and Farrington, 2007). Similarly,

studies also showed that viral hepatitis could predispose the drugs to cause liver injury at an otherwise non-toxic dose (Hussaini and Farrington, 2007). Such findings strongly suggest that inflammation could possibly be associated in lowering the threshold of drugs to cause hepatotoxicity. As idiosyncratic drug-induced hepatotoxicity pose a great challenge in drug development due to the factors mentioned above, before we discuss the postulated underlying mechanisms, the following section will highlight the different drug-induced hepatotoxicity studies with some widely studied direct and idiosyncratic hepatotoxins in infections and inflammation.

Table 1.2 Few examples of drugs which were withdrawn from the market or those which carry a black-box warning label (Ernst, 2002; Goldkind and Laine, 2006; Lasser *et al.*, 2002; Smith and Schmid, 2006). (Year the drug was withdrawn)

Drugs which are withdrawn	**Drugs which carry a black-box warning**
Temafloxacin HCl (1992)	TYLENOL (acetaminophen)
ORAFLEX (benoxaprofen) (1982)	Isoniazid
Ibufenac † (1970)	Valproate sodium
DURACT (bromfenac) (1998)	Sulindac
REZULIN (troglitizone) (2000)	Ketoconazole
Kava Kava*	Pemoline
Mibefradil dihydrochloride (1998)	Ketorolac

* withdrawn from German market, † withdrawn from UK market,

Drug-induced hepatotoxicity pose an even greater challenge when promising therapeutic drugs such as troglitazone (an antidiabetic drug) and bromfenac (an analgesic) were withdrawn from the market due to unacceptable liver injury observed in phase IV clinical studies (Hunter *et al.*, 1999; Kohlroser *et al.*, 2000). Collective information on the occurrences of adverse drug reactions (ADRs) was represented in a recent article which employed 18,820 patients out of which 1225 were admitted due to ADRs (> 6%). The number of patients died or the mortality rate during the 6 month study period was 28 patients (>2%) (Pirmohamed *et al.*, 2004). However, this number can be significantly greater due to unaccountable incidences of underreporting suspected (Bagheri *et al.*, 2000). ADRs should not only be viewed in terms of its threat to human health, but also the increasing number of ADRs lead to significant losses of financial revenues of the pharmaceutical companies, time and efforts invested and eventually lead to emergence of poor management of new diseases.

1.6.3. Significance of these findings

Inflammation is a characteristic phenomenon elicited as a result of tissue injury and causes local irritation along with redness, swelling, pain, heat and loss of function. The inflammatory stress hypothesis studied in detail by Roth *et al* states that: “an acute episode of inflammation has the potential of interacting with co-administered drugs to precipitate idiosyncratic drug induced hepatotoxicity” (Roth *et al.*, 2003). Although, inflammation plays a highly important role in detoxification of foreign agents, prolonged stimulation can lead to toxic reactions by production and release of pro-inflammatory

mediators and activation of cell signaling systems. Inflammation encompasses a wide array of cells such as the Kupffer cells, polymorpho nuclear neutrophils (PMNs), endothelial cells, hepatic stellate cells along with the parenchymal cells (hepatocytes) (Ganey *et al.*, 2004).

The data presented in this dissertation highlights novel mechanisms likely to affect drug-induced hepatotoxicity in inflammation. This study suggests that the threshold for toxic drug reactions is lowered in infections or inflammation which can lead to significant drug-induced hepatotoxicity. Identification of novel receptors and cell-signaling components paves the way for molecular intervention in early identification using specific biomarkers for prevention of drug-induced hepatotoxicity.

1.7. Changes in drug-induced hepatotoxicity in infections and inflammation

1.7.1. Bacterial infections

The gram-negative bacterial endotoxin, LPS, has been extensively used as a model of bacterial sepsis and induces inflammation to study the role of inflammatory stress in idiosyncratic drug-induced hepatotoxicity. The effects of LPS on induction of pro-inflammatory genes involved in production of cytokines and cell signaling molecules such as p-38 or c-Jun-N-terminal kinase (JNK) involved in cell growth and differentiation have led to the widespread use of LPS in mammals to study drug-induced hepatotoxicity. In addition, various pathophysiological conditions such as alcohol intake, gastrointestinal distress, changes in diet or surgery can lead to increased plasma concentrations of LPS (Roth *et al.*, 1997).

Table 1.3 List of idiosyncratic hepatotoxins in known to cause adverse drug reactions humans and LPS-treated animals (Abdel-Bakky *et al.*, 2010; Deng *et al.*, 2009; Ikeda, 2011; Lewis *et al.*, 1990; Lu *et al.*, 2012)

Drugs	Adverse drug reactions in humans	LPS-DRUG interactions in rodents
Chlorpromazine	Yes	Yes
Trovafloxacin	Yes	Yes
Levofloxacin	No	No
Ranitidine	Yes	Yes
Monocrotaline	Yes	Yes
Famotidine	No	No
Halothane	Yes	Yes
Sulindac	Yes	Yes
Diclofenac	Yes	Yes
Troglitazone	Yes	Yes
Amiodarone	Yes	Yes

Ranitidine (RAN), a histamine-2 (H2)-receptor antagonist used for treating duodenal ulcers, gastric hypersecretory diseases and gastroesophageal reflux disease is associated with idiosyncratic hepatotoxicity in humans observed in 1 of every 1000 patients taking the medication (Vial *et al.*, 1991). Studies showed that a nontoxic dose of RAN was rendered hepatotoxic in rats pretreated with an otherwise nontoxic dose of LPS 44.4X10 EU/kg) (Luyendyk *et al.*, 2003). The authors showed that, only ranitidine (30 mg/kg), but not famotidine (FAM, 6 mg/kg), significantly increased serum ALT, AST

and γ-glutamyl transferase (GGT) activity at 6, 12 and 24 hafter RAN treatment. Histopathologic examination of liver tissues revealed presence of midzonal hepatic necrosis in LPS/RAN cotreated rats (Luyendyk *et al.*, 2003). Interestingly, prodromal indicators consistent with endotoxin-induced inflammation are commonly reported in patients on RAN therapy. For e.g. evaluation of 34 cases of RAN-associated liver injury demonstrated diarrhea, fever, nausea/vomiting, and/or abdominal pain in nearly 60% of the cases (Barr and Piper, 1981). Indeed, RAN-treated patients showed signs of inflammation/endoxemia related changes in serum liver enzyme levels (Barr and Piper, 1981; Halparin, 1984). It is also believed that RAN idiosyncrasy leads to translocation of LPS to the GI tract as observed during high alcohol intake or surgery (Halparin, 1984). A recent study showed interesting correlation of LPS/RAN hepatotoxicity with metabonomic changes as demonstrated with distinct metabolite profiles in urine by non invasive techniques such as ^{1}H-nuclear magnetic resonance (NMR) or mass spectroscopy (Maddox *et al.*, 2006). The predominant changes included decreases in citrate, hippurate, and 2-oxoglutarate, and increases in acetate, creatine, creatinine, taurine, and trimethylamine *N*-oxide, which were consistent with results obtained from animals with hepatocellular injury (Beckwith-Hall *et al.*, 2002; Clayton *et al.*, 2003).

It would be a great boon to the society by bringing drugs back to the shelf which were once withdrawn due to serious ADRs. One classic example is the fluoroquinolone antibiotic agent, trovafloxacin (TVX). Approved in 1997 by the FDA, TVX was used to treat bacterial infections with a better sensitivity against the gram-positive pathogens.

Although a block buster drug with immense clinical benefit, the drug was withdrawn in 1999 due to fatal hepatotoxicity reported in 14 cases, including six deaths and four patients who underwent liver transplantation (Ball *et al.*, 1999). In order to better understand the mechanisms of TVX hepatotoxicity, several animal models have been developed. TVX led to significant increases in serum ALT and TNF-α levels and histopathologic changes evident only in LPS-treated mice compared to saline controls (Shaw *et al.*, 2007). Interestingly, the authors did not observe any hepatotoxicity-related changes in mice treated with levofloxacin (LVX), a structurally similar analogue of TVX. These erratic observations again point to the fact that inflammation-mediated changes in drug-induced hepatotoxicity can be dependent on several factors.

Similarly, various studies with the LPS model have shown the utility of LPS as a potent inflammagen in understanding the mechanisms involved in drug induced hepatotoxicity with clinically relevant drugs such as chlorpromazine (Buchweitz *et al.*, 2002), diclofenac (Deng *et al.*, 2006), sulindac (Zou *et al.*, 2009a), allyl alcohol (Tukov *et al.*, 2006), amiodarone (Lu *et al.*, 2012) or acetaminophen (Maddox *et al.*, 2010), monocrotaline (Yee *et al.*, 2003c) and aflatoxin B1 (Luyendyk *et al.*, 2002).

1.7.2. Viral infections

Viral infections have also shown to cause serious drug-induced hepatotoxicities in animal models. Studies have shown contrasting results with APAP-induced hepatotoxicity in animal models of viral infections. For e.g. studies have reported the inductive effect of viral infections on APAP-induced hepatotoxicity. Mice infected with

reovirus showed reduced threshold for APAP-induced hepatotoxicity as demonstrated by significantly increased ALT levels and centrilobular necrosis with marked accumulation of polymorphonuclear neutrophils in livers of reovirus/APAP co-treated mice compared to mice treated with saline, reovirus or APAP alone (Maddox *et al.*, 2010). The authors concluded that normally noninjurious doses of APAP are rendered hepatotoxic by modest inflammation, induced by either bacterial or viral components.

According to the 2010 statistical report, more than 38 million people are infected with HIV worldwide and AIDS accounted for approximately one third of all deaths in South Africa in 2011 (http://www.ips.org/). The management of AIDS becomes very complex considering the fact that HIV infected patients have a compromised immune system and are traditionally put on combination drug therapies which can lead to severe drug-drug interactions and increases the metabolic burden on the liver. A prospective report from the Data collection on adverse events of Anti-HIV Drugs (D:A:D) Study Group (Weber *et al.*, 2006) showed that mortality from liver disease was second only to AIDS-related mortality. Moreover, of these liver-related deaths, 66% were secondary to hepatitis C virus (HCV), 17% were attributed to active hepatitis B virus (HBV), and 3% were directly related to combination anti-retroviral drug therapy (cART), respectively (Weber *et al.*, 2006). Drug-induced hepatotoxicity in HIV infections is a topic of great attention. Severe hepatotoxicities have been reported in HIV-infected patients receiving cART in which the rise in ALT levels were raised significantly in 8.5 to 23% patients (Kovari *et al.*, 2010; Servoss *et al.*, 2006; Sulkowski *et al.*, 2000). Although observed

rarely, the most widely used anti-retro viral agents, efavirenz and nevirapine, were prone to cause serious hepatotoxicities in humans infected with HIV, HBV or HCV alone (Ena *et al.*, 2003; Rivero *et al.*, 2007; Sulkowski *et al.*, 2002). Moreover, the risk of drug-induced hepatotoxicity due to cART increased severely in HIV patients co-infected with HBV or HCV compared to those without co-infection (den Brinker *et al.*, 2000). Furthermore, asymptomatic aminotransferase elevation, although not clinically relevant for the patient, can add to increased costs due to additional tests and clinic visits, and medication changes. Overall, HIV, HBV or HCV alone or together pose a great challenge in designing the drug dosage regimen owning to their unwanted effects on the liver.

Other viral components such as viral RNA mimetic polyI:C was also known to exacerbate halothane-induced liver injury in mice (Cheng *et al.*, 2009b). The authors observed distinct halothane-induced liver injury upon pre- or post-treatment with polyI:C. Specifically, pre-treatment with polyI:C attenuated halothane-induced liver injury where as post-treatment proved to significantly aggravate the liver injury (Cheng *et al.*, 2009b). The authors linked reduced halothane-induced liver injury upon pre-treatment with polyI:C may be due to down-regulation of DMEs involved in metabolism of halothane. In addition, the pan-caspase inhibitor, z-VAD-fmk, suppressed liver injury induced by polyI:C/halothane cotreatment, implying that the increased hepatocyte apoptosis can lead to exacerbation of liver injury. The data showed that, post-treatment with polyI:C also activated the cells of the immune system such as hepatic Kupffer cells (KC) and natural

killer (NK) cells and up-regulated multiple pro-apoptotic mediators, including TNF-α, NK receptor group 2, and Fas ligand in mice.

Of particular attention are the hepatotoxicity reports of anti-tuberculosis (TB) drugs such as isoniazid (INH), rifampin (RIF), and pyrazinamide (PZA) which have drawn considerable attention when administered to patients with TB with underlying chronic hepatitis or liver cirrhosis. More than 3 decades ago, INH treatment led to significant hepatocellular injury in 114 patients with underlying TB (Black *et al.*, 1975). The authors reported 13 fatalities, 9 with submassive necrosis and 4 with massive necrosis as assessed by the histological demonstration of patients. From the other 20 patients, 16 developed moderately severe acute hepatocellular injury (4 had a mixed hepatocellular-cholestatic pattern), and 4 with chronic hepatic diseases. A recent clinical study with 107 patients (49 with chronic hepatitis and 58 with liver cirrhosis) suspected or confirmed with TB were endrolled in the study to assess anti-TB induced DILI (Park *et al.*, 2010). Out of the 18 patients who met the criteria for DILI, 11 patients with chronic hepatitis and 7 patients with liver cirrhosis developed DILI with anti-TB medications as demonstrated by increased ALT, AST and ALP levels. Detailed univariate analyses indicated that female sex, underlying immunesuppressed state, increased number of hepatotoxic anti-TB drugs and elevation of baseline ALP were potential risk factors for anti-TB DILI.

1.8. Mechanisms of idiosyncratic drug-induced hepatotoxicity

Despite of several advances in biochemical, toxicological, and pharmaceutical approaches to understand idiosyncratic drug-induced hepatotoxicity, the underlying mechanisms still remain to be completely proven. Various limitations and challenges in identifying idiosyncratic drug-induced hepatotoxicity has led to an overwhelming investment of scientific resources and theories to build models which can be used for successfully used in early drug development. This has led to the emergence of several hypotheses which may individually or as a combination play an important role in elicitation of drug-induced hepatotoxicity. These hypotheses are briefly overviewed as shown below:

1.8.1. Reactive intermediate hypothesis

Idiosyncratic drug-induced hepatotoxicity is broadly classified into immune-mediated and metabolism-mediated idiosyncrasy (Zimmerman, 1993) The reactive metabolic hypothesis assumes that a drug forms reactive metabolites which can covalently bind to cellular proteins, lead to membrane instability and alter intracellular signaling mechanisms which can lead to cell death (Kaplowitz *et al.,* 1986). Drugs or their reactive metabolites can have significant effects on alterations of gene expression and cellular homeostasis in hepatocytes (Boelsterli and Lim, 2007). Several studies shed light on this theory suggesting drugs such as APAP, tamoxifen, diclofenac, and troglitazone form reactive metabolites leading to adverse effects on the liver (Park *et al.*, 2005; Walgren *et al.*, 2005). One classic example is the anti-diabetic agent troglitazone,

which has been linked with serious idiosyncratic hepatotoxicity (Murphy *et al.*, 2000). Metabolic activation of troglitazone by CYP3A4 results in reactive metabolites capable of binding to proteins and other nucleophiles which can have profound effects on normal liver physiology (He *et al.*, 2004), however the link between the reactive metabolites of troglitazone to liver injury has not yet been established completely. Thus, although the reactive intermediate hypothesis can be certainly linked with occurrence of hepatotoxicity, there is a lack of supporting data for many drugs that cause idiosyncratic drug-induced hepatotoxicity.

1.8.2. Genetic polymorphism hypothesis

This theory relies on the fact that differences in genetic compositions of DMEs can lead to inter-individual differences in pharmacokinetics as well as in reactive intermediate formation. These polymorphisms can either result in potentially toxic plasma drug concentrations or even render individuals susceptible to therapeutic doses of drugs, resulting in idiosyncratic drug-induced hepatotoxicity. For e.g. a genetic polymorphism in an anti-inflammatory cytokine could alter the toxicity threshold in individuals for some drugs, further contributing to IDILI. Notably, the genetic polymorphism hypothesis can explain why some individuals experience different rates of metabolic activation from the same drug dosage regimen, as a result of faster achievement of critical threshold needed for toxicity. A classic example backing this hypothesis comes from several studies analyzing isoniazid-induced hepatotoxicity (Bose *et al.*, 2011; Leiro-Fernandez *et al.*, 2010; Mitchell *et al.*, 1976; Sotsuka *et al.*, 2011).

These studies showed that genetic variations in NAT2 or CYP2E1 were particularly linked for isoniazid-induced hepatotoxicity. Similarly, others have shown that genetic polymorphisms in phase II enzymes such as UGTs or GSTs also play a role in susceptibility to toxic effects of drugs on the liver (Lee *et al.*, 2011; Sun *et al.*, 2008; Wang *et al.*, 2010). However, some studies have failed to find such associations (Chatterjee *et al.*, 2010; Gurumurthy *et al.*, 1984). Overall, the association of a specific polymorphism with adverse drug reactions does not by itself constitute proof of cause and effect.

1.8.3. Hapten hypothesis

This is another prevalent hypothesis which states that prodrugs or more likely their reactive metabolites form drug-protein adducts through covalent binding (Macher and Chase, 1969). This protein adduct is then recognized as a foreign antigen which initiates an immunological response (Park *et al.*, 1987). These adducts are recognized as foreign antigens by the immune system and presented to helper T cells. Subsequent drug exposure results in the formation of autoantibodies by the immune cells eliciting an immune response. Common examples include drugs such as diclofenac, troglitazone, halothane, and tienilic acid (Maniratanachote *et al.*, 2005; Nguyen *et al.*, 2008; Sallie *et al.*, 1991). Although repeated halothane-exposure can lead to liver injury (Bird and Williams, 1989), 39% of patients developed halothane-induced hepatitis which were not previously exposed to halothane (Eghtesadi-Araghi *et al.*, 2008). These observations make us rethink whether sensitization and challenge exposures are needed to precipitate

severe drug-induced hepatotoxicity. Animal models of drug-induced autoimmunity have been developed with penicillamine and nevirapine (Shenton *et al.*, 2003; Tournade *et al.*, 1990). However, liver injury was not observed in these animal models. Thus, development of animal models to study this hypothesis in context of liver injury remains a major challenge.

1.8.4. Danger hypothesis

This hypothesis is similar to the hapten hypothesis and states that an activated immune response occurs when a drug or its reactive metabolite binds to a protein and causes a stress response only in the presence of an adjuvant resulting in a "danger signal". This signal can be in the form of cell necrosis or cytokine release upon subsequent exposure of the drug (Uetrecht, 1999). Activation of the innate immune system as a result of underlying inflammation, was proposed to be a potential danger signal (Kaplowitz, 2005). However, the danger hypothesis does not apply to all the drugs forming reactive metabolites. For e.g. tienilic acid treatment in rats induced changes in genes involved in oxidative stress, inflammation, cytotoxicity, and liver regeneration (Pacitto *et al.*, 2007). On the other hand, sulfamethoxazole, generally associated with idiosyncratic drug reactions and forms reactive metabolites did not lead to any effects on the immune system as observed with tienilic acid (Pacitto *et al.*, 2007). Thus, the danger signal can be considered as a collective event elicited from a number of independent factors including intestinal microbial distress or an infection causing an innate immune response resulting in inflammatory stress (Shaw *et al.*, 2010).

1.8.5. Mitochondrial abnormality hypothesis

Another possible hypothesis known to be involved in IDILI is drug-induced mitochondrial abnormality or drug interaction with the compromised mitochondria. Factors such as reduction in endogenous ATP production, generation of mitochondrial ROS and alteration of mitochondrial membrane potential usually contribute in leading to mitochondrial dysfunction. Altered mitochondrial function could render cells sensitive to the drug, resulting in idiosyncratic toxicity (Waring and Anderson, 2005). An uncommon but distinctive form of drug-induced hepatotoxicity as characterized by microvesicular fatty liver can result from tetracycline, amiodarone, valproate and various antiviral nucleoside analogues treatment (Bissell *et al.*, 2001; Bryant and Dreifuss, 1996; McKenzie *et al.*, 1995). This hepatotoxicity is further characterized by the accumulation of microvesicular fat in hepatocytes and reduced numbers of mitochondria. Several reverse transcriptase inhibitors such as anti-HIV drugs including zalcitabine, didanosine, stavudine, lamivudine, zidovudine and abacavir led to inhibition of mitochondrial DNA polymerase γ with zalcitabine showing the highest potency followed by the above listed drugs (Kakuda, 2000). In vitro studies showed that drug-induced hepatotoxicities with drugs such as troglitazone, tolcapone, nimesulide and valproic acid were linked with severe mitochrondrial dysfunction (Bedoucha *et al.*, 2001; Bjorge and Baillie, 1991; Haasio *et al.*, 2002; Mingatto *et al.*, 2000). In addition, data from clinical studies also show a strong relationship between in IDILI and mitochondrial abnormality as assessed by polymorphisms in the mitochondrial superoxide dismutase 2 and glutathione

peroxidase 1 genes and susceptibility to DILI among 185 Spanish patients with DILI and population controls (Lucena *et al.*, 2010). Overall, it can be concluded that alterations in mitochondrial function can regulate the modes of action of IDILI.

1.8.6. Failure to adapt hypothesis

This hypothesis proposes that although a large proportion of population 'adapt' to the increasing exposure of drug and can recover from the liver injury, a small fraction of this population fails to adapt and this can lead to overt liver injury (Watkins, 2005). For e.g. mild elevations in plasma ALT levels were observed in ~15% of patients treated with isoniazid, however less than 1% developed symptomatic hepatitis with continued treatment (Black *et al.*, 1975). Although the underlying mechanisms remain to be fully elucidated, environmental stresses or genetic disposition can affect an individual's susceptibility to drug toxicity. Animal models to study this hypothesis are also rare.

1.8.7. Multiple determinant hypothesis

This hypothesis proposes that liver injury precipitates as a collective stimulation of multiple discrete factors with the probability of occurrence of liver injury is dependent the probability of each event (Li, 2002). This hypothesis holds true only in an event when all these discrete variables occur in a predetermined fashion. Unlike the other hypotheses, the determining factors in causing liver injury can be physicochemical properties of the drug, exposure, environmental stress and genetic factors (Shaw *et al.*, 2010).

1.8.8. The inflammatory stress hypothesis

This hypothesis will be discussed in much detail highlighting the roles of different inflammatory mediators, immune cells and various cell signaling components. This hypothesis states that an acute underlying inflammation can render the individual susceptible to drug-induced hepatotoxicity even at sub-therapeutic dosage (Roth *et al.*, 2003). Although drug-induced hepatotoxicity occurs at high doses of drugs out of the therapeutic window, inflammation could lower this therapeutic window eventually leading to increased sensitivity of the liver to cause hepatotoxicity (Roth and Ganey, 2010). It is difficult to indentify IDILI mediated by inflammation, as inflammation occurs as daily-life event among all the individuals. We will discuss various mechanisms of IDILI induced by inflammation or other pathophysiological conditions.

Inflammation associated conditions can decrease the threshold for maximum tolerated dose such that it drops below the mean plasma concentration during drug therapy and this leads to the occurrence of idiosyncratic immune drug responses in humans. Fig. 1.3 illustrates this intriguing phenomenon.

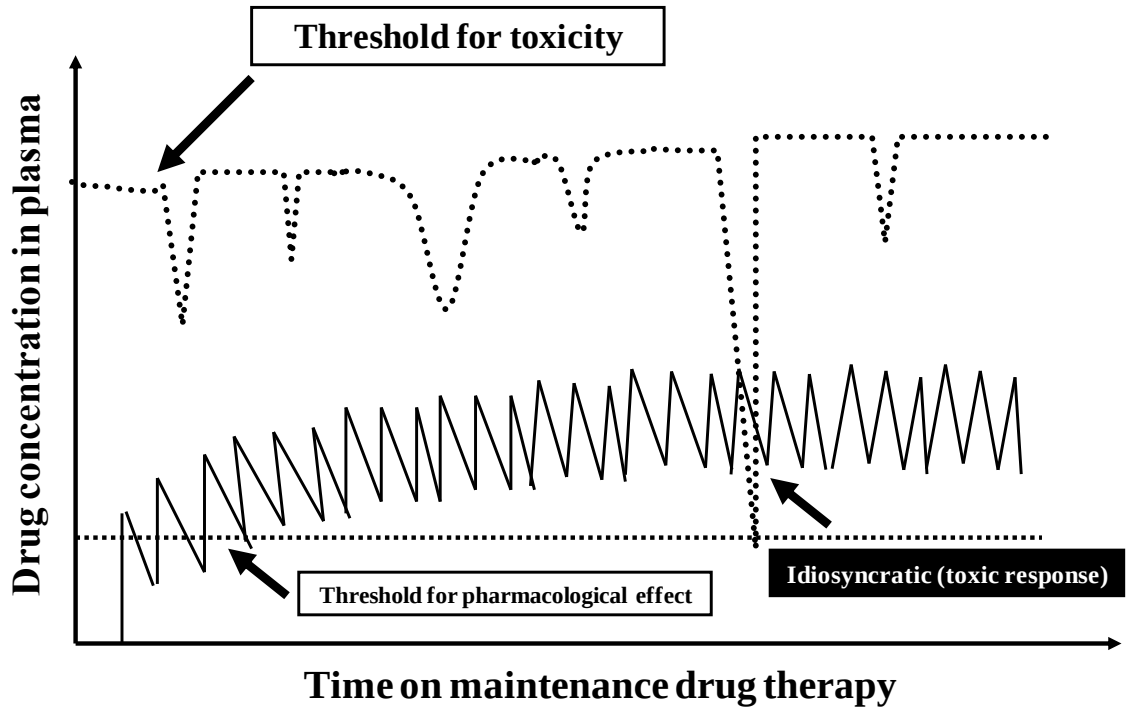

Figure 1.3 A schematic explaining idiosyncratic drug reactions in humans (adapted from (Deng *et al.*, 2009))

1.8.8.1. Role of TLR signaling and cytokines

The TLRs play an important role in recognizing microbial components such as of bacterial, viral or fungal origin and further mediating the inflammatory response in the liver by activation of downstream cell signaling molecules such as NF-κB or JNK which are known to regulate the gene expression of several pro- and anti-apoptotic genes involved in cell growth and differentiation. Out of the 13 TLRs identified in mammals, the TLR4 and TLR2 are very widely studied due to their recognition by gram-negative and gram-positive bacteria. A recent study showed that APAP-induced hepatotoxicity

was potentiated in alcohol-pretreated endotoxin-responsive C3H/HeN mice, with increases in liver damage, including severe steatosis and elevated plasma levels of TNF-α (Yohe *et al.*, 2006). Similarly, APAP-induced hepatotoxicity was shown as a result of activated TLR9 by the free DNA released from apoptotic hepatocytes (Imaeda *et al.*, 2009). This was associated with triggering of signaling cascade that increases transcription of the genes encoding pro-IL-1β and pro-IL-18 in sinusoidal endothelial cells. Others showed that hepatotoxic interaction between trovafloxacin and LPS (TLR4 ligand) or LTA (TLR2 ligand) also induced liver injury (Shaw *et al.*, 2009d). However, levofloxacin, a fluoroquinolone that is not associated with idiosyncratic hepatotoxicity in humans, did not demonstrate any synergistic effect with LPS in causing liver injury (Shaw *et al.*, 2007). We have also previously shown a modest though significant increase in hepatotoxicity of APAP or CPZ in *in vitro* mouse hepatocyte model in presence of the TLR4 or TLR2 ligands (Gandhi *et al.*, 2010). Although, TLRs are activated in various pathophysiological and inflammatory conditions, studies assessing their roles in DILI in conditions such as RA, CNS-related disorders or steatohepatitis are still lacking.

The identification of the first signaling pathway to modulate APAP-induced liver injury was the the JNK pathway. JNK exists in 3 distinct isoforms, JNK1, 2 and 3, of which JNK1 and JNK2 have been associated with DILI in different animal models. JNK plays an important role in responding to environmental stresses, and growth factors, as well as to cytokines, however sustained activation of JNK is believed to promote cell death (Singh and Czaja, 2007). Studies reported reduced APAP-induced liver injury in

mice pretreated with a JNK inhibitor or in $JNK^{-/-}$ mice without affecting APAP metabolism (i.e., GSH depletion and covalent binding) (Gunawan *et al.*, 2006; Hanawa *et al.*, 2008). A complex JNK-mitochondria signaling loop involving various pathways have been shown to participate in modulating the effects of activated JNK-induced hepatocyte death following APAP (Han *et al.*, 2010). However, as JNK1 and JNK2 are both expressed in the liver, studies have observed contrasting evidences on the contribution of individual JNK isoforms in DILI with maximum protection observed when both the isoforms are knocked out. For e.g. neither JNK1 nor JNK2 offered protection against APAP-induced liver injury when APAP was dissolved in PBS (Hanawa *et al.*, 2008), however JNK2 was shown to confer a major hepato-protection when APAP was dissolved in DMSO (which is known to down-regulate CYP2E1) (Gunawan *et al.*, 2006). Nonetheless, maximum protection was again observed when both JNK1 and JNK2 were simultaneously knocked down in mice irrespective of vehicle used for dissolving APAP.

In a very recent study, increased serum ALT levels, inflammatory infiltration, and central necrosis were observed in the $JNK2^{-/-}$ and *wild type* mice treated with pyrazole plus TNF-α, but not in the $JNK1^{-/-}$ mice (Wang *et al.*, 2011). The authors also observed a significant increase of malondialdehyde, 4-hydroxynonenal adducts, 3-nitrotyrosine, and iNOS in the $JNK2^{-/-}$ and *wild type* mice, compared to the $JNK1^{-/-}$ mice, upon pyrazole plus TNF-α treatment, or compared to mice treated with either pyrazole alone or TNF-α alone. These findings doubt the potential involvement of JNK1 activation related to alcoholic liver injury. These inconsistencies in the effect of activation of the JNK

pathway on apoptosis can be attributed to several factors such as the cell type, the nature of the death stimulus, the duration of its activation and probably, most importantly, the activity of other signaling pathways (Davis, 2000; Lin, 2003). We also previously showed that JNK played a significant role in regulating hepatotoxicities of APAP and CPZ in TNF-α treated primary mouse hepatocytes (Gandhi *et al.*, 2010).

As already discussed, various nuclear receptors are known to regulate drug metabolism and the down-stream cell signaling pathways involved in cell cycle differentiation and apoptosis. Here we will discuss their roles in mediating DILI. A recent study demonstrated the hepato-protective role of LXR in attenuating APAP-induced liver injury in mice (Saini *et al.*, 2011). The authors reported that activation of LXR in transgenic (Tg) mice or by an LXR agonist conferred resistance to the hepatotoxicity of APAP, whereas the effect of LXR agonist on APAP toxicity was disappeared in LXR-deficient mice. Furthermore, detailed analysis suggested that the increased APAP resistance in LXR Tg mice was associated with increased APAP clearance and increased APAP sulfation (resulting from the induction of antitoxic phase II conjugating enzymes, such as Gst and Sult2a1), and decreased formation of toxic APAP metabolites (resulting from suppression of protoxic Cyp3a11 and Cyp2e1 enzymes). On the other hand, another study determined the effects of human PXR activation and CYP3A4 induction on APAP-induced hepatotoxicity using rifampicin as a PXR agonist (Cheng *et al.*, 2009a). Further analysis demonstrated that, hPXR activation and CYP3A4 induction enhanced APAP-induced hepatotoxicity as revealed by significant increases in serum ALT and AST

activities, and hepatic necrosis after co-administration of rifampicin and APAP, compared with APAP treatment alone (Cheng *et al.*, 2009a). On the contrary, hPXR mice, *wild type* mice, and Pxr-null mice exhibited significantly lower ALT/AST levels compared with TgCYP3A4/hPXR mice after APAP administration. The authors concluded that the toxicity was coincident with depletion of hepatic glutathione and increased production of hydrogen peroxide, suggesting increased oxidative stress upon hPXR activation. Thus, drawing the data from the above two studies, it can be concluded that the suppression of Cyp3a11 may be accounted for by the inhibitory effect of LXR on the PXR-responsive transactivation of Cyp3a11 and the protective effect of LXR on APAP toxicity is opposite to the sensitizing effect of PXR.

However, PXR induction does not always to aggravated hepatotoxicity as increased protection of $PXR^{+/+}$ mice against cholic acid-induced hepatotoxicity by PCN (PXR activator) was associated with the induction of MRP3 and CYP3A11 expression which support the fact that changes in MRP3 can lead to cholestatic liver injury (Teng and Piquette-Miller, 2007). Recently, ligand activation of PPARβ/δ in mice led to significantly reduced serum ALT and hepatic TNF-α mRNA in CCl4-treated *wild-type* mice compared to PPARβ/δ-null mice (Shan *et al.*, 2008). The authors concluded that their findings demonstrate that ligand activation of PPARβ/δ protects against chemically induced hepatotoxicity by down-regulating expression of pro-inflammatory genes such as TNF-alpha, S100A6, monocyte chemoattractant protein-1 (MCP1), and TWEAKr in *wild-type* mice, compared to PPARbeta/delta-null mice. On the other hand,

activation of CAR was shown to cause CCl4-induced hepatotoxicity while CAR inhibition resulted in partial protection against CCl4-induced hepatotoxicity. Also, there were no differences in the expression of CYP2E1, the main metabolizing enzyme for CCl4, between $CAR^{+/+}$ and $CAR^{-/-}$ mice.

Various pro-inflammatory cytokines have been associated with IDILI. Hepatotoxicity of dicloxacilin was mediated by IL-4 in mice as evidenced by increased plasma ALT and IL-4 levels, and total bilirubin levels (Higuchi *et al.*, 2011). The authors reported that hepatotoxicity of dicloxacilin was attenuated upon neutralization of IL-4 and was induced upon recombinant mouse IL-4 administration. However, the effects of IL-4 on IDILI remain quite intriguing as IL-4 was shown to suppress regulatory responses to CYP2E1 autoantigens but induce pro-inflammatory responses to drug haptens (Njoku, 2010). Similarly, there are numerous studies with TNF-α-mediated drug-induced hepatotoxicity due to its pro-inflammatory and apoptotic properties. Recent studies showed that trovafloxacin-induced liver injury in LPS-induced inflammation was as a result of prolonged plasma TNF-α level by trovafloxacin pretreatment (Shaw *et al.*, 2007). In addition, this study was later confirmed by inhibiting TNF-α which led to significantly attenuated trovafloxacin-induced increases in plasma concentrations of several pro-inflammatory cytokines and thus reduced liver injury (Shaw *et al.*, 2009e). The same group of researchers also showed that trovafloxacin-induced liver injury was not due to increased production (or increased mRNA) of TNF-α gene, but as a result of sustained occurrence and reduced clearance of TNF-α which led to enhanced effects of

trovafloxacin on sensitizing the cells to TNF-mediated cell death (Shaw *et al.*, 2009a). Similar effects of TNF-α were shown to be associated with drug-induced hepatotoxicities of several drugs including diclofenac, sulindac, aflatoxin B1, amiodarone, ranitidine, cadmium, APAP, etc (Barton *et al.*, 2001; Gardner *et al.*, 2002; Kayama *et al.*, 1995; Lu *et al.*, 2012; Tukov *et al.*, 2007; Zou *et al.*, 2009a).

However, the pro-inflammatory effects of TNF-α on mediating DILI does not hold true for all the drugs (He and Sharma, 2005). Notably, the contribution of the soluble TNF receptors, TNFR1 (p55) and TNFR2 (p75), in mediating the hepatotoxic effects of TNF-α in DILI remain controversial. For e.g. it has been shown that TNFR1 majorly contributes in regulating APAP-induced liver injury as evidenced by significantly attenuated plasma ALT level, reduced mortality, reduced centrilobular hepatic necrosis and leukocyte infiltration, reduced IFN-γ, and inducible nitric oxide synthase (iNOS), and reduction in expression of cytotoxic proteins in TNFR1/p55$^{-/-}$ mice compared to *wild type* mice (Ishida *et al.*, 2004). On the contrary, mice lacking an active TNFR1/p55 were prone to severe APAP-induced liver injury due to delayed cytokine signaling which may account for reduced hepatocyte proliferation as well as rapid and prolonged induction of NOS in the liver (Chiu *et al.*, 2003; Gardner *et al.*, 2003). Similar results have been observed with other compounds such as cadmium and fumonisin B1 (Harstad and Klaassen, 2002; Sharma *et al.*, 2001; Sharma *et al.*, 2002). Other cytokines such as IL-1β, IL-1α, IL-6, IL-10, IL-13 and IFN-γ also play important roles in mediating DILI in animal species with IL-6 and IL-13 playing hepatoprotective roles (Blazka *et al.*,

1996; Blazka *et al.*, 1995; Gardner *et al.*, 2003; Gardner *et al.*, 2002; Masubuchi *et al.*, 2003; Yee *et al.*, 2007). Trovafloxacin induced liver injury was also shown to be attenuated in IFN-$\gamma^{-/-}$ and IL-$18^{-/-}$ mice previously exposed to LPS (Shaw *et al.*, 2009b).

1.8.8.2. Cell-types involved in regulation of drug-induced hepatotoxicity

Various immune cells also mediate hepatotoxic effects of drugs by activating the downstream signaling components during the course of inflammation. In an in vitro model, hepatocytes were incubated with activated polymorpho nuclear neutrophils (PMNs) at various concentrations (0, 25 or 50%) with or without ranitidine or famotidine for 16 h (Luyendyk *et al.*, 2003). The results demonstrated a significant increase in ALT level in a concentration dependent manner with PMNs implying hepatocellular damage. Famotidine showed modest, although significant, hepatotoxic responses only at the highest concentration used. Dendritic cells are known to regulate inflammatory responses in liver diseases.

A recent study showed that APAP-induced hepatotoxicity was exacerbated in dendrictic cell depleted mice along with centrilobular necrosis which was further shown to be associated with natural killer (NK) cell activation and induced neutrophil apoptosis, respectively (Connolly *et al.*, 2011). Similarly, neutrophils were shown to play a major role in protecting against LPS-induced liver injury in mice (Hewett *et al.*, 1992). Thus, the DILI of from monocrotaline and trovafloxacin were shown to be mediated by hepatic accumulation of neutrophils upon LPS-coexposure in mice and rats (Shaw *et al.*, 2009a; Waring *et al.*, 2006; Yee *et al.*, 2003b).

In mice, out of the mature T cells, NKT cells are most frequent in the liver (30–50%) and bone marrow (20–30%), while they represent a smaller proportion of T cells in the spleen (3%) and lymph nodes (0.3%) (Godfrey *et al.*, 2000). The mouse hepatic NKT cells were shown to inhibit hepatitis B viral replication as well as suppressing hepatocellular carcinoma (Kakimi *et al.*, 2000; Margalit *et al.*, 2005). Recent studies showed significant involvement of NK and NKT cells in mediating APAP-induced liver injury in mice. One study reported that reduced APAP-induced liver injury and increased survival in mice was dependent on reduction of NK and NKT cells (Liu *et al.*, 2004). The authors concluded that the secretion of IFN-γ by NK or NKT cells may induce inflammatory chemokines or enhance leukocyte recruitment which are known exacerbate liver injury. On the other hand, another study reported that APAP-induced liver injury mediated by NK cells was as a result of presence of DMSO used as a solvent vehicle which resulted in a significant increase in both the number and activation of hepatic NK or NKT cells (Masson *et al.*, 2008). Similarly, a very recent study reported that halothane-induced liver injury in mice was attenuated in NKT cells depleted $CD1d^{-/-}$ mice (Cheng *et al.*, 2010). The authors also showed that activation of NK cells by halothane led to recruitment of neutrophils to the liver which further worsen the injury (Cheng *et al.*, 2010; You *et al.*, 2006).

Kupffer cells (KC) are considered as the resident macrophages in the liver and play an important role in regulating the immune responses by release of pro-inflammatory cytokines and chemokines upon stimulation by hepatotoxins. Several

studies report the essential role of KCs in maintaining the normal physiology and homeostasis of the liver as well as participating in the acute and chronic responses of the liver to toxic compounds. Monocrotaline-induced liver injury in presence of LPS stimulation was greatly reduced in KC depleted mice as compared to their *wild type* counterparts (Yee *et al.*, 2000). In this study, not only the hepatocytes, but also sinusoidal endothelial cells were protected against the toxic effects of monocrotaline in gadolinium chloride (GdCl), which inhibits KC function, pretreated mice. KC-mediated hepatotoxicity of LPS-monocrotaline mouse model was shown to be due to release of plasma TNF-α level in and neutralization of TNF-α reversed this effect (Yee *et al.*, 2003a; Yee *et al.*, 2003b). Similarly, *in vitro* studies using primary rat and human HC-KC cocultures have shown the potential involvement of KCs in mediating the inflammatory responses leading to DILI (Edling *et al.*, 2009; Tukov *et al.*, 2006). On the contrary, others have shown the protective role of KCs in APAP-induced liver injury in mice (Holt *et al.*, 2010; Ju *et al.*, 2002). The authors reported reduced APAP-induced liver injury in mouse model of liposome-entrapped clodronate (an effective Kupffer cell-depleting agent) and attributed these results due to increased production of anti-inflammatory cytokines such as IL-6, IL-10 and IL-18 by activated KCs (Ju *et al.*, 2002). In another study, the aggravation of APAP-induced hepatic sinusoidal endothelial cell disturbance upon depletion of KCs correlated with increased hepatic vascular permeability and red blood cell accumulation (Holt *et al.*, 2010). Thus, contrasting evidences suggesting both pro-toxicant and hepatoprotective role of KCs in DILI can be likely attributed to the

heterogeneity and/or plasticity of macrophages and the difficulty in distinguishing and differentially studying subpopulations of macrophages in the liver (Holt *et al.*, 2008).

1.8.9. Role of transporters in drug-induced hepatotoxicity

Transporters are involved in handling of drugs are also known to cause drug-induced cholestasis. Drug-induced cholestasis can result from injury to cholangiocytes caused by the hepatobiliary excretion of a toxic metabolite or from the drug-mediated inhibition of either hepatobiliary bilirubin or the bile acid uptake and efflux systems (Pauli-Magnus and Meier, 2006). Major canalicular transporters such as ABC group of transporters including BSEP, MRP2 and MDR3 play pivotal roles in transporting various metabolites across the biliary tract. Genetic polymorphisms in genes encoding the ABC family of transporters can lead to reduced transporter expression and activity. Twenty-three patients with drug-induced cholestasis and 13 patients with drug-induced hepatocellular injury were linked to reduced BSEP expression (Lang *et al.*, 2007). Another study, demonstrated that both genetic and clinical factors could lead to 20–100-fold variation (in large populations) in the expression levels of the hepatic OCT1 and OCT3 transporters (Nies *et al.*, 2009) further leading variation in the pharmacodynamic effects of drugs that are substrates for these transporters and possibly to cholestatic DILI.

CHAPTER 2

Hypotheses and Specific Aims

2.1. Hypotheses

The broad picture of this dissertation is that drug metabolism and drug-induced hepatotoxicity is altered in inflammation induced by LPS or LTA. Although, previous studies have shown that inflammatory conditions lead to a reduction in gene expression and functional activity of DMEs, detailed mechanistic studies in both LPS- and LTA-induced inflammation models are lacking. We hypothesize that LPS- and LTA-induced down-regulation of Cyp3a11 (analog of human CYP3A4) will alter the PK and PD of the CYP3A specific substrate, midazolam (MDZ). Although TIRAP is known to differentially regulate Cyp3a11 gene expression in LPS- and LTA-treated mice, the role of TIRAP in regulating MDZ metabolism remains unexplored. So we also hypothesize that, TIRAP plays a crucial role in regulating Cyp3a11 protein expression and activity in LPS- or LTA-induced inflammation in mice.

Drug-induced hepatotoxicity is exacerbated in bacterial infections and inflammation. And sustained activation of the kinase, JNK, is associated with cell death. We hypothesize that APAP- or CPZ-induced hepatotoxicities are triggered by sustained activation of JNK in presence of LPS- or LTA-induced inflammation in mice. Also, the role of TIRAP and individual pro-inflammatory cytokines will also be evaluated in mediating the hepatotoxic responses of APAP or CPZ.

2.2. SPECIFIC AIM 1

1A: We will test the hypothesis that reduction of hepatic Cyp3a11 in LPS- or LTA-induced inflammation will significantly alter PK of MDZ further leading to increased pharmacological activity of MDZ in mice.

1B: We will test the hypothesis that TIRAP is involved in regulating decreased Cyp3a11 protein expression and activity only in LTA-induced inflammation and not in LPS-induced inflammation.

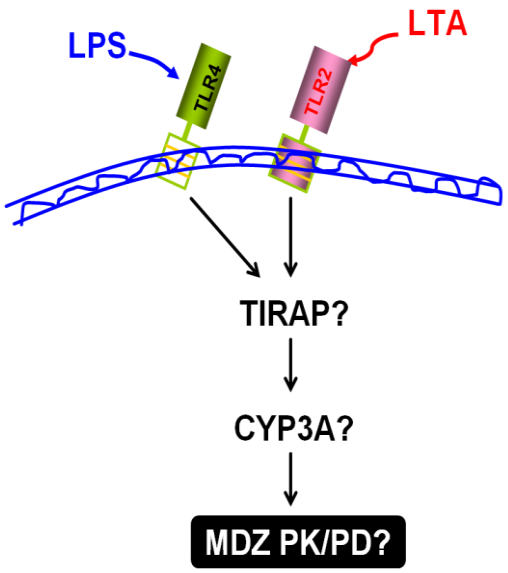

Figure 2.1 Regulation of drug metabolism in inflammation

2.3. SPECIFIC AIM 2

2A: We will test the hypothesis that hepatotoxicity of CPZ in augmented in LPS- or LTA-induced inflammation is dependent on TIRAP and most likely involves increased serum TNF-α and sustained activation of JNK.

2B: We will test the hypothesis that hepatotoxicity of APAP or CPZ is augmented only in presence of TNF-α which further mediates its apoptotic actions by sustained activation of JNK in primary mouse hepatocytes.

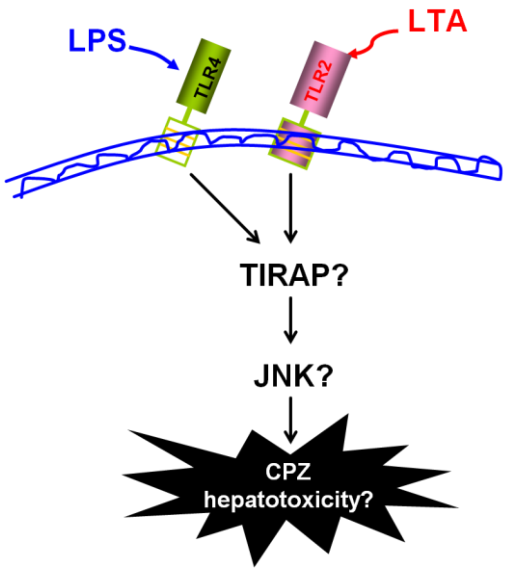

Figure 2.2 Regulation of drug-induced hepatotoxicity in inflammation

CHAPTER 3

Experimental methods employed throughout the dissertation

3.1. MDZ metabolism, PK and PD experiments

3.1.1. Preparation of MDZ and its metabolite standards for calibration curve

Five mg of MDZ (BD Biosciences, San Diego, CA, Cat # 451028) was dissolved in 50:50 saline:methanol mixture to get a final concentration of 0.5 mg/ml. This solution was aliquoted in different Eppendorf tubes (500 µL per tube) and stored at -80 ^{0}C covered and protected from light. Similarly, 1'-OHMDZ (Sigma-Aldrich, St. Louis MO, Cat # UC430) was dissolved in 100% methanol to get a final concentration of 1 mg/ml and aliquoted and stored at -80 ^{0}C. The secondary metabolite, 1'-OHMDZ-gluc (a kind donation from Dr. Gerard Fabre's Lab, Sanofi-Aventis, France) was dissolved in 100% dd water to get a final concentration of 2 mg/ml, aliquoted (20 µL per tube) and stored at 4 ^{0}C. The internal standard, phenacetin (Sigma-Aldrich, St. Louis, MO, Cat # 77440), was prepared by adding 10 mg of standard powder in 10 ml of 100% methanol to get a stock solution of 1 mg/ml and stored at -80 ^{0}C for further use.

3.1.2. Preparation of LPS and LTA

Lipopolysaccharide (*E. coli*, Cat # tlrl-pslta) and lipoteichoic acid (*S. aureus*, Cat # tlrl-pelps) were purchased from InvivoGen (San Diego, CA) and dissolved in pyrogen free sterile water to get a stock solution with a concentration of 5 mg/mL of LPS and 5 mg/mL of LTA and stored at -20 ^{0}C.

3.1.3. Treatment of animals

The animals used in this study followed critical care of the animals and experimental procedures complied strictly with the Institutional Animal Care and Use

Committee guidelines of the University of Houston. Adult, male C57BL/6 mice, aged 5-6 weeks with approximate weight of 20-22 g were purchased from The Harlan Laboratory (Houston, Texas, USA). The $TIRAP^{+/+}$ and $TIRAP^{-/-}$ mice (8–10 weeks weighing 25-30 g) on a C57BL/6×SV129; F3 genetic background were a kind donation from Dr. Ruslan Medzhitov (Yale University School of Medicine, New Haven, CT, USA). All the animals were maintained in a temperature and humidity controlled environment and 12 h light/dark cycle with free access to water and rodent chow *ad libitum*.

For injections with LPS, 50 µL of the 5 mg/ml stock was freshly reconstituted with 1200 µL of sterile dd water. For injections with LTA, 150 µL of 5 mg/ml stock was freshly reconstituted with 1100 µL of sterile dd water. A 10 µL of each reconstituted solution was injected by the intra peritoneal (i.p.) route for every 1 g of mouse weight. For *in vitro* studies, the animals were injected with saline, 2 mg/kg of LPS or 6 mg/kg of LTA. The animals were returned to their cages and sacrificed after 16 h to prepare liver microsomes as described in the subsequent sections.

For PK studies, C57BL/6 mice pre-treated with saline, LPS or LTA for 16 h were treated with MDZ (5 mg/kg, i.p.) and returned to their cages as one animal per cage. Midazolam hydrochloride solution for injections was purchased from Baxter Healthcare Corporation (Deerfield, IL, USA, NDC # 0409-2308-02) at a concentration of 5 mg/ml stock solution. For injections at a dose of 5 mg/kg, MDZ-HCl was diluted 5X to get a concentration of 1 mg/ml. Then 100 µL of 1 mg/ml of MDZ-HCl solution was injected i.p. for every 20 g of mouse weight.

For PD studies, C57BL/6 mice pre-treated with saline, LPS or LTA for 16 h were treated with MDZ (80 mg/kg, i.p.). For 80 mg/kg dose, MDZ-HCl solution was directly injected by the i.p. route at volume of 320 µL for every 20 g of mouse weight. The mice were returned to their cages as one animal per cage.

3.1.4. Perfusion of mouse liver followed by harvesting

The microsomal fractions are widely used to study drug metabolizing enzyme activity and drug-drug interaction studies. But in order to obtain the purest form of microsomal fractions, the livers need to be perfused to remove any remaining blood which may interfere in the assays. For preparation of liver microsomes, the livers were perfused with homogenization buffers A and B. Perfusion buffer A comprised of 8 mM KH_2PO_4, 5.6 mM Na_2HPO_4, 1.5 mM KCl and 96 mM NaCl. Perfusion buffer B comprised of 8 mM KH_2PO_4, 5.6 mM Na_2HPO_4, and 1.5 mM EDTA dehydrate. Both the buffers were stored at 4 ^{0}C and prepared the day before the experiments. On the day of the experiments, 10 µL of 2 mM dithioerythritol (DTT, Sigma-Aldrich, Cat # D9779) and 10 µL of PMSF solution (Sigma-Aldrich, Cat # P7626) 1000X prepared by adding 24 mg in 0.6 ml of methanol) were added to 100 ml of perfusion buffer. Perfusion buffer A contained only PMSF. An incision was cut in the abdomen of the mice and the livers were perfused with buffer A for 2-3 min followed by buffer B for an additional 2-3 min until there was no blood visible in the liver. The livers were then excised and put in a beaker containing cold sterile saline solution. The livers were placed on ice all the time after harvesting.

3.1.5. Preparation of liver microsomes

The microsomes were prepared to study CYP3A-mediated reaction to study the metabolism of MDZ in inflammation. The perfused livers were then minced on a glass plate placed on ice with a sharp and clean blade to make the liver ready for homogenization. The minced livers were then transferred into 10 ml cylindrical homogenization glass tubes (Wheaton, Millville, NJ, Cat # 358007) placed on ice. The livers were then homogenized using a motorized homogenization gun fitted with a teflon pestle in ice-cold homogenization buffer comprised of 10 mM potassium phosphate solution (pH 7.4), 250 mM sucrose, 1 mM EDTA at a ratio of 1:3 i.e. 3 ml of homogenization buffer for every 1 g of liver. The mixture was then transferred into clean polycarbonate centrifuge tubes (Beckman Coulter, Palo Alto, CA, Cat # 357000) and centrifuged at 15,400 rpm for 15 min at 4°C. The pellet which contained cell debris and unwanted waste was discarded and the supernatant was collected into clean polycarbonate ultracentrifuge tubes (Beckman Coulter, Palo Alto, CA, Cat # 355618) and centrifuged again at 35,000 rpm for 60 min at 4°C. The fat layer on the top was carefully aspirated using rubber droppers to yield the microsomal pellets. The microsomal pellet was then washed twice with 500 µL of 250 mM sucrose solution. The pellet was then resuspended in approximately 500-700 µL of 250 mM sucrose and mixed with a teflon pestle. The mixture was then pipette with a 1000 µL pipette into a clean 2 ml cylindrical homogenization glass tube (Wheaton, Cat # 358003) which was placed on ice. The mixture was manually homogenized by grinding the microsomal pellet with 10-12

strokes of the teflon pestle. The microsomes were then aliquoted (~50 µL per tube) and stored at -80 ^{0}C. Protein concentration was determined in one tube from each mouse using a BCA protein assay kit on the same day.

3.1.6. BCA Assay for protein quantification

To perform this experiment, microsomes placed on ice all the time. Three µL of sample was added to 57 µL or 117 µL of dd water to get 20 or 40 folds dilution, respectively. The Pierce® BCA protein assay kit was purchased from Thermo Scientific, Rockford, IL, Cat # 23225). The standards were prepared from the stock of 2 mg/ml to get final concentrations of 0.1, 0.2, 0.4, 0.6, 0.8 and 1 mg/ml respectively. Water served as a blank or 0 mg/ml concentration. All the standards prepared were at least 30 µL as 20 µL was to be used in the calibration curve. Then 10 µL of microsome samples or standards were added in duplicates in a clear bottom 96 well plate. The working reagent was prepared by mixing 50 parts of solution A with 1 part of solution B as per the manufacturer's recommendation. Then 200 µL of working reagent was added to each well containing the samples or standards. The plate was then covered with aluminum foil and incubated for 30-35 min at 35 – 37^{o}C in an incubator. Once this time elapsed, the plate was cooled to room temperature for 2-3 min and the absorbance was read on a Biotek plate reader (Biotek, Winooski, VT, USA). The plate reader used to read the absorbance was set to quick read, single settling, 96 well plate, and 570 nm wavelength.

3.1.7. Cyp3a11 activity assays

Typical Phase I reactions were carried out in liver microsomes using MDZ as a CYP3A specific probe substrate. The Glucose-6-phosphate (Cat # G6378-500UN), $MgCl_2$ (Cat # 208337), glucose-6-phosphate dehydrogenase (Cat # G6378-2KU) and $NADP^+$ (Cat # N0505) were purchased from Sigma-Aldrich, St. Louis, MO). For determining Cyp3a11 activity, 0.05 mg/ml of microsomal protein was incubated with various concentrations of MDZ (0-16 µM). The reaction mixture consisted of 50 mM KPi solution (pH 7.4), 25 µL of regenerating system solution (final concentrations as 3.3 mM of Glucose-6-phosphate, 3.3 mM of $MgCl_2$ and 1.3 mM of $NADP^+$), 10 µL of MDZ stock solutions (25 fold concentrated) and 0.05 mg/ml of final microsomal protein concentration. The reactions were carried out in duplicate and the reaction mixtures were placed in an ice water bath all the time. The reactions were initiated by adding 25 µL of 100 units/ml of glucose-6-phosphate dehydrogenase solution to get a final concentration of 1 unit/ml in the reaction mixture. The volume of KPi solution was adjusted according to the microsome concentration for which the volume was fixed at 25 µL. The tubes were tightly capped and reversed upside-down to mix the solution properly. The tubes were then incubated for 5 min at 37 ^{0}C in a shaking water bath (40 horizontal oscillations per min). After 5 min, the reactions were stopped by the adding 100 µL of 100% acetonitrile containing phenacetin (IS, 1 µg/ml).

3.1.8. Immunoblotting for Cyp3a11 protein determination

Immunoblot, commonly known as western blot, analysis was used to determine the protein expression of Cyp3a11 in liver microsomes. Beta actin was used as a loading control or as a housekeeping gene for all the samples. After determination of protein concentration by BCA assay, the samples were diluted with a homogenization buffer comprising each of 50 mM Tris HCl, 0.5 M NaCl, 2 mM EDTA, 2 mM EGTA, 1% Triton X-100 and 0.25% deoxycholate, 1 mM sodium fluoride (NaF), 1 mM sodium vanadate (Na_3VO_4), 2 mM of DTT and 100 µL of protease inhibitor cocktail solution per 10 ml of homogenization buffer. The samples were diluted so as to load 10 µg of protein per well in the gel. After dilution of the microsomal samples with the buffer, the tubes were tightly capped and gently vortexed. Then an equal amount of 1X loading dye was added to all the wells. 1X loading dye was prepared by mixing 950 µL of Laemmeli sample buffer with 50 µL of 2-mercaptoethanol. The protein samples were then briefly vortexed and spun down and then heated at 90-95 ^{0}C in a heating block to break the linear disulfide bonds. By this time, the gels, prepared the previous day, were loaded into the chambers to check any leakage of the buffer. After 10 min, the samples were cooled on ice for 10 more min and then spun down for 10 seconds again. The first well of the gel was loaded with 5 µL of protein Fisher-EZ run Pre stained *Rec* protein ladder (Fisher Scientific, Cat # BP 3603-500) which consists of a mixture of different proteins with varying molecular weights. Then 10 µL of microsome samples were loaded into the respective wells and the gel was run at 200 V electrophoretically on a electrophoresis

chamber (Bio-Rad, Hercules, CA, USA) for about 35-40 min. After the run, the gels were transferred onto the nitrocellulose membranes as a sandwich consisting of this sequence: 1 wet sponge, 1 sheet of 3 mm wet paper, 1 pre-wet nitrocellulose membrane, gel, 1 sheet of 3 mm wet paper and then the wet sponge again. Care was taken to avoid any air bubbles in this step. The gel was set up for transfer in the transferring buffer with continuous stirring at 250 mAmp for 90 min at 4 ^{0}C. After this the membranes were removed and blocked in a 5% non-fat dry milk (NFDM) solution for 1 h at room temperature on a horizontal shaker to avoid any non-specific binding. Then the membranes were washed 2 times in Tris-buffered saline containing 0.1% Tween-20 (TBST) for 5 min each. The membranes were then incubated overnight at 4 ^{0}C with the anti-mouse Cyp3a11 antibody (a kind gift from Dr. Robert J. Edwards, Department of Medicine, Imperial College, London, UK) in 50 ml conical tubes consisting of 5 ml of 5% bovine serum albumin (BSA, Sigma Aldrich, St. Louis, MO, Cat # A3059) solution prepared in TBST. The final dilution of the antibody was determined to be 1:4000.

Next day, the membranes were washed thrice with TBST followed by incubation with the goat anti-rabbit IgG-alkaline phosphatase secondary antibody (Santa Cruz Biotechnology Inc., Santa Cruz, CA, Cat # sc-2007) at a dilution of 1:2000 in 5% NFDM for 1 h at room temperature with continuous shaking. Then the membranes were washed for the final 3 times with TBST and incubated with an electro chemiluminescence reagent (~ 1 ml of reagent was added per membrane) for 10 min covered in dark (I use a box cover to protect my membranes from exposure to light). The bands were then analyzed

on a FluorChem FC2 Imaging System with chemiluminescence filter initially for 2 min. Depending on the intensity of the bands, exposure time was determined accordingly.

3.1.9. Collection of blood and isolation of plasma

Approximately 10-15 µL of blood samples were collected at predetermined time points (0, 5, 15, 30, 60, 120, 240, 360 and 480 min) from the tail vein in heparinized Eppendorf tubes. The heparinized tubes were prepared on the day before the experiment by coating the tubes with cotton gauze immersed in a solution of 1000 units heparin prepared in dd water. Plasma was immediately isolated from the blood by centrifuging the tubes at 9000 rpm for 3 min at room temperature.

3.1.10. Drug extraction from plasma samples

Various organic solvents can be used to extract drugs and its metabolites from the plasma. We isolated MDZ and its metabolites in 5 µL of plasma which was diluted 10 folds using blank mouse plasma with sodium heparin purchased from Equitech-Bio, Inc., Kerrville, TX, Cat # SMPH-0100) Therefore, 5 µL of plasma sample + 40 µL of blank plasma + 5 µL of 1 µg/mL of IS was added and tubes were briefly vortexed. Standard samples were prepared by serial dilutions of 45 µL of highest standard (1000 ng/ml of MDZ, 1'-OHMDZ or 1'-OHMDZ-gluc) with 45 µL of blank plasma. Then 5 µL of 1 µg/ml of IS was added and the tubes were briefly vortexed. After precipitation of protein with 450 µL acetonitrile (ACN), the tubes were briefly vortexed and centrifuged. Liquid-liquid extraction was carried by adding 450 µL of methyl t-butyl ether (MTBE) followed by vortexing for at least 30 seconds and centrifuging at 13,200 rpm for 10 min at 4 ^{0}C.

The supernatant organic solvent (~810 µL) was transferred to clean Eppendorf tubes and evaporated under a gentle stream of air at room temperature and the dried extracts were reconstituted in 30% ACN.

3.1.11. PD study – monitoring sleep time

Sleep time was used as a specific marker of pharmacological effect of MDZ. In this study, mice injected with the drug (as described in section 3.1.3) went to sleep after ~10 min. To record the exact time, the mice were turned on their back and the sleep time was recorded as the time between when the mice turned on their back and returned to their original positions.

3.1.12. Liquid chromatography tandem mass spectrometry (LC-MS/MS) analysis of MDZ and its metabolites

For quantification of analytes in plasma samples, LC-MS/MS method was utilized. An API 3200 Qtrap® triple quadrupole mass spectrometer (Applied Biosystems/MDS SCIEX, Foster City, CA, USA) equipped with a TurboIonspray™ source, operated in a positive ion mode, was used to quantitatively measure MDZ, 1'-OHMDZ, 1'-OHMDZ-gluc and phenacetin in plasma. The following compound dependent parameters were optimized: declustering potential (DP), entrance potential (EP), cell exit potential (CXP) and the collision energy (CE). The following instrument dependent parameters were optimized for the compounds: ion spray voltage, ion source temperature, nebulizer gas (gas 1), turbo gas (gas 2) and the curtain gas. The flow rate of the sample during Mass method optimization was set between 7 - 20 µL/min. The method

was analyzed for the MRM transitions with monitoring of the ion pair transitions of the compounds (MS2 peaks). The following transitions were selected: m/z 326.1→ m/z 291.1 for MDZ, 342.1 → 324.1 for 1′-OHMDZ, 518.1 → 324.1 for 1′-OHMDZ-gluc and 180.0 → 110.0 for phenacetin. The selection of the fragment ions depended on the highest intensity of the fragment. All the data collected was analyzed with Analyst 1.4.2 software (AB Sciex, USA).

The UPLC conditions for the compounds were: system, Waters Acquity™ (Milford, MA, USA) with DAD detector; column, Acquity UPLC BEH C18 column (50×2.1mm I.D., 1.7μm, Waters); mobile phase A, 0.1% formic acid; mobile phase B, 100%, acetonitrile; gradient, 0-0.5 min, 10% B, 0.5-1 min, 25% B, 1-2 min, 40% B, 2-2.5 min, held constant at 40% B, 2.5-3 min, 10% B, respectively. Flow rate was 0.4 ml/min, column temperature, 45 degree; injection volume, 10 μL. The chromatographs of MDZ and its metabolites are shown in Fig. 3.2.

3.1.13. Pharmacokinetic analysis

The PK data was analyzed using the WinNonlin 3.3 PK modeling software from Pharsight Corporation (Mountain View, California). The data was fitted to a non-compartmental model for pharmacokinetic analysis of MDZ and its metabolites. Pharmacokinetic parameters, including maximum plasma concentration (Cmax), time to reach Cmax (Tmax), elimination rate constant (ke), half-life ($t_{1/2}$), rate at which drug is cleared from the body (CL), volume of distribution (Vd), mean residence time (MRT)

and plasma exposure or area under the curve (AUC) were directly derived from WinNonlin.

3.2. *In vivo* experiments with CPZ-induced hepatotoxicity in inflammation

3.2.1. Preparation of LPS and LTA

Same as described in section 3.1.2.

3.2.2. Preparation of drugs CPZ solution for animal injections

CPZ-HCl (Sigma-Aldrich, St. Louis, MO, Cat # C8138-5) was dissolved in sterile saline solution (0.9% NaCl). A fresh stock solution was prepared every time on the day of the experiment. The stock solution was made by dissolving 10 mg of CPZ-HCl poweder in 10 ml of sterile saline to yield a final concentration of 1 mg/ml which was used for injections in mice.

3.2.3. Treatment of animals

The C57BL/6 male mice, aging 5-6 weeks and weighing ~ 18-20 g were purchased from The Harlan Laboratories, Houston, TX. All the mice were housed in cages with free access to food and water for at least 1 week prior to the experiments. The mice when aged 6-7 weeks were used in the study. The breeding pair of $TIRAP^{+/+}$ and $TIRAP^{-/-}$ mice (8–10 weeks, weighing 25-30 g) on a C57BL/6×SV129; F3 genetic background was a kind donation from Dr. Ruslan Medzhitov (Yale University School of Medicine, New Haven, CT, USA). Saline, LPS or LTA were injected in the mice as described previously in section 3.1.3. CPZ injections were carried out by injecting 100 µL o 1 mg/ml of CPZ-HCl stock solution for every 20 g of mouse by the i.p. route.

3.2.4. Collection of blood and isolation of serum from whole blood

For collection of blood, a minimally invasive procedure was used. Mice were lightly anesthetized (putting the mice in a glass jar containing a cotton ball wetted with Isoflurane) followed by cervical dislocation. An incision was made by holding a small piece of skin near the abdominal region and cut upto to neck. The blood was collected using a 1000 µL pipette in 1.5 mL of Eppendorf tubes. The blood was allowed to sit at room temperature for ~ 1h and then centrifuged at 5000 rpm for 10 min at 4^0C. The supernatant was collected as the serum and stored at -80^0C for further analysis.

3.2.5. Tumor necrosis factor (TNF)-α assay

The pro-inflammatory cytokine, TNF-α is usually analyzed as a biomarker in inflammatory conditions. The TNF-α ELISA Max^{TM} Deluxe assay kit (Cat # 430904) was purchased from BioLegend, San Diego, CA and stored at 4 ^{0}C. To detect TNF-α in serum samples, for a full 96-well plate, 5X coating buffer was diluted to 1X with dd water. Then 60µL of Capture Antibody was diluted in 11.94 µL of 1X Coating buffer and 100 µL of this solution was added to the wells of a 96-well plate and the plate was sealed and incubated overnight (16 – 18 h) at 4^oC. To block non-specific binding and reduce the background, 200 µL of 1X assay diluent (prepared by diluting 5X assay diluent to 1X with PBS solution, pH 7.4) was added per well and the plate was sealed and incubated at room temperature for 1 h. One hundred microliters of 10-fold diluted serum or standard samples were added per well and incubated for 2 h at room temperature. The standards were prepared by reconstituting the lyophilized vial with 0.2 mL of 1X assay diluents and

setting it aside for 15 min to dissolve. A total of 8 standards were prepared ranging from 500-7.8 pg/ml. The 1X assay diluent served as a zero concentration. The plate was washed 4 times with 300 µL of wash buffer per well. The wash buffer consisted of PBS + 0.05% Tween-20 (pH 7.4). Approximately 1L of wash buffer was prepared for a full 96 well plate. The samples were then incubated with 100 µL of diluted Biotinylated detection antibody (prepared by adding 60 µL of antibody to 11.94 µL of 1X assay diluents) solution at room temperature for 1 h with shaking. After washing the plate for four times with the wash buffer, 100 µL of diluted Avidin-HRP (12 µL in 11.99 µL of 1X assay diluent) was added to each well; the plate was sealed and incubated at room temperature for 30 minutes with shaking. Thereafter, again washing the plate 4 times, 100 µL of freshly mixed 3,3', 5,5' tetramethylbenzidine (TMB) substrate solution (prepared by mixing 6 ml of TMB substrate solution A + 6 ml of TMB substrate solution B) was added and the plate was incubated in the dark (covered with aluminum foil) for 15 minutes (with shaking). Positive wells turned blue. To stop the reaction, 100 µL of Stop Solution was added to each well. The stop solution was prepared by adding 0.98 ml of concentrated H_2SO_4 in 10 ml of dd water to get a 2N H_2SO_4 solution. Positive wells changed colors from blue to yellow. The absorbance was read at 450 nm with a background at 570 nm within 30 min. The concentration of TNF-α in unknown samples was determined by using the calibration curve prepared using the TNF-α standards.

3.2.6. Preparation of whole cell extracts from liver tissues

To prepare whole cell extracts, ~0.1g of mouse liver tissue was homogenized in 1 mL of homogenization buffer. The homogenization buffer consisted of 50mM Tris HCl (pH 7.5), 0.5M NaCl, 2mM EDTA, 2mM EGTA, 1% Triton X-100, and 0.25% Deoxycholate. Then, it was supplemented with 1mM NaF, 1mM Na_3VO_4, 2mM DTT, and Protease Inhibitor. The samples were placed in glass homogenizing tubes and minced with ten strokes of Dounce A, and with ten strokes of Dounce B. Afterwards, the samples were transferred to Eppendorf tubes and spun at 13,000 rpm for ten minutes at 4^oC. The supernatant was collected and stored in aliquots in -80^oC. The protein concentration was then determined by using BCA Assay.

3.2.7. Immunoblot analysis for protein determination

In this study, the activation of JNK in inflammation was studied in presence or absence of CPZ. The experimental procedures and conditions for running the gel, transferring the gel on the nitrocellulose membrane and blocking in 5% NFDM for immunoblotting of JNK and p-JNK were similar as described in section 3.1.8 except for the antibodies used. For determination of JNK protein, the anti-JNK antibody (Cell Signaling, Beverly, MA, USA Cat # 9252) was used at a dilution of 1:500 in 5% BSA prepared in TBST buffer. For p-JNK determination, anti-phospho-JNK antibody (Cell Signaling, Beverly, MA, USA Cat # 9251) was used at a dilution of 1:1000 in 5% BSA prepared in TBST buffer. Total JNK was used as a loading control for accurate protein loading. After incubating with the secondary antibody, the membranes were exposed toa

camera set under chemiluminescence filter for 2 min and then depending on the band intensity the membranes were exposed for additional 15-20 min.

3.2.8. Fixation of liver tissues for histological analysis

The liver tissues were harvested from mice at the end of the experiment and allowed to fix in 10% neutral formalin solution for 24 h at 4 ^{0}C. Approximately 15 ml of formalin solution was used to fix the liver from one mouse. The fixation is done in order to prevent the degradation of the tissue. They were processed with different alcohol gradients, embedded in paraffin, sectioned to a thickness of 4–5 μm and stained with hematoxylin and eosin (H&E) for morphological evaluation or with Periodic acid Schiff's reagent (PAS) for qualitative analysis of glycogen content.

3.2.9. mRNA isolation and qRT-PCR for hepatic cytokine expression

Total RNA was isolated from mouse liver tissues using TRIzol reagent (Sigma-Aldrich, St. Louis, MO, Cat # T9424) according to the manufacturer's instructions. The details are: Approximately 0.1 g of liver tissues stored at -80 ^{0}C were collected in 2 ml of microcentrifuge tubes. Then 0.75 ml of cold TRIzol reagent was added. The tubes were placed on ice and homogenized with a hand-held Beckman Polytron homogenizer (highest setting) for ~ 1 min. After each tube, the homogenizer was washed in the sequence with RNA Zap reagent, 70% ethanol, MilliQ water and TRIzol reagent. The samples were incubated at room temperature for 5 min. Then 0.2 ml of chloroform (Sigma-Aldrich, Cat # C2432) was added. The tubes were tightly capped and vigorously shaken for 15 sec and incubated for an additional 15 min at room temperature. The tubes

were centrifuged at 12,000 rpm for 15 min at 4 ^{0}C. After this step, the upper colorless phase was transferred (~70% of the volume of TRIzol) to another clean Eppendorf tubes. Then 0.5 ml of isopropyl alcohol was added and tubes were mixed vigorously and incubated for 10 min at room temperature. The tubes were then centrifuged at 12,000 rpm for 10 min at 4 ^{0}C. The supernatant was removed and the RNA pellet (often invisible formed at the bottom) was mixed with 1 ml of 75% ethanol, vortex mixed and centrifuged at 7600 rpm for 5 min at 4 ^{0}C. All the ethanol was removed and the RNA pellet was allowed to dry in the hood for 2-3 min. The pellet was then dissolved in 50-70 µL of RNAase-free water or diethylpyrocarbonate **(**DEPC, 0.1% v/v solution) water by passing the solution several times with a pipette tip. If necessary, the tubes were warmed for 5-10 min in a water bath preset at 55 ^{0}C.

Total RNA was measured by diluting 1 µL of sample in 500 µL of TE buffer (pH 8.8) in 1.5 ml clear disposable plastic cuvettes (purchased from VWR, Cat # Z330388) on a UV-vis spectrophotometer (Beckman Coulter, DU800) at 260 and 280 nm wavelengths. The ratio of 260/280 was used to quantitatively determine the RNA concentration. RNA preparations with a ratio of > 1 were used in the subsequent experiments.

The cDNA synthesis was performed using a High Capacity Reverse Transcription Kit from Applied Biosystems (Foster City, CA, Cat # 4368813). The following reagents per reaction were used as follows: 4 µL of 10X RT buffer, 1.6 µL of 25X dNTP mix (100 nm), 4 µL of 10X random primers, 2 µL of multiscribe reverse transcriptase, 2 µL of RNAase inhibitor, 6.4 µL of DEPC water. So a total of 20 µL of these reagents were

added to 20 µL of RNA samples in PCR tubes (0.2 ml capacity) to get the final reaction volume of 40 µL. The tubes were gently tapped and placed in the PCR cycler to construct the cDNA. The conditions for PCR were: 25 ^{0}C for 0-10 min, 37 ^{0}C for 11-70 min, held constant at 37 ^{0}C from 71-130 min, 85 ^{0}C for 5 sec, then cooled down to 4 ^{0}C for 90 min.

Real-time PCR was performed using an ABI PRISM 7300 Sequence Detection System instrument and software (Applied Biosystems, Foster City, CA). For each 10 µL of sample, 15 µL of PCR mix reagent was added which contained 50 to 100 ng of cDNA, 300 nM forward primer, 300 nM reverse primer, 200 nM TaqMn probe, 11.25 µL of Roche PCR Master Mix (Roche Diagnostics, Indianapolis, IN, Cat # 04914058001) and 3.55 µL of dd water in a PCR plate. The reaction volume was 25 µL per well. The plate was tightly sealed and centrifuged for 10-15 sec to allow proper mixing of the reagents. The reaction conditions were 50 ^{0}C for 2 min (stage 1), denaturing at 95 ^{0}C for 10 min (stage 2), denaturing at 95 ^{0}C for 15 sec and annealing at 60 ^{0}C for 1 min (stage 3, 50 cycles). Quantitative expression values were normalized to cyclophilin. The sequences of the primers and probes are shown in Table 3.1.

Table 3.1 Probe and primer sequences of cytokine genes

Gene	Forward primer	Reverse primer	Probe sequence
TNF-α	5'-CATCTTCTCAA AATTCGAGTGACAA	5'-TGGGAGTAGA CAAGGTACAACCG	5'-6 CACGTCGTAGCA AACCACCAAGTGGA0
IL-1β	5'-CAACCAACAAGTG ATATTCTCCATG	5'-GATCCACACT CTCCAGCTGCA	5'-6CTGTGTAATGAA AGACGGCACACCCACC0
IL-6	Mm00446190-m1 purchased from AB Sciex as a 20X mix		
Cyclophilin	5'-GGCCGATGAC GAGCCC	5'-TGTCTTTGGAA CTTTGTCTGCA	5'-6TGGGCCGCGTCT CCTTCGA0

3.3. *In vitro* experiments

3.3.1. Isolation of primary mouse hepatocytes

Prior the experiment, water bath was warmed at 40 ^{0}C, the ultracentrifuge was fast cooled at 4 ^{0}C and perfusion buffers 1 and 2 were warmed in the water bath. Perfusion buffer 1 was purchased from VWR Chemicals (Cat # 45000-446) and consisted of EGTA, 95 mg; PBS (without Ca/Mg), 500 ml and 1 M HEPES solution, 5 ml. M HEPES was prepared by adding 131 g of HEPES powder to 1L of dd water with the pH adjusted to 7.4 and stored at 4 ^{0}C. The pH was already adjusted to 7.4. Similarly, perfusion buffer 2 (VWR, Cat # 45000-430) consisted of PBS with Ca/Mg. The perfusion buffer 2 was prepared by adding 20 mg of collagenase Type IV (Sigma-Aldrich, C-5138) to 62.5 ml of the buffer. The mixture was vigorously shaken to ensure proper dissolution of collagenase in the buffer. A total of 50 ml of buffer 1 and 62.5 ml of buffer 2 were pre-warmed in the water bath for one mouse.

For isolation of primary mouse hepatocytes, the mouse was lightly anesthetized in a jar containing a cotton ball wet in Isoflurane. The mouse was allowed to remain in the jar for less than a min after which the mouse was placed on a sterile Styrofoam lid covered with aluminum foil. The head of the mouse was pushed in a conical tube containing a cotton ball lightly wet with the Isoflurane. The fore and hind legs of the mouse were fixed by piercing pins so that a tight and flat abdominal surface is available for the experiment. An incision was cut on holding the abdominal skin of the mouse tightly with a forcep. Then the abdomen was cut wide open by moving the scissors so as to avoid damage to any other internal organs. The intestine was gently pushed away with cotton tips to expose the inferior vena cava (IVC) and portal vein (PV). The muscles next to the IVC were gently ruptured with a curved forcep so that the hemostat can pass. A silk thread was curved in the hemostat at the tip and put under through the IVC. The thread was pulled from the other end and a loose knot was tied with 2 throws. At an angle parallel to the IVC, a catheter was inserted in the IVC till the needle went ¾ inside and the knot was tightened. Then the needle was carefully removed and after checking the blood flow from the white end of the needle and the tubing was attached. The PV was quickly cut and the pump was turned on to perfuse the liver first with perfusion buffer 1. The liver was perfused for 4-5 min at a flow rate of 6-8 ml/min (~ 30-40 ml was perfused). Then the tube was removed from buffer 1 and immersed in buffer 2 which was perfused for an additional 3-4 min until the liver begins dissociating under glisson's

capsule. We check the liver by poking holes with a curved forcep. The pump was then stopped; the liver was then removed and immersed in cold plating cell culture medium.

3.3.2. Hepatocyte culture

The compositions of the cell culture medium are listed below.

(1) Plating medium: Williams medium E, 500 ml; penicillin/streptomycin, 5 ml of stock; glutamine/gentamycin, 5 ml of stock; ITS (25 mg/10ml), 1 ml of stock to get final conc. of 5 µg/ml; glucagon, 20 µL of stick (2 µg/500 ml) and fetal bovine serum (FBS), 50 ml.

(2) Treatment medium: Williams medium E, 500 ml; penicillin/streptomycin, 5 ml of stock and glutamine/gentamycin, 5 ml of stock.

Both the mediums were filter sterilized in the cell culture hood and stored at 4 ^{0}C for further use. The liver, which was placed in 40 ml of cold plating medium was shaken vigorously enough to break the liver. The suspension was then poured through a 70 micron cell strainer and collected in another tube. Some debris is left and do not worry to tear that as it may damage the hepatocytes. The 40 ml crude suspension was centrifuged at 50 rcf for 2 min at 4 ^{0}C. The supernatant was discarded as it contained the non-parenchymal cells. Then, 25 ml of fresh medium was added with 12 ml of 100% Percoll solution. Percoll is used to establish a density gradient which allows efficient removal of dead cells. The tube was inverted 4-5 times gently to mix the cells and then spun down at 50 rcf for 10 min at 4 ^{0}C. The supernatant was aspirated and the cells were again washed 2 times with 30 ml of ice cold plating medium and spun at 50 rcf for 2 min each. The supernatant was aspirated and the cells were resuspended in 10 ml of ice cold plating

medium. The cells were gently mixed and then counted on a hemocytometer under a light microscope set at 20X. A good preparation yielded around 2 million cells/ml. Only preparations with a viability >85% was used in further experiments. A seeding density of 100,000 cells/0.5 ml/well in 24-well plates (BD PharMingen, Cat # 353847) was used.

The plates were incubated at 37 ^{0}C in a humidified incubator supplied with 95% relative humidity and 5%CO^2. The cells were allowed to attach for 3-4 h after which the medium was changed to treatment medium and the cells were returned to the incubator for overnight. The treatments were carried out on the next day after changing the medium again.

3.3.3. Treatment of primary mouse hepatocytes

The hepatocytes were treated with the bacterial endotoxins (LPS/LTA), cytokines (TNF-α, IL-1β or IL-6) or PBS containing 0.0001% BSA as a control. For toxicity studies, hepatocytes were pre-treated with 10 ng/mL each of IL-1β, IL-6 or TNF-α, or PBS containing 0.0001% BSA for 30 min. The stock solutions for the cytokines were prepared at a concentration of 10 µg/ml and store at -20 ^{0}C. The 10 µg/ml stock was diluted in PBS/BSA mixture to get 5 µg/ml and 1 µL of this solution was added in 0.5 ml of medium to get a final concentration of 10 ng/ml. This was followed by addition of APAP (2.5 mM, Sigma-Aldrich, Cat # A7085) or CPZ (20 µM, Sigma-Aldrich, Cat # C8138) or their corresponding vehicles (0.1 % DMSO for APAP and saline for CPZ). The DMSO was purchased from Sigma-Aldrich, St. Louis, MO (Cat # D8418). Similarly, the cells were treated with 1 µg/ml each of LPS or LTA or saline control 30 min prior to

drug treatments. For LPS or LTA treatments, the 5 mg/ml of stock were diluted to 0.8 µg/ml and a 5 µL was added in 0.5 ml of medium. The cells were returned to the incubator set at 37 ^{0}C for an additional 24 h. After this, supernatant samples (400 µL) were collected in Eppendorf tubes. The samples were stored at 4 ^{0}C for toxicity assays as described below.

For investigating the role of JNK in drug-induced hepatotoxicity, cells were pre-treated with 0.5 µL of 30 mM JNK inhibitor, SP600125 (final concentration 30 µM) for 30 min, followed by TNF-α treatment for 30 min, after which the cells were treated with APAP or CPZ. DMSO served as a vehicle control for SP600125. The concentration of DMSO in the well did not exceed 0.25%. The supernatant samples were then collected after 24 h and stored as described above.

To study the activation of JNK, cells were treated with the pro-inflammatory cytokines (TNF-α, IL-1β, or IL-6) or LPS or LTA at the above mentioned concentrations from 0 - 6 h. In order to measure JNK activation by APAP or CPZ in presence of cytokines, hepatocytes were pre-treated with the cytokines for 30 min, followed by treatment with APAP (2.5 mM) or CPZ (20 µM) from 0 to 2 h. Therefore, the cells were exposed to the cytokines for a total of 2.5 h and the drugs at the indicated time points. After the end of the last time point, the supernatant was aspirated and discarded. The attached cells were washed 2 times with ice cold PBS (0.5 ml/well, gently swirled and aspirated). Then the cells were scraped in the homogenization buffer (described in section 3.3.5) and stored for protein quantification by BCA assay and immunoblotting.

3.3.4. Toxicity assays

A. Alanine aminotransferase assay

Alanine Aminotransferase (ALT) is routinely used as a marker to assess liver toxicity due to pathophysiological conditions or chemical insults. The reagent was reconstituted with the volume of distilled or deionized water as stated on the vial label (ALT-GPT Infinity, Thermo Scientific, Middletown, VA, USA, Cat # TR18503) and stored at 4^0C for future use. For determination of ALT activity in samples, 5 μL of serum specimen or 20 μL of cell culture supernatant was added in a half-area UV absorbance 96-well plate. Then 50 μL or 200 μL of ALT reagent was added into the plate. The plate was mixed well and after 30 seconds the absorbance was recorded at 340 nm for 3 min at 1 min intervals. The change in absorbance per min (ΔA/min) was calculated from using the mean from the 3 readings. To get the final ALT activity in U/L, the ΔA/min was multiplied by a predefined factor based on the manufacturer's instructions.

B. Lactate dehydrogenase assay

Lactate dehydrogenase (LDH) is also commonly used to assess cytotoxicity in biological specimens. The LDH assay kit was purchased from Roche Pharmaceuticals Ltd., Nutley, NJ, Cat # 11644 793 001). In order to determine the LDH release from the hepatocytes, 100uL of supernatant medium from each well was collected and stored for analysis at 4^0C (samples can be used up to 48 hours for LDH if stored in 4^0C). The lyophilized Catalyst reagent (Blue Cap) was reconstituted by adding 1mL of distilled water directly to the vial, followed by through mixing and incubating at room

temperature for 10 minutes. Two μL of sample was aliquoted to a 96-well plate. Then 250 μL of Catalyst (blue cap) was mixed with 11.25mL of Dye Solution (red cap) in 15 mL conical tube and the reagent was transferred to solution basin. Using a multichannel pipette, 100 μL of reagent was added to each well of the 96-well plates containing the 2 μL sample. This was done quickly as this is a time and light sensitive procedure. The plate was incubated at room temperature in a dark space for 25 minutes (I like to use my workbench drawer covered with tape so I don't mistakenly open it during the incubation time). The change in absorbance of samples was recorded at 492nm (reference 655nm) using the Gen5 software on the Synergy II plate reader (Biotek, Winooski, VT). The percent control in LDH release was calculated using the following equation:

% Control = (Sample - Blank) / (2% Triton X - Blank) * 100

The 2% Triton X served as a positive control and untreated cells as Blank.

3.3.5. Preparation of whole cell extracts from hepatocytes

To prepare whole cell extracts from liver cells, a 6-well plate was placed on top of packed ice. The media was quickly aspirated. Then, the plate was washed two times with 1 mL of cold PBS. Ice cold PBS was added once and swirled gently. PBS was aspirated off and the washing was repeated. Two hundred micro-liters of homogenization buffer, which consisted of 50mM Tris HCl (pH 7.5), 0.5M NaCl, 2mM EDTA, 2mM EGTA, 1% Triton X-100, and 0.25% Deoxycholate, was added to each well. Then, it was supplemented with 1mM NaF, 1mM Na_3VO_4, 2mM DTT, and Protease Inhibitor. The plate was incubated on ice for 30 minutes. Once this time elapsed, the cells were scraped

with a cell scraper and pipetted up and down ten times. The solutions were transferred to Eppendorf tubes and spun at maximum speed for 10 minutes at 14,000 rpm and 4^{o}C. The supernatant was saved as total lysate, aliquoted into Eppendorf tubes and stored at -80^{o}C.

3.3.6. Immunoblot analysis for protein measurement

Immunoblot analysis was used to determine the protein expression of p-JNK and JNK in cell culture extracts. Total JNK was used as a loading control. The experimental procedures and antibody conditions were similar to as described in sections 3.1.8 and 3.2.7, respectively.

CHAPTER 4

CYP3A-dependent drug metabolism is reduced in bacterial inflammation in mice

4.1. Abstract

Background and purpose: Gene expression of Cyp3a11 is reduced by activation of Toll-like receptors (TLRs) by gram-negative or gram-positive bacterial components, lipopolysaccharide (LPS) or lipoteichoic acid (LTA), respectively. The primary adaptor protein in the TLR signaling pathway, TIRAP, plays differential roles in LPS- and LTA-mediated down-regulations of Cyp3a11 mRNA. Our goal was to determine the functional relevance of these findings by pharmacokinetic/pharmacodynamic (PK/PD) analysis of the Cyp3a substrate, midazolam (MDZ) in mice. MDZ is also metabolized by Cyp2c in mice.

Experimental approach: Adult, male, C57BL/6, $TIRAP^{+/+}$ and $TIRAP^{-/-}$ mice were pre-treated with saline, LPS (2 mg/kg) or LTA (6 mg/kg). Cyp3a11 protein expression, activity and PK/PD studies using MDZ were performed.

Key results: Cyp3a11 protein expression in LPS- or LTA-treated mice reduced by 95% and 60% compared to saline. Cyp3a11 activity was reduced by 70% in LPS- or LTA-treated mice. There was 2-3 folds increase in the plasma AUC of MDZ in LPS- and LTA-treated mice. Plasma levels of 1'-OHMDZ decreased significantly only in LTA-treated mice. Both LPS and LTA decreased AUC of 1'-OHMDZ-glucuronide. In the PD study, sleep time was increased by ~2 fold in LPS- and LTA-treated mice. LTA-mediated decrease in Cyp3a11 protein expression and activity was dependent on TIRAP. In PK/PD correlation, AUC of MDZ was increased only in LPS-treated mice compared to saline.

Conclusions and implications: MDZ PK/PD was altered by LPS and LTA. This is the first study to demonstrate the mechanistic differences in the regulation of metabolite formation of a clinically relevant drug by gram-negative or gram-positive bacterial endotoxins.

Key words: Inflammation, lipopolysaccharide, lipoteichoic acid, midazolam, pharmacokinetics and pharmacodynamics.

4.2. Introduction

Inflammation is a complex immunological response elicited during many disease states, making it a critical phenomenon in clinical therapies. An acute inflammatory reaction can be initiated by a wide variety of pathological stimuli, such as bacterial or viral infections, tissue damage, or cellular stress which results in the release of pro-inflammatory cytokines and alteration in the expression of several hepatic proteins. Several studies have shown that inflammation can lead to an impairment of expression and activity of drug metabolizing enzymes (DMEs) in rodents and humans (Giannini *et al.*, 2003; Morgan, 1997; Sewer *et al.*, 1996; Siewert *et al.*, 2000). Literature reports indicate that DME regulation during inflammation is dependent on the type of inflammatory stimuli (Barclay *et al.*, 1999; Chaluvadi *et al.*, 2009; Sewer *et al.*, 1996, 1997). However, it is not known whether reductions in DMEs by different inflammatory stimuli are responsible for reducing the metabolite formation of drugs metabolized by specific DMEs. Reduced metabolite formation during inflammation can lead to increased accumulation of the parent compound in the plasma. This can change the pharmacological activity of clinically-relevant medications leading to reduced efficacy or increased toxicity.

Among the phase I and phase II DMEs, the human CYP3A subfamily is responsible for metabolizing approximately half of currently marketed drugs (Guengerich, 1999; Shimada *et al.*, 1994; Thummel *et al.*, 1996). Studies have shown that the gram-negative bacterial endotoxin, LPS, can induce acute phase response in animals

which can lead to decreased expression and activity of key phase I and II DMEs (Morgan, 1989; Renton and Nicholson, 2000), ultimately leading to decreased hepatic drug metabolism (Monshouwer *et al.*, 1996a). Also, a clinical study showed that LPS injection led to a significant decrease in the clearance of antipyrine (Shedlofsky *et al.*, 1994). Recently, we showed that LPS-mediated down-regulation of hepatic Cyp3a11 mRNA levels was mediated through activation of the pathogen recognition receptor, known as Toll-like receptor 4 (TLR4) (Ghose *et al.*, 2008). In comparison with gram-negative organisms, gram-positive bacteria such as *Enterococcus faecalis*, *Staphylococcus aureus* or *Streptococcus pneumoniae* are also highly prevalent. Statistically, infections caused by gram-positive antigens account for >50% of total organisms causing sepsis (Martin *et al.*, 2003). Gram-positive infections are commonly implicated in producing the toxic shock syndrome which is an acute, multi-organ illness, typically resulting in shock (Sriskandan and Cohen, 1999). We have shown that activation of TLR2 by the gram-positive bacterial endotoxin, LTA, reduced the gene expression of hepatic DMEs and transporters (Ghose *et al.*, 2009; Ghose *et al.*, 2011a). A recent clinical study also showed that LTA treatment elicited a different response in the lungs compared with LPS (Hoogerwerf *et al.*, 2008). However, there is a limited understanding of how alterations in DME genes by LPS or LTA cause changes in metabolism and clearance of clinically-relevant medications. It is known that TLR4 or TLR2 activation by LPS or LTA, respectively, is initiated by the primary adaptor protein, Toll-interleukin 1 receptor domain containing adaptor protein (TIRAP)-dependent

pathway. In our previous studies, we have shown that the down-regulation of mRNA levels of key phase I and II DMEs by LTA was mediated by TIRAP; while LPS-mediated effects on these DMEs was not dependent on TIRAP (Ghose *et al.*, 2011a; Ghose *et al.*, 2008). Thus, gram-negative and gram-positive bacteria may regulate drug metabolism by distinct mechanistic pathways.

In this study, we determined the metabolism of MDZ as it is a clinically relevant drug, widely used for anesthesia in surgical and dental procedures. MDZ is also used as a sedative for acutely agitated patients in intensive care units due to its favorable PK properties. It is considered to be a specific CYP3A substrate and routinely used as a marker of CYP3A4 activity in humans (Greenblatt *et al.*, 2003; von Moltke *et al.*, 1996). However, *in vivo* studies have shown a 5-fold variation (in 98% of study population) (Floyd *et al.*, 2003) and 11-fold variation (in 90% of study population) (He *et al.*, 2005) in the clearance of MDZ. Although MDZ is used to study Cyp3a activity in mice, recent studies in $Cyp3a^{-/-}$ mouse showed a significant contribution of Cyp2c enzymes in MDZ metabolism (Perloff *et al.*, 2000; Perloff *et al.*, 2003; van Waterschoot *et al.*, 2008; Warrington *et al.*, 2000). It is not reported to be a P-glycoprotein (Pgp) substrate and is therefore mainly cleared by hepatic and/or intestinal metabolism owing to its intermediate extraction ratio (E=0.3-0.7) (Gorski *et al.*, 2003; Polli *et al.*, 2001). In humans, MDZ is oxidized by CYP3A4 to form the primary metabolite, 1'-hydroxymidazolam (1'-OHMDZ), (Heizmann et al., 1983). In mice, Cyp3a and Cyp2c are involved in formation of 1'-OHMDZ and 4'-OHMDZ (van Waterschoot *et al.*, 2008).

Studies in humans have shown that 1'-OHMDZ further undergoes *o*-glucuronidation to form 1'-hydroxymidazolam-glucuronide (1'-OHMDZ-gluc) by UGT2B4 and 2B7 (Zhu *et al.*, 2008). 1'-OHMDZ has ~50% pharmacological activity as the parent compound and the affinity of 1'-OHMDZ to the benzodiazepine receptors in the brain is ~60% of that of MDZ. Because of its very short half-life and lower pharmacological activity, 1'-OHMDZ is referred to have negligible clinical effects (Bornemann *et al.*, 1985). On the other hand, clinical studies have shown that, accumulation of 1'-OHMDZ-gluc caused prolonged sedation in patients suffering from acute renal failure (Bauer *et al.*, 1995; Driessen *et al.*, 1991; Swart *et al.*, 2005).

To investigate the effects of MDZ and its metabolites on the pharmacological activity in mice, we performed PK/PD correlation using model independent linear regression analysis. We find that, the PK and PD profiles of MDZ and its metabolites showed significant differences in LPS- or LTA-treated mice compared to the control. This corresponds to reduced expression and activity of Cyp3a11 in mice. This study provides direct evidence that inflammation reduces the metabolism and clearance of MDZ, which leads to prolonged sedation in mice. This study warrants further investigation of inflammation-mediated alterations in drug metabolism and its effects on the safety and efficacy of therapeutics.

4.3. Materials and methods

4.3.1. Chemicals

Midazolam (Cat # 451028) was purchased from BD Biosciences (San Diego, CA, USA). Phenacetin (Cat # 77440) and 1'-hydroxymidazolam (Cat # UC430) were purchased from Sigma Aldrich (St. Louis, MO, USA). 1'-hydroxymidazolam glucuronide was a kind donation from Dr. Gérard Fabre, (Sanofi-Aventis, France). Midazolam hydrochloride solution for injections was purchased from Baxter Healthcare Corporation (Deerfield, IL, USA). Lipopolysaccharide (*E. coli*) and lipoteichoic acid (*S. aureus*) were purchased from InvivoGen (San Diego, CA, USA) and freshly diluted to 5 mg mL^{-1} in pyrogen-free 0.9% NaCl solution. The anti-CYP3A antibody was a generous gift from Dr. Robert J. Edwards, Department of Medicine, Imperial College (London, UK). All solvents were of HPLC grade and were obtained from VWR International, LLC (Suwanee, GA, USA). Unless otherwise noted, all other chemicals were purchased from Sigma-Aldrich (St. Louis, MO, USA).

4.3.2. Animals

Adult, male, C57BL/6, $TIRAP^{+/+}$ and $TIRAP^{-/-}$ mice (8-10 weeks) weighing 20-25 g were maintained in a temperature and humidity controlled environment and 12 h light/dark cycle with free access to water and rodent chow ad libitum. All animal experimental and surgical procedures were strictly performed as per the Institutional Animal Care and Use Committee guidelines.

4.3.3. Preparation of liver microsomes

Mouse liver microsomes were prepared using a procedure adopted from the literature with minor modifications as described below (Chen *et al.*, 2003). Mice were intraperitoneally (i.p.) injected with saline, LPS (2 mg/kg) or LTA (6 mg/kg) and the livers were perfused after 16 h with sodium phosphate buffer (pH 7.4) to remove the blood and harvested for preparation of microsomes. Livers were homogenized using a motorized homogenizer in ice-cold homogenization buffer [50 mM potassium phosphate buffer (pH 7.4), 250 mM sucrose, 1 mM EDTA] and centrifuged at 15,400 rpm for 15 min at 4°C. The pellet was discarded and the supernatant was collected and centrifuged again at 35,000 rpm for 60 min at 4°C to yield the microsome pellets. The microsome pellet was resuspended in 250 mM sucrose. Protein concentration was determined using a BCA protein assay kit (Pierce, Rockford, IL, USA) using bovine serum albumin (BSA) as the standard.

4.3.4. Cyp3a11 protein expression

Protein expression of Cyp3a11 in mouse liver microsomes was determined by immunoblotting analysis as described previously (Gandhi *et al.*, 2010; Ghose *et al.*, 2008), with minor modifications. Hepatic microsomal proteins (10 μg) were separated by SDS-polyacrylamide gel electrophoresis (SDS-PAGE) on a 12% polyacrylamide resolving gel (Bio-Rad, Hercules, CA, USA). Samples were then transferred to nitrocellulose membrane. Membranes were blocked with 5% nonfat milk in TBS-Tween-20 washing buffer for 1 h and then incubated with primary anti-rabbit Cyp3a11 antibody

(1:4000) in 5% BSA in TBS-Tween20 overnight at 4°C. Membranes were subsequently washed and probed with a goat anti-rabbit IgG-alkaline phosphatases (IgG-AP) secondary antibody (1:2000) and incubated with Tropix® CDP Star® Nitro block II™ ECL reagent as per the manufacturer's instructions (Applied Biosystems, Foster City, CA, USA). Membranes were analyzed on FluorChem FC Imaging System (Cell Biosciences, Santa Clara, CA, USA).

4.3.5. Cyp3a11 enzyme activity

MDZ hydroxylation was measured using mouse liver microsomes as described in detail previously (He *et al.*, 2006), with minor modifications. The formation of 1'-OHMDZ was used as a specific indicator for mouse Cyp3a11 activity. In brief, incubation mixtures (performed in duplicate) contained 0.05 mg of total microsomal protein, MDZ (0-16 µM), 1.3 mM NADPH and reaction cofactors in 50 mM potassium phosphate buffer (pH 7.4). The reaction mixtures were incubated at 37°C. The reaction was initiated by addition of glucose-6-phosphate dehydrogenase (1 unit mL^{-1}). After 5 min, the reactions were stopped by the addition of 100 µL of acetonitrile containing phenacetin (IS). The incubation mixture was centrifuged and the supernatant was analyzed by LC-MS/MS analysis. The identity of 1'OHMDZ and IS was verified by comparing with authenticated standards. The data were fit to the substrate inhibition model and analyzed by GraphPad Prism 4.0 software (GraphPad Inc., La Jolla, CA).

4.3.6. Liquid chromatography tandem mass spectrometry analysis (LC-MS/MS)

To determine the concentrations of MDZ and its metabolites in microsomal and plasma samples, an API 3200 Q-trap triple quadrupole mass spectrometer (Applied Biosystems/MDS SCIEX, Foster City, CA, USA) was used by MRM (Multiple Reaction Monitoring) method in the positive ion mode. A UPLC system, Waters Acquity™ with diode-arrayed detector was used. The UPLC conditions for analyzing MDZ, 1'-OHMDZ, 1'-OHMDZ-gluc and phenacetin (IS) were: column, Acquity UPLC BEH C18 column (50 mm × 2.1 mm I.D., 1.7 μm, Waters, Milford, MA, USA); mobile phase A, 0.1% formic acid; mobile phase B, 100% acetonitrile performed in a gradient from 0 to 3 min as follows: 0-0.5 min: 90% A; 0.5-1.0 min: 75% A; 1.0-2.0 min: 60% A and 2.0-2.5 min: held constant at 60% A, 2.5-3.0 min: 90% A, respectively. The quantification was performed using MRM method with the transitions of *m*/*z* 326.1 → *m*/*z* 291.1 for MDZ, 342.1 → 324.1 for 1'-OHMDZ, 518.1 → 324.1 for 1'-OHMDZ-gluc and 180.0 → 110.0 for phenacetin. The retention times were: MDZ, 1.98 min; 1'-OHMDZ, 1.93 min; 1'-OHMDZ-gluc, 1.72 min and phenacetin, 1.79 min.

4.3.7. Pharmacokinetic study of MDZ

Mice were i.p. injected with saline, LPS or LTA followed by i.p. injection of MDZ (5 mg/kg) 16 h later. Blood samples (10–15 μL) were collected from the tail vein in heparinized tubes at 0, 5, 15, 30, 60, 120, 240, 360 and 480 min, respectively. For extraction of MDZ and its metabolites, 50 μL of diluted plasma (10-fold dilution) was mixed with 450 μL of acetonitrile and 450 μL of methyl *t*-butyl ether. The samples were

vortex-mixed, centrifuged and the organic layer was evaporated under a gentle stream of air and reconstituted in 150 μL of 30% acetonitrile. The lower limits of quantification in this study were 1.95 ng ml^{-1} for MDZ, 3.91 ng ml^{-1} for 1'-OHMDZ and 15.63 ng ml^{-1} for 1'-OHMDZ-gluc. The linear range for MDZ was 1.95-1000 ng ml^{-1}, 1'-OHMDZ was 7.81-1000 ng ml^{-1} and 1'-OHMDZ-gluc was 62.5–1000 ng ml^{-1}, respectively. The within-day variability did not exceed 15.3% and the between-day variability did not exceed 13.9%, respectively. Pharmacokinetic parameters such as maximum plasma concentration (C_{max}), time to reach C_{max} (T_{max}), area under the plasma concentration-time curve ($AUC_{0–8h}$), volume of distribution (V), clearance (CL) and half-life ($t_{1/2}$) for MDZ or the metabolites were derived from the plasma concentration-time data by non-compartmental model using WinNonlin 3.3, respectively (Pharsight, Mountain View, CA).

4.3.8. Pharmacodynamic study of MDZ

For pharmacodynamic studies, mice were pretreated with saline, LPS or LTA followed by i.p. injection of MDZ (80 mg/kg) 16 h later. Sleep time (time between the loss and regaining of righting reflex) in minutes was used as a marker for the pharmacodynamic activity of MDZ.

4.3.9. PK-PD correlation of MDZ and its metabolites with the sleep time

Adult, C57BL/6 mice were divided into 3 groups (n = 3-5 per group) and treated with saline, LPS or LTA. Mice were i.p. injected with a pharmacological dose of MDZ (80 mg/kg) 16 h later. Mice were allowed to turn on their back and blood samples were

collected in heparinized tubes at 30, 60, 180 and 300 minutes, respectively. Plasma concentrations of MDZ, 1'-OHMDZ and 1'-OHMDZ-gluc were determined by LC-MS/MS. The AUCs were calculated by the trapezoidal rule. A correlation between the AUC of MDZ and its metabolites with the sleep time was fitted using linear regression analysis.

4.3.10. Statistical analysis

All the experiments were conducted with n = 3-5 mice in each group. The numerical data were presented as mean ± S.D. and analyzed by one-way ANOVA followed by Tukey post hoc analysis if $p<0.05$. The enzyme kinetic data with the TIRAP mice was analyzed by 2-way ANOVA followed by Bonferroni's multiple comparison test if $p<0.05$.

4.4. Results

4.4.1. Regulation of Cyp3a11 expression and activity in inflammation

Our recent studies showed that activation of TLR4 by LPS or TLR2 by LTA down-regulated the gene expression of hepatic Cyp3a11 (Ghose *et al.*, 2009; Ghose *et al.*, 2011a; Ghose *et al.*, 2008). In the present study, we determined the protein expression and activity of Cyp3a11. We observed ~25 fold down-regulation of Cyp3a11 protein expression in LPS-treated mice and ~3 fold in LTA-treated mice compared to saline (Fig. 4.1.A). We determined Cyp3a11 activity by measuring hydroxylation of the *Cyp3a* substrate, MDZ, as described previously (Thummel *et al.*, 1994). Cyp3a11 activity (V_{max}) decreased significantly (~4-5 fold) in both, LPS- and LTA-treated mice compared to saline (Fig. 4.1.B). There was no significant difference in the K_M values between saline (6.58 ± 1.44 μM) and LTA-treated mice (4.85 ± 2.87 μM). However, the K_M was significantly lower in LPS-treated mice (3.24 ± 0.29 μM) compared to saline (Table 4.1). The intrinsic clearance (CL_{int}) was significantly lower in LPS- or LTA-treated mice (~2-3 fold reduction in CL_{int}) compared to saline. The substrate inhibition constant (K_i) did not change significantly among the three groups (Table 4.1).

Table 4.1 Enzyme kinetic parameters of MDZ

Parameters	Saline	LPS	LTA
V_{max} (nmol/min/mg)	14.14 ± 4.15	2.88 ± 0.41*	3.42 ± 2.46*
K_M (µM)	6.58 ± 1.44	3.24 ± 0.29*	4.85 ± 2.87
CL_{int} (ml/min/mg)	2.14 ± 0.27	0.89 ± 0.07*	0.67 ± 0.08*
K_i (µM)	9.65 ± 2.09	24.75 ± 12.99	13.51 ± 6.54

*p<0.05 when compared against saline.

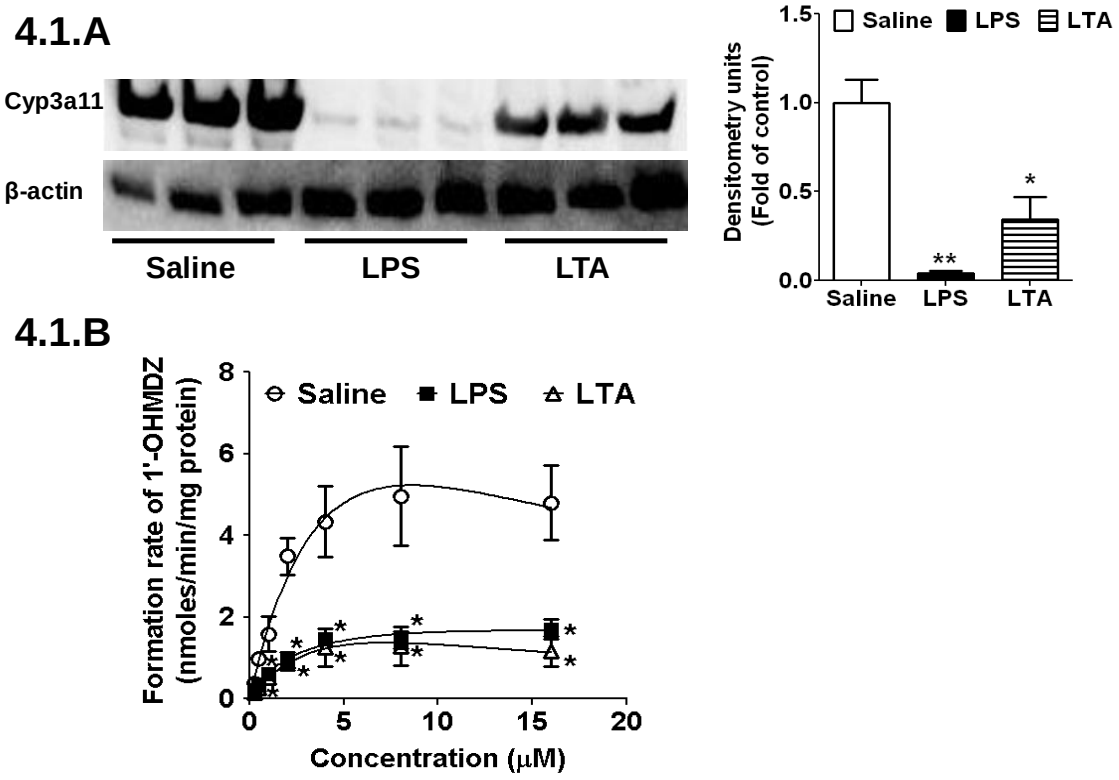

Figure 4.1 Regulation of Cyp3a11 protein expression and activity

Mice were i.p-injected with saline, LPS (2 mg/kg) or LTA (6 mg/kg). Livers were harvested after 16 h (n=4 per group). Microsomes were prepared as described previously in *Materials and Methods*. (A) Cyp3a11 expression was analyzed by western blot analysis of microsomal fractions (10 μg protein per well) using anti-rabbit Cyp3a11 antibody. *p<0.05 and **p<0.01 when compared to saline. (B) Hydroxylation of MDZ was used as a marker of Cyp3a11 activity. Data are shown as mean ± S.D. Significant difference at p<0.05 when compared to saline.

4.4.2. LC-MS/MS validation

The LC-MS/MS method was validated for MDZ and its metabolites before the actual PK experiments and the results are summarized in the table below.

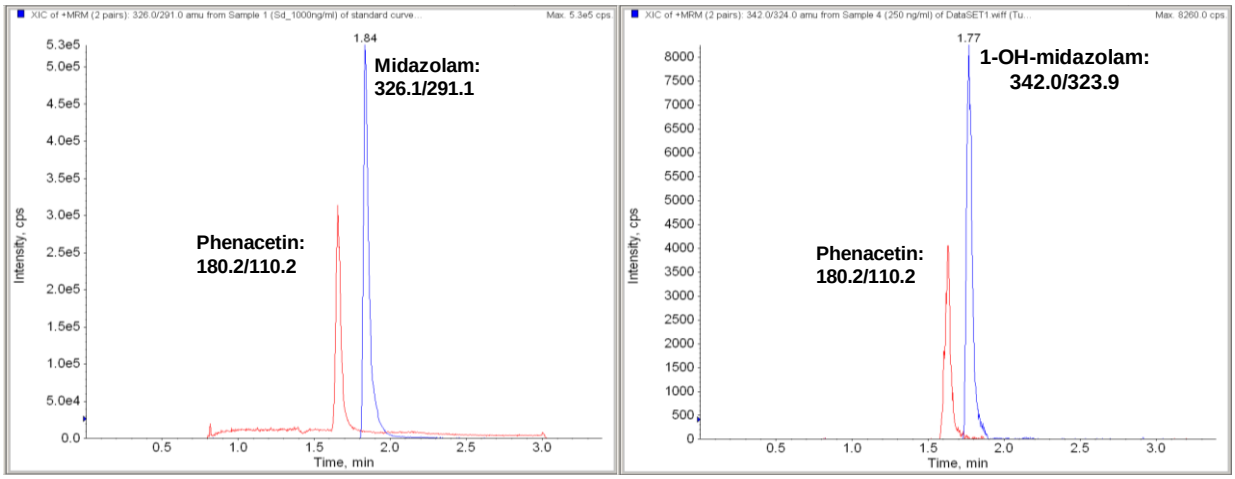

Figure 4.2 Peaks of MDZ and its metabolites are observed in LC-MS/MS

Table 4.2 LC-MS/MS validation parameters of MDZ and its metabolites

Parameter	**MDZ**	**1'-OHMDZ**	**1'-OHMDZ-gluc**
Linear rage	1.95 – 1000.0 ng/ml	7.81 – 1000.0 ng/ml	62.5 – 1000.0 ng/ml
Specificity	No interference from blank plasma sample		
LLOQ	1.95 ng/ml	3.91 ng/ml	15.63 ng/ml
Accuracy	95 – 102 %	99 – 101 %	
Recovery	Exceeded 85-90%		
Intra-day precision	Did not exceed more than 16%		
Inter-day precision	Did not exceed more than 14%		

4.4.3. Pharmacokinetics of midazolam

Since hepatic Cyp3a11 protein expression and activity were reduced by LPS or LTA, we determined the plasma PK profiles of MDZ. The results demonstrate a significant increase in the AUC of MDZ in LPS- or LTA-treated mice (~2-3 folds) compared to saline (Fig. 4.3, Table 4.3.A). Similarly, there was a significant decrease in the clearance of MDZ in LPS or LTA groups (~2-3 folds) compared to saline (Table 4.3.A). The pharmacokinetic parameters for 1'-OHMDZ showed an interesting outcome in LPS- or LTA-treated mice. There was a significant decrease in the C_{max} of 1'-OHMDZ with a corresponding decrease in AUC (~2 fold reduction) in LTA-treated mice compared to saline (Fig 4.3, Table 4.3.B). These parameters were unchanged in LPS-treated mice. On the other hand, AUC of the secondary metabolite, 1'-OHMDZ-gluc, was significantly decreased (~1.5 fold reduction) in LPS- or LTA-treated mice compared to saline (Fig. 4.3, Table 4.3.C).

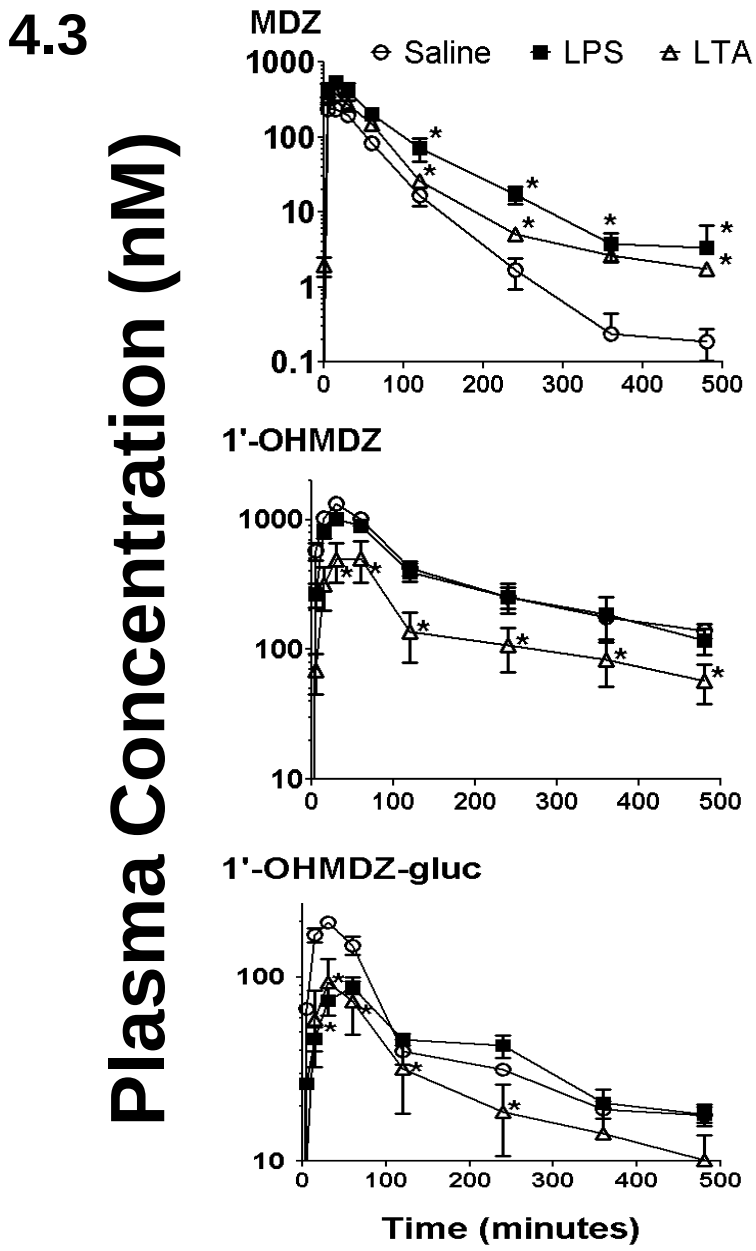

Figure 4.3 Pharmacokinetics of MDZ in LPS or LTA induced inflammation

Plasma concentration versus time profiles from 0 to 8 h for MDZ, 1'-OHMDZ and 1'-OHMDZ-gluc in saline, LPS (2 mg/kg) or LTA (6 mg/kg) treated mice followed by i.p. administration of MDZ (5 mg/kg) are shown. Plasma samples were processed as

described in Materials and Methods. n = 4-5. Data are shown as mean ± S.D. *p<0.05 when compared to saline.

Table 4.3 PK parameters of (A) MDZ, (B) 1'-OHMDZ and (C) 1'-OHMDZ-gluc

Parameter	Saline	LPS	LTA
A. MDZ			
$AUC_{0\rightarrow 8h}$ (µmol.min/L)	13.69±3.36	37.24±14.13*	24.63±6.94*
C_{max} (µmol/L)	0.24±0.02	0.41±0.11*	0.40±0.18
T_{max} (min)	10.00±5.77	15.00±0.00	12.5±5.00
$T_{1/2}$ (min)	31.52±17.23	54.92±13.36	99.91±46.67*
CL (L/min/kg)	1.13±0.22	0.46±0.18*	0.65±0.19*
Vd (L/kg)	47.57±16.05	35.36±13.59	92.52±35.58*
B. 1'-OHMDZ			
$AUC_{0\rightarrow 8h}$ (µmol.min/L)	216.42±56.78	168.09±36.98	117.60±26.52*
Tmax (min)	29.54±6.98	36.46±7.67	34.74±8.78
Cmax (µmol L-1)	1.56±0.49	1.03±0.16	0.84±0.27*
B. 1'-OHMDZ-gluc			
$AUC_{0\rightarrow 8h}$ (µmol.min/L)	24.50±3.06	18.13±2.44*	16.20±0.50*
Tmax (min)	29.42±4.67	49.63±6.80*	33.31±12.08
Cmax (µmol/L)	0.20±0.02	0.08±0.01*	0.12±0.01*

*p<0.05 when compared against saline.

4.4.4. Pharmacodynamics of midazolam

Being a short acting benzodiazepine, MDZ is commonly used in surgical and dental procedures for mild anesthesia. Therefore, we used sleep time as a marker for the pharmacological activity of MDZ. We observed ~2 fold increase in the sleep time in LPS- (288.75 min) or LTA- (220.0 min) treated mice compared to saline (151.33 min).

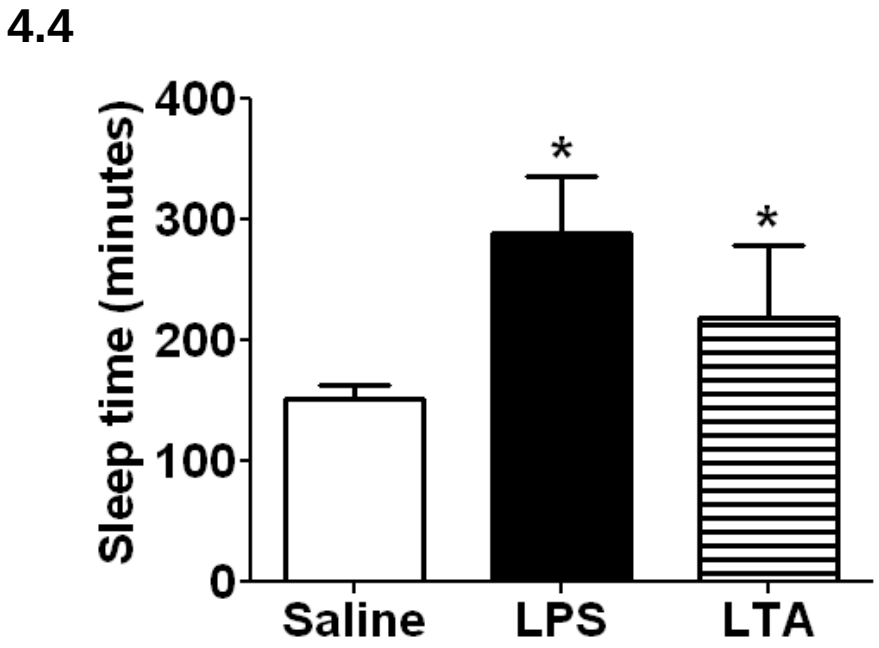

Figure 4.4 Pharmacodynamics of MDZ in LPS or LTA induced inflammation

Mice were i.p- injected with saline, LPS (2 mg/kg) or LTA (6 mg/kg) followed by MDZ (80 mg/kg) 16 h later. Sleep time was recorded as a marker of pharmacodynamic activity of MDZ. n = 4-5. Data are shown as mean ± S.D. *p<0.05 when compared to saline.

4.4.5. PK-PD correlation of midazolam and its metabolites with the sleep time

Due to the formation of an active metabolite of MDZ, another goal of this study was to determine a correlation between the plasma levels of MDZ or its metabolites to the pharmacological activity of MDZ in mice. Pharmacological potency of 1'-OHMDZ compared to the parent compound remains controversial (Mandema *et al.*, 1992; Reed *et al.*, 2001). Therefore, in this study, we examined whether the sedative-hypnotic activity of MDZ is related to plasma concentrations of either MDZ, or its metabolites following the administration of a single i.p. dose of MDZ (80 mg/kg) in mice using conventional model-independent analysis. This dose of MDZ was shown to induce sleep in mice. Plasma concentration-time profiles of MDZ, 1'-OHMDZ or 1'-OHMDZ-gluc in saline, LPS- or LTA-treated mice are shown in Fig 4.5.A. We observed a significant increase in the plasma levels of MDZ in LPS group at 3 and 5 h compared to saline. Whereas, plasma levels of MDZ in LTA group were significantly different only at 5 h compared to saline (Fig. 4.5.A). We also observed significantly reduced plasma levels of 1'-OHMDZ in LPS group at 30 and 60 minutes compared to saline. Plasma level of 1'-OHMDZ was lower in LTA group only at 30 minutes. On the other hand, we also observed significantly reduced plasma levels of 1'-OHMDZ-gluc in LPS group at 30 and 60 minutes. Surprisingly, the plasma levels of 1'-OHMDZ-gluc increased at 5 h in LPS group compared to saline (Fig. 4.5.A). However, in the LTA group, the plasma levels of 1'-OHMDZ-gluc were significantly reduced only at 30 minutes (Fig. 4.5.A).

Next aim was to determine the correlation between AUCs of MDZ and the metabolites with the sleep time. Our results demonstrate that higher AUC of MDZ in LPS-group corresponded with the increased sleep time in mice compared to saline (Fig. 4.5.B). However, AUC of MDZ in the LTA group did not show a significant increase compared to saline. On the other hand, the AUC of 1'-OHMDZ or 1'-OHMDZ-gluc in LPS or LTA groups did not show a significant difference compared to saline (Fig. 4.5.B). Thus, increased sleep-time of mice correlated with increased AUC of MDZ. Furthermore, there was an inverse correlation between sleep-time and AUC of metabolites. This study therefore confirms that the increase in the pharmacological activity of MDZ is associated with the concentrations of the parent compound in LPS-treated mice, and not to any of the metabolites studied.

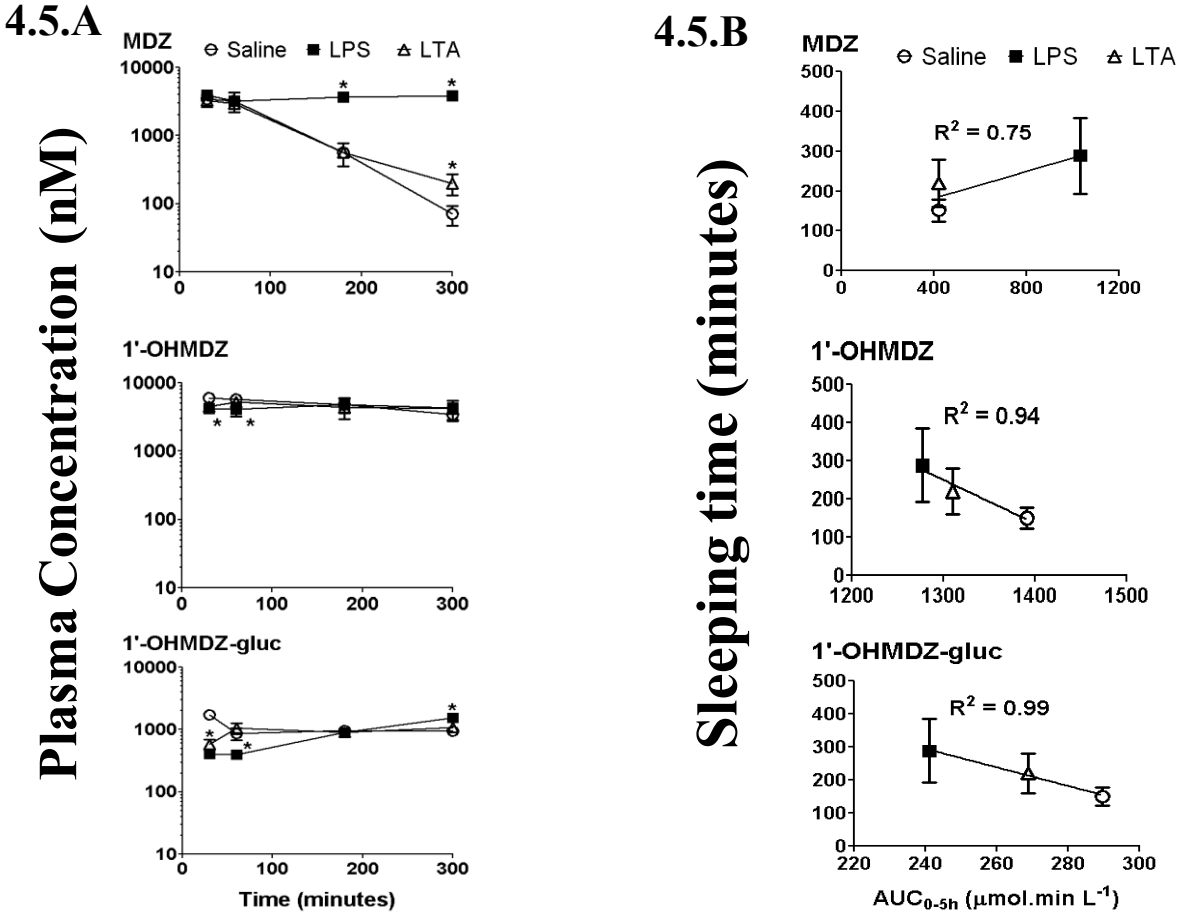

Figure 4.5 PK-PD correlation of MDZ and its metabolites with the sleep time

Mice were i.p- injected with saline, LPS (2 mg/kg) or LTA (6 mg/kg) followed by MDZ (80 mg/kg) 16 h later. Blood samples were collected at 30 and 60 minutes and 3 and 5h, respectively. (A) PK profiles of MDZ, 1'-OHMDZ and 1'-OHMDZ-gluc. (B) Correlation of plasma AUC of MDZ and its metabolites with the sleep time was calculated by linear regression analysis. Data are shown as mean ± S.D. *p<0.05 when compared to saline.

4.4.6. Role of TIRAP in Cyp3a11 expression and activity

Our previous studies showed that TIRAP played a differential role in regulating the gene expression of various phase I and phase II enzymes in LPS or LTA induced-inflammation (Ghose *et al.*, 2009; Ghose *et al.*, 2011a; Ghose *et al.*, 2008). Therefore, we sought to determine whether TIRAP also played a role in MDZ metabolism upon LPS or LTA treatment. We observed ~2-3 folds reduction in Cyp3a11 protein expression in liver microsomes from LPS- or LTA-treated $TIRAP^{+/+}$ mice compared to saline (Fig. 4.6). We also observed ~2-3 folds decrease in Cyp3a11 activity (V_{max}) and CL_{int} in LPS- or LTA-treated $TIRAP^{+/+}$ mice compared to saline (Fig. 4.7). However, this reduction in Cyp3a11 protein expression and activity was attenuated only in the LTA-treated $TIRAP^{-/-}$ mice (Figs. 4.6 and 4.7, Table 4.4). Cyp3a11 expression and activity were comparable in saline-treated $TIRAP^{+/+}$ and $TIRAP^{-/-}$ mice. There was no significant difference in the K_M values between saline and LTA-treated mice however, the K_M was significantly lower in LPS-treated mice compared to saline (3.24 ± 1.19 µM vs. 6.50 ± 2.47 µM) respectively.

Table 4.4 Enzyme kinetic parameters of MDZ in TIRAP mice

Parameters	TIRAP $^{+/+}$			TIRAP $^{-/-}$		
	Saline	**LPS**	**LTA**	**Saline**	**LPS**	**LTA**
V_{max} (nmol/min/mg)	8.88±1.83	4.32±0.86*	4.02±2.50*	13.72±3.78	5.18±1.59*	9.17±3.54
K_M (μM)	4.04±1.00	3.06±0.82	3.05±2.33	6.50±2.47	3.24±1.19*	4.19±2.31
CL_{int} (ml/min/mg)	2.22±0.18	1.45±0.27*	1.41±0.24*	2.17±0.22	1.64±0.20*	3.12±1.35
K_i (μM)	13.47± 3.91	23.89± 14.55	63.02± 64.55	9.29± 3.66	14.26± 3.25	15.42± 7.57

*p<0.05 when compared against saline in the respective group

4.6

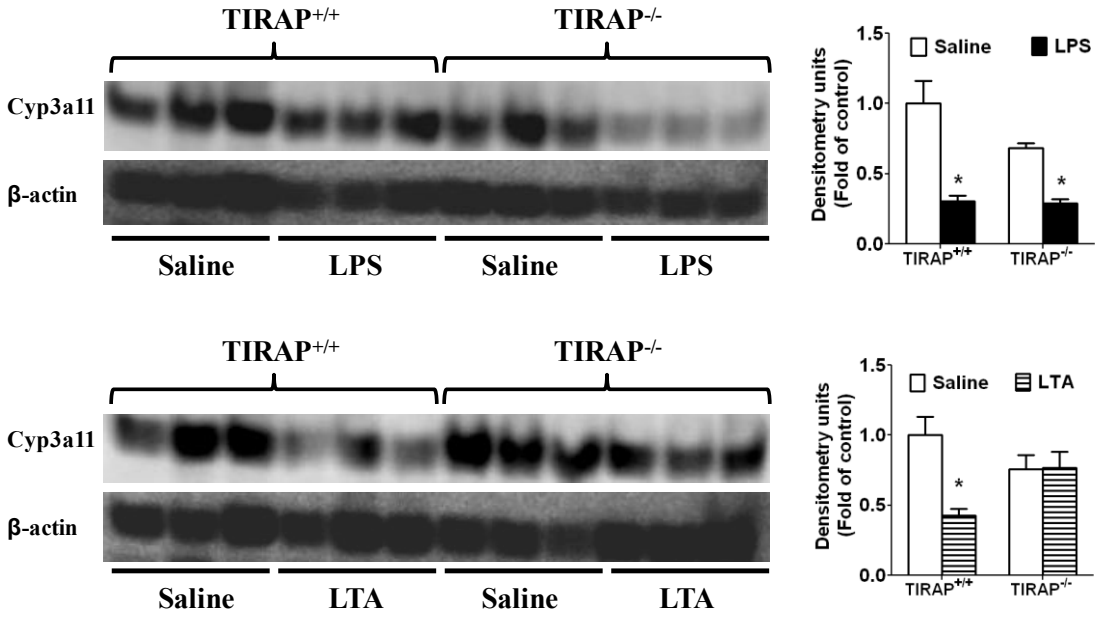

Figure 4.6 Role of TIRAP in Cyp3a11 protein expression

Mice were i.p-injected with saline, LPS (2 mg/kg) or LTA (6 mg/kg). Livers were harvested after 16 h (n=4 per group). Microsomes were prepared as described previously in *Materials and Methods*. Cyp3a11 expression was analyzed by western blot analysis of microsomal fractions (10 μg protein/well) using anti-rabbit Cyp3a11 antibody. Data are shown as mean ± S.D. *p<0.05 when compared to saline.

4.7

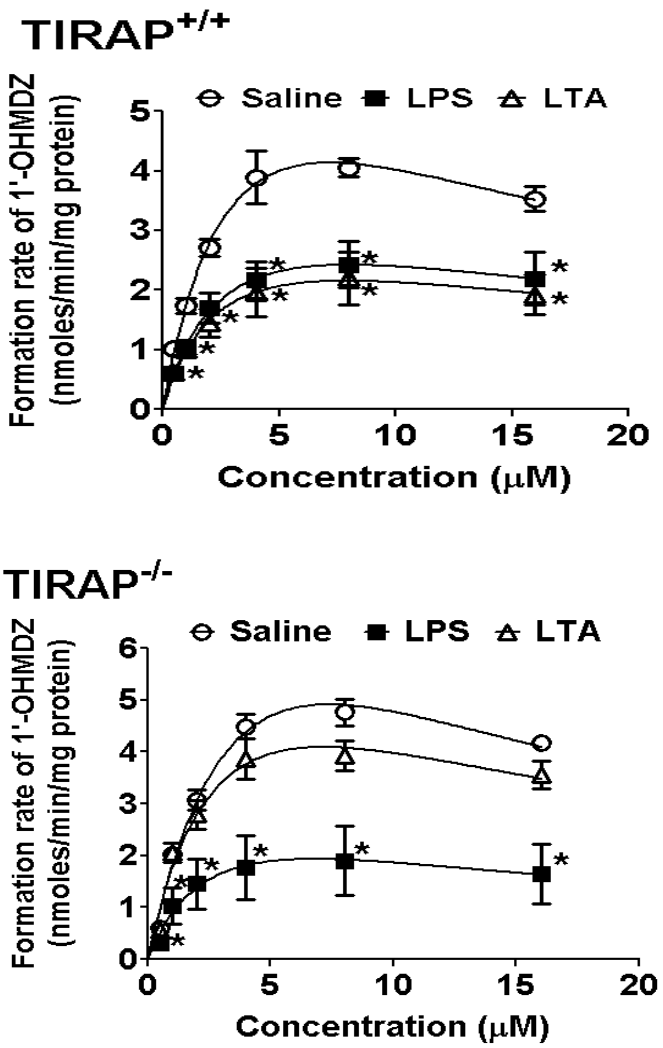

Figure 4.7 Role of TIRAP in Cyp3a11 activity

Mice were i.p-injected with saline, LPS (2 mg/kg) or LTA (6 mg/kg). Livers were harvested after 16 h (n=4 per group). Microsomes were prepared as described previously in *Materials and Methods*. Hydroxylation of MDZ was determined as a marker of Cyp3a11 activity in microsomes. Data are shown as mean ± S.D. *p<0.05 when compared to saline.

4.5. Discussion

In this study, we report that inflammation-induced by the bacterial endotoxins can significantly impact Cyp3a11 enzyme activity and PK/PD of the Cyp3a11 specific substrate, MDZ. The regulation of MDZ metabolism by gram-negative or gram-positive bacterial components occurs by distinct mechanistic pathways.

We observed a significant reduction in Cyp3a11 protein expression as well as activity in LPS- or LTA-induced inflammation compared to saline (Fig. 4.1.A). Also, the reduction in Cyp3a11 protein expression and activity, (as shown by reduced formation of 1'-OHMDZ (Fig. 4.1.B), in mouse liver microsomes by LPS was comparable to studies reported in the literature (Barclay *et al.*, 1999). To further extend the significance of this finding, our next goal was to study the effect of inflammation on PK/PD of MDZ in mice.

In the PK studies, we observed a significant increase in the plasma exposure ($AUC_{0\text{-}8h}$) and a significant decrease in the CL of MDZ in LPS- as well as LTA-treated mice (Fig 4.3; Table 4.3.A). Changes in the PK profiles of MDZ by LPS or LTA can have serious implications on the efficacy and safety of MDZ. Several studies have shown clinically relevant drug-drug interactions with MDZ in animals as well as humans (Kotegawa *et al.*, 2002; Palkama *et al.*, 1999). Increased MDZ plasma levels can lead to respiratory depression further leading to a requirement for intubation and ventilatory support. Our results can serve as a paradigm for MDZ dosage optimization in patients with underlying bacterial infections. Although, LPS did not have a significant effect on the reduction in plasma levels of 1'-OHMDZ, LTA treatment showed a significant effect

on reduced 1'-OHMDZ plasma levels compared to saline (Fig. 4.3). There can be several possible explanations for this intriguing observation. First, although LPS was shown to down-regulate Cyp3a11 protein expression and activity, regulation of other CYPs might be involved in hepatic metabolism of MDZ. A recent study showed that MDZ was metabolized even in the *Cyp3a*$^{-/-}$ mouse model (van Waterschoot *et al.*, 2008). The authors reported that absence of Cyp3a11 was compensated by up-regulation of other CYP enzymes, such as CYP2C. Although, LPS has been known to suppress CYP2C enzymes at the transcriptional level (Morgan, 1997), the role of LPS on CYP2C activity still remains unknown. In addition, a recent study showed a slight, but significant tendency of increase in CYP2C activity in rats treated with LPS isolated from *E. coli* Nissle 1917 (Matuskova *et al.*, 2009). Midazolam is primarily metabolized by Cyp3a11; however, studies have also shown a significant contribution of Cyp2c11, which was studied using anti-Cyp2c11 antibody, in mouse liver microsomes (Perloff *et al.*, 2000; Warrington *et al.*, 2000). Thus, the reduction in MDZ metabolism by LPS or LTA in mice may also be due to reduced expression and activity of both Cyp3a11 and Cyp2c enzymes. It was recently shown that, LPS treatment induced serum β-glucuronidase activity in rats (Shimoi *et al.*, 2001). β-glucuronidases are responsible for hydrolyzing hydrophilic conjugates such as luteolin glucuronide. β-glucuronidases can thereby play an essential role in either detoxification of reactive metabolites or in reducing the pharmacological action of active metabolites. During inflammation, β-glucuronidases, which are present in immune cells such as neutrophils and eosinophils, are released in

blood (Marshall *et al.*, 1988). This drives us to hypothesize that the glucuronide conjugate of 1'-OHMDZ might be hydrolyzed back into the 1'-OHMDZ by the serum β-glucuronidases. However, in contrast to the *Shimoi et al's* study, we did not observe any change in serum β-glucuronidase activity in LPS-treated mice up to 8 h compared to saline (data not shown). This can be possibly a species dependent effect (rat vs. mouse) or the route of administration of LPS (i.v. vs. i.p.), which needs further evaluations.

Mostly, phase II metabolites are considered less active due to their hydrophilic properties which lead them to increased elimination. However, a clinical study reported that accumulation of 1'-OHMDZ-gluc led to increased sedation in patients with renal impairment (Bauer *et al.*, 1995). Therefore, we evaluated the PK profiles of 1'-OHMDZ-gluc in LPS- or LTA-treated mice. Interestingly, we observed a significant reduction in the C_{max} and AUC of 1'-OHMDZ-gluc in LPS- as well as LTA-treated mice (Fig. 4.3) compared to saline. Thus, further work will be required to elucidate the pharmacological potency of 1'-OHMDZ-gluc across species. It has been shown that LPS-induced inflammation down-regulate the gene expression of several hepatic and renal UGT isoforms (Richardson *et al.*, 2006). Therefore, the decreased AUC of 1'-OHMDZ-gluc may be attributed to down-regulation of hepatic UGTs.

In the PD studies, we observed ~2 fold increase in the sleep time in LPS-treated mice compared to saline. Similar to the LPS study, compared to saline, the sleep time in LTA-treated mice was increased by ~1.5 fold (Fig. 4.4). LPS treatment in mice was shown to be associated with decreased plasma protein content (Hartmann *et al.*, 2005).

As MDZ is >97% protein bound drug and only the unbound drug is pharmacologically active, the reduced protein binding of MDZ in LPS-treated mice can contribute to increased distribution and retention of MDZ in the brain. It is not known whether the decrease in the protein content in LTA-treated mice is responsible for increased V_d of MDZ suggesting higher fraction unbound (fu).

The fact that many psychotropic drugs are converted into active metabolites has major implications for PK/PD modeling. Usually, the metabolites of MDZ are considered less active due to their hydrophilic nature and thereby rapid elimination by the kidneys. However, several studies have also shown that 1'-OHMDZ is about 50% active as MDZ in producing the sedative-hypnotic effects in healthy volunteers (Mandema *et al.*, 1992; Ziegler *et al.*, 1983). Another clinical study also showed that, prolonged sedation in ICU patients suffering with renal failure was correlated with significantly increased plasma levels of 1'-OHMDZ-gluc (Bauer *et al.*, 1995). Due to its short half-life and rapid conversion to the glucuronide conjugate, we examined the relationship between the plasma concentrations of 1'-OHMDZ and its glucuronide conjugate with the sleep time induced by MDZ administration in mice. The pharmacological effect of MDZ or its metabolites is determined by their ability to penetrate the blood–brain barrier, which in turn is dependent on their plasma protein binding and lipophilicity. As mentioned earlier, MDZ is >97% plasma protein bound drug and is an intermediate-to-high hepatic extraction ratio drug (ER = 0.3 to 0.7). Therefore, its metabolism is dependent on liver blood flow as well as protein binding. Previous *in vitro* and *in vivo* studies have shown

that LPS treatment can decrease the albumin synthesis by prevention of albumin transcription (Ruot *et al.*, 2000; Wang *et al.*, 2005). Since only the plasma unbound fractions of MDZ and its metabolites can penetrate the brain, any differences between MDZ and its metabolites plasma protein binding can affect their relative *in vivo* potency. MDZ is more lipophilic than its metabolites. We can therefore postulate that concentration ratio of MDZ/total metabolites in the brain, in the absence of any differences in plasma protein binding, is even greater than that found in plasma. This further supports that MDZ contributes the major effect on the overall sedative activity exerted. Also, our data show overall higher levels of plasma MDZ concentration in LPS groups as compared to saline. In the PK study with the lower dose (5 mg/kg), we observed very high levels of MDZ plasma concentrations in LTA-treated mice. Although, we observed a significant increase in the PD effect of MDZ with LTA treatment, the AUC of MDZ in LTA group did not differ significantly from saline treated mice at the higher dose (80 mg/kg). However, we observed a significant increase in the V_d and $t_{1/2}$ of MDZ in LTA group compared to saline, which can possibly lead to prolonged sedation in mice. The increase in V_d and $t_{1/2}$ can be attributed to an increased fu.

A key adaptor of the TLR signaling pathway, namely TIRAP, is known to regulate the inflammatory responses of LPS or LTA on cell surfaces of immune cells (Fitzgerald *et al.*, 2001; Horng *et al.*, 2002). We recently showed that the gene expression of Cyp3a11 in mice was dependent on TIRAP in LTA-induced inflammation (Ghose *et al.*, 2011a). However, TIRAP was not involved in regulating gene expression of Cyp3a11

in LPS-induced inflammation (Ghose *et al.*, 2008). In agreement with our previous studies, our results show that, TIRAP played a significant role not in LPS, but only in LTA-mediated down-regulation of Cyp3a11 protein expression as well as activity (Figs. 4.6 and 4.7). This differential role of TIRAP in regulating LPS- or LTA-induced inflammation provides new approaches to counteract changes in drug metabolism during infection and inflammation.

In conclusion, we observed significant effects of the two inflammatory mediators (gram-positive and gram-negative bacterial endotoxins) on metabolic profiles of MDZ. Both, LPS and LTA, significantly altered the PK profiles of MDZ and a differential role in regulating the PK profiles of 1'-OHMDZ. The plasma levels of 1'-OHMDZ-gluc were significantly reduced in LPS as well as LTA-treated mice. In the PD study, both LPS and LTA played significant roles in increasing the pharmacological activity of MDZ. This is a first study, demonstrating a detailed analysis of MDZ and its metabolites (phase I and phase II) during gram-negative and gram-positive acute phase response on the PK/PD of MDZ. We also show that TIRAP plays a significant role in the regulation of *in vitro* metabolism of MDZ by LTA. As about 50% of cases of sepsis and septic shock are caused by gram-positive bacteria, examination of Cyp3a11 regulation by LTA may prove to be a useful tool to study the PK/PD of clinically relevant medications. These studies show that activation of TLR-signaling pathways impact drug metabolism in mice. However, future studies are needed to investigate the impact of these signaling pathways on drug disposition in human diseases.

CHAPTER 5

Chlorpromazine-induced hepatotoxicity in inflammation is mediated by TIRAP-dependent signaling pathway in mice

5.1. Abstract

Idiosyncratic adverse drug reactions pose a serious concern leading to approved drug withdrawals. Chlorpromazine (CPZ), a typical antipsychotic used to treat schizophrenia, has a long history of hepatotoxicity during its therapeutic use in humans. To understand the molecular mechanism, we studied the role of an adaptor in the Toll-like receptor (TLR) signaling pathway, Toll-interleukin 1 receptor domain containing adaptor protein (TIRAP), which mediates the inflammatory responses of TLR4 and TLR2. In addition, prolonged activation of the downstream kinase, c-Jun-N-terminal kinase (JNK), can lead to cell death. We tested the hypothesis that CPZ-induced hepatotoxicity in lipopolysaccharide- (LPS) or lipoteichoic acid (LTA)-induced inflammation is mediated by TIRAP involving sustained activation of JNK. Male, C57BL/6, TIRAP$^{+/+}$ and TIRAP$^{-/-}$ (C57BL/6×SV129; F3) mice were pretreated with saline, LPS (6 mg/kg) or LTA (2 mg/kg) for 30 min or 16 h followed by CPZ (5 mg/kg) or saline (vehicle control) upto 24 h. Blood samples were analyzed for serum ALT and tumor necrosis factor (TNF)-α release, and histopathology and activation of JNK was studied in the liver tissues. In C57BL/6 and TIRAP$^{+/+}$ mice, only in the presence of CPZ, we observed a ~3-4 fold increase in serum ALT levels, a marked reduction in hepatic glycogen, significant induction of serum TNF-α and prolonged activation of JNK (upto 4 h), compared to LPS or LTA alone. These observations were reversed in TIRAP$^{-/-}$ mice. We, for the first time, show that inflammation-mediated hepatotoxicity of CPZ is dependent on TIRAP. The

TIRAP mouse model can be used to understand and predict idiosyncratic drug-induced hepatotoxicity.

Key words: Inflammation, chlorpromazine, lipopolysaccharide, lipoteichoic acid, c-Jun-N-terminal kinase and Toll-interleukin 1 receptor domain containing adaptor protein.

5.2. Introduction

Drug induced liver injury (DILI) accounts for more than 50% of acute liver failure cases in the United States (Bissell *et al.*, 2001) and remains to be a major concern in significant attrition of new drug molecules reaching phase III clinical trials and the single major cause of "black-box" warning for several clinically relevant drugs. Inflammation, induced by bacterial or viral stimulants, or by underlying disease conditions, has been shown to increase the toxic responses to known hepatotoxic drugs such as trovafloxacin (Shaw *et al.*, 2009d), diclofenac (Deng *et al.*, 2006). sulindac (Zou *et al.*, 2009a) or chlorpromazine (Buchweitz *et al.*, 2001). The gram negative bacterial endotoxin, lipopolysaccharide (LPS), is commonly used to induce inflammation in animal models and in cell-culture, and toxicity of drugs was shown to be increased in LPS-treated rodent models (Shaw *et al.*, 2007; Tukov *et al.*, 2007). Similarly, the gram positive bacterial endotoxin, lipoteichoic acid (LTA) has been shown to augment drug-induced hepatotoxicity in animals (Shaw *et al.*, 2009d). However the molecular mechanism by which LPS or LTA increases the toxicity of drugs is not completely known. In this study, we sought to determine the mechanism by which LPS or LTA regulate the hepatotoxicity of the anti-psychotic agent, chlorpromazine.

Chlorpromazine (CPZ) is widely used as a sedative or antiemetic. There is a long known history of CPZ-induced hepatotoxicity in humans characterized by elevated serum alkaline phosphatases or biliary cirrhosis (Breuer, 1965; Read *et al.*, 1961). Animal models and *in vitro* studies indicate that CPZ is an intrinsic hepatotoxin (Abernathy *et al.*,

1977; Mullock *et al.*, 1983). CPZ was shown to be toxic to the liver in rats treated with LPS (Buchweitz *et al.*, 2002; Gandhi *et al.*, 2010). Furthermore, our recent *in vitro* study using primary mouse hepatocytes, we showed that hepatotoxicity of CPZ was markedly augmented when pre-treated with the pro-inflammatory cytokine, tumor necrosis factor (TNF)-α, or bacterial endotoxins, LPS or LTA (Gandhi *et al.*, 2010). Thus, we selected CPZ as the model drug for our in vivo studies.

The bacterial components, LPS or LTA activate Toll-like receptors (TLRs) 4 or 2, respectively. This leads to the recruitment of the first adaptor protein, TIRAP (TIR-domain containing adaptor protein) to the intracellular domain of TLRs (Akira *et al.*, 2001). Using $TIRAP^{-/-}$ mice, we and others have shown that, TIRAP played a significant role in attenuating the production of inflammatory cytokines in response to activated TLR4 or TLR2 (Fitzgerald *et al.*, 2001; Ghose *et al.*, 2008). However, TIRAP was shown to have a differential role in mediating the effects of LPS or LTA on hepatic detoxification genes (Ghose *et al.*, 2011a; Ghose *et al.*, 2008). In particular, TIRAP was involved in mediating the alteration of hepatic detoxification genes by LTA, but was not involved in mediating the effects of LPS on these genes. Thus, in this study, our goal is to determine the role of TIRAP in mediating the effects of LPS or LTA on the hepatotoxicity of CPZ.

A key component of the TIRAP-dependent TLR-signaling pathway is the MAP-kinase, c-Jun N-terminal kinase (JNK). JNK exists in 3 distinct isoforms (JNK1-3) and is expressed in various tissues such as liver, heart, brain, etc. (Ip and Davis, 1998). JNK

activation by TNF-α or UV radiation (Whitmarsh and Davis, 1996) displays two distinct activation profiles: early/transient and late/sustained (Guo *et al.*, 1998; Roulston *et al.*, 1998). Transient activation of JNK was shown to be involved in cell survival, whereas sustained activation led to apoptosis. Recently, sustained activation of JNK was shown to play a significant role in acetaminophen-induced liver injury *in vivo* (Gunawan *et al.*, 2006; Hanawa *et al.*, 2008; Henderson *et al.*, 2007). We had observed that augmentation of CPZ toxicity by TNF-α in primary mouse hepatocytes was associated with sustained activation of JNK. Furthermore, TNF-α mediated increase in CPZ hepatotoxicity in primary mouse hepatocytes was attenuated by treatment with a JNK inhibitor.

Owing to the lack of effective animal models in indentifying idiosyncratic drug-induced hepatotoxicity and to improve the quality of treatment options to patients (by reducing the occurrence of adverse events reported in post-marketing studies), we need to understand the mechanism by which certain drugs have the propensity of causing serious hepatotoxicity in a subset of population. We observed that LPS or LTA treatment led to increased CPZ-induced hepatotoxicity involving sustained activation of JNK and release of serum TNF-α. Furthermore, TIRAP played a central role in regulating the effects of LPS or LTA on CPZ-induced hepatotoxicity.

5.3. Materials and methods

5.3.1. Materials

Highly purified LPS (*Escherichia coli* serotype 0111:B4) and lipoteichoic acid (*Staphylococus aureus*) were purchased from InvivoGen (San Diego, CA, USA) and freshly diluted to the desired concentration in pyrogen-free 0.9% saline before injection. Anti-JNK (#9252) and anti-phospho-JNK (#9251) (Cell-Signaling, Beverly, MA, USA) were used according to the manufacturer's instructions. Chlorpromazine and all other chemicals were purchased from Sigma-Aldrich (St. Louis, MO, USA).

5.3.2. Animals

C57BL/6 mice were obtained from The Harlan Laboratory (Houston, Texas, USA). $TIRAP^{+/+}$ and $TIRAP^{-/-}$ mice (C57BL/6×SV129; F3) were obtained from Dr. Ruslan Medzhitov (Yale University School of Medicine, New Haven, CT, USA). The animals were maintained in a temperature and humidity-controlled environment and were provided with water and rodent chow ad libitum. All animal experimental and surgical procedures were approved by the Institutional Animal Care and Use Committee. Experiments were repeated 4 – 5 times.

5.3.3. Treatment of animals and sample collection

For toxicity studies, C57BL/6, $TIRAP^{+/+}$ or $TIRAP^{-/-}$ mice were pretreated with saline, LPS (2 mg/kg body wt.) or LTA (6 mg/kg body wt.) or saline for 16 h. All the mice were treated with CPZ (5 mg/kg) or saline (vehicle control) for 24 h. Blood was removed by cardiac puncture and serum was separated and stored at -80^0C for further

analysis. Livers were removed and snap frozen in liquid nitrogen and stored at -80^{0}C for further studies. For immunoblotting studies, C57BL/6, TIRAP$^{+/+}$ or TIRAP$^{-/-}$ mice were pre-treated with saline, LPS or LTA for 30 min followed by CPZ up to 8 h. Livers were harvested and stored as described above.

5.3.4. Alanine aminotransferase (ALT) assay

ALT assay was performed according to the manufacturer's instructions (Thermo Fisher Scientific Inc., Middletown, VA, USA) with slight modifications. Briefly, 5 µL of serum was added to 50 µL of ALT reagent and incubated at 37^{0}C for 3 min. The change in absorbance per min was recorded at 340 nm. Change in ALT activity was reported as ALT release in U/L.

5.3.5. Serum TNF-α analysis

Serum TNF-α was quantified by ELISA kit according to the manufacturer's instructions (BioLegend, San Diego, CA, USA). A standard curve was performed in duplicate and concentration of TNF-α was calculated using the standard curve as reference. The optical density at 450 nm and background at 570 nm was measured with a microplate reader (Synergy II, Biotek, Winooski, VT, USA).

5.3.6. mRNA quantification of cytokines by qRT-PCR

Total RNA was isolated from mouse liver tissues using TRIzol reagent (Sigma-Aldrich, St. Louis, MO) according to the manufacturer's instructions. cDNA synthesis was performed using a High Capacity Reverse Transcription Kit from Applied Biosystems. Real-time PCR was performed using an ABI PRISM 7300 Sequence

Detection System instrument and software (Applied Biosystems). In brief, each amplification reaction (25 µl) contained 50 to 100 ng of cDNA, 300 nM forward primer, 300 nM reverse primer, 200 nM fluorogenic probe, and 15 µl of TaqMan Universal PCR Master Mix. Quantitative expression values were extrapolated from standard curves and were normalized to cyclophilin.

5.3.7. Immunoblotting

Whole cell extracts were prepared from liver tissues pre-treated with LPS/LTA as described previously (Ghose et al., 2008, 2009, Gandhi et al., 2010). The protein concentration was determined by BCA assay according to the manufacturer's protocol (Pierce Chemical, Rockford, IL, USA). The samples were separated by SDS-polyacrylamide gel electrophoresis (SDS-PAGE), transferred to nitrocellulose membrane and probed with JNK (1:500), phospho (P)-JNK (1:1000) or MKP-1 (1:500) antibodies. Membranes were subsequently washed and probed with a goat anti-rabbit IgG-AP secondary antibody (1:2000) for 1 h at room temperature. The blots were then washed with TBS-Tween-20 and incubated with Tropix® CDP Star® Nitro block II™ ECL reagent as per the manufacturer's instructions (Applied Biosystems, Foster City, CA, USA). Membranes were analyzed on FluorChem FC2 Imaging System (Cell Biosciences, Inc., Santa Clara, CA, USA) and quantified by densitometry using the AlphaEase software.

5.3.8. Histopathological analysis

The liver tissues were fixed in 10% neutral buffered formalin. They were processed with different alcohol gradients, embedded in paraffin, sectioned to a thickness

of 4–5 μm and stained with hematoxylin and eosin (H&E) for morphological analysis of the liver or Periodic acid Schiff's reagent (PAS) for qualitative analysis of glycogen content.

5.3.9. Data analysis

All the data are presented as mean ± S.D. with 4-5 animals per group. Differences between experimental groups were assessed for statistical significance by one-way, or two-way ANOVA where appropriate, using GraphPad Prism 4.0 (GraphPad Software, Inc., La Jolla, CA, USA). Unpaired Student's t-test was used when the means of only 2 groups were compared. Statistical significance was demonstrated at $p < 0.05$.

5.4. Results

5.4.1. Hepatotoxicity of CPZ is augmented upon LPS or LTA treatment

Hepatotoxicity of CPZ is very well established in humans (Breuer, 1965; Derby *et al.*, 1993). Treatment with the bacterial endotoxins, LPS or LTA, is known to augment the hepatotoxicity of known hepatotoxins (Luyendyk *et al.*, 2003; Shaw *et al.*, 2009d). In the present study, mice were pretreated with the TLR4 ligand, LPS (2 mg/kg), or the TLR2 ligand, LTA (6 mg/kg) 16 h prior to saline (vehicle control) or CPZ treatment (5 mg/kg). Serum samples collected after 24 h were analyzed for ALT release. The 5 mg/kg dose of CPZ was chosen as a non-hepatotoxic dose based on the data from our dose escalation studies (data not shown). We find that hepatotoxicity of CPZ, as demonstrated by ALT release, was significantly increased by 3-4 folds in mice pretreated with LPS (Fig. 5.1.A) or LTA (Fig. 5.1.B). The ALT levels did not differ significantly in mice treated with CPZ, LPS or LTA alone from saline controls upto 24 h (Figs. 5.1.A and 5.1.B).

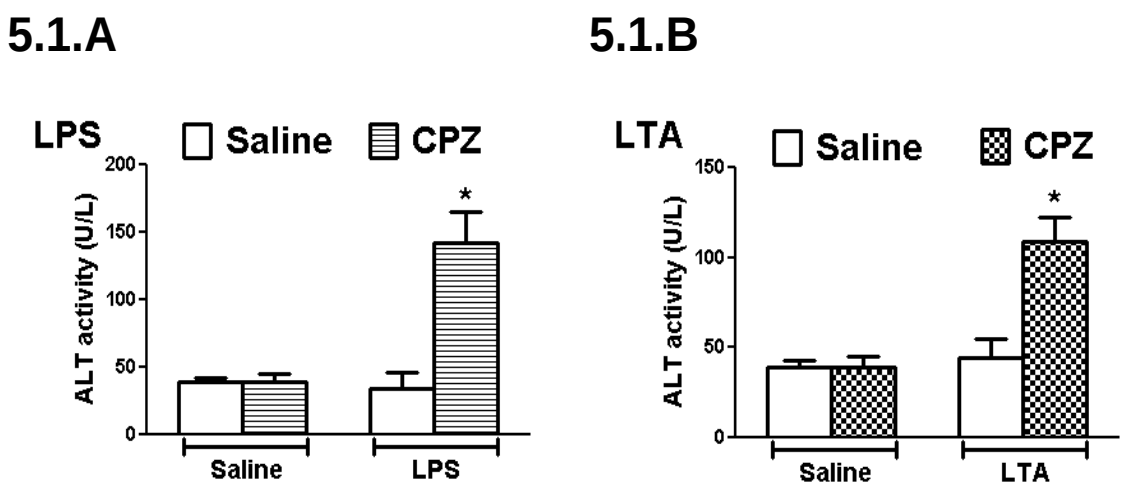

Figure 5.1 Regulation of hepatotoxicity of CPZ in presence of LPS or LTA

C57BL/6 mice were pre-treated with saline, LPS (2 mg/kg) (A) or LTA (6 mg/kg) (B) for 16 h followed by CPZ (5 mg/kg, i.p.) or saline (vehicle control). Blood samples were collected 24 h after CPZ treatment and ALT assays performed. All the data represented are mean ± S.D. from 4-5 mice per group. * $p<0.05$ indicates statistical significance when compared to LPS/Sal or LTA/Sal.

5.4.2. Histopathological examination of liver tissues upon LPS or LTA treatment

Several studies have shown abnormal histopathology of the liver tissue during LPS or LTA treatment (Shaw *et al.*, 2009b; Shaw *et al.*, 2009d). From the qualitative H&E stains, we did not observe any histopathologic abnormalities such as necrotic hepatocytes or immune cell infiltration in liver sections from mice treated with LPS/CPZ or LTA/CPZ compared to saline, LPS, LTA or CPZ alone (Figs 5.2.A and 5.2.B).

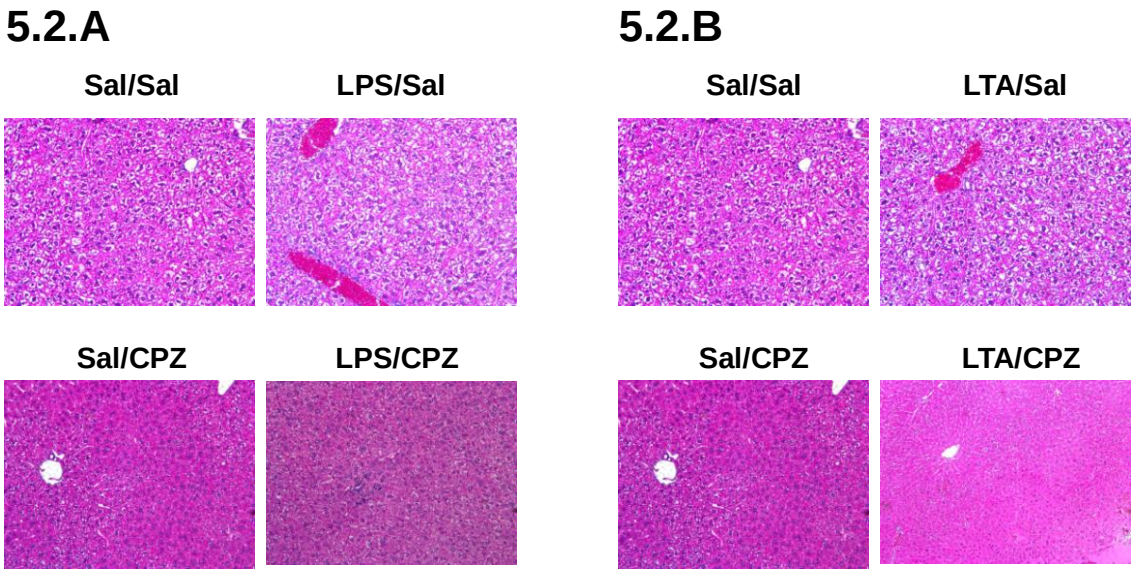

Figure 5.2 Morphological analysis of liver tissue using H&E

C57BL/6 mice were pre-treated with saline, LPS (2 mg/kg) (A) or LTA (6 mg/kg) (B) for 16 h followed by CPZ (5 mg/kg, i.p.) or saline (vehicle control). Liver tissues were harvested 24 h after CPZ treatment and liver histology was studied by H&E staining. The images are represented from one individual mouse although the analysis was done on liver tissues from 3-4 mice per group.

Hepatic glycogen is known to prevent the liver from injury induced by drugs or ischemia-reperfusion (Tang *et al.,* 2002). Depletion of glycogen stores can lead a deficiency in energy reserve, further affecting the cellular metabolic processes and can lead to cell death. However, depletion of hepatic glycogen does not necessarily correlate with the rise in ALT levels, as observed in the case of acetaminophen (Beitia *et al.,* 2000; Hinson *et al.,* 1983). CPZ has been shown to cause glycogen depletion in mice and rats (Mullock *et al.*, 1983; Samorajski *et al.*, 1965; Siddiqui *et al.*, 1979). Changes in liver histopathology such as hepatocellular necrosis, midzonal necrotic foci or accumulation of neutrophils have been observed in LPS-drug costimulation hepatotoxicity animal models. However, we did not observe any marked hepatocellular damage in our studies. As glycogen is involved in maintaining the plasma membrane stability, we wanted to study whether the increase in ALT levels was due to any changes in hepatic glycogen content. Thus, using PAS staining, liver glycogen content in mice pretreated with LPS or LTA prior to saline or CPZ was determined qualitatively. We observed marked depletion of glycogen content (diminished pink area which resembles glycogen) in the liver sections of LPS- (Fig. 5.3.A) or LTA-pretreated mice (Fig. 5.3.B) only in the presence of CPZ. The glycogen content in liver sections of CPZ-, LPS- or LTA-treated mice alone did not differ significantly compared to saline treatment (Figs. 5.3.A and 5.3.B).

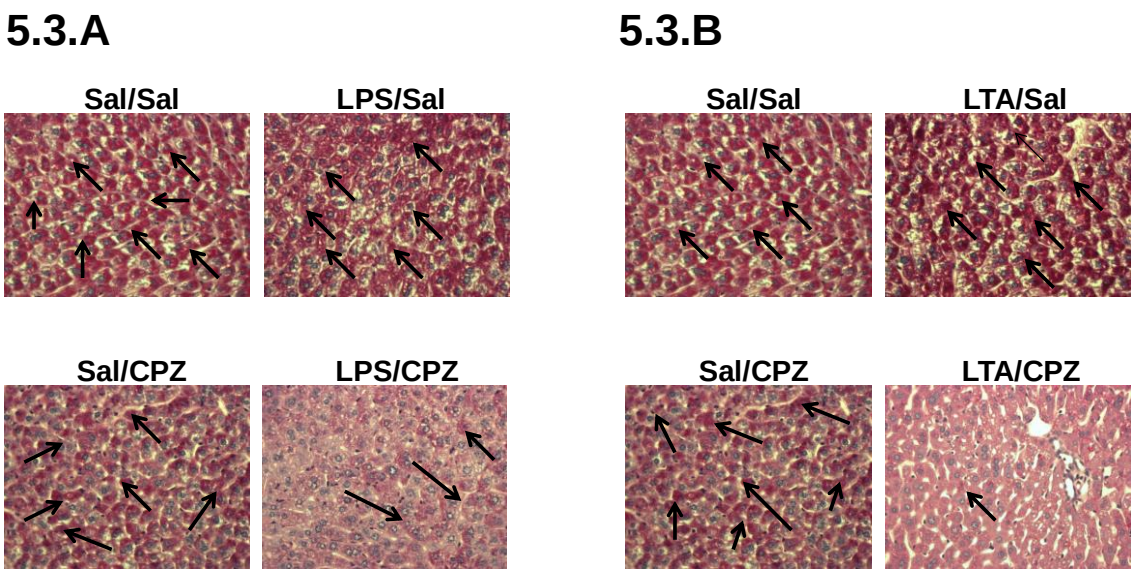

Figure 5.3 Qualitative evaluation of hepatic glycogen content

C57BL/6 mice were pre-treated with saline, LPS (2 mg/kg) (A) or LTA (6 mg/kg) (B) for 16 h followed by CPZ (5 mg/kg, i.p.) or saline (vehicle control). Liver tissues were harvested 24 h after CPZ treatment and hepatic glycogen content was determined using PAS staining. The images are represented from one individual mouse although the analysis was done on liver tissues from 3-4 mice per group. The pink area represents areas with abundant glycogen content.

5.4.3. Increase in serum TNF-α concentration is associated with CPZ-induced hepatotoxicity in presence of LPS or LTA

Previous studies with LPS have shown that TNF-α plays an important role in exacerbating the hepatotoxic responses to drugs in animal models of DILI (Lu *et al.*, 2012; Tukov *et al.*, 2007). We have also previously shown that TNF-α played a major role in increasing the hepatotoxicity of CPZ in primary mouse hepatocytes (Gandhi *et al.*, 2010). On the other hand, IL-1β or IL-6 were not involved. In the present study, mice were pretreated with LPS or LTA 30 min prior to saline or CPZ upto 4 h. Our results demonstrated that serum TNF-α level at 1 h were comparable in LPS or LTA treated mice in presence or absence of CPZ (Figs. 5.4.A and 5.4.B). However, at 2 h, compared to LPS/Sal or LTA/Sal group, serum TNF-α levels were 5-6 folds higher in LPS/CPZ or LTA/CPZ group (Figs. 5.4.A and 5.4.B). Similarly, at 4 h, serum TNF-α levels were 3-4 folds higher in LPS- or LTA-treated mice only in the presence of CPZ Serum TNF-α levels were upon CPZ treatment alone were similar to the saline-treated vehicle control.

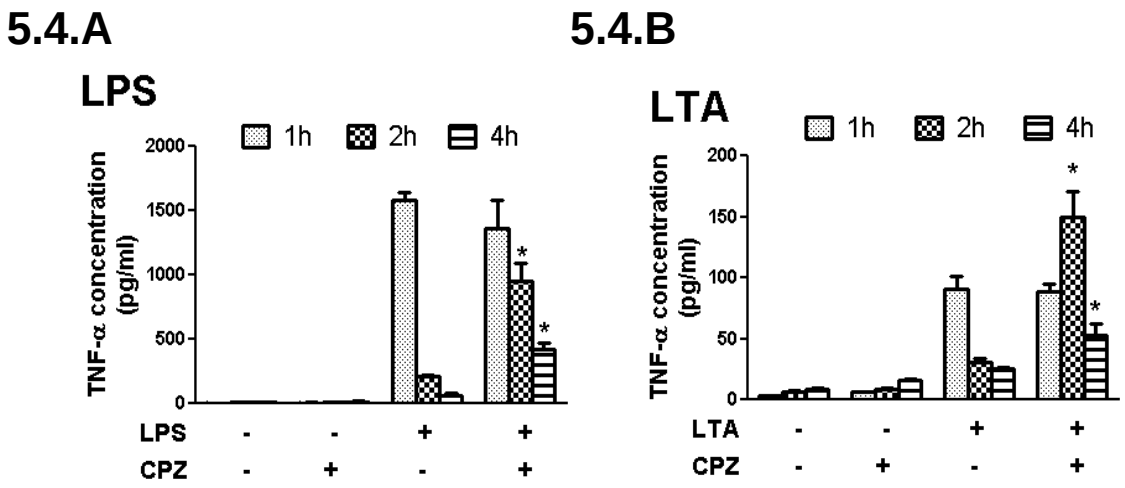

Figure 5.4 Induction of serum TNF-α level upon LPS or LTA treatment

C57BL/6 mice were pre-treated with saline, LPS (2 mg/kg) (A) or LTA (6 mg/kg) (B) for 30 min followed by CPZ (5 mg/kg, i.p.) or saline (vehicle control). Blood samples were collected upto 4 h after CPZ treatment. Determination of serum TNF-α was performed by ELISA as described in the *Materials and Methods* section. All the data represented are mean ± S.D. from 4-5 mice per group. * $p<0.05$ indicates statistical significance when compared to LPS/Sal or LTA/Sal at the corresponding time point.

5.4.4. Sustained activation of JNK by CPZ in the presence of LPS or LTA

Although JNK plays a crucial role in regulation of cell growth, differentiation and proliferation, prolonged activation by inflammatory stress can lead to apoptosis or even hepatic necrosis. We have previously shown that sustained activation of JNK by TNF-α likely played a significant role in CPZ-induced hepatotoxicity in primary mouse hepatocytes (Gandhi *et al.*, 2010). In the present study, liver tissues were harvested from mice pretreated for 30 min with saline, LPS or LTA followed by saline or CPZ upto 4 h. Our immunoblotting studies indicate that LPS alone activated JNK (as evidenced by phosphorylation of JNK) up to 1 h only (Fig. 5.5.A). However in combination with CPZ, the activation of JNK was sustained up to 4 h (Fig. 5.5.A). Similarly, LTA by itself activated JNK upto 1 h. However, JNK was activated up to 4 h in the livers of LTA-pretreated mice only in the presence of CPZ (Fig. 5.5.B). JNK activation was not detected at the 8 h time point in LPS- or LTA-treated mice in presence or absence of CPZ (data not shown). Saline or CPZ by itself did not activated JNK at any of the time points tested.

5.5.A

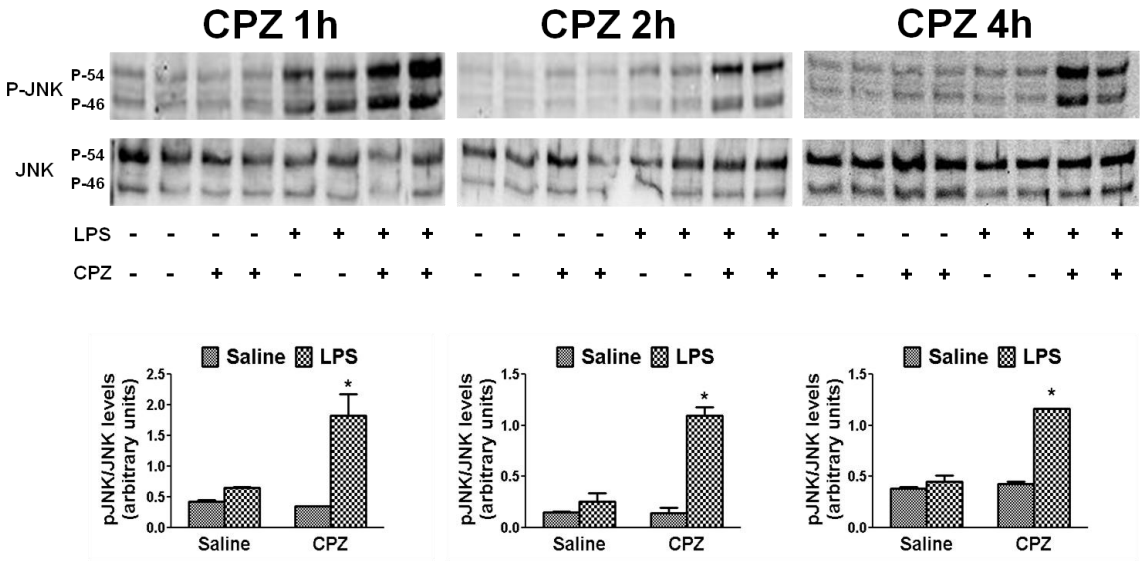
CPZ 1h
CPZ 2h
CPZ 4h
P-JNK
P-54
P-46
JNK
P-54
P-46
LPS
CPZ
Saline
LPS
pJNK/JNK levels (arbitrary units)
Saline
CPZ

5.5.B

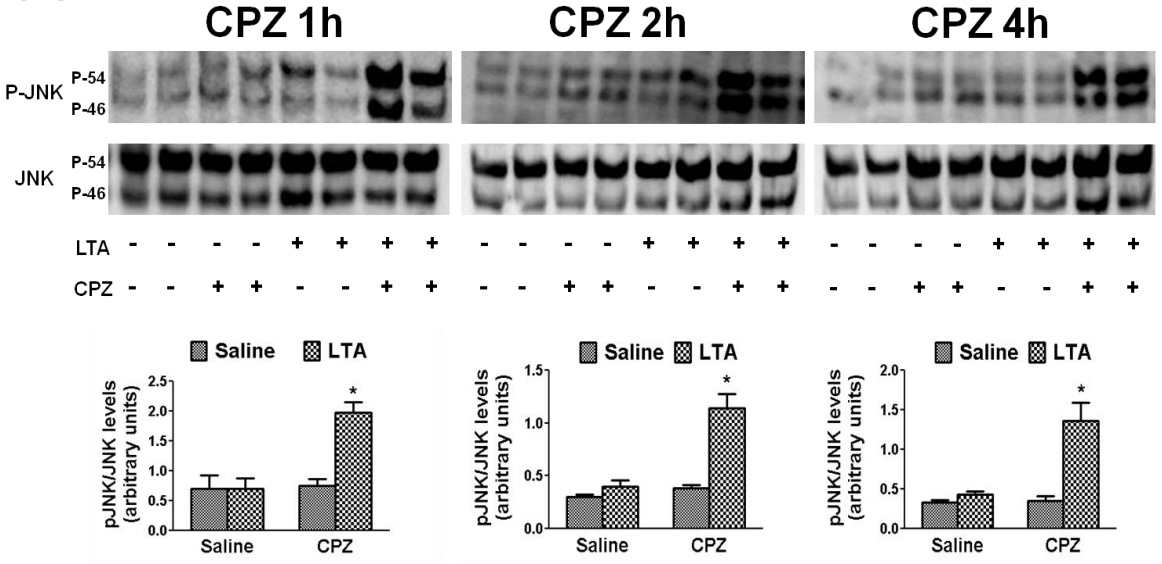
CPZ 1h
CPZ 2h
CPZ 4h
P-JNK
P-54
P-46
JNK
P-54
P-46
LTA
CPZ
Saline
LTA
pJNK/JNK levels (arbitrary units)
Saline
CPZ

Figure 5.5 Activation of JNK by LPS or LTA is prolonged is presence of CPZ

C57BL/6 mice were pre-treated with saline, LPS (2 mg/kg) (A) or LTA (6 mg/kg) (B) for 30 min followed by CPZ (5 mg/kg, i.p.) or saline (vehicle control). Liver tissues were collected upto 4 h after CPZ treatment. Activation of JNK was determined by western blotting as described under the *Materials and Methods* section. Protein bands were quantified using densitometry software. * $p<0.05$ indicates statistical significance when compared to LPS/Sal or LTA/Sal at the corresponding time point.

5.4.5. TIRAP mediates CPZ-induced hepatotoxicity upon LPS or LTA treatment by regulating serum TNF-α release and activation of JNK

To study the role of TIRAP in regulating CPZ-induced hepatotoxicity and hepatic glycogen content in LPS- or LTA-induced inflammation, $TIRAP^{+/+}$ or $TIRAP^{-/-}$ mice were pretreated with saline, LPS (2 mg/kg) or LTA(6mg/kg) 16 h prior to saline or CPZ (5 mg/kg). Serum samples collected after 24 h were analyzed for ALT release. Only in the presence of CPZ, ALT levels were significantly increased (3-4 folds) in LPS- or LTA-treated $TIRAP^{+/+}$ mice. This rise in ALT level was attenuated in the $TIRAP^{-/-}$ mice (Figs. 5.6.A and 5.6.B). ALT levels did not differ significantly in saline, LPS, LTA or CPZ treatment alone in both $TIRAP^{+/+}$ and $TIRAP^{-/-}$ mice (Figs. 5.6.A and 5.6.B).

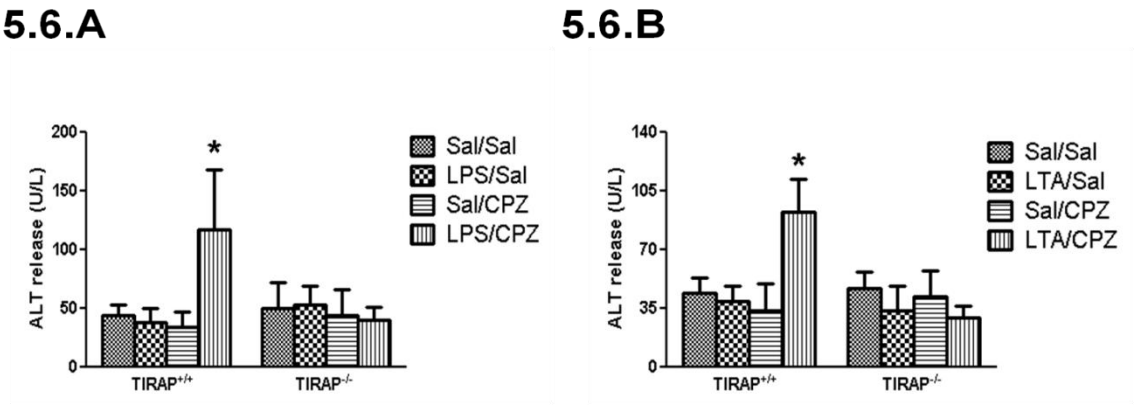

Figure 5.6 Role of TIRAP in LPS- or LTA-induced hepatotoxicity of CPZ

TIRAP$^{+/+}$ and TIRAP$^{-/-}$ mice were pre-treated with saline, LPS (2 mg/kg) (5) or LTA (6 mg/kg) (5) for 16 h followed by CPZ (5 mg/kg, i.p.) or saline (vehicle control). Blood samples were collected 24 h after CPZ treatment and ALT assays performed. All the data represented are mean ± S.D. from 4-5 mice per group. * p<0.05 indicates statistical when compared to LPS/Sal or LTA/Sal in TIRAP$^{+/+}$ mice.

5.4.6. Histopathological examination of liver tissues upon LPS or LTA treatment

In the TIRAP mice, we observed similar results as seen with the C57BL/6 mice for H&E analysis. Surprising, neither LPS/CPZ nor LTA/CPZ from $TIRAP^{+/+}$ group showed any morphological damage to the liver when compared to $TIRAP^{-/-}$ mice. The H&E stains with different treatments are shown in Fig 5.7.A for LPS and 5.7.B for LTA treated $TIRAP^{+/+}$ and $TIRAP^{-/-}$ mice.

5.7.A

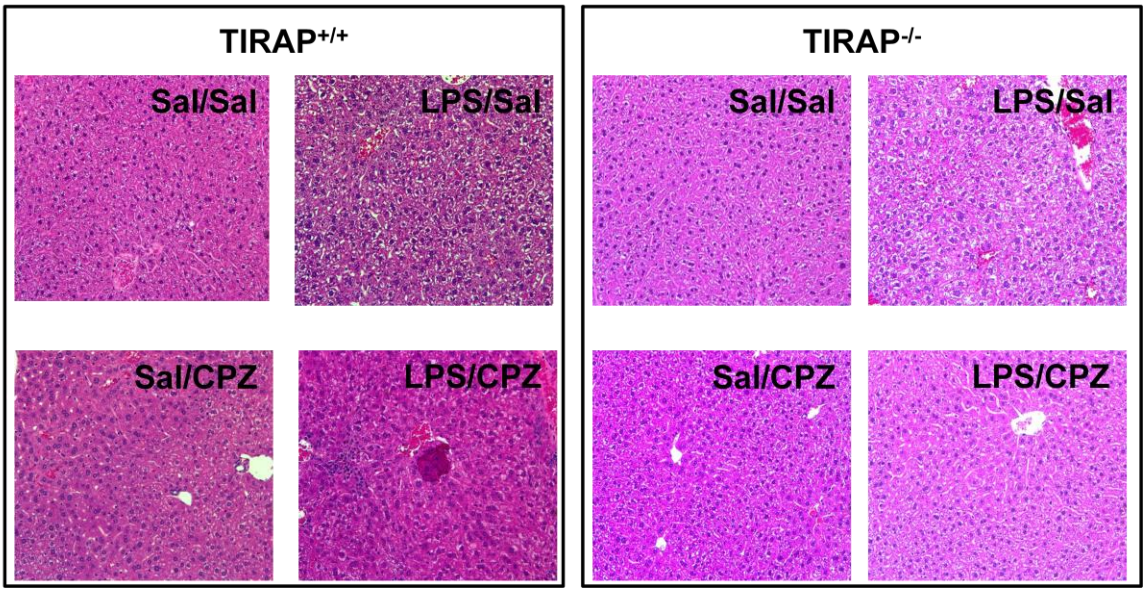

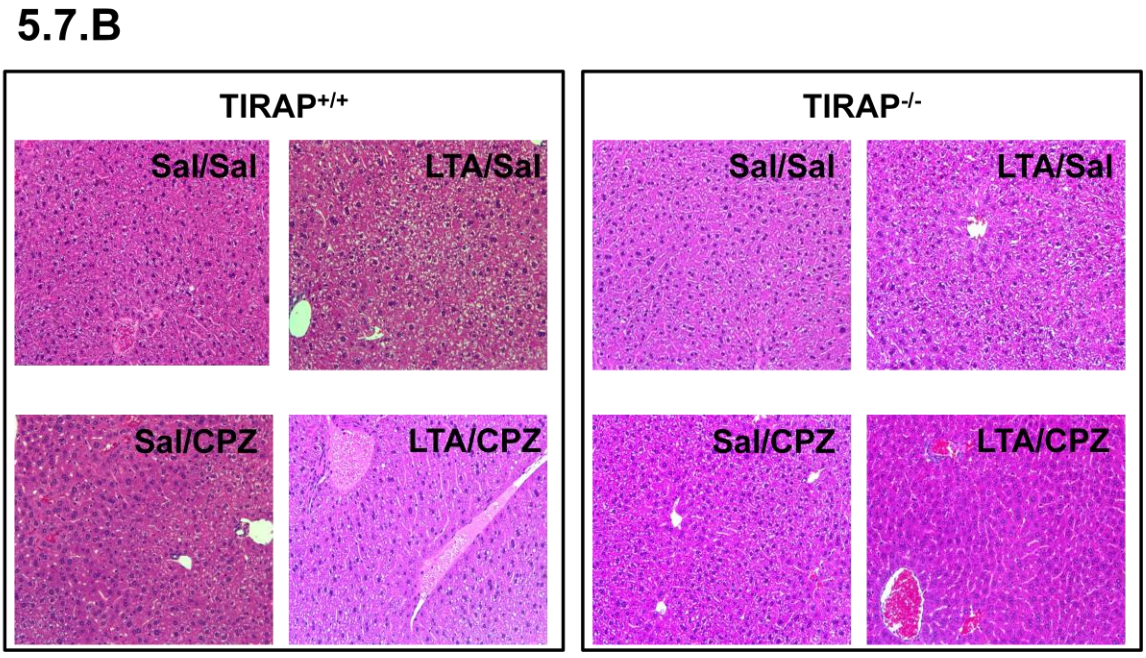

Figure 5.7 Morphological analysis of liver tissue using H&E

$TIRAP^{+/+}$ and $TIRAP^{-/-}$ mice were pre-treated with saline, LPS (2 mg/kg) (A) or LTA (6 mg/kg) (B) for 16 h followed by CPZ (5 mg/kg, i.p.) or saline (vehicle control). Liver tissues were harvested 24 h after CPZ treatment and liver histology was studied by H&E staining. The images are represented from one individual mouse although the analysis was done on liver tissues from 3-4 mice per group.

Surprisingly, although CPZ-induced hepatotoxicity was augmented in LPS or LTA-treated $TIRAP^{+/+}$ mice, we did not observe any marked changes in hepatic glycogen content in LPS/Sal or LTA/Sal compared to LPS/CPZ or LTA/CPZ (Figs. 5.8.A and

5.8.B). This leads us to think that TIRAP does not play a major role in regulating liver glycogen content during drug-induced hepatotoxicity.

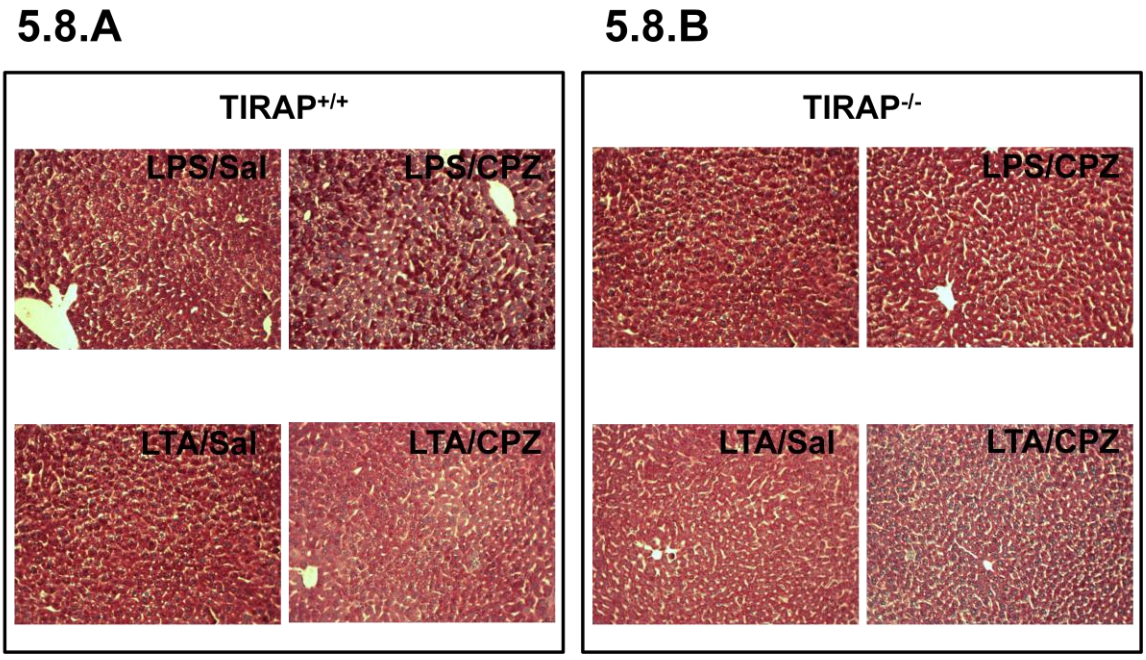

Figure 5.8 Qualitative evaluation of hepatic glycogen content

$TIRAP^{+/+}$ or $TIRAP^{-/-}$ mice were pre-treated with saline, LPS (2 mg/kg) (A) or LTA (6 mg/kg) (B) for 16 h followed by CPZ (5 mg/kg, i.p.) or saline (vehicle control). Liver tissues were harvested 24 h after CPZ treatment and hepatic glycogen content was determined using PAS staining. The images are represented from one individual mouse although the analysis was done on liver tissues from 3-4 mice per group. The pink area represents areas with abundant glycogen content.

5.4.7. TIRAP-dependent regulation of serum TNF-α can be associated with CPZ-induced hepatotoxicity in presence of LPS or LTA

TIRAP also plays an important role in regulating serum TNF-α levels (Ghose *et al.*, 2011a; Ghose *et al.*, 2008). Therefore, to study the role of TIRAP in regulating serum TNF-α levels in CPZ-induced hepatotoxicity, $TIRAP^{+/+}$ or $TIRAP^{-/-}$ mice were pretreated with LPS or LTA followed by saline or CPZ for upto 2 h. We observed significant increase in serum TNF-α levels in LPS or LTA treated $TIRAP^{+/+}$ mice only in the presence of CPZ (Fig. 5.9.A and 5.9.B). On the other hand, serum TNF-α level was attenuated in $TIRAP^{-/-}$ mice in both, LPS/CPZ or LTA/CPZ groups.

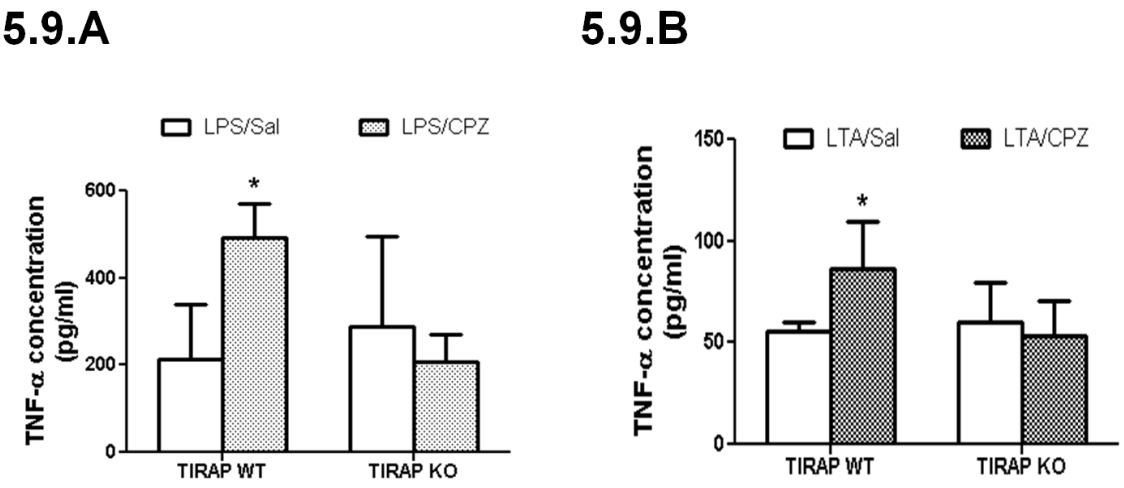

Figure 5.9 Regulation of serum TNF-α upon LPS or LTA treatment

$TIRAP^{+/+}$ and $TIRAP^{-/-}$ mice were pre-treated with saline, LPS (2 mg/kg) (A) or LTA (6 mg/kg) (B) for 30 min followed by CPZ (5 mg/kg, i.p.) or saline (vehicle control). Blood samples were collected 2 h after CPZ treatment. Determination of serum TNF-α was

performed by ELISA as described in the *Materials and Methods* section. All the data represented are mean ± S.D. from 4-5 mice per group. *p<0.05 indicates statistical significance when compared to LPS/Sal or LTA/Sal in TIRAP$^{+/+}$ mice.

5.4.8. Changes in mRNA of cytokines in TIRAP mice

Based on the observations in increase in serum TNF-α in LPS/CPZ or LTA/CPZ TIRAP$^{+/+}$ mice, we wanted confirm whether this increase is specific to the liver. Therefore, we analyzed mRNA of cytokines in the livers of TIRAP$^{+/+}$ and TIRAP$^{-/-}$ mice. Surprisingly, we did not observe any induction of mRNA of TNF-α, IL-1β or IL-6 in LPS-treated TIRAP$^{+/+}$ mice in presence of CPZ (Figs. 5.10.A, B and C). Similarly, mRNA of TNF-α in LTA-treated TIRAP$^{+/+}$ mice in presence of CPZ did not differ significantly compared to LPS/Sal group in the TIRAP$^{+/+}$ mice (Fig. 5.10.D). However, TIRAP$^{-/-}$ mice displayed a decreasing trend in the induction of mRNA of all the three cytokines when compared against TIRAP$^{+/+}$ mice.

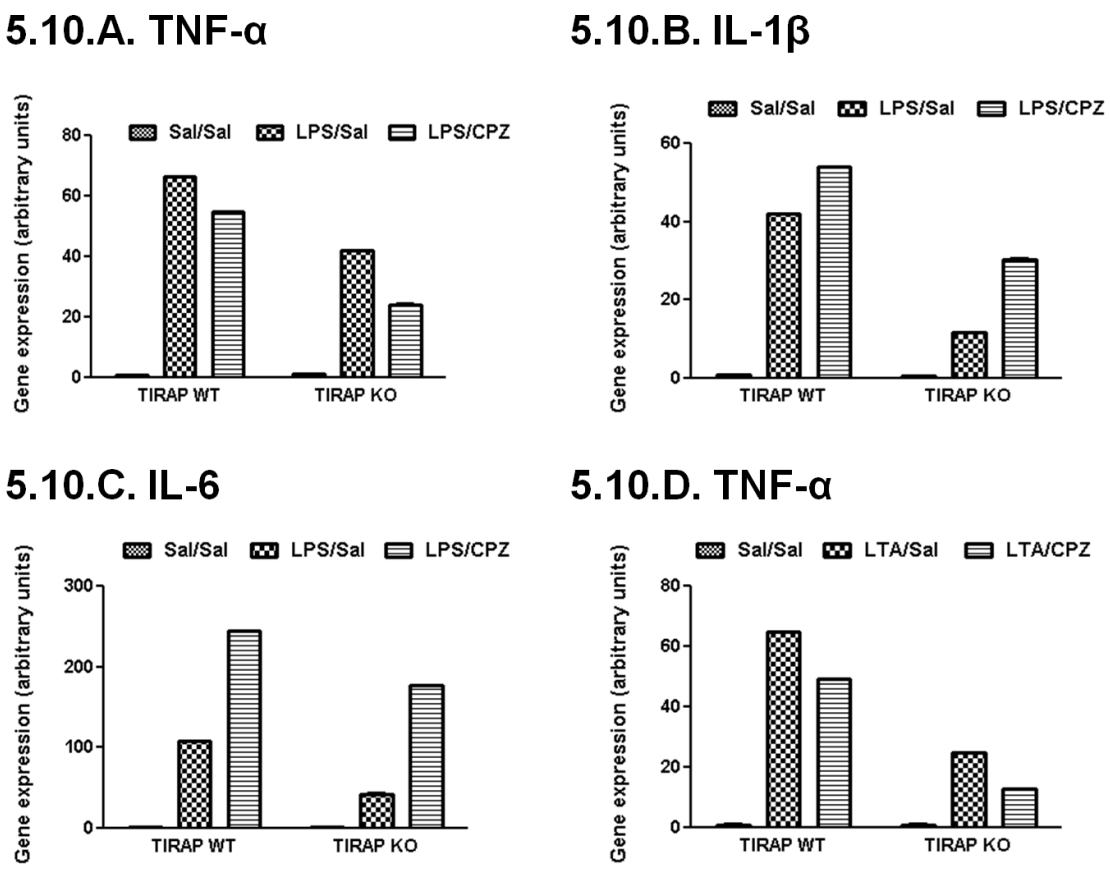

Figure 5.10 Regulation of mRNA of TNF-α, IL-1β and IL-6 upon LPS or LTA treatment in presence or absence of CPZ

TIRAP$^{+/+}$ and TIRAP$^{-/-}$ mice were pre-treated with saline, LPS (2 mg/kg) (A) or LTA (6 mg/kg) (B) for 30 min followed by CPZ (5 mg/kg, i.p.) or saline (vehicle control). Liver tissues were collected 2 h after CPZ treatment. Determination of mRNA of TNF-α was performed by qRT-PCR as described in the *Materials and Methods* section. All the data represented are mean ± S.D. from 4 mice per group.

5.4.9. Activation of JNK is attenuated in TIRAP$^{-/-}$ mice even in presence of CPZ in LPS- or LTA-induced inflammation

In order to study the role of TIRAP in activation of JNK, mouse liver tissues pretreated with LPS or LTA 30 min prior to CPZ were harvested after 2 or 4 h respectively. We observed activation of JNK in LPS/CPZ group at 4 h or LTA/CPZ group at 2 h in TIRAP$^{+/+}$ mice. However, JNK activation in LPS/CPZ or LTA/CPZ groups was blocked in TIRAP$^{-/-}$ mice (Figs. 5.11.A and 5.11.B). Also, CPZ, LPS or LTA did not activate JNK by itself up to 4 h in either of the groups (Figs 5.11.A and 5.11.B). Thus CPZ-induced hepatotoxicity may likely be mediated by TIRAP involving sustained activation of JNK.

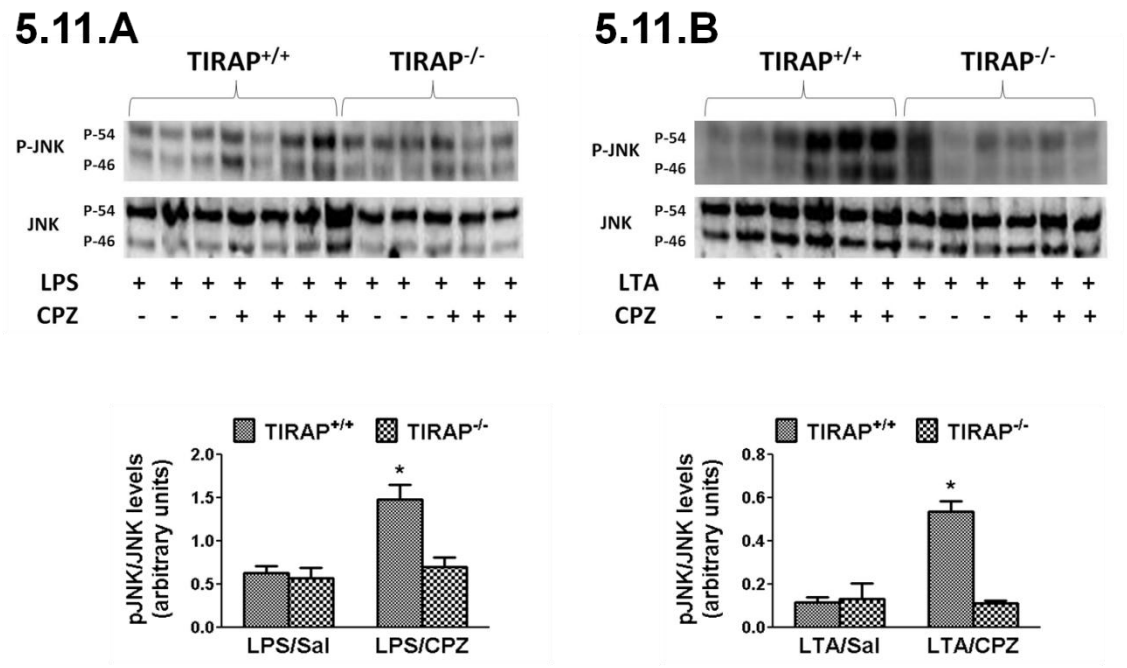

Figure 5.11 Activation of JNK by LPS or LTA in presence of CPZ is TIRAP-dependent

TIRAP$^{+/+}$ and TIRAP$^{-/-}$ mice were pre-treated with saline, LPS (2 mg/kg) (A) or LTA (6 mg/kg) (B) for 30 min followed by CPZ (5 mg/kg, i.p.) or saline (vehicle control). Liver tissues were collected 2 h after CPZ treatment. Activation of JNK was determined by western blotting as described under the *Materials and Methods* section. Protein bands were quantified using densitometry software. * p<0.05 indicates statistical significance when compared to LPS/Sal or LTA/Sal in TIRAP$^{+/+}$ mice.

5.5. Discussion

The underlying mechanisms involved in idiosyncratic DILI in humans are widely debated. Immune-mediated hypersensitivity reactions (Uetrecht, 2003), role of the hemostatic system (Shaw *et al.*, 2009c), accumulation of polymorphonuclear neutrophils (Zou *et al.*, 2011), genetic polymorphisms in drug metabolizing enzymes (Poolsup *et al.*, 2000) are some of the contributing factors to IDILI.

Inflammation is considered to be an underlying factor determining the susceptibility for the toxic effects of xenobiotic agents including CPZ (Buchweitz *et al.*, 2002; Roth *et al.*, 1997). In the present study, we observed that CPZ treatment in mice led to ~3 folds rise in rise in serum ALT levels in LPS/CPZ or LTA/CPZ groups (Figs. 5.1.A and 5.1.B). Previous studies have shown a ~1.5-fold increase in ALT levels in CPZ-treated rats in the presence of LPS (Buchweitz *et al.*, 2002). Thus, considering similar hepatotoxic responses in both, rats (~1.5 folds increase in ALT) and mice (~3 folds increase in ALT), it may be stated that the development of CPZ-inflammation interaction leads to a common phenomenon which may independent of the species and might share similar mechanisms which could be extrapolated to CPZ mediated ADRs in humans. The molecular mechanism by which LPS or LTA increases hepatotoxic responses to CPZ is unknown. LPS- or LTA-treatment of rodents or cells are known to down-regulate drug metabolizing enzymes, leading to altered drug metabolism (Gandhi *et al.*, 2012; Ghose *et al.*, 2009; Ghose *et al.*, 2008; Richardson *et al.*, 2006; Sewer *et al.*, 1996). Similarly, LPS-induced changes in drug metabolizing enzymes were linked linked with altered

pharmacokinetics and pharmacodynamics of drugs such as midazolam, verapamil and ketoprofen in animals (de Boever *et al.*, 2010; Gandhi *et al.*, 2012; Sermsappasuk *et al.*, 2008). Metabolism of CPZ is very complex. The major metabolic pathways include 7-hydroxylation, N-dealkylation, N-oxidation and S-oxidation (Hartmann *et al.*, 1983). Of these, the 7-hydroxylation pathway, catalyzed mainly by CYP2D6 and partially by CYP1A2, is considered to be the major metabolic pathway for CPZ metabolism in humans (Yeung *et al.*, 1993; Yoshii *et al.*, 2000). It was shown that the ring-hydroxylated metabolites of CPZ are highly potent than the sulfoxidation product in causing jaundice in humans (Watson *et al.*, 1988). Another study showed that the demethylated metabolites, mono- and didesmethyl-CPZ, were three and six times, respectively, more potent than CPZ in causing the release of aspartate aminotransferase from isolated rat hepatocytes (Abernathy *et al.*, 1977). 7-hydroxyhchlorpromazine is equally potent as CPZ (Manian *et al.*, 1965). Although, LPS down-regulates the gene expression of several CYP isoforms in mice, the effects of LPS or LTA on regulation of CYP2D6 and the enzymes responsible for catalyzing the demethylaion of CPZ are not known. Therefore, the possibility that the hepatotoxic effects of CPZ is a function of a reactive metabolite demands for further studies.

In rats, LPS-CPZ co-exposure led to marked histopathological changes demonstrated by numerous midzonal and subserosal lesions (Buchweitz *et al.*, 2002). In our study, histopathological examinations revealed no parenchymal cell damage in CPZ, LPS or LTA treated mice compared to the saline controls (Figs. 5.2.A and 5.2.B). To our

surprise, however, we did not observe any subserosal or midzonal necrotic foci (Figs. 5.2.A and 5.2.B) which is in contrast to the previous reports in rats and humans (Buchweitz *et al.*, 2002; Ishak and Irey, 1972). In addition to species-specific differences, dosing schedules can lead to this discrepancy. For e.g. the dosing protocol of LPS and CPZ used in the rat study was different compared to the present study. In rats, the 70 mg/kg dose of CPZ translates to ~10 mg/kg in mice, which is twice than that used in the present study. Next, in rats, LPS was administered intravenously only 2 h before CPZ as opposed to 16 h intraperitoneal pretreatment in our study.

It has been previously shown that non-hepatotoxic doses of APAP decreased liver glycogen content and this may be used as a sensitive marker to study metabolic changes in the liver (Hinson *et al.*, 1983). CPZ-mediated periportal loss of hepatic glycogen and centrilobular fatty liver have been reported in rats in relation to hepatotoxicity (Mullock *et al.*, 1983). Based on the fact that phenothiazine therapy (particularly CPZ) is commonly associated with a marked reduction in the liver glycogen content (Samorajski *et al.*, 1965), we evaluated whether there was any synergistic effect of LPS or LTA with CPZ on reducing liver glycogen. Compared to saline treated mice, the liver glycogen content did not change among CPZ, LPS or LTA by themselves (Figs. 5.3.A and 5.3.B). However, LPS-CPZ or LTA-CPZ co-exposure led to a marked reduction in glycogen content compared to CPZ, LPS or LTA alone (Figs. 5.3.A and 5.3.B). This significant loss of liver glycogen can be critical as hepatocytes with high glycogen content have abundant energy source in the form of ATP, which plays an important role in stabilizing

cell membrane and metabolic functionality of drug metabolizing enzymes (Fouts, 1963; Tang *et al.*, 2002). As less than 1% of CPZ is excreted unchanged and ~70% is recovered as various metabolites, a decrease in drug metabolism can lead to accumulation, further leading to hepatotoxic effects of CPZ in inflammation. However, the exact mechanism by which CPZ may lead to a decrease in liver glycogen needs further investigation.

The pro-inflammatory cytokine, TNF-α, plays an important role in mediating hepatotoxic responses of several xenobiotics (Shaw *et al.*, 2007; Tukov *et al.*, 2007; Zou *et al.*, 2009a). We find that LPS- or LTA-mediated increase in serum TNF-α levels were sustained upto 4 h only in the presence of CPZ (Figs. 5.4.A and 5.4.B). However, the data from the present study are in contrast to the previous reports in which it was shown that, CPZ injected prior to LPS plays a hepatoprotective role in attenuating the toxic effects of LPS and increased TNF-α levels in mice (Gadina *et al.*, 1991; Ghezzi *et al.*, 1996). This discrepancy can arise due to several factors. Although the doses of CPZ were not significantly different (4 mg/kg in earlier studies vs. 5 mg/kg in the current study), *Gadina et al* used 75 µg/kg and 30 mg/kg of LPS and *Ghezzi et al* used 2.5 µg/mouse of LPS, respectively. Also, the earlier studies used CD-1 mice (Gadina *et al.*, 1991; Ghezzi *et al.*, 1996) where as C57/BL6 mice were used in the present study. Thus, strain differences can account to the disparate observations. Also, CPZ was administered before LPS in the previous studies as opposed to 30 min post-treatment of CPZ in the present study. In addition, *in vitro* studies also showed that CPZ blocked the cytotoxic effects of TNF-α by inhibiting its synthesis in human monocytic leukemia cells or inhibition of

mRNA for TNF-α in human thymocytes (Schleuning *et al.*, 1989; Zinetti *et al.*, 1995). Thus, the dosing regimen of CPZ may determine its hepatoprotective or hepatotoxic nature. Altogether, the therapeutic effectiveness of CPZ in lowering TNF-α in human requires intensive investigation.

Recently, JNK has been targeted as a major contributor in APAP-induced liver injury (Gunawan *et al.*, 2006; Hanawa *et al.*, 2008; Henderson *et al.*, 2007). In our recent publication, we showed that TNF-α-induced hepatotoxicities of APAP or CPZ in primary mouse hepatocytes were blocked when pretreated with the JNK inhibitor (Gandhi *et al.*, 2010). We also showed that TNF-α-mediated activation of JNK was sustained up to 2 h only in the presence of APAP or CPZ. These findings are in accordance with our data from the present study in which we observed sustained activation of JNK (upto 4 h) in LPS- or LTA-treated mice only in the presence of CPZ (Figs. 5.5.A and 5.5.B). Although JNK plays an important role in stress response in cells, sustained activation is believed to promote cell injury and death by activation of downstream pro-apoptotic genes (Singh and Czaja, 2007). The link between sustained activation of JNK and cell death may possibly be related to increase in TNF-α production (Henderson *et al.*, 2007). However, further work will be needed to study the synergistic interaction between bacterial endotoxins and CPZ in causing prolonged activation of JNK.

TIRAP plays an important role in regulating gene expression of key hepatic phase I and phase II drug metabolizing enzymes only in TLR2 and not in TLR4-mediated signaling pathway (Ghose *et al.*, 2011a; Ghose *et al.*, 2008). The increase in serum ALT

upon CPZ treatment in LPS- or LTA-pretreated TIRAP$^{+/+}$ mice was blocked in TIRAP$^{-/-}$ mice (Figs. 5.6.A and 5.6.B). TIRAP is the proximal adaptor molecule involved in LPS-induced TLR4 or LTA-induced TLR2 activation. It is also known to regulate the LPS-induced apoptosis in macrophages by regulating the activation of NF-κB which plays an important role in transcription of genes involved in apoptosis (Fitzgerald *et al.*, 2001; Horng *et al.*, 2001). Recently, TIRAP was shown to regulate LPS-mediated caspase activation in endothelial cells (Bannerman *et al.*, 2002). However, further studies will be needed to determine if TIRAP-dependent hepatotoxicity of CPZ is due to altered drug metabolism due to the fact that TIRAP is differentially involved in regulation of drug metabolizing enzyme genes in LPS- or LTA-induced inflammation.

Although we did not observe any morphological changes in the histology of liver tissue treated with LPS or LTA in presence of CPZ in TIRAP$^{+/+}$ mice compared to TIRAP$^{-/-}$ mice, there were also no significant differences in the hepatic glycogen content between LPS/Sal or LTA/Sal when compared to LPS/CPZ or LTA/CPZ in TIRAP$^{+/+}$ mice. Thus, additional studies will be needed to delineate the mechanisms involved in hepatic glycogen synthesis in TIRAP$^{+/+}$ mice.

We previously showed that mRNA levels of pro-inflammatory cytokines induced by LPS or LTA treatment in livers of TIRAP$^{+/+}$ mice did not differ from the TIRAP$^{-/-}$ mice (Ghose *et al.*, 2011a; Ghose *et al.*, 2008). In accordance with these studies, even in the presence of CPZ, we observed no changes in mRNA levels of the cytokine genes in LPS- or LTA-treated TIRAP$^{+/+}$ mice compared to TIRAP$^{-/-}$ mice (Figs. 5.9.A, B, C and

D). Based on these observations, we conclude that changes in cytokine gene expression may not be the major determinant in predisposing drugs in causing hepatotoxicity. We previously showed that serum cytokine levels were significantly attenuated in $TIRAP^{-/-}$ mice (Ghose *et al.*, 2011a; Ghose *et al.*, 2008). Similarly, in the present study, significant induction of serum TNF-α levels by CPZ in LPS- or LTA-treated $TIRAP^{+/+}$ mice was attenuated in $TIRAP^{-/-}$ mice (Figs. 5.10.A and 5.10.B). Activation of JNK in LPS or LTA-treated $TIRAP^{+/+}$ mice in presence of CPZ was attenuated in $TIRAP^{-/-}$ mice (Figs. 5.11.A and 5.11.B). We and others have shown that TIRAP is essential for regulation of JNK in LPS or LTA-induced inflammation (Ghose *et al.*, 2011a; Horng *et al.*, 2001).

In conclusion, the novel finding in our study was that a non-hepatotoxic dose of CPZ was rendered hepatotoxic by LPS or LTA by a TIRAP-dependent mechanism. Thus, the underlying mechanisms responsible for precipitating idiosyncratic hepatotoxicity of CPZ could be attributed to TIRAP which was shown to regulate serum secretion of the pro-inflammatory cytokine, TNF-α, and activation of JNK in presence of LPS or LTA. Thus, the TIRAP-dependent signaling pathway may be effectively targeted to prevent DILI to restrict the progression and severity of liver injury during acute inflammatory episodes.

CHAPTER 6

Role of c-jun N-terminal kinase (JNK) in regulating tumor necrosis factor-alpha (TNF-α) mediated increase of acetaminophen (APAP) and chlorpromazine (CPZ) toxicity in murine hepatocytes

6.1. Abstract

Drug Induced Liver Injury (DILI) accounts for more than 50% of the cases of acute liver failure in this country, and is the major cause of drug withdrawal from the market. DILI has been associated with the induction of pro-inflammatory cytokines, including tumor necrosis factor-alpha (TNF-α). Pro-inflammatory cytokines activate the mitogen activated protein kinase, c-Jun-N-terminal kinase (JNK) in the liver. Recent studies have shown that JNK can regulate the hepatotoxicity of the analgesic, acetaminophen (APAP). Several reports have shown that inflammation induced by the endotoxin, lipopolysaccharide (LPS) augments the toxic response to hepatotoxicants *in vivo*. However, the mechanism by which inflammation alters drug-induced hepatotoxicity is not known. This study investigated the role of inflammatory mediators in regulating the toxicity of the hepatotoxic drugs, APAP or chlorpromazine (CPZ) in primary mouse hepatocytes. We found that, pre-treatment with TNF-α resulted in ~50 to 60% increase in alanine aminotransferase (ALT) levels by APAP or CPZ, while IL-1β or IL6 treatments showed only 15-20% increase in ALT release. The bacterial components, LPS or lipoteichoic acid (LTA) increased ALT release by ~35 to 38% upon drug treatment of the hepatocytes. The JNK inhibitor, SP600125 significantly diminished APAP and CPZ toxicity with or without TNF-α. Pre-treatment with TNF-α resulted in prolonged activation of JNK (upto 2 hours) in the presence of APAP or CPZ. These results show that TNF-α is the major cytokine involved in sensitizing hepatocytes to APAP- or CPZ-induced hepatotoxicity, likely by a mechanism involving sustained activation of JNK.

6.2. Introduction

Drug-induced liver injury (DILI) has been reported with more than 1100 toxins including herbals and is the leading cause of approved drug withdrawals in the US (Temple and Himmel, 2002). Recent evidence shows that treatment with the Gram-negative bacterial endotoxin; lipopolysaccharide (LPS) predisposes the liver to toxic effects of several xenobiotics (Roth *et al.*, 1997) including the known hepatotoxicants, acetaminophen (APAP) and chlorpromazine (CPZ) (Buchweitz *et al.*, 2002; Roth *et al.*, 1997). Furthermore, LPS has been shown to alter the expression of hepatic drug metabolizing enzymes and transporters, and the pro-inflammatory cytokines, tumor necrosis factor-alpha (TNF-α), interleukin-1β (IL-1β) and IL-6 were involved in this process (Aitken *et al.*, 2006; Ghose *et al.*, 2008; Ghose *et al.*, 2004). In addition, we have recently shown that the Gram-positive bacterial component, lipoteichoic acid (LTA) can also induce pro-inflammatory cytokines and regulate key hepatic genes involved in drug metabolism and transport (Ghose *et al.*, 2009). Thus, induction of inflammatory responses can potentially alter the toxic responses to select drugs.

The pro-inflammatory cytokine, TNF-α stimulates a number of cellular responses including cell proliferation, production of other inflammatory mediators and programmed cell death. TNF-α is also one of the major mediator of inflammatory response stimulated by LPS. Recently, TNF-α dependent hepatotoxicity of trovafloxacin was demonstrated in mice exposed to LPS (Shaw *et al.*, 2007). Elevation of pro-inflammatory cytokines has been associated with APAP-induced liver injury (Blazka *et al.*, 1996; Blazka *et al.*, 1995;

James *et al.*, 2003b). In addition, Blazka showed that inhibition of TNF-α or IL-1α with specific antibodies had protective effect against APAP-induced liver injury in mice (Blazka *et al.*, 1996). On the other hand, TNF-α was shown to exhibit no influential role on APAP toxicity in tumor necrosis factor/lymphotoxin-alpha gene knockout mice (Boess *et al.*, 1998). Recently, APAP was rendered hepatotoxic in mice by an otherwise nontoxic dose of LPS (Newport et al., 2005). In contrast, LPS was shown to be protective against APAP-induced liver injury (Ishikawa *et al.*, 1990b; Ishikawa *et al.*, 1990c; Liu *et al.*, 2000). These studies imply a controversial role of LPS and cytokines in APAP-induced liver injury, with both increase and decrease in toxicity reported in the presence of these inflammatory mediators. Thus the role of pre-existing inflammation in modulation of the toxic effects of APAP needs to be further investigated.

The anti-psychotic drug, CPZ, is mostly shown to induce cholestatic liver injury rather than conventional parenchymal damage and has caused several idiosyncratic responses during its therapeutic use (Buchweitz *et al.*, 2002). Clinical evidence suggests that underlying inflammation are risk factors for the appearance of these responses (Buchweitz *et al.*, 2002). However, animal models (Ros *et al.*, 1979) and *in vitro* studies (Abernathy *et al.*, 1977) have indicated that CPZ is also intrinsically toxic to the liver. It has been reported that pre-treatment with a non-toxic dose of LPS can enhance the toxic responses to CPZ (Buchweitz *et al.*, 2002) by unknown mechanisms.

The pro-inflammatory cytokines and the bacterial components, LPS or LTA, are known to activate the mitogen-activated kinase, c-Jun-N-terminal kinase (JNK) in the

liver (Ghose *et al.*, 2009; Ghose *et al.*, 2008; Moriguchi *et al.*, 1997). JNK plays a key role in regulation of cell growth, differentiation and apoptosis. Sustained activation of JNK was shown to be a major contributor to APAP induced liver injury, and inhibition of JNK was protective to APAP hepatotoxicity (Bourdi *et al.*, 2008; Gunawan *et al.*, 2006; Kaplowitz *et al.*, 2008). CPZ-induced activation of JNK was observed in renal epithelial A6 cells (Niisato *et al.*, 1999). However, it is not known whether JNK is involved in inflammation-mediated regulation of the toxic responses to drugs.

Therefore, in this study we sought to determine the role of inflammatory mediators in APAP- or CPZ-induced hepatotoxicity *in vitro*. We find that pre-treatment of primary mouse hepatocytes with the pro-inflammatory cytokine, TNF-α significantly increased the toxic response to APAP or CPZ. No such induction was observed with pre-treatment of hepatocytes with IL-1β or IL-6. Sustained activation of JNK was detected after treatment of hepatocytes with APAP or CPZ in the presence of TNF-α. Our results show that sustained activation of JNK by APAP or CPZ in combination with TNF-α contributes to hepatocyte damage.

6.3. Materials and methods

6.3.1. Materials

Lipopolysaccharide (*E. coli*) and lipoteichoic acid (*S. aureus*) were purchased from InvivoGen (San Diego, CA) and freshly diluted to 5 mg/mL of LPS and 1 mg/mL of LTA in pyrogen-free 0.9% NaCl solution. TNF-α, IL-1β and IL-6 were purchased from R and D Systems, Minneapolis, MN. The anti-JNK (# 9252) and anti-phospho JNK antibodies (# 9251) were purchased from Cell Signaling Technology, Beverly, MA. Unless otherwise stated, all other chemicals were purchased from Sigma-Aldrich, St. Louis, MO.

6.3.2. Animals

Male, C57BL/6 mice (~8 weeks) weighing 20-25 g were obtained from The Harlan Laboratories, Houston, TX. The animals were maintained in a temperature and humidity controlled environment and 12 h light/dark cycle with free access to water and rodent chow *ad libitum*. All animal experimental and surgical procedures were strictly performed as per the Institutional Animal Care and Use Committee guidelines.

6.3.3. Cell culture

Primary mouse hepatocytes were isolated using a two-step collagenase perfusion method with modifications as described previously (Li et al., 2002). Briefly, after digestion, liver was excised and transferred to a sterile 50 ml conical tube containing William's medium E supplemented with 1% streptomycin, glutamine, 0.1% gentamycin, glucagon and 10% fetal bovine serum. Hepatocytes were purified through a Percoll

gradient followed by two washings. Cell viability was assessed by Trypan blue dye exclusion method. Only isolations yielding more than 85% viable hepatocytes were used in the study. Hepatocytes were plated in 24-well primaria plates (BD PharMingen) at a density of $1x10^5$ cells/ml/well in serum-containing William's medium E. Four hours later, medium was replaced with pre-warmed serum-starved medium and cells were allowed to incubate overnight before any treatments.

6.3.4. Treatment of hepatocytes

Hepatocytes were pre-treated with 10 ng/mL each of IL-1β, IL-6 or TNF-α, or 0.0001% bovine serum albumin in phosphate-buffered saline for 30 min. This was followed by addition of APAP (2.5 mM) or CPZ (20 µM) or their corresponding vehicles (0.1 % DMSO for APAP and saline for CPZ). Similarly, the cells were treated with 1 µg/ml each of LPS or LTA or saline control 30 min prior to drug treatments. Supernatants were collected after 24 h for toxicity assays. For investigating the role of JNK, cells were pre-incubated with the JNK inhibitor, SP600125 (30 µM) for 30 min, followed by TNF-α treatment for 30 min, after which the cells were treated with APAP or CPZ. For JNK activation, cells were treated with the pro-inflammatory cytokines (TNF-α, IL-1β, or IL-6) or LPS or LTA up to 6 h. In order to measure JNK activation by APAP or CPZ in presence of cytokines, hepatocytes were pre-treated with the cytokines for 30 min, followed by treatment with APAP or CPZ from 0 to 2 h. Therefore, the cells were exposed to the cytokines for 2.5 h and the drugs at the indicated time points.

6.3.5. Alanine aminotransferase assay (ALT) assay

ALT assay was performed according to the manufacturer's instructions with slight modifications (ALT Infinity GPT, Thermo Fisher Scientific Inc., Middletown, VA). Briefly, 20 µl of supernatant was added to 200 µl of ALT reagent and incubated at 37 $^{\circ}$C for 8 minutes. The change in absorbance was recorded per minute at 340 nm. ALT release in the medium is expressed as a percentage of total ALT (intracellular + extracellular). Two percent Triton-X 100 served as a positive control to induce 100% cell lysis.

6.3.6. Lactate dehydrogenase (LDH) assay

The amount of LDH leaked out of the cells into the medium was determined by LDH assay as per the manufacturer's instructions (Roche Pharmaceuticals Ltd., Nutley, NJ). Briefly, 100 µl of cell culture supernatant was mixed with 100 µl of LDH assay reagent followed by 30 min incubation in dark at room temperature. Cells incubated with only medium served as the blank. Cytotoxicity was expressed as the percentage of LDH released in the supernatants compared to the total LDH from 2% Triton X-100 lysed cells. The calculations are similar to as described above for ALT assay.

6.3.7. Cell fractionation and immunoblotting

Whole cell extracts were prepared from hepatocytes pre-treated with LPS/LTA or cytokines as described previously (Ghose et al., 2008, 2009). Briefly cells were homogenized in 0.2 mL buffer containing 50 mM Tris-HCl, pH 7.5, 0.5 M NaCl, 2 mM each of EDTA and EGTA, 1.0% Triton X-100, 0.25% deoxycholate, 1 mM NaF, 1 mM

Na_3VO_4, and protease inhibitor cocktail (VWR, # 80053-846) for 30 minutes on ice. The samples were analyzed by SDS-polyacrylamide gel electrophoresis, transferred to nitrocellulose membrane and probed with JNK (1:500) or phospho (P)-JNK antibodies (1:1000). Membranes were subsequently washed and probed with a goat anti-rabbit IgG-AP secondary antibody (1:2000) for 1 h at room temperature. The blots were then washed with TBS-Tween20 and incubated with Tropix® CDP Star® Nitro block II™ ECL reagent as per the manufacturer's instructions (Applied Biosystems, Foster City, CA, USA). Membranes were analyzed on FluorChem FC Imaging System (Alpha Innotech). Protein bands were quantified by densitometry using the AlphaEase software.

6.3.8. Statistical analysis

All numerical data were presented as mean ± S.D. from at least four independent experiments and analyzed using the two-way ANOVA followed by Bonferroni's multiple comparison test. Statistical significance was demonstrated with $p<0.05$.

6.4. Results

6.4.1. Inflammatory mediators enhance toxic responses to APAP in hepatocytes

Several studies have reported either an increase or decrease in toxic responses to APAP by LPS (Blazka *et al.*, 1995; Laskin *et al.*, 1986). Although, pro-inflammatory cytokines are known to mediate the effect of LPS in the liver (Aitken *et al.*, 2006; Ghose *et al.*, 2008), it is not known whether individual cytokines can augment the hepatotoxic effects of drugs. Therefore, we studied the role of individual pro-inflammatory cytokines and endotoxins in hepatocytes. Based on our initial dose-response experiments, 2.5 mM APAP was selected due to minimal toxicity in hepatocytes (data not shown). Hepatocytes were pre-treated with cytokines or endotoxins for 30 min followed by APAP or the vehicle, 0.1 % DMSO for 24 h. As expected, we find that percent ALT release by 2.5 mM APAP by itself was comparable to the DMSO control (Fig. 6.1). Interestingly, ALT release was significantly increased (~60% increase, $p<0.001$) in the TNF-α group as compared with APAP by itself (Fig. 6.1.A, Table 6.1). IL-1β or IL-6 treatment resulted in ~15-20% increase in APAP toxicity, however this increase was not statistically significant. The cytokines by themselves did not show any significant increase in toxicity. Treatment with the bacterial components, LPS or LTA, resulted in a moderate, though significant increase in ALT release (30-40% increase, $p<0.05$) (Fig. 6.1.B, Table 6.1). The above results were further confirmed by LDH assay that was in agreement with the ALT assay (Table 6.2).

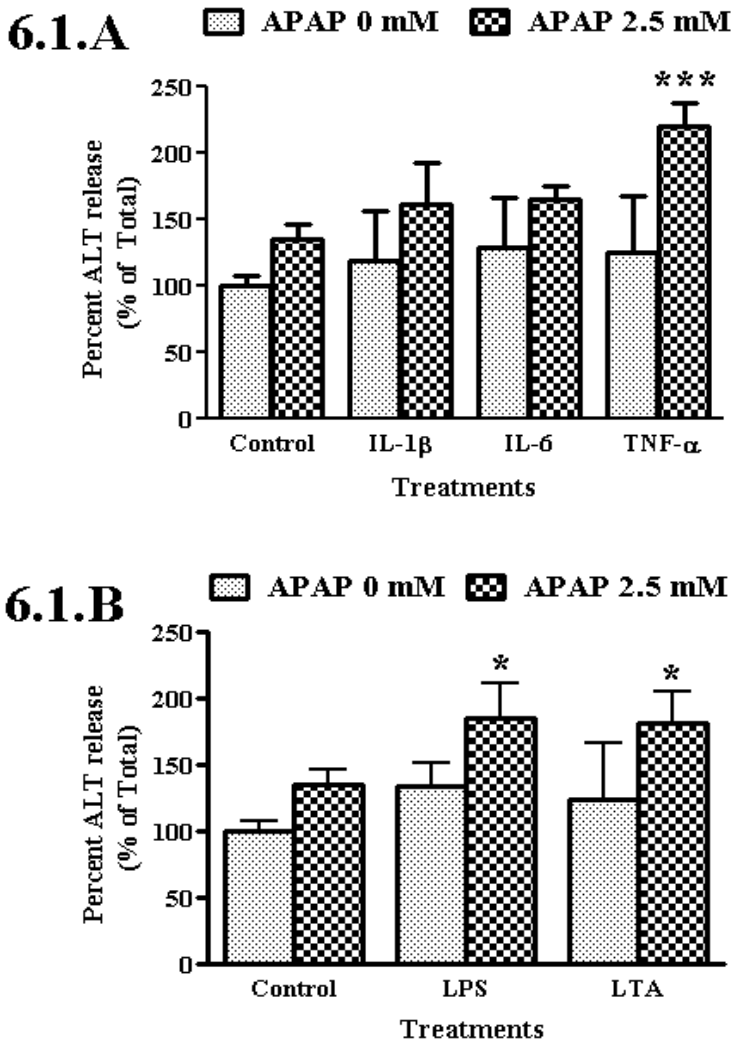

Figure 6.1 Inflammatory mediators enhance hepatotoxic responses to APAP in hepatocytes

Hepatocytes were treated with 2.5 mM APAP or the vehicle, DMSO after pre-treatment with (A) cytokines or 0.0001% BSA/PBS or (B) LPS/LTA or saline. Cells were treated as described under *Materials and Methods*. Cell culture supernatant was collected after 24 h.

n = 4-6 hepatocyte isolations from different mice. * $p<0.05$, ** $p<0.01$, *** $p<0.001$, significantly different when compared to 2.5 mM APAP in presence of BSA or saline treatments. Triplicate readings were used to calculate the mean.

6.4.2. Inflammatory mediators enhance toxic responses to CPZ in hepatocytes

Based on our initial dose-response experiments, 20 μM CPZ was selected due to minimal toxicity in hepatocytes (data not shown). Hepatocytes were pre-incubated with cytokines or endotoxins for 30 min, followed by a non-toxic dose of 20 μM CPZ for 24 h. We find that percent ALT release by 20 μM CPZ was comparable to the saline control (Fig. 6.2.A). As seen with APAP, the effect of CPZ on elevating ALT activity in presence of TNF-α was found to be the most significant (~60% increase, $p<0.01$) as compared to IL-1β or IL-6 (<12% increase) (Fig. 6.2.A). The cytokines by themselves did not show any significant increase in toxicity. LPS or LTA treatment resulted in a moderate, though significant effect on increased ALT activity (~23% increase, $p<0.05$) (Fig. 6.2.B, Table 6.1). Similar results were obtained by LDH assay (Table 6.2).

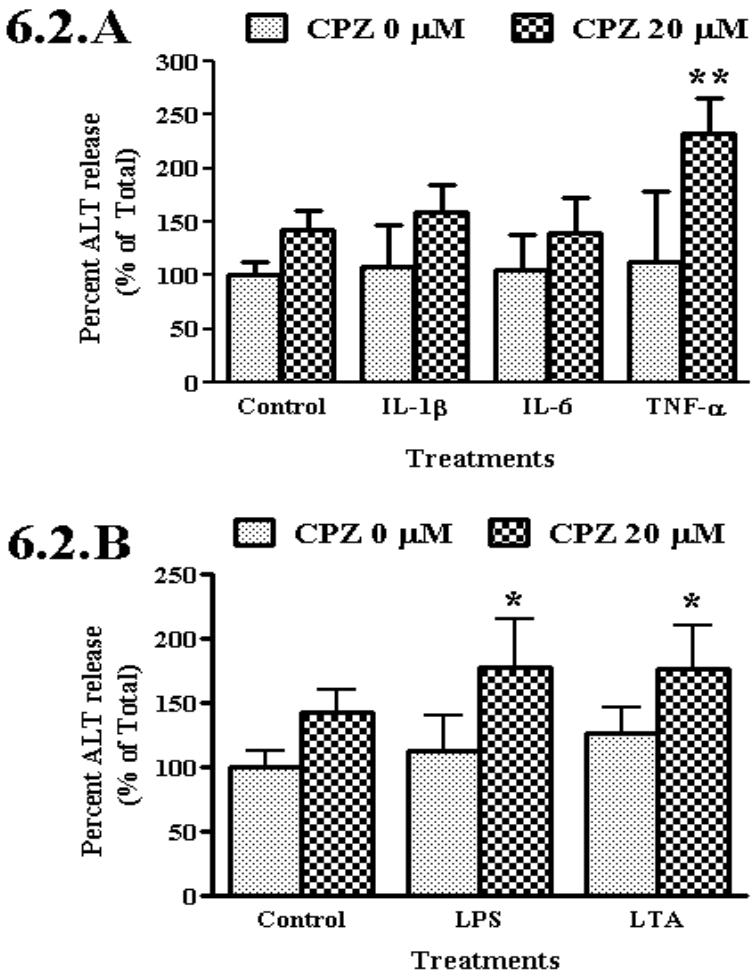

Figure 6.2 Inflammatory mediators enhance hepatotoxic responses to CPZ in hepatocytes

Hepatocytes were treated with 20 µM CPZ or the vehicle, saline after pre-treatment with (A) cytokines or 0.0001% BSA/PBS or (B) LPS/LTA or saline. Cells were treated as described under *Materials and Methods*. Cell culture supernatant was collected after 24 h. n = 4-6 hepatocyte isolations from different mice. * $p<0.05$, ** $p<0.01$, *** $p<0.001$, significantly different when compared to 20 µM CPZ in presence of BSA or saline treatments. Triplicate readings were used to calculate the mean.

Table 6.1 Comparison of ALT release from individual inflammatory mediators on enhancing drug-induced liver toxicity

Treatments	Drug	
	APAP (2.5 mM)	**CPZ (20 μM)**
IL-1β	119.59 ± 20.00	112.09 ± 15.70
IL-6	113.06 ± 15.25	96.76 ± 14.52
TNF-α	159.17 ± 15.16***	164.57 ± 21.23**
LPS	136.54±23.47*	124.00 ± 16.10*
LTA	133.43±13.57*	123.70 ± 18.60*

Table 6.2 Comparison of LDH release from individual inflammatory mediators on enhancing drug-induced liver toxicity

Treatments	Drug	
	APAP (2.5 mM)	**CPZ (20 μM)**
IL-1β	108.41 ± 17.40	120.03 ± 32.87
IL-6	98.75 ± 17.61	115.56 ± 40.68
TNF-α	161.16 ± 39.16**	166.42 ± 22.15**
LPS	140.02 ± 46.72*	134.23 ± 16.48*
LTA	135.57 ± 48.65*	143.31 ± 22.56*

Table 6: (6.1) Percent ALT or **(6.2)** percent LDH change by APAP (2.5 mM) or CPZ (20 μM) in the presence of cytokines or LPS/LTA was compared to the control sample. The control was APAP (2.5 mM) or CPZ (20 μM) without cytokines or LPS/LTA treatment. * $p<0.05$, ** $p<0.01$, *** $p<0.001$, significantly different when compared to the drugs alone.

6.4.3. Inhibition of JNK attenuates TNF-α mediated induction of APAP or CPZ toxicity

Recently, JNK was shown to be involved in APAP-induced hepatotoxicity (Gunawan *et al.*, 2006; Nakagawa *et al.*, 2008). Although activation of JNK by CPZ was reported in renal epithelial A6 cells (Niisato *et al.*, 1999), the role of JNK in CPZ-induced toxic responses is not known. TNF-α and IL-1β can activate JNK *in vivo* (Swantek *et al.*, 1997; Wang *et al.*, 2006) and activated JNK can contribute to hepatocellular necrosis (Nakagawa *et al.*, 2008). In our study, hepatocytes were pre-treated with the JNK inhibitor, SP600125 (30 μM) for 30 min followed by TNF-α treatment. After 30 min, the cells were treated with APAP (2.5 mM) or CPZ (20 μM). ALT release by APAP or CPZ was significantly increased with TNF-α pre-treatment, and the JNK inhibitor (Figs. 6.3.A and 6.3.B) attenuated this increase. SP600125 by itself had no effect on ALT release in the absence of APAP or CPZ. These results show that JNK is likely involved in mediating APAP- or CPZ-induced hepatotoxicity in presence of TNF-α. Interestingly,

pre-incubation with SP600125 reduced the ALT release induced by 2.5 mM APAP or 20 μM CPZ, indicating that JNK was involved in regulating the toxicity of these drugs.

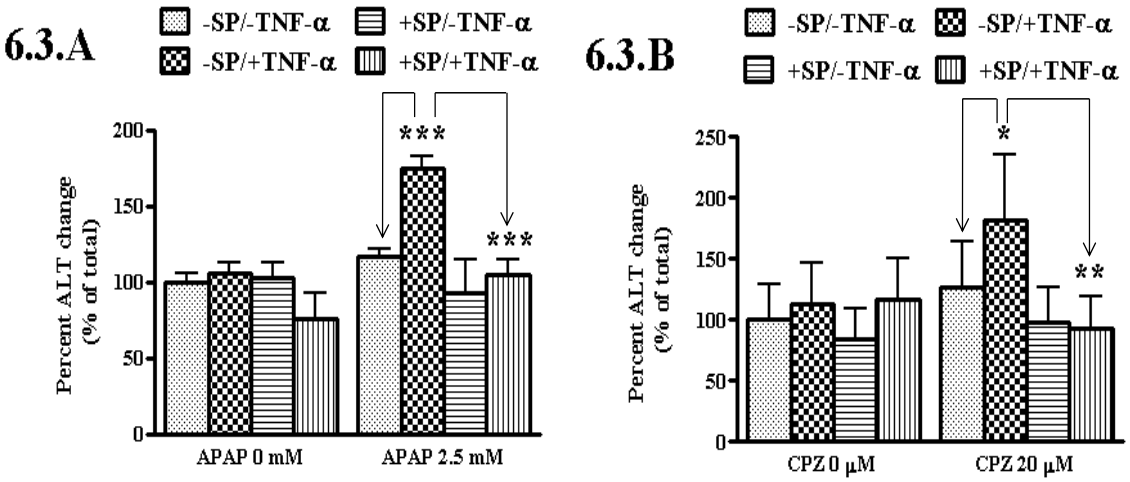

Figure 6.3 Treatment with the JNK inhibitor, SP600125, attenuates TNF-α mediated induction of APAP/CPZ toxicity

Cells were treated with TNF-α and 30 μM SP600125 (SP) or DMSO in the presence of (A) APAP or (B) CPZ as described under *Materials and Methods*. * $p<0.05$, ** $p<0.01$, *** $p<0.001$ significantly different for –SP/+TNF-α samples compared to –SP/-TNF-α samples and significantly different for +SP/+TNF-α samples compared to –SP/+TNF-α samples.

6.4.4. TNF-α, but not IL-1β treatment results in sustained JNK activation by APAP or CPZ

Since inhibition of JNK attenuated the effect of TNF-α on APAP or CPZ toxicity, we were interested in determining JNK activation by APAP/CPZ in the presence of TNF-α. The pro-inflammatory cytokines, TNF-α and IL-1β significantly activated JNK from 5 to 30 min compared to the control as evidenced by increased levels of phospho (P)-JNK (Figs. 6.4.A and 6.4.B). Levels of total JNK protein remained constant as expected. P-JNK levels were not detected from 60 min to 6 h, indicating that the early JNK activation by TNF-α or IL-1β was transient. No activation of JNK was detected with IL-6, LPS or LTA treatments.

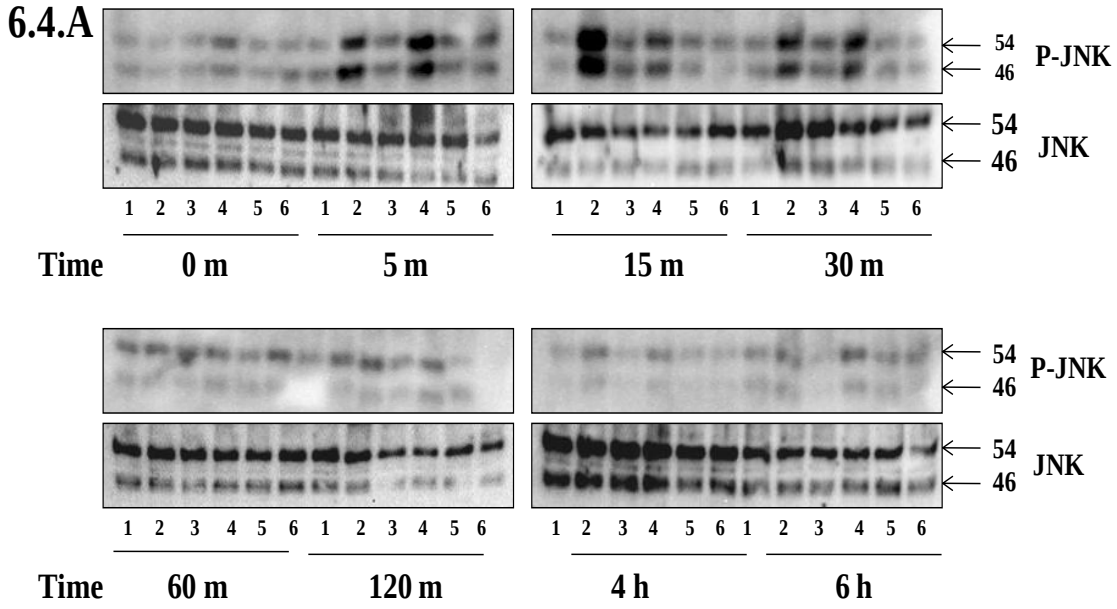

Figure 6.4 Effect of individual cytokines or endotoxins on time-dependent activation of JNK

(A) Immunoblot of differentially expressed phospho (P)-JNK after IL-1β, IL-6, TNF-α, LPS or LTA treatments for 0, 5, 15, 30, 60, 120, 240 or 360 min as described in *Materials and Methods*. The numbers represent the treatments as follows: **1**. Control, **2**. IL-1β, **3**. IL-6, **4**. TNF-α, **5**. LPS and **6**. LTA

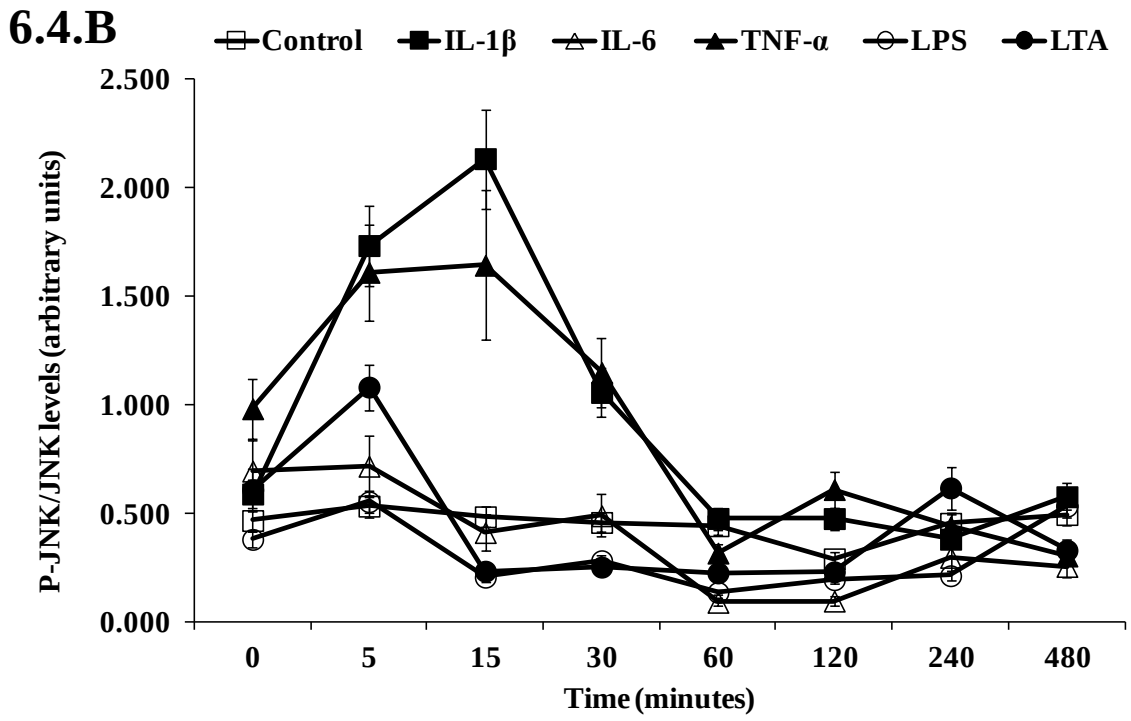

Figure 6.4 Effect of individual cytokines or endotoxins on time-dependent activation of JNK

(B) Quantification of blots by densitometry after normalizing the P-JNK levels over total JNK. Replicates from three experiments were quantified by densitometry.

Treatment of hepatocytes with TNF-α followed by 2.5 mM APAP resulted in increased expression of P-JNK from 0 to 2 h (Figs. 6.5.A and 6.5.C). A subsequent decrease of P-JNK levels was detected from 4 to 24 h (data not shown). Similar profile of JNK activation was detected in case of TNF-α and CPZ treated hepatocytes (Figs. 6.5.B and 6.5.D). No significant induction of JNK was detected by treatment with APAP or CPZ alone without TNF-α pre-treatment (Figs. 6.5.A and 6.5.B). Expression levels of the total JNK did not change. This implies that TNF-α pre-treatment result in sustained JNK activation by APAP or CPZ, which can contribute to enhanced toxicity of these drugs.

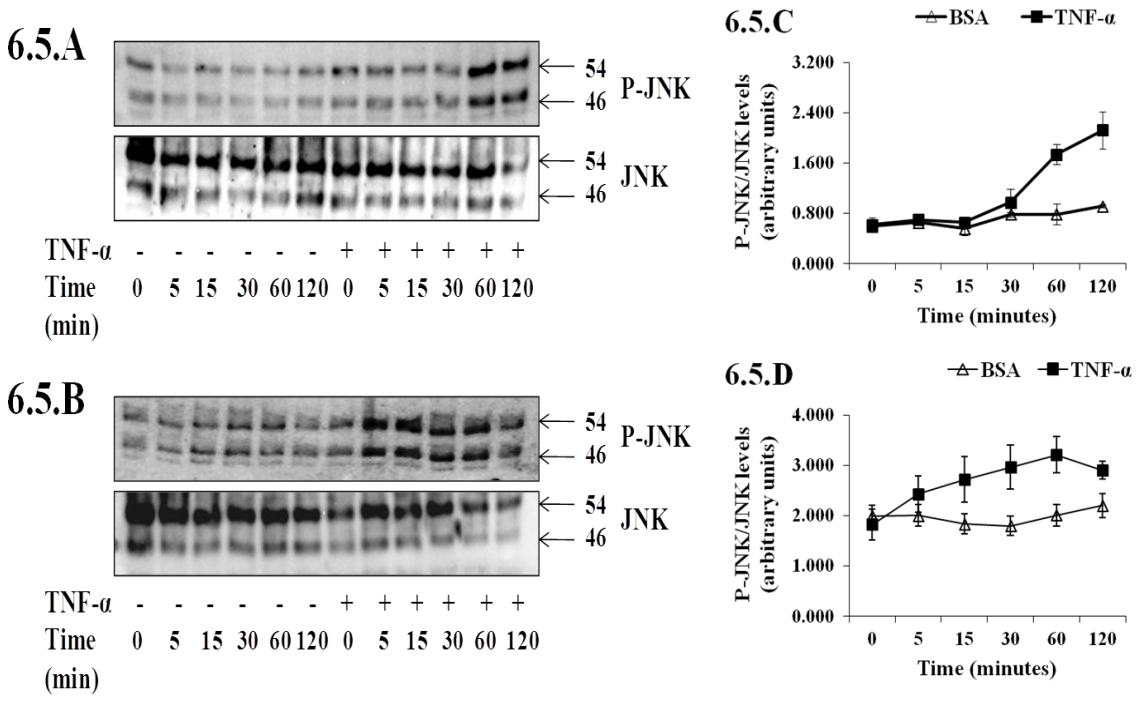

Figure 6.5 TNF-α pre-treatment result in sustained JNK activation by APAP or CPZ

Hepatocytes were treated with 10 ng/ml TNF-α for 30 min followed by a non-toxic dose of **(A)** 2.5 mM of APAP or **(B)** 20 µM of CPZ from 0 – 2 h as described in *Materials and Methods*. Whole cell extracts were analyzed by immunoblotting. TNF-α treated cells showed a sustained activation of JNK up to 2 h as seen by increased expression of phospho (P)-JNK. Total JNK levels did not change for control as well as TNF-α treated cells. **(C)** and **(D)** Quantification of blots by densitometry after normalizing the P-JNK levels over total JNK. Replicates from three experiments were quantified by densitometry.

Since IL-1β also activated JNK (Fig. 6.4.A), we pre-treated the hepatocytes with IL-1β followed by APAP or CPZ. Surprisingly, we did not detect any JNK activation in IL-1β pre-treated hepatocytes in presence of APAP (Figs. 6.6.A and 6.6.C) or CPZ (Figs. 4.6.B and 6.6.D). Lack of JNK activation was associated with lack of effect of IL-1β on APAP or CPZ toxicity (Figs. 6.1.A and 6.2.A).

In these experiments, the hepatocytes were exposed to the cytokines for a total of 2.5 h and APAP or CPZ for up to 2 h. So, we did not detect JNK activation in presence of IL-1β or TNF-α without the drugs (Figs. 6.5.A and 6.5.B), since cytokine-induced transient JNK activation occurs from 0-30 min. (Fig. 6.4.A).

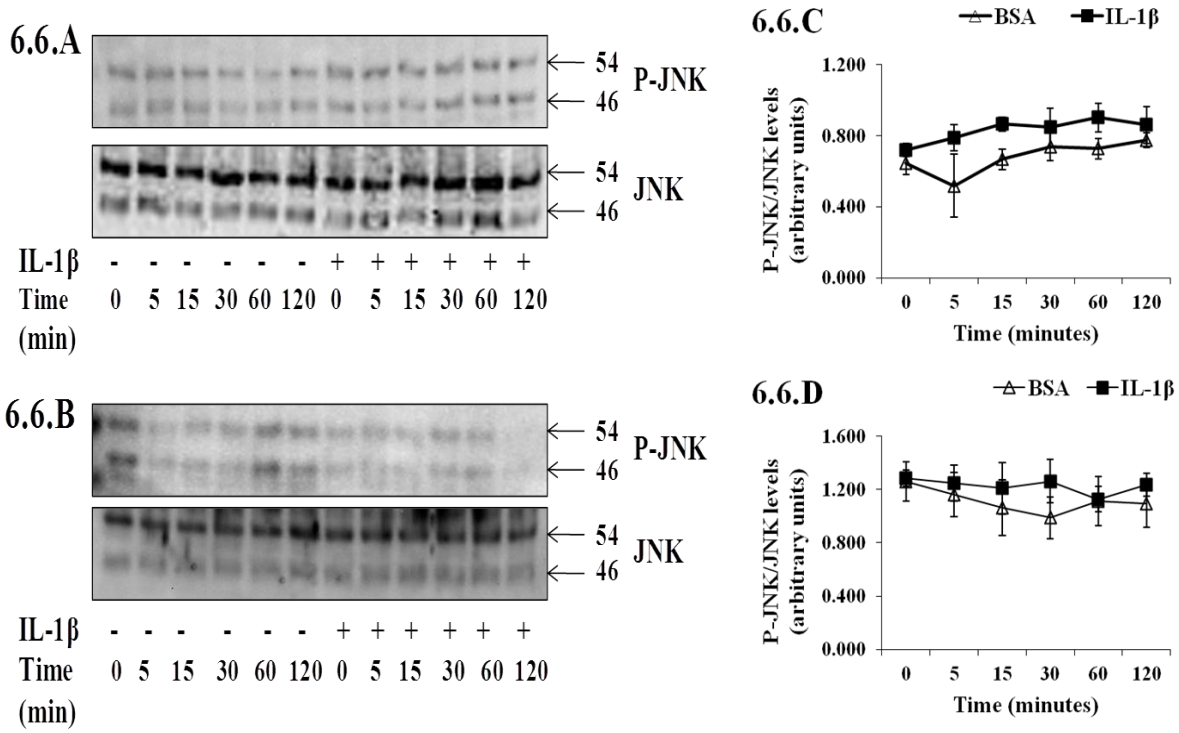

Figure 6.6 IL-1β pre-treatment did not result in JNK activation by APAP or CPZ

Hepatocytes were treated with 10 ng/ml IL-1β for 30 min followed by a non-toxic dose of **(A)** 2.5 mM of APAP or **(B)** 20 μM of CPZ from 0 – 2 h as described in *Materials and Methods*. Whole cell extracts were analyzed by immunoblotting. IL-1β treated cells did not show any significant activation of JNK for the duration of drug treatments as evidenced by lack of increase in P-JNK levels. Total JNK levels did not change for control as well as IL-1β treated cells **(C)** and **(D)** Quantification of blots by densitometry after normalizing the P-JNK levels over total JNK. Replicates from three experiments were quantified by densitometry.

6.5. Discussion

Drug-induced liver injury has been reported for more than 1100 classical drugs (Zimmerman., 1999). It is the most frequent reason cited for the withdrawal of approved drugs from the market, and accounts for more than 50% of the cases of acute liver failure in the United States (Lee, 2003). Despite innovations and early-assessment of biomarkers of liver toxicity in drug development, there is a wide array of drugs which show an abnormal effect on the liver. Recent studies have shown that underlying inflammation enhances the toxic effects of select drugs (Buchweitz *et al.*, 2002; Roth *et al.*, 1997); although the mechanism is not well-established. Our previous studies have shown that LPS or LTA can induce the pro-inflammatory cytokines (IL-1β, IL6 and TNF-α) in the liver, and modulate the gene expression of drug metabolizing enzymes and transporters (Ghose *et al.*, 2009; Ghose *et al.*, 2008; Ghose *et al.*, 2004). These cytokines are known to be the major determinants of acute-phase response (Ramadori *et al.*, 1988) and play a key role in regulation of several liver disorders including fever and cirrhosis (Fey and Gauldie, 1990).

Our studies suggest that pre-treatment with the pro-inflammatory cytokine, TNF-α can enhance the toxic responses to APAP or CPZ in primary mouse hepatocytes. Though relatively safe at low doses, APAP can lead to critical complications in the liver at higher doses. On the other hand, CPZ has been studied extensively due to its idiosyncratic behavior in humans.

The role of pro-inflammatory cytokines in APAP toxicity is controversial. It has been known that APAP can activate the Kupffer cells (Laskin *et al.*, 1986), leading to the release of pro-inflammatory cytokines (Blazka *et al.*, 1995; James *et al.*, 2003b; Laskin *et al.*, 1986). In addition, several studies have shown that cytokines are involved in exacerbation of APAP toxicity (Blazka *et al.*, 1996; Tukov *et al.*, 2006). On the other hand, Boess showed that TNF-α was unlikely to be involved in regulating APAP-induced acute hepatotoxicity in TNF/lymphotoxin-alpha knockout mice (Boess *et al.*, 1998). Furthermore, previous studies have shown that co-administration of APAP and TNF-α results in sensitization to TNF-α-induced apoptosis in hepatocytes due to glutathione depletion (Nagai *et al.*, 2002). Recent studies had shown that a nontoxic dose of APAP was rendered hepatotoxic in mice by LPS-induced inflammation (Newport et al., 2005). These findings are in contradiction to previous reports showing that LPS was protective against hepatotoxicity of APAP (Liu *et al.*, 2000). As toxicity of APAP is generally linked to its toxic metabolite, N-acetyl-p-benzo-quinone imine (NAPQI); Liu concluded the hepatoprotective role of LPS is regulated by IL-1α, which suppresses the cytochrome P450 enzyme involved in bioactivation of APAP to NAPQI (Liu *et al.*, 2000). Since hepatocytes were exposed to LPS *in vitro*, our results indicate that endotoxin exposure can sensitize these cells towards enhanced toxicity by APAP. A recent study showed that APAP hepatotoxicity as a result of APAP overdose in mice and humans was associated with increased glutamate dehydrogenase activity and mitochondrial DNA concentration in plasma from patients with abnormal liver function tests suggesting the possible role of

mitochondrial damage (McGill *et al.*, 2012). However, the authors reported that APAP-induced hepatotoxicity was not apoptotic rather necrotic in nature due to unchanged caspase-3 activity and cleaved caspase-3 levels in plasma from overdosed mice and humans.

The role of inflammatory mediators on CPZ toxicity remains to be fully elucidated. Buchewitz et al. have shown that co-treatment of rodents with non-toxic doses of CPZ and LPS induces toxicity, mimicking human idiosyncratic responses (Buchweitz *et al.*, 2002). Furthermore, co-treatment of a co-culture of Kupffer cells and hepatocytes with non-toxic doses of LPS and CPZ resulted in enhanced release of TNF-α (Tukov *et al.*, 2006).

We find that exposure to TNF-α can potentially sensitize hepatocytes to toxic effects of drugs at low doses. These results indicate that induction by TNF-α may be associated with enhanced toxicity of known hepatotoxicants even at sub-therapeutic doses. Since elevation of pro-inflammatory cytokines is associated with disease states, these findings can have serious implications in terms of drug safety in susceptible individuals. We were also interested in studying the role of two more cytokines, namely, IL-1β and IL-6 on mediating APAP or CPZ induced liver injury, as these cytokines are also involved in inflammatory response in the liver (Aitken *et al.*, 2006; Ghose *et al.*, 2009; Ghose *et al.*, 2008), and are also induced in response to APAP treatment (James *et al.*, 2003b). Our results indicate that pre-treatment of hepatocytes with IL-1β or IL-6 has no influence on the toxicity of APAP. Previous studies with IL-6-deficient mice had

shown protective effect of this cytokine against liver injury by APAP (James *et al.*, 2003a; Masubuchi *et al.*, 2003). The lack of effect of IL-6 on toxic responses to APAP in hepatocytes indicates that the protective effect *in vivo* is likely due to a mechanism independent of the hepatocytes.

Interestingly, LPS or LTA treatment of hepatocytes also moderately increased the toxic responses to these drugs, likely by direct action on hepatocytes through the Toll-like receptors present on the cell-surface. Although the effects of LPS or LTA are primarily mediated by Toll-like receptors present on the non-parenchymal cells including the Kupffer cells (Aitken *et al.*, 2006; Ghose *et al.*, 2009; Ghose *et al.*, 2008), recent studies have shown that the hepatocytes themselves express these receptors, which mediate the uptake of LPS by hepatocytes (Liu *et al.*, 2002).

The mechanism by which underlying inflammation contributes towards drug toxicity is not known. Recent studies have shown that the hemostatic system contributes towards liver injury induced by co-exposure to LPS with trovafloxacin or sulindac (Shaw *et al.*, 2007; Zou *et al.*, 2009b). In addition, TNF-α was shown to be involved in mediating hepatotoxicity from trovafloxacin/LPS co-exposure (Shaw *et al.*, 2007). We find that inhibition of the MAPK, JNK, attenuated the effects of TNF-α on APAP or CPZ toxicity. Furthermore, the JNK inhibitor, SP600125 reduced the percent ALT release by APAP or CPZ. The involvement of JNK in APAP toxicity has been reported recently (Bourdi *et al.*, 2008; Gunawan *et al.*, 2006; Kaplowitz *et al.*, 2008; Wang *et al.*, 2006). In mammals, JNK exists in 3 distinct isoforms. JNK 1 and 2 are ubiquitously expressed,

whereas JNK3 is limited to brain, testis and cardiomyocytes. Thus, the overall effect of JNK activation depends on the cellular context of study. JNK1 was shown to play a major role in insulin resistance and fatty liver disease, whereas JNK2 induced apoptosis in a TNF-α dependent liver injury model (Conze *et al.*, 2002). Gunawan et al demonstrated that JNK acts as a downstream signaling mediator, and maximum protection against APAP-induced liver injury was observed by inhibition of both JNK1 and JNK2 (Gunawan *et al.*, 2006). Since the JNK inhibitor, SP600125 can inhibit both forms of JNK, it is likely that maximal protection against TNF-α-induced drug toxicity is attained by inhibition of both JNK1 and JNK2; however, the role of individual isoforms of JNK needs to be further investigated.

Our results show that IL-1β or TNF-α induced JNK as early as 5 min upto 30 min with no activation detected thereafter. Interestingly, only TNF-α, but not IL-1β, resulted in prolonged JNK activation lasting upto 2 h in presence of APAP or CPZ. JNK activation profile correlated with enhanced drug toxicity by TNF-α, but no such increase was observed with IL-1β. We did not detect any activation of JNK at the non-toxic doses of APAP or CPZ by themselves. Transient early JNK activation (≤ 30 min) is a non-toxic response of the cells induced by stress or injury, while prolonged JNK activation (≥ 1h) is indicative of cellular injury (Kaplowitz *et al.*, 2008). Thus, it is likely that sustained JNK activation in the hepatocytes by APAP or CPZ upon TNF-α pre-treatment plays a major role in enhancing the toxic responses to these drugs. The mechanism of TNF-α-induced JNK activation in augmenting drug toxicity remains to be investigated. In accordance

with previous studies with APAP, it is plausible that inhibition of mitochondrial bioenergetics due to translocation of activated JNK to mitochondria may contribute to enhanced drug toxicity (Hanawa *et al.*, 2008). Pre-treatment of hepatocytes with LPS or LTA increased the toxic responses to APAP or CPZ. However, the activation of JNK was minimal, indicating the potential involvement of additional MAPKs, including p38 kinase which is known to be activated in LPS-treated hepatocytes (Scott and Billiar, 2008).

This study demonstrates that TNF-α, but not IL-1β or IL-6 pre-treatment of primary mouse hepatocytes elevate the toxic response to APAP or CPZ. In addition, treatment of hepatocytes with LPS or LTA can also significantly enhance the toxic responses to these drugs. Previous studies have shown that APAP/TNF-α treatment sensitizes hepatocytes to TNF-α-induced apoptosis (Nagai *et al.*, 2002). Our studies show for the first time that pre-treatment with TNF-α enhances the toxic responses to APAP. Since many diseases and altered physiological states are associated with elevation of pro-inflammatory cytokines, it is important to assess the effect of pre-existing inflammation on drug toxicity. Inhibition of JNK attenuated the effects of TNF-α on drug toxicity, and sustained activation of JNK by APAP or CPZ in presence of TNF-α was associated with enhanced toxicity of these drugs. Prolonged JNK activation by these drugs in inflammation may be a novel mechanism of regulation of drug-induced hepatotoxicity.

CHAPTER 7

Summary and conclusions

7.1. Summary and conclusions

As inflammation is known to affect DME gene expression and has been linked with exacerbation of drug-induced hepatotoxicity in various animal models and human subjects, the purpose of this project was to delineate the underlying mechanisms responsible in mediating these effects. In this project, we tested the hypothesis that bacterial endotoxin-induced inflammation alters drug metabolism and hepatotoxicity of prototypical compounds which involved the TLR signaling pathway. A mouse model of inflammation was developed to characterize these effects. The results from this study strengthen the hypothesis that inflammation is a major determining factor which needs to be taken into account while designing dosage regimen in patients with a compromised liver function.

First, we determined the changes in Cyp3a11 protein expression and activity in LPS- or LTA-induced inflammation mouse model. After confirming this data, we carried out systematic PK and PD studies with the Cyp3a11 substrate, MDZ. The data showed that LPS and LTA treatments led to a significant increase (~2 fold) in the plasma exposure (AUC) of MDZ and a significant decrease (~2 fold) in the total clearance. We, for the first time, characterized the changes in the primary and secondary metabolites of MDZ in LPS- or LTA-induced inflammation in mice. An increase in the AUC of MDZ correlated with increased pharmacological activity in both LPS- or LTA-treated mice (assessed by sleep time). This study shows that inflammation-induced down-regulation of functional activity of Cyp3a11 can lead to undesirable effects of MDZ. Thus, as opposed

to healthy subjects, critical monitoring of patients infected with bacterial infections is required if given the same dose. Subsequent studies were performed to establish a correlation between the PK and PD of MDZ and its metabolites in presence of inflammation.

Based on the literature data which reports that the metabolites (1'-OHMDZ and 1'-OHMDZ-glcu), if not more, are equally potent in carrying the pharmacological activity, we conducted a PK/PD correlation analysis to determine the major moiety involved in mediating the sedative properties of MDZ. Unlike the metabolites, our data revealed that the parent compound was the most active form in carrying the pharmacological potency in inducing sedation in LPS- or LTA-treated mice.

TIRAP was shown to play a differential role in regulating Cyp3a11 gene expression in LPS- or LTA-treated mice. Additional evidence from the study showed that TIRAP was involved in mediating Cyp3a11 protein expression and activity only in LTA-treated mice. As LPS mediates its inflammatory actions by either TIRAP or TRIF pathways, these results show that additional compensatory pathways may be involved in regulating Cyp3a11-mediated metabolism in LPS-induced inflammation. Molecular intervention by targeting TIRAP should be considered as a potential pathway to prevent down-regulation of Cyp3a11.

A mouse model of acute inflammation was also used to study the changes in drug-induced hepatotoxicity with a known hepatotoxin, CPZ. Our observations revealed significant induction of ALT level in LPS- or LTA-treated mice only in the presence of

CPZ. The dose of CPZ was chosen to be below the therapeutic dose so as to test the hypothesis that inflammation reduces the threshold of drugs to cause hepatotoxicity.

Histological evaluations of liver tissue demonstrate that although LPS or LTA treatment even in the presence of CPZ did not cause overt liver damage, it was just enough to precipitate changes in liver glycogen stores. These observations can be used for safety assessment of drugs by considering liver glycogen as a biomarker in early detection of drug-induced hepatotoxicity.

Inflammation is a collective event of induction of various pro-inflammatory cytokines. Among the various cytokines studied, TNF-α is mostly associated with drug-induced hepatotoxicity. We observed that LPS- or LTA-induced release of serum TNF-α was augmented in presence of CPZ. These results were also confirmed in primary mouse hepatocytes which were pre-treated with IL-1β, IL-6 or TNF-α in presence of CPZ.

Sustained activation of JNK is associated with cell death. However, the effects of inflammation-drug interactions on activation of JNK are unknown. We observed that LPS- or LTA-induced activation of JNK (upto 1 h) was prolonged upto 4 h only in the presence of CPZ. Furthermore, we provide a better understanding that CPZ-induced sustained activation of JNK is dependent on TNF-α and not on IL-1β which was also involved in early activation of JNK. We conducted subsequent mechanistic studies to study the role of TIRAP, a TLR signaling adaptor molecule, in CPZ-induced hepatotoxicity.

Although, TIRAP was shown to play a differential role in regulating gene expression of DMEs, we observed CPZ-mediated induction of serum ALT and TNF-α levels, and activation of JNK was dependent on TIRAP in both, LPS- and LTA-treated mice. Thus, the complex role of TIRAP can make it a potential target for drug-induced hepatotoxicity in inflammation.

In summary, accumulating evidence suggests that inflammation induced by bacterial endotoxins can lead to adverse drug reactions. The novel molecular mechanisms presented in this project will help reduce these undesirable effects precipitated by inflammatory conditions. Also, as inflammation is a common factor involved in various pathophysiological conditions, these studies can be extended to help understand the effects of these conditions on drug metabolism and hepatotoxicity.

7.2. Future studies

The data presented in this project provided several novel mechanisms involved in regulation of altered DMEs, drug metabolism and hepatotoxicity. However, additional studies can further aid in understanding of these mechanisms.

Although LPS or LTA treatment increased the plasma concentration and pharmacological activity of MDZ, the effects of LPS or LTA on the functional activity of $GABA_A$ receptor (target receptor of MDZ) remains unknown. The effects of LPS or LTA on increasing or decreasing the binding affinity of MDZ or its metabolites can be worth investigating.

LPS activates TLR4 and mediates its action by TIRAP or TRIF adaptor proteins. As TIRAP was not involved in regulating Cyp3a mediated drug metabolism in LPS-induced inflammation, the TRIF pathway could be investigated.

Although, plasma protein content is significantly reduced in LPS-induced inflammation, there is no data of such effects in LTA-induced inflammation. MDZ being a highly protein-bound drug (>97%), additional studies could be performed in investigating the effects of LPS or LTA on changes in plasma protein levels and their subsequent effects on distribution of MDZ and its metabolites to the brain.

Next, LPS or LTA treatment significantly increased ALT levels in presence of CPZ. Also, CPZ is known to produce hepatic cholestasis by obstructing the bile flow. LPS is known to alter hepatic transporters involved in bile acid disposition. Additional

studies could be performed on investigating the effects of LPS or LTA on CPZ-induced hepatotoxicity in context of changes in the hepatobiliary transporters.

Although we showed that CPZ treatment was accompanied with a significant increase in LPS- or LTA-mediated induction of serum TNF-α, additional mechanism based studies highlighting the changes in increased gene expression of TNF-α or using specific TNF-α inhibitors could be worth evaluating.

The metabolites of CPZ have been shown to be hepatotoxic and LPS or LTA are known to alter DMEs. However, the effects of LPS or LTA on DMEs involved in metabolism of CPZ remain unknown. Therefore, additional studies could be performed in evaluating the role of inflammation in alteration of the metabolic pathway of CPZ.

These studies hold lot of potential for expansion to include other clinically relevant drugs, especially those with a narrow therapeutic window. These studies could be extrapolated in humans, as people tend to take multiple medications in hospital settings, and therefore the effects of inflammation on drug-drug interactions is worth considering.

APPENDIX

Altered metabolism of irinotecan (CPT-11) in diet-induced obese mice

Abstract

Background: Colorectal cancer is the second most common cause of cancer related deaths in the United States. A significant number of colorectal cancer patients have colorectal liver metastasis (CLM) due to the cancer which has spread to the liver. Due to its potent anticancer activity, irinotecan (CPT-11) by itself or in combination with other drugs is used for CLM treatment. Irinotecan metabolizes to form the active compound, SN-38, which then undergoes glucuronidation by the enzyme, uridine glucuronosyl transferase (UGT) 1A1 to form SN-38 glucuronide (SN-38G). Dose-limiting toxicity such as life threatening diarrhea and neutropenia occur due to increased plasma concentrations of SN-38. Although irinotecan treatment is associated with steatohepatitis (fatty liver with inflammatory infiltrate) in ~12% of patients with BMI<25 kg/m^2, the prevalence of steatohepatitis is more than double (~25%) in patients with BMI>25 kg/m^2. However, the mechanism by which irinotecan causes steatohepatitis in patients with higher BMI is not known.

Purpose: To determine the role of obesity in affecting metabolism of irinotecan in mice.

Methods: For drug metabolism studies, liver S9 fractions were prepared from diet-induced obese (DIO, 60 kcal % fat) and lean mice (10 kcal % fat). UGT1A-mediated metabolism of SN-38 was studied in liver S9 fractions (2 mg/ml protein) incubated with SN-38 (15 µmol) for 60 min. For pharmacokinetic (PK) studies, mice were injected with a single oral dose of 10 mg/kg irinotecan. Serial blood sampling was performed from 0 to 8h. Plasma and feces samples were analyzed for irinotecan and SN-38 concentrations

using LC-MS/MS. Liver tissues were harvested for real-time PCR studies. The mRNA and serum TNF-α levels were measured in liver and plasma samples, respectively.

Results: We find that formation of SN-38G was ~2 folds lower in the S9 fractions from DIO mice compared to the lean controls ($p<0.05$). This corresponded with reduced expression of UGT1A1 in DIO mice livers. In PK studies, we did not observe significant changes in the area under the curve (AUC) or clearance of irinotecan between the DIO and lean mice. However, plasma, liver and fecal concentrations of SN-38 increased significantly by ~2 folds in the DIO mice compared to the lean controls ($p<0.05$). Next, compared to lean mice, we also observed significantly higher (~3 fold in mRNA) and serum levels of TNF-α in the DIO mice. Higher TNF-α levels are known to be associated with steatohepatitis.

Conclusion: SN-38 concentration is increased in obesity with a concurrent induction of the pro-inflammatory cytokine, TNF-α. Dosage of irinotecan should be closely monitored for effective and safe chemotherapy in obese patients who are at a higher risk of developing steatohepatitis.

Introduction

Colorectal cancer (CRC) is the second most leading cause of cancer related deaths in the United States. Globally, approximately one half of the one million CRC patients develop liver metastases at some point of time in their cancer related history (Abdalla *et al.*, 2004). The survival of patients with untreated colorectal liver metastases (CLM) is as low as 4 months. Secondary liver resection is considered to be an effective treatment for CLM (Saif, 2009). However, only 15-20% of patients with CLM are candidates for surgical resection at the time of diagnosis (Scheele *et al.*, 1995). Studies have shown that treatment with chemotherapy drugs significantly such as 5fluorouracil and oxaliplatin can cure the originally unresectable tumors, and the five-year survival rates have been reported to be ~ 58% in patients when rescection is combined with chemotherapy (Choti *et al.*, 2002; Fernandez *et al.*, 2004).

Among the various chemotherapeutic agents, the topoisomerase I inhibitor, irinotecan (CPT-11, Camptosar) has been highly effective to treat malignant colorectal cancers. The use of irinotecan has dramatically increased in treating CRC (Czejka *et al.*, 2011). It is a prodrug which is metabolized by carboxylesterases (CES 1&2) to form the active metabolite 7-ethyl-10-hydroxycamptothecin (SN-38) (Weekes *et al.*, 2009). SN-38 is a potent topoisomerase-1 inhibitor that causes breaks in double-stranded DNA, leading to cell death. Its inactivation is catalyzed by uridine diphosphate glucuronosyltransfereses (UGTs) 1A1 and 1A9, forming SN-38 glucuronide (SN-38G). SN-38G is eliminated through the bile, and it is believed that SN-38G is hydrolyzed back

into SN-38 by enteric bacterial β-glucuronidases (Takasuna *et al.*, 1996). A schematic of irinotecan metabolic pathway is shown in Fig. 8.1.

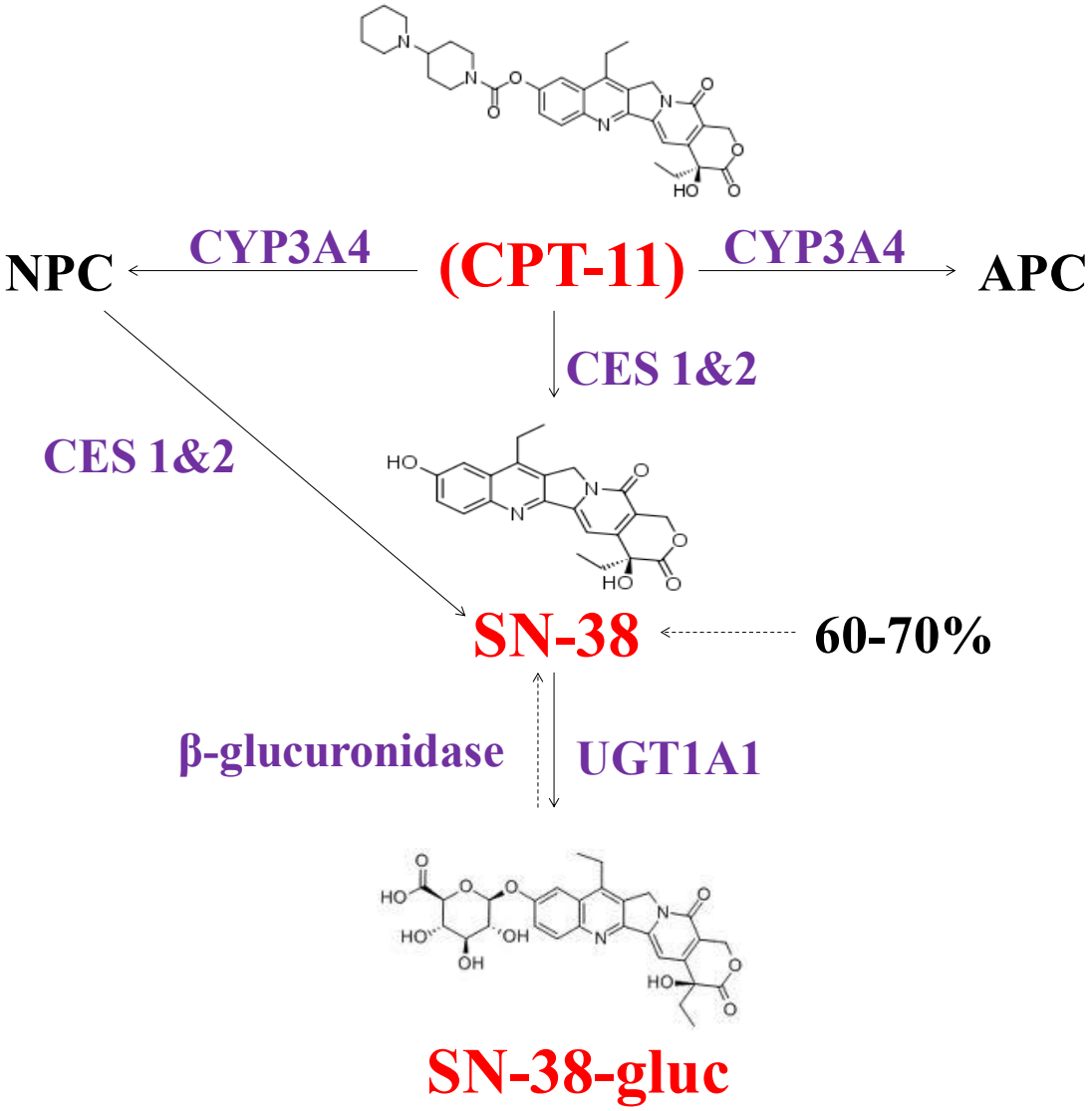

Fig. 8.1 Metabolic pathway of irinotecan

Although being a potent anticancer agent, irinotecan is associated with many side effects, including shortness of breath, neutropenia, which may increase the risk of infection or bleeding, vomiting and temporary hair loss (Weekes *et al.*, 2009). One of the major side effects of irinotecan is the life threatening diarrhea which accounts for the dose limiting toxicity of irinotecan. Irinotecan–induced diarrhea could be related to its inhibitory activity on acetylcholinesterase, or delayed onset diarrhea, which is possibly linked to accumulation of the active metabolite of irinotecan in the bowel (Hecht, 1998).

Several studies have reported the potential hepatotoxicity of irinotecan used in patients to treat stage IV CRC (Fernandez *et al.*, 2005; Morris-Stiff *et al.*, 2008; Pilgrim *et al.*, 2012; Vauthey *et al.*, 2006; Zorzi *et al.*, 2007). It was shown that irinotecan-induced liver damage could also progress to fibrosis and cirrhosis. The types of pathology observed in liver specimens from patients treated with irinotecan included steatosis and NASH (non alcoholic steatohepatitis). Nevertheless, NASH can be severe and over a 10 year period can lead to cirrhosis in 9-20% of patients (Ong and Younossi, 2007) and of these cirrhotic patients, 22-233% develop end-stage liver disease (Ong and Younossi, 2007). These patients have permanent damage to the liver with significant scars and impaired liver functioning. Irinotecan was also shown to cause hepatotoxicity in primary cultures of rat hepatocytes (Fulco *et al.*, 2000). In addition, camptothecin (CPT) was shown to induce apoptosis in primary mouse hepatocytes and *in vivo* only in the presence of TNF-α (Hentze *et al.*, 2004). Recently, irinotecan treatment along with etoposide in patients with Non-Hodgkin's lymphoma developed hepatotoxicities which were possibly

linked with higher plasma levels of the SN-38 (toxic metabolite of irinotecan) (Ohtsu *et al.*, 1998).

A recent study reported statistical comparison of steatohepatitis in patients receiving irinotecan based on the body mass index (BMI) (Vauthey *et al.*, 2006). According to this study, steatohepatitis was observed in 12% of patients with a BMI < 25 kg/m^2 whereas 25% of the patients with BMI > 25 kg/m^2 were prone to irinotecan-induced steatohepatitis. This study strongly suggests that irinotecan plays a role in steatohepatitis development. However, the mechanism was not investigated.

Based on these observations, we hypothesize that SN-38 might be playing a major role in the increased incidence of steatohepatitis in obesity. Alongside, our goal was to identify key factors which may likely play a role in augmenting irinotecan-induced liver toxicity using diet-induced obese mice. The high fat diet animal models of obesity hold clinical significance due to the fact that they resemble consumption of diets high in fat in humans which subsequently lead to higher body weight and increased plasma concentrations of circulating free fatty acids (Collins *et al.*, 2004). This data presented in this project can be used in clinical settings to determine the clinical PK of irinotecan and its metabolites in obese cancer patients and to effectively treat obese CLM patients with irinotecan.

Materials and methods

Materials

Irinotecan hydrochloride for injections was purchased from APP Pharmaceuticals LLC, Schaumburg, IL (Cat # NDC-63323-19305). Standard CPT-11 and camptothecin (CPT, internal standard) were purchased from Sigma-Aldrich, St. Louis, MO. SN-38 and SN-38G were a kind gift from Dr. Ming Hu's lab at the University of Houston, Houston, TX. The TNF-α ELISA Max^{TM} Deluxe assay kit (Cat # 430904) was purchased from BioLegend, San Diego, CA. All the solvents for chromatography were of LC-MS grade and purchased from VWR International, LLC (Suwanee, GA, USA).

Animals

Male, 12 weeks old DIO mice (weighing 25-30 g) and their age matched lean counterparts (weighing 22-25 g) on a C57BL/6 genetic background were purchased from The Jackson Laboratory, Bar Harbor, ME. All the mice were allowed to acclimatize for 1 week before the start of the experiment with free access to food and water. The DIO mice were put on a 60 kcal % high fat diet whereas the lean mice were fed a 10 kcal % regular diet.

Preparation of drug solutions

The standard irinotecan was dissolved in 50:50 methanol:water to get a stock solution with a concentration of 1 mM. This solution was sonicated for 15-20 min in a water bath maintained at room temperature. The solution was aliquoted into Eppendorf tubes with 1 ml of 1 mM solution each and stored at -20 ^{0}C for future use. The internal

standard (CPT), SN-38 and SN-38G were dissolved in 50:50 methanol:DMSO to get stock solutions with a concentration of 1 mg/ml, 100 µM and 100 µM respectively. All the solutions were aliquoted and stored at -20 ^{0}C for future use.

Preparation of S9 fractions

The S9 fractions were prepared to study UGT-mediated metabolism of SN-38. The livers (~1 g) from the DIO and lean mice were perfused and homogenized using a motorized homogenizer in ice-cold homogenization buffer (~3 ml) [50 mM potassium phosphate buffer (pH 7.4), 250 mM sucrose, 1 mM EDTA] and centrifuged at 15,400 rpm for 15 min at 4°C as described in section 3.1.4 and 3.1.5. The supernatant fractions were collected by carefully avoiding the fat layer and stored at -80 ^{0}C. Protein was quantified by BCA assay as described in section 3.1.6.

UGT1A1 reaction with SN-38

To study UGT-mediated reactions, S9 fractions are frequently employed. We added 2 mg/ml of hepatic S9 fractions and 15 µM of SN-38 (1.7 µL of 15 mM) along with the 24 µL of solution A and 30 µL of solution B and incubated the tubes (in duplicates, total volume 170 µL per tube) in 0.05 M KPi (pH 7.4) for 90 min in a shaking water bath at 37 ^{0}C. Solution A contained 25 mM UDPGA triammonium salt. Solution B contained 25 mM saccharolactone, 5 mM $MgCl_2$ and with 0.125 mg/ml alamethicin. A 50 mg/ml stock of alamethicin was prepared in 100% methanol. Both, solutions A and B were aliquoted as 1 ml in Eppendorf tubes and stored at -20 ^{0}C for future use. The reactions were then stopped by adding 50 µL of 94% ACN and 6% glacial acetic acid

containing 1 µg/ml of CPT (IS). Calibration curve was prepared using S9 and various concentrations of standard SN-38 (0-15 µM) except the cofactors. The samples were then analyzed for SN-38 and SN-38G by LC-MS/MS as described below.

Treatment of animals

For PK studies, the injectable irinotecan (20 mg/ml) was diluted in sterile dd water 10X to get a concentration of 2 mg/ml for injections. One hundred microliters of 2 mg/ml of irinotecan was injected for every 20 g mouse. Therefore, the DIO and lean mice received a final dose of 10 mg/kg of irinotecan by the oral route. The animals were returned to their cages and blood sampling was performed at various time points from 0 – 8 h as described in section 3.1.9. The plasma samples were processed as described in section 3.1.9. For analysis of serum TNA-α, approximately 100-150 µL of blood was collected at 1 h and at the end of the study (8 h).

Preparation of feces samples

Feces samples were collected to quantify irinotecan and its metabolites in DIO and lean mice. The feces were collected from time 0 to 8 h combined together. The feces were immediately stored at -80 ^{0}C to prevent loss of enzyme activity. For evaluating the drug concentrations, feces were accurately weighed and homogenized in 50:50 water:methanol and stored at -80 ^{0}C until further analysis. Roughly, 1 ml of solvent mixture was taken for 1 g of feces.

LC-MS/MS analysis of CPT-11 and its metabolites

The optimization of the LC-MS/MS conditions for analysis of irinotecan and its metabolites was performed as described in section 3.1.12. The m/z transition for irinotecan was 587.1/124.1, m/z transition for SN-38 was 393.1/349.1, m/z transition for SN-38G was 569.5/393.1, m/z for CPT was 349.0/305.1 in positive ion mode. The instrument dependent and compound dependent parameters for all the compounds were optimized as described in section 3.1.12.

β-glucuronidase reaction in feces samples

The β-glucuronidase activity in the feces samples was determined using a DU800 absorbance spectrophotometer (Beckman Coulter Inc., Indianapolis IN). Briefly, the reaction mixture (total volume of 0.5 ml) contained 0.2 ml of 1 mM p-nitrophenyl-β-D-glucuronide (Sigma-Aldrich, Cat # N1627) for, 0.25 ml of a 0.1 M phosphate buffer, pH 7.0, and 0.05 ml of the fecal suspension. The assay mixture was incubated at 37 ^{0}C water bath for 30 min. The reaction was quenched by adding 0.5 ml of 0.5 N NaOH. The mixture was then centrifuged at 3000 rpm for 10 min and the supernatant (700 µL) was transferred to clear plastic UV disposable cuvettes and the absorbance was measured at 540 nm using the UV lamp.

mRNA isolation, cDNA synthesis and quantification of mRNA with RT-PCR

The livers were harvested after 8 h and liver tissue extracts were prepared for mRNA analysis of TNF-α in DIO and lean mice as described in section 3.2.9. RT-PCR was performed as described in section 3.2.9. The primers and probe sequence of TNF-α is shown in Table 2.1.

Statistical analysis

All the data presented are mean ± S.D. from 3-4 mice per group. The data were analyzed by unpaired Student's t-test using GraphPad Prism 4.0 software (GraphPad Inc., La Jolla, CA) *$p<0.05$ was considered to be statistically significant.

Results

Ugt1a1 mediated glucuronidation of SN-38

Obesity is known to increase (Xu *et al.*, 2012) or decrease (Ghose *et al.*, 2011b) the gene expression and activity of Ugt1a1 in mice. We determined the role of Ugt1a1 in glucuronidation of SN-38 in hepatic S9 fractions as no glucuronide was detected in hepatic microsomes. As compared to lean mice which had an SN-38G concentration of 16.71 nM, the SN-38G concentration in DIO mice was 10.02 nM ($p<0.05$, Fig. 8.2). Thus, the down-regulation of Ugt1a1 in this study in DIO mice is in accordance to our earlier study (Ghose *et al.*, 2011b).

Fig. 8.2

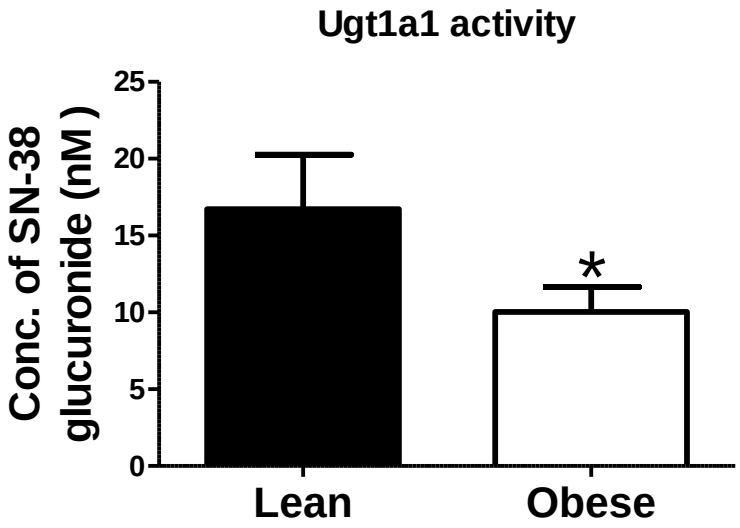

Fig. 8.2 Ugt1a1 mediated glucuronidation of SN-38 in DIO and lean mice

Livers were harvested from DIO (n=3) and lean mice (n=4). S9 fractions were prepared as described previously in *Materials and Methods*. Glucuronidation of SN-38 was used as a marker of Ugt1a1 activity. Data are shown as mean ± S.D. * indicates statistical significance at $p<0.05$ when compared to the lean group.

Pharmacokinetics of irinotecan

In order to measure the changes in irinotecan and its metabolites we performed PK studies in DIO and lean mice. The PK data was analyzed by non-compartmental analysis using WinNonlin software 3.3 (Pharsight Corporation (Mountain View, California). The plasma PK data revealed no significant differences in the AUC and CL of irinotecan in DIO mice compared to the lean controls (Fig. 8.3.A, Table 8.1). Similarly, the concentration of irinotecan in liver tissue and fecal extracts did not vary significantly in DIO mice compared to lean control. However, plasma concentrations of SN-38 were significantly increased in DIO mice (Fig. 8.3.B). The $AUC_{0\text{-}8h}$ of SN-38 in DIO mice was >2 times that of the lean controls (Table 8.1). Similarly, the concentrations of SN-38 in liver tissues and fecal extracts in DIO mice were significantly increased as compared to the lean controls. The concentrations of SN-38 in liver tissues and fecal extracts are shown in Figs. 8.4.A and 8.4.B respectively. Due to unexplained limitations, the limit of detection for SN-38G was very low as a result of which we could not quantify SN-38G levels in plasma as well as fecal extracts.

Fig. 8.3.A

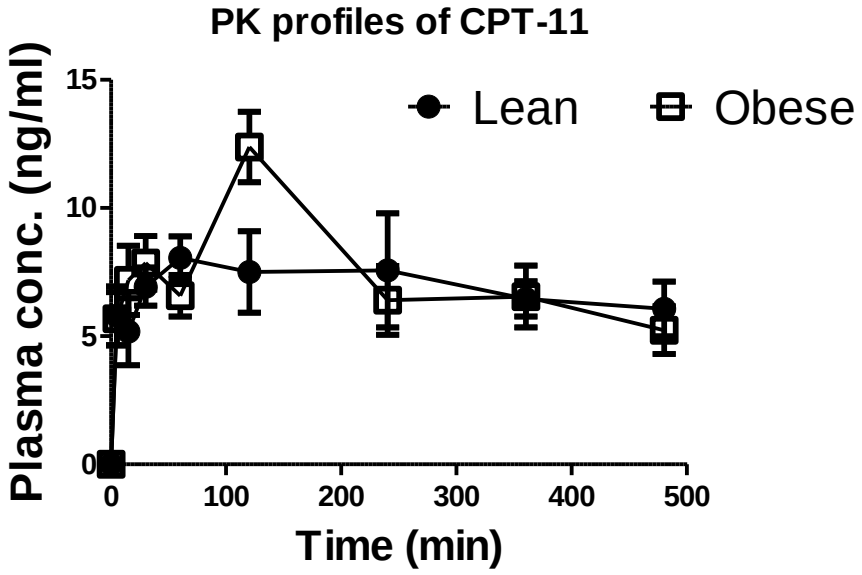

Fig. 8.3.B

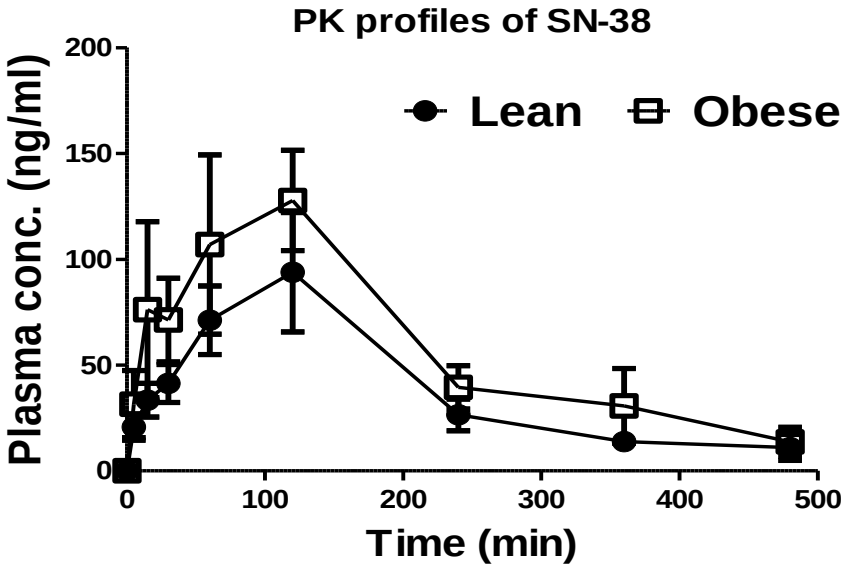

Fig. 8.3 PK profiles of irinotecan and SN-38

Plasma concentrations versus time profiles from 0 to 8 h for irinotecan (A) and SN-38 (B) in DIO and lean mice upon oral injection of irinotecan (10 mg/kg) are shown. Plasma samples were processed as described in *Materials and Methods*. *n* = 3-4. Data are shown as mean ± S.D.

Table 8.1 PK parameters of irinotecan and SN-38

Parameter	CPT-11		SN-38	
	Lean	Obese	Lean	Obese
AUC $_{0 \longrightarrow 8h}$ (ng.min/ml)	3349.81 ± 916.41	3587.92 ± 868.13	18654.1 ± 4486.83	28353.37 ± 7311.38*
T_{max} (min)	280.0 ± 183.3	97.5 ± 45.0	80.0 ± 34.64	48.75 ± 22.5
C_{max} (ng/ml)	8.25 ± 3.72	12.60 ± 2.34	108.2 ± 36.30	191.25 ± 30.31*
CL (L/min)	1.37 ± 0.49	1.64 ± 0.65	-----	-----
V_d (L/min)	1010.60 ± 345.56	776.39 ± 218.12	-----	-----

*** *p*<0.05 compared to the lean mice**

Fig. 8.4.A

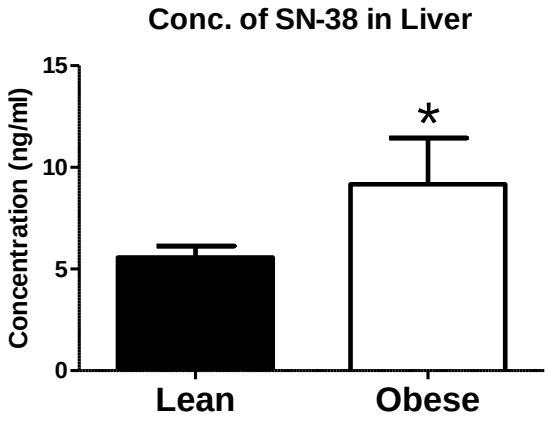

Fig. 8.4.B

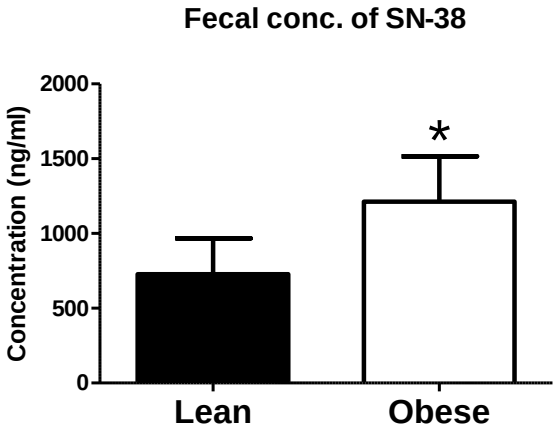

Fig. 8.4 Concentrations of SN-38 in liver and feces

Concentrations of SN-38 were measured in liver tissues and fecal extracts. (A) SN-38 in liver and (B) SN-38 in feces of DIO and lean mice upon oral injection of irinotecan (10 mg/kg) are shown. n = 3-4. Data are shown as mean ± S.D. * indicates statistical significance at $p<0.05$ when compared to the lean group.

Effect of obesity on β-glucuronidase activity

Studies have shown that intestinal β-glucuronidase enzyme may play an important role in causing increased toxicity of irinotecan due to increase in circulating SN-38 concentration (Takasuna *et al.*, 1996). In our study, we observed ~ 2 fold induction in fecal β-glucuronidase enzyme activity in irinotecan-treated DIO mice compared to the lean controls (Fig. 8.5).

Fig. 8.5.

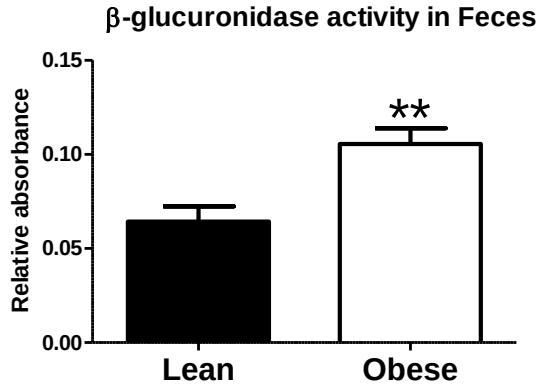

Fig. 8.5 Fecal β-glucuronidase enzyme activity

DIO and lean mice were treated with irinotecan (10 mg/kg, orally). Feces were collected from 0 to 8 h. β-glucuronidase enzyme activity was determined as described in *Materials and Methods*. All the data represented are mean ± S.D. from 3-4 mice per group. ** indicates statistical significance at $p<0.01$ when compared to the lean group.

Effect of obesity on hepatic TNF-α mRNA expression and TNF-α concentration in plasma

TNF-α is known to induce apoptosis in cells. Also, CPT along with TNF-α when injected in mice was shown to cause significant liver damage (Hentze *et al.*, 2004). Compared to lean mice, we observed ~3 fold induction in the mRNA expression of TNF-α in irinotecan-treated DIO mice (Fig. 8.6.A). Similarly, we observed a moderate, though significant increase in plasma concentration of TNF-α in irinotecan-treated DIO mice compared to the lean controls (Fig. 8.6.B).

Fig. 8.6.A

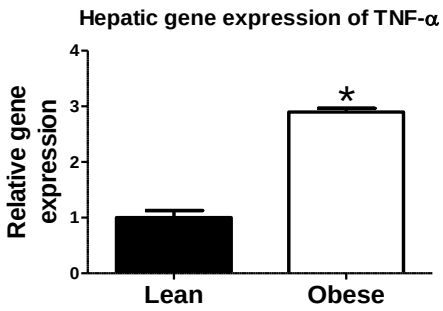

Fig. 8.6.B

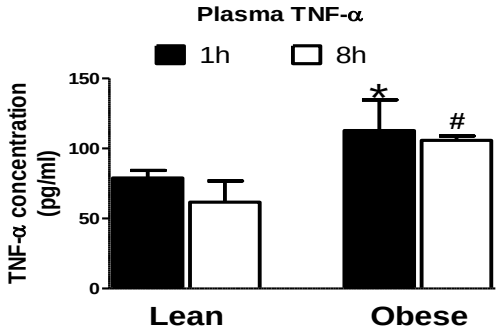

Fig. 8.6 Quantification of TNF-α in irinotecan-treated DIO and lean mice

DIO and lean mice were treated with irinotecan (10 mg/kg). (A) mRNA expression of TNF-α was determined by RT-PCR as described in *Materials and Methods* section. (B) Plasma levels of TNF-α were determined at 1 and 8 h after irinotecan administration by ELISA. All the data represented are mean ± S.D. from 3-4 mice per group. * and # indicates statistical significance at $p<0.05$ and $p<0.01$ when compared to the lean group.

Discussion

In this study, we observed significant down-regulation of hepatic Ugt1a1 activity in DIO mice compared to the lean controls. The plasma, liver and fecal concentrations of SN-38 were also significantly higher in DIO animals. In addition, hepatic mRNA and plasma levels of TNF-α increased greatly in irinotecan-treated DIO mice. The activity of β-glucuronidase enzyme in fecal extracts of DIO mice was ~ 2 fold compared to the lean controls.

Several studies have reported changes in hepatic Ugt1a1 activity in obese animal models. Although, our previous study showed that Ugt1a1 enzyme activity is decreased in DIO mice (Ghose *et al.*, 2011b), the expression and activity of hepatic Ugt1a1 was shown to be increased in genetically obese mice deficient in leptin signaling (*ob/ob*) (Xu *et al.*, 2012). Thus, these two studies provide contrasting evidences on regulation of hepatic Ugt1a1 activity in obese animal models. In the present study, we observed significant down-regulation of SN-38G formation in DIO mice due to decreased hepatic Ugt1a1 activity. High levels of SN-38 have been associated with life-threatening diarrhea. Irinotecan-induced toxicity (even at low doses) such as neutropenia or diarrhea in humans were correlated with alterations in UGT1A1 activities due to genetic polymorphisms in the UGT1A1*28/*28 allele (Hu *et al.*, 2010). The authors also concluded that the dose-dependent manner of SN-38 glucuronidation could possible explain the link between UGT1A1*28 and neutropenia. Thus, the results from our study

hold clinical significance in justifying that UGT1A1 activity in obese human patients should be monitored in cases of irinotecan-induced hepatotoxicities such as NASH.

Clinical PK of irinotecan is widely reported. However, PK of irinotecan in context of obesity has not been studied before. Obesity is associated with serious comorbidities with a steep global increase in its prevalence. Increased BMI is considered as a risk factor in causing recurrence of CRC (Calle *et al.*, 2003; Renehan *et al.*, 2008). As irinotecan treatment led to significant development of steatohepatitis in CRC patients with a BMI > 25 kg/m^2 (Vauthey *et al.*, 2006), however the cause was not explored. Our results showed more than double the AUC of SN-38 with no significant changes in the parent compound in DIO mice compared to lean mice. It is plausible that increased plasma levels of SN-38 might be playing a role in causing liver injury in obese patients. Several factors, individually or collectively, can possibly play a role in these observations. First, down-regulation of Ugt1a1 can account for increased plasma and liver concentration of SN-38. However, we could not detect SN-38G in mouse liver microsomes as well *in vivo*. We speculate that this intriguing observation could be due to release of lysosomal β-glucuronidase enzyme which is released from intact hepatocytes during microsome preparation. However, lack of detection of SN-38G *in vivo* in our study could not be explained. Second, obesity induces CES1 expression in human adipose tissues (Jernas *et al.*, 2009). Thus, increased CES levels in DIO mice could also play a role in increased production of SN-38 from irinotecan. Also, cancer is known to induce CES2 expression (Xu *et al.*, 2002) in humans. Therefore, further studies exploring the role of obesity on

CES will be of clinical relevance in studying irinotecan-induced steatohepatitis in obese population. Third, intestinal bacterial β-glucuronidases have been shown to increase circulating levels of SN-38 in animals (Kaneda *et al.*, 1990; Takasuna *et al.*, 1996) as well as humans (Sparreboom *et al.*, 1998). This observation is commonly termed as enterohepatic recirculation accounted by the second peak of SN-38. To assess the importance of SN-38G deconjugation with respect to potential increase in concentration of SN-38, we therefore also evaluated β-glucuronidase activity in fecal extracts of DIO and lean mice. Our observations of increased SN-38 concentrations in the feces were in accordance with increased fecal β-glucuronidase activity.

We also explored the role of obesity in irinotecan-induced increases in hepatic and plasma TNF-α levels. Steatohepatitis encompasses steatosis (fatty liver) with infiltration of inflammatory cells and mediators including TNF-α (Kleiner *et al.*, 2005). The significant increase in mRNA (3 fold) and plasma concentration of TNF-α suggests a strong interaction of between obesity and irinotecan or its metabolite (SN-38) in causing steatohepatitis in obese patients.

In conclusion, as obese patients are at a higher risk for irinotecan-induced steatohepatitis, our study provides novel findings on the probable role of increased concentration of SN-38 in producing such effects. Thus, in addition to the DIO animal model, additional studies using different obese animals (such as ob/ob mouse model) and multiple dosing regimen (as used in clinical settings) should also be explored for a more in-depth understanding of mechanisms likely to be involved in irinotecan-induced

steatohepatitis. Overall, our observations that altered hepatic Ugt1a1 and fecal β-glucuronidase activity leading to a prolonged retention of SN-38 in DIO mice should be considered as potential therapeutic targets for preventing adverse reactions of irinotecan.

BIBLIOGRAPHY

Abdalla, E. K., Vauthey, J. N., Ellis, L. M., Ellis, V., Pollock, R., Broglio, K. R., Hess, K., and Curley, S. A. (2004). Recurrence and outcomes following hepatic resection, radiofrequency ablation, and combined resection/ablation for colorectal liver metastases. *Ann Surg* **239**, 818-25; discussion 825-7.

Abdel-Bakky, M. S., Hammad, M. A., Walkerit, L. A., and Ashfaqi, M. K. (2010). Developing and characterizing a mouse model of hepatotoxicity using oral pyrrolizidine alkaloid (monocrotaline) administration, with potentiation of the liver injury by co-administration of LPS. *Nat Prod Commun* **5**, 1457-62.

Abdel-Razzak, Z., Loyer, P., Fautrel, A., Gautier, J. C., Corcos, L., Turlin, B., Beaune, P., and Guillouzo, A. (1993). Cytokines down-regulate expression of major cytochrome P-450 enzymes in adult human hepatocytes in primary culture. *Molecular pharmacology* **44**, 707-15.

Abdulla, D., Goralski, K. B., Del Busto Cano, E. G., and Renton, K. W. (2005). The signal transduction pathways involved in hepatic cytochrome P450 regulation in the rat during a lipopolysaccharide-induced model of central nervous system inflammation. *Drug metabolism and disposition: the biological fate of chemicals* **33**, 1521-31.

Abernathy, C. O., Lukacs, L., and Zimmerman, H. J. (1977). Adverse effects of chlorpromazine metabolites on isolated hepatocytes. *Proc Soc Exp Biol Med* **155**, 474-8.

Adachi, O., Kawai, T., Takeda, K., Matsumoto, M., Tsutsui, H., Sakagami, M., Nakanishi, K., and Akira, S. (1998). Targeted disruption of the MyD88 gene results in loss of IL-1- and IL-18-mediated function. *Immunity* **9**, 143-50.

Adam-Stitah, S., Penna, L., Chambon, P., and Rochette-Egly, C. (1999). Hyperphosphorylation of the retinoid X receptor alpha by activated c-Jun NH2-terminal kinases. *J Biol Chem* **274**, 18932-41.

Aggarwal, B. B. (2004). Nuclear factor-kappaB: the enemy within. *Cancer Cell* **6**, 203-8.

Aitken, A. E., and Morgan, E. T. (2007). Gene-specific effects of inflammatory cytokines on cytochrome P450 2C, 2B6 and 3A4 mRNA levels in human hepatocytes. *Drug metabolism and disposition: the biological fate of chemicals* **35**, 1687-93.

Aitken, A. E., Richardson, T. A., and Morgan, E. T. (2006). Regulation of drug-metabolizing enzymes and transporters in inflammation. *Annu Rev Pharmacol Toxicol* **46**, 123-49.

Akira, S., Takeda, K., and Kaisho, T. (2001). Toll-like receptors: critical proteins linking innate and acquired immunity. *Nature immunology* **2**, 675-80.

Aliprantis, A. O., Yang, R. B., Mark, M. R., Suggett, S., Devaux, B., Radolf, J. D., Klimpel, G. R., Godowski, P., and Zychlinsky, A. (1999). Cell activation and apoptosis by bacterial lipoproteins through toll-like receptor-2. *Science* **285**, 736-9.

Bagheri, H., Michel, F., Lapeyre-Mestre, M., Lagier, E., Cambus, J. P., Valdiguie, P., and Montastruc, J. L. (2000). Detection and incidence of drug-induced liver injuries in hospital: a prospective analysis from laboratory signals. *British journal of clinical pharmacology* **50**, 479-84.

Ball, P., Mandell, L., Niki, Y., and Tillotson, G. (1999). Comparative tolerability of the newer fluoroquinolone antibacterials. *Drug Saf* **21**, 407-21.

Bannerman, D. D., Erwert, R. D., Winn, R. K., and Harlan, J. M. (2002). TIRAP mediates endotoxin-induced NF-kappaB activation and apoptosis in endothelial cells. *Biochemical and biophysical research communications* **295**, 157-62.

Barclay, T. B., Peters, J. M., Sewer, M. B., Ferrari, L., Gonzalez, F. J., and Morgan, E. T. (1999). Modulation of cytochrome P-450 gene expression in endotoxemic mice is tissue specific and peroxisome proliferator-activated receptor-alpha dependent. *J Pharmacol Exp Ther* **290**, 1250-7.

Barker, C. W., Fagan, J. B., and Pasco, D. S. (1992). Interleukin-1 beta suppresses the induction of P4501A1 and P4501A2 mRNAs in isolated hepatocytes. *J Biol Chem* **267**, 8050-5.

Barr, G. D., and Piper, D. W. (1981). Possible ranitidine hepatitis. *The Medical journal of Australia* **2**, 421.

Barton, C. C., Barton, E. X., Ganey, P. E., Kunkel, S. L., and Roth, R. A. (2001). Bacterial lipopolysaccharide enhances aflatoxin B1 hepatotoxicity in rats by a mechanism that depends on tumor necrosis factor alpha. *Hepatology* **33**, 66-73.

Bauer, T. M., Ritz, R., Haberthur, C., Ha, H. R., Hunkeler, W., Sleight, A. J., Scollo-Lavizzari, G., and Haefeli, W. E. (1995). Prolonged sedation due to accumulation of conjugated metabolites of midazolam. *Lancet* **346**, 145-7.

Beckwith-Hall, B. M., Holmes, E., Lindon, J. C., Gounarides, J., Vickers, A., Shapiro, M., and Nicholson, J. K. (2002). NMR-based metabonomic studies on the biochemical effects of commonly used drug carrier vehicles in the rat. *Chemical research in toxicology* **15**, 1136-41.

Bedoucha, M., Atzpodien, E., and Boelsterli, U. A. (2001). Diabetic KKAy mice exhibit increased hepatic PPARgamma1 gene expression and develop hepatic steatosis upon chronic treatment with antidiabetic thiazolidinediones. *J Hepatol* **35**, 17-23.

Beitia, G., Cobreros, A., Sainz, L., and Cenarruzabeitia, E. (2000). Ecstasy-induced toxicity in rat liver. *Liver* **20**, 8-15.

Bica, I., McGovern, B., Dhar, R., Stone, D., McGowan, K., Scheib, R., and Snydman, D. R. (2001). Increasing mortality due to end-stage liver disease in patients with human immunodeficiency virus infection. *Clin Infect Dis* **32**, 492-7.

Bird, G. L., and Williams, R. (1989). Detection of antibodies to a halothane metabolite hapten in sera from patients with halothane-associated hepatitis. *J Hepatol* **9**, 366-73.

Bissell, D. M., Gores, G. J., Laskin, D. L., and Hoofnagle, J. H. (2001). Drug-induced liver injury: mechanisms and test systems. *Hepatology* **33**, 1009-13.

Bjorge, S. M., and Baillie, T. A. (1991). Studies on the beta-oxidation of valproic acid in rat liver mitochondrial preparations. *Drug Metab Dispos* **19**, 823-9.

Black, M., Mitchell, J. R., Zimmerman, H. J., Ishak, K. G., and Epler, G. R. (1975). Isoniazid-associated hepatitis in 114 patients. *Gastroenterology* **69**, 289-302.

Blazka, M. E., Elwell, M. R., Holladay, S. D., Wilson, R. E., and Luster, M. I. (1996). Histopathology of acetaminophen-induced liver changes: role of interleukin 1 alpha and tumor necrosis factor alpha. *Toxicol Pathol* **24**, 181-9.

Blazka, M. E., Wilmer, J. L., Holladay, S. D., Wilson, R. E., and Luster, M. I. (1995). Role of proinflammatory cytokines in acetaminophen hepatotoxicity. *Toxicol Appl Pharmacol* **133**, 43-52.

Boelsterli, U. A., and Lim, P. L. (2007). Mitochondrial abnormalities--a link to idiosyncratic drug hepatotoxicity? *Toxicol Appl Pharmacol* **220**, 92-107.

Boess, F., Bopst, M., Althaus, R., Polsky, S., Cohen, S. D., Eugster, H. P., and Boelsterli, U. A. (1998). Acetaminophen hepatotoxicity in tumor necrosis factor/lymphotoxin-alpha gene knockout mice. *Hepatology* **27**, 1021-9.

Bornemann, L. D., Min, B. H., Crews, T., Rees, M. M., Blumenthal, H. P., Colburn, W. A., and Patel, I. H. (1985). Dose dependent pharmacokinetics of midazolam. *Eur J Clin Pharmacol* **29**, 91-5.

Bose, P. D., Sarma, M. P., Medhi, S., Das, B. C., Husain, S. A., and Kar, P. (2011). Role of polymorphic N-acetyl transferase2 and cytochrome P4502E1 gene in antituberculosis treatment-induced hepatitis. *J Gastroenterol Hepatol* **26**, 312-8.

Bourdi, M., Korrapati, M. C., Chakraborty, M., Yee, S. B., and Pohl, L. R. (2008). Protective role of c-Jun N-terminal kinase 2 in acetaminophen-induced liver injury. *Biochem Biophys Res Commun* **374**, 6-10.

Breuer, R. I. (1965). Chlorpromazine Hepatotoxicity Manifested by a Selective and Sustained Rise of Serum Alkaline Phosphatase Activity; Report of a Case. *The American journal of digestive diseases* **10**, 727-31.

Bryant, A. E., 3rd, and Dreifuss, F. E. (1996). Valproic acid hepatic fatalities. III. U.S. experience since 1986. *Neurology* **46**, 465-9.

Buchweitz, J. P., Ganey, P. E., Bursian, S. J., and Roth, R. A. (2001). Underlying endotoxemia augments toxic responses to chlorpromazine: is there a relationship to drug idiosyncrasy? *The Journal of pharmacology and experimental therapeutics* **300**, 460-7.

Buchweitz, J. P., Ganey, P. E., Bursian, S. J., and Roth, R. A. (2002). Underlying endotoxemia augments toxic responses to chlorpromazine: is there a relationship to drug idiosyncrasy? *J Pharmacol Exp Ther* **300**, 460-7.

Callahan, S. M., Ming, X., Lu, S. K., Brunner, L. J., and Croyle, M. A. (2005). Considerations for use of recombinant adenoviral vectors: dose effect on hepatic cytochromes P450. *J Pharmacol Exp Ther* **312**, 492-501.

Calle, E. E., Rodriguez, C., Walker-Thurmond, K., and Thun, M. J. (2003). Overweight, obesity, and mortality from cancer in a prospectively studied cohort of U.S. adults. *N Engl J Med* **348**, 1625-38.

Carlson, T. J., and Billings, R. E. (1996). Role of nitric oxide in the cytokine-mediated regulation of cytochrome P-450. *Mol Pharmacol* **49**, 796-801.

Chalasani, N., and Bjornsson, E. (2010). Risk factors for idiosyncratic drug-induced liver injury. *Gastroenterology* **138**, 2246-59.

Chalasani, N., Fontana, R. J., Bonkovsky, H. L., Watkins, P. B., Davern, T., Serrano, J., Yang, H., Rochon, J., and Drug Induced Liver Injury, N. (2008). Causes, clinical features, and outcomes from a prospective study of drug-induced liver injury in the United States. *Gastroenterology* **135**, 1924-34, 1934 e1-4.

Chaluvadi, M. R., Kinloch, R. D., Nyagode, B. A., Richardson, T. A., Raynor, M. J., Sherman, M., Antonovic, L., Strobel, H. W., Dillehay, D. L., and Morgan, E. T. (2009). Regulation of hepatic cytochrome P450 expression in mice with intestinal or systemic infections of citrobacter rodentium. *Drug Metab Dispos* **37**, 366-74.

Chatterjee, S., Lyle, N., Mandal, A., and Kundu, S. (2010). GSTT1 and GSTM1 gene deletions are not associated with hepatotoxicity caused by antitubercular drugs. *J Clin Pharm Ther* **35**, 465-70.

Chen, J., Lin, H., and Hu, M. (2003). Metabolism of flavonoids via enteric recycling: role of intestinal disposition. *J Pharmacol Exp Ther* **304**, 1228-35.

Chen, Y., Tang, Y., Guo, C., Wang, J., Boral, D., and Nie, D. (2012). Nuclear receptors in the multidrug resistance through the regulation of drug-metabolizing enzymes and drug transporters. *Biochem Pharmacol* **83**, 1112-26.

Cheng, J., Ma, X., Krausz, K. W., Idle, J. R., and Gonzalez, F. J. (2009a). Rifampicin-activated human pregnane X receptor and CYP3A4 induction enhance acetaminophen-induced toxicity. *Drug Metab Dispos* **37**, 1611-21.

Cheng, L., You, Q., Yin, H., Holt, M., Franklin, C., and Ju, C. (2009b). Effect of polyI:C cotreatment on halothane-induced liver injury in mice. *Hepatology* **49**, 215-26.

Cheng, L., You, Q., Yin, H., Holt, M. P., and Ju, C. (2010). Involvement of natural killer T cells in halothane-induced liver injury in mice. *Biochem Pharmacol* **80**, 255-61.

Chiu, H., Gardner, C. R., Dambach, D. M., Durham, S. K., Brittingham, J. A., Laskin, J. D., and Laskin, D. L. (2003). Role of tumor necrosis factor receptor 1 (p55) in hepatocyte

proliferation during acetaminophen-induced toxicity in mice. *Toxicol Appl Pharmacol* **193**, 218-27.

Choti, M. A., Sitzmann, J. V., Tiburi, M. F., Sumetchotimetha, W., Rangsin, R., Schulick, R. D., Lillemoe, K. D., Yeo, C. J., and Cameron, J. L. (2002). Trends in long-term survival following liver resection for hepatic colorectal metastases. *Ann Surg* **235**, 759-66.

Clark, M. A., Williams, J. F., Gottschall, P. E., and Wecker, L. (1996). Effects of phenobarbital and interleukin-6 on cytochrome P4502B1 and 2B2 in cultured rat hepatocytes. *Biochem Pharmacol* **51**, 701-6.

Clayton, T. A., Lindon, J. C., Everett, J. R., Charuel, C., Hanton, G., Le Net, J. L., Provost, J. P., and Nicholson, J. K. (2003). An hypothesis for a mechanism underlying hepatotoxin-induced hypercreatinuria. *Arch Toxicol* **77**, 208-17.

Collins, S., Martin, T. L., Surwit, R. S., and Robidoux, J. (2004). Genetic vulnerability to diet-induced obesity in the C57BL/6J mouse: physiological and molecular characteristics. *Physiol Behav* **81**, 243-8.

Connolly, M. K., Ayo, D., Malhotra, A., Hackman, M., Bedrosian, A. S., Ibrahim, J., Cieza-Rubio, N. E., Nguyen, A. H., Henning, J. R., Dorvil-Castro, M., Pachter, H. L., and Miller, G. (2011). Dendritic cell depletion exacerbates acetaminophen hepatotoxicity. *Hepatology* **54**, 959-68.

Conze, D., Krahl, T., Kennedy, N., Weiss, L., Lumsden, J., Hess, P., Flavell, R. A., Le Gros, G., Davis, R. J., and Rincon, M. (2002). c-Jun NH(2)-terminal kinase (JNK)1 and JNK2 have distinct roles in CD8(+) T cell activation. *J Exp Med* **195**, 811-23.

Corbett, T. H., and Nettesheim, P. (1973). Effect of PR-8 viral respiratory infection of benz[a]pyrene hydroxylase activity in BALB/c mice. *J Natl Cancer Inst* **50**, 779-82.

Czejka, M., Kiss, A., Koessner, C., Terkola, R., Ettlinger, D., and Schueller, J. (2011). Metabolic activation of irinotecan during intra-arterial chemotherapy of metastatic colorectal cancer. *Anticancer Res* **31**, 3573-8.

Davis, R. J. (2000). Signal transduction by the JNK group of MAP kinases. *Cell* **103**, 239-52.

de Boever, S., Neirinckx, E. A., Meyer, E., de Baere, S., Beyaert, R., de Backer, P., and Croubels, S. (2010). Pharmacodynamics of tepoxalin, sodium-salicylate and ketoprofen

in an intravenous lipopolysaccharide inflammation model in broiler chickens. *J Vet Pharmacol Ther* **33**, 564-72.

Delaporte, E., and Renton, K. W. (1997). Cytochrome P4501A1 and cytochrome P4501A2 are downregulated at both transcriptional and post-transcriptional levels by conditions resulting in interferon-alpha/beta induction. *Life sciences* **60**, 787-96.

den Brinker, M., Wit, F. W., Wertheim-van Dillen, P. M., Jurriaans, S., Weel, J., van Leeuwen, R., Pakker, N. G., Reiss, P., Danner, S. A., Weverling, G. J., and Lange, J. M. (2000). Hepatitis B and C virus co-infection and the risk for hepatotoxicity of highly active antiretroviral therapy in HIV-1 infection. *AIDS (London, England)* **14**, 2895-902.

Deng, X., Luyendyk, J. P., Ganey, P. E., and Roth, R. A. (2009). Inflammatory stress and idiosyncratic hepatotoxicity: hints from animal models. *Pharmacol Rev* **61**, 262-82.

Deng, X., Stachlewitz, R. F., Liguori, M. J., Blomme, E. A., Waring, J. F., Luyendyk, J. P., Maddox, J. F., Ganey, P. E., and Roth, R. A. (2006). Modest inflammation enhances diclofenac hepatotoxicity in rats: role of neutrophils and bacterial translocation. *J Pharmacol Exp Ther* **319**, 1191-9.

Derby, L. E., Gutthann, S. P., Jick, H., and Dean, A. D. (1993). Liver disorders in patients receiving chlorpromazine or isoniazid. *Pharmacotherapy* **13**, 353-8.

Dixon, R. L., Hart, L. G., and Fouts, J. R. (1961). The metabolism of drugs by liver microsomes from alloxan-diabetic rats. *J Pharmacol Exp Ther* **133**, 7-11.

Driessen, J. J., Vree, T. B., and Guelen, P. J. (1991). The effects of acute changes in renal function on the pharmacokinetics of midazolam during long-term infusion in ICU patients. *Acta Anaesthesiol Belg* **42**, 149-55.

Edling, Y., Sivertsson, L. K., Butura, A., Ingelman-Sundberg, M., and Ek, M. (2009). Increased sensitivity for troglitazone-induced cytotoxicity using a human in vitro co-culture model. *Toxicol In Vitro* **23**, 1387-95.

Eghtesadi-Araghi, P., Sohrabpour, A., Vahedi, H., and Saberi-Firoozi, M. (2008). Halothane hepatitis in Iran: a review of 59 cases. *World J Gastroenterol* **14**, 5322-6.

Ena, J., Amador, C., Benito, C., Fenoll, V., and Pasquau, F. (2003). Risk and determinants of developing severe liver toxicity during therapy with nevirapine-and efavirenz-containing regimens in HIV-infected patients. *International journal of STD & AIDS* **14**, 776-81.

Ernst, E. (2002). Safety concerns about kava. *Lancet* **359**, 1865.

Fernandez, F. G., Drebin, J. A., Linehan, D. C., Dehdashti, F., Siegel, B. A., and Strasberg, S. M. (2004). Five-year survival after resection of hepatic metastases from colorectal cancer in patients screened by positron emission tomography with F-18 fluorodeoxyglucose (FDG-PET). *Ann Surg* **240**, 438-47; discussion 447-50.

Fernandez, F. G., Ritter, J., Goodwin, J. W., Linehan, D. C., Hawkins, W. G., and Strasberg, S. M. (2005). Effect of steatohepatitis associated with irinotecan or oxaliplatin pretreatment on resectability of hepatic colorectal metastases. *J Am Coll Surg* **200**, 845-53.

Ferrari, L., Peng, N., Halpert, J. R., and Morgan, E. T. (2001). Role of nitric oxide in down-regulation of CYP2B1 protein, but not RNA, in primary cultures of rat hepatocytes. *Mol Pharmacol* **60**, 209-16.

Fey, G. H., and Gauldie, J. (1990). The acute phase response of the liver in inflammation. *Prog Liver Dis* **9**, 89-116.

Fitzgerald, K. A., Palsson-McDermott, E. M., Bowie, A. G., Jefferies, C. A., Mansell, A. S., Brady, G., Brint, E., Dunne, A., Gray, P., Harte, M. T., McMurray, D., Smith, D. E., Sims, J. E., Bird, T. A., and O'Neill, L. A. (2001). Mal (MyD88-adapter-like) is required for Toll-like receptor-4 signal transduction. *Nature* **413**, 78-83.

Floyd-Smith, G., Slattery, E., and Lengyel, P. (1981). Interferon action: RNA cleavage pattern of a (2'-5')oligoadenylate--dependent endonuclease. *Science (New York, N.Y* **212**, 1030-2.

Floyd, M. D., Gervasini, G., Masica, A. L., Mayo, G., George, A. L., Jr., Bhat, K., Kim, R. B., and Wilkinson, G. R. (2003). Genotype-phenotype associations for common CYP3A4 and CYP3A5 variants in the basal and induced metabolism of midazolam in European- and African-American men and women. *Pharmacogenetics* **13**, 595-606.

Fouts, J. R. (1963). Factors Affecting Hepatic Microsomal Enzyme Systems Involved in Drug Metabolism. *Advances in enzyme regulation* **1**, 225-33.

Frapolli, R., Zucchetti, M., Sessa, C., Marsoni, S., Vigano, L., Locatelli, A., Rulli, E., Compagnoni, A., Bello, E., Pisano, C., Carminati, P., and D'Incalci, M. (2010). Clinical pharmacokinetics of the new oral camptothecin gimatecan: the inter-patient variability is related to alpha1-acid glycoprotein plasma levels. *Eur J Cancer* **46**, 505-16.

Fulco, R. A., Costa, C., Germano, M. P., Torre, E. A., Viscomi, M. G., Salimbeni, V., Maisano, R., Giudice, A., and Costa, G. (2000). Hepatotoxicity of camptothecin derivatives in a primary culture system of rat hepatocytes. *J Chemother* **12**, 345-51.

Gadina, M., Bertini, R., Mengozzi, M., Zandalasini, M., Mantovani, A., and Ghezzi, P. (1991). Protective effect of chlorpromazine on endotoxin toxicity and TNF production in glucocorticoid-sensitive and glucocorticoid-resistant models of endotoxic shock. *The Journal of experimental medicine* **173**, 1305-10.

Galloway, E., Shin, T., Huber, N., Eismann, T., Kuboki, S., Schuster, R., Blanchard, J., Wong, H. R., and Lentsch, A. B. (2008). Activation of hepatocytes by extracellular heat shock protein 72. *Am J Physiol Cell Physiol* **295**, C514-20.

Gandhi, A., Guo, T., and Ghose, R. (2010). Role of c-Jun N-terminal kinase (JNK) in regulating tumor necrosis factor-alpha (TNF-alpha) mediated increase of acetaminophen (APAP) and chlorpromazine (CPZ) toxicity in murine hepatocytes. *The Journal of toxicological sciences* **35**, 163-73.

Gandhi, A. S., Guo, T., Shah, P., Moorthy, B., Chow, D. S., Hu, M., and Ghose, R. (2012). CYP3A-dependent drug metabolism is reduced in bacterial inflammation in mice. *Br J Pharmacol*.

Ganey, P. E., Luyendyk, J. P., Maddox, J. F., and Roth, R. A. (2004). Adverse hepatic drug reactions: inflammatory episodes as consequence and contributor. *Chemico-biological interactions* **150**, 35-51.

Garcia Del Busto Cano, E., and Renton, K. W. (2003). Modulation of hepatic cytochrome P450 during Listeria monocytogenes infection of the brain. *J Pharm Sci* **92**, 1860-8.

Gardner, C. R., Laskin, J. D., Dambach, D. M., Chiu, H., Durham, S. K., Zhou, P., Bruno, M., Gerecke, D. R., Gordon, M. K., and Laskin, D. L. (2003). Exaggerated hepatotoxicity of acetaminophen in mice lacking tumor necrosis factor receptor-1. Potential role of inflammatory mediators. *Toxicol Appl Pharmacol* **192**, 119-30.

Gardner, C. R., Laskin, J. D., Dambach, D. M., Sacco, M., Durham, S. K., Bruno, M. K., Cohen, S. D., Gordon, M. K., Gerecke, D. R., Zhou, P., and Laskin, D. L. (2002). Reduced hepatotoxicity of acetaminophen in mice lacking inducible nitric oxide synthase: potential role of tumor necrosis factor-alpha and interleukin-10. *Toxicol Appl Pharmacol* **184**, 27-36.

Ghezzi, P., Garattini, S., Mennini, T., Bertini, R., Delgado Hernandez, R., Benigni, F., Sacco, S., Skorupska, M., Mengozzi, M., Latini, R., Kurosaki, M., Lombet, A., Fradin, A., Bonnet, J., Rolland, Y., and Brion, J. D. (1996). Mechanism of inhibition of tumor necrosis factor production by chlorpromazine and its derivatives in mice. *European journal of pharmacology* **317**, 369-76.

Ghose, R., Guo, T., and Haque, N. (2009). Regulation of gene expression of hepatic drug metabolizing enzymes and transporters by the Toll-like receptor 2 ligand, lipoteichoic acid. *Arch Biochem Biophys* **481**, 123-30.

Ghose, R., Guo, T., Vallejo, J. G., and Gandhi, A. (2011a). Differential role of Toll-interleukin 1 receptor domain-containing adaptor protein in Toll-like receptor 2-mediated regulation of gene expression of hepatic cytokines and drug-metabolizing enzymes. *Drug Metab Dispos* **39**, 874-81.

Ghose, R., Omoluabi, O., Gandhi, A., Shah, P., Strohacker, K., Carpenter, K. C., McFarlin, B., and Guo, T. (2011b). Role of high-fat diet in regulation of gene expression of drug metabolizing enzymes and transporters. *Life Sci* **89**, 57-64.

Ghose, R., White, D., Guo, T., Vallejo, J., and Karpen, S. J. (2008). Regulation of hepatic drug-metabolizing enzyme genes by Toll-like receptor 4 signaling is independent of Toll-interleukin 1 receptor domain-containing adaptor protein. *Drug metabolism and disposition: the biological fate of chemicals* **36**, 95-101.

Ghose, R., Zimmerman, T. L., Thevananther, S., and Karpen, S. J. (2004). Endotoxin leads to rapid subcellular re-localization of hepatic RXRalpha: A novel mechanism for reduced hepatic gene expression in inflammation. *Nucl Recept* **2**, 4.

Giannini, E., Fasoli, A., Botta, F., Romagnoli, P., Malfatti, F., Chiarbonello, B., Mamone, M., Savarino, V., and Testa, R. (2003). Helicobacter pylori infection is associated with greater impairment of cytochrome P-450 liver metabolic activity in anti-HCV positive cirrhotic patients. *Dig Dis Sci* **48**, 802-8.

Gilmore, T. D. (2006). Introduction to NF-kappaB: players, pathways, perspectives. *Oncogene* **25**, 6680-4.

Ginsburg, I. (2002). Role of lipoteichoic acid in infection and inflammation. *Lancet Infect Dis* **2**, 171-9.

Godellas, C. V., Williams, J. F., and Fabri, P. J. (1995). Mixed-function oxidase activity in sepsis. *J Surg Res* **59**, 783-6.

Godfrey, D. I., Hammond, K. J., Poulton, L. D., Smyth, M. J., and Baxter, A. G. (2000). NKT cells: facts, functions and fallacies. *Immunol Today* **21**, 573-83.

Goldkind, L., and Laine, L. (2006). A systematic review of NSAIDs withdrawn from the market due to hepatotoxicity: lessons learned from the bromfenac experience. *Pharmacoepidemiol Drug Saf* **15**, 213-20.

Goodwin, S. D., Gallis, H. A., Chow, A. T., Wong, F. A., Flor, S. C., and Bartlett, J. A. (1994). Pharmacokinetics and safety of levofloxacin in patients with human immunodeficiency virus infection. *Antimicrobial agents and chemotherapy* **38**, 799-804.

Gorski, J. C., Vannaprasaht, S., Hamman, M. A., Ambrosius, W. T., Bruce, M. A., Haehner-Daniels, B., and Hall, S. D. (2003). The effect of age, sex, and rifampin administration on intestinal and hepatic cytochrome P450 3A activity. *Clin Pharmacol Ther* **74**, 275-87.

Gous, A. G., Dance, M. D., Lipman, J., Luyt, D. K., Mathivha, R., and Scribante, J. (1995). Changes in vancomycin pharmacokinetics in critically ill infants. *Anaesth Intensive Care* **23**, 678-82.

Gray, J. D., Renton, K. W., and Hung, O. R. (1983). Depression of theophylline elimination following BCG vaccination. *Br J Clin Pharmacol* **16**, 735-7.

Greenblatt, D. J., von Moltke, L. L., Harmatz, J. S., Chen, G., Weemhoff, J. L., Jen, C., Kelley, C. J., LeDuc, B. W., and Zinny, M. A. (2003). Time course of recovery of cytochrome p450 3A function after single doses of grapefruit juice. *Clin Pharmacol Ther* **74**, 121-9.

Gu, X., Ke, S., Liu, D., Sheng, T., Thomas, P. E., Rabson, A. B., Gallo, M. A., Xie, W., and Tian, Y. (2006). Role of NF-kappaB in regulation of PXR-mediated gene expression: a mechanism for the suppression of cytochrome P-450 3A4 by proinflammatory agents. *J Biol Chem* **281**, 17882-9.

Guengerich, F. P. (1999). Cytochrome P-450 3A4: regulation and role in drug metabolism. *Annual review of pharmacology and toxicology* **39**, 1-17.

Guirguis, M. S., and Jamali, F. (2003). Disease-drug interaction: Reduced response to propranolol despite increased concentration in the rat with inflammation. *J Pharm Sci* **92**, 1077-84.

Gunawan, B. K., Liu, Z. X., Han, D., Hanawa, N., Gaarde, W. A., and Kaplowitz, N. (2006). c-Jun N-terminal kinase plays a major role in murine acetaminophen hepatotoxicity. *Gastroenterology* **131**, 165-78.

Guo, Y. L., Baysal, K., Kang, B., Yang, L. J., and Williamson, J. R. (1998). Correlation between sustained c-Jun N-terminal protein kinase activation and apoptosis induced by tumor necrosis factor-alpha in rat mesangial cells. *The Journal of biological chemistry* **273**, 4027-34.

Gurumurthy, P., Krishnamurthy, M. S., Nazareth, O., Parthasarathy, R., Sarma, G. R., Somasundaram, P. R., Tripathy, S. P., and Ellard, G. A. (1984). Lack of relationship between hepatic toxicity and acetylator phenotype in three thousand South Indian patients during treatment with isoniazid for tuberculosis. *Am Rev Respir Dis* **129**, 58-61.

Haasio, K., Koponen, A., Penttila, K. E., and Nissinen, E. (2002). Effects of entacapone and tolcapone on mitochondrial membrane potential. *Eur J Pharmacol* **453**, 21-6.

Halparin, L. S. (1984). Adverse effects of ranitidine therapy. *Canadian Medical Association journal* **130**, 668, 672.

Han, D., Shinohara, M., Ybanez, M. D., Saberi, B., and Kaplowitz, N. (2010). Signal transduction pathways involved in drug-induced liver injury. *Handb Exp Pharmacol*, 267-310.

Hanada, K., Nakai, K., Tanaka, H., Suzuki, F., Kumada, H., Ohno, Y., Ozawa, S., and Ogata, H. (2011). Effect of nuclear receptor downregulation on hepatic expression of cytochrome P450 and transporters in chronic hepatitis C in association with fibrosis development. *Drug metabolism and pharmacokinetics*.

Hanawa, N., Shinohara, M., Saberi, B., Gaarde, W. A., Han, D., and Kaplowitz, N. (2008). Role of JNK translocation to mitochondria leading to inhibition of mitochondria bioenergetics in acetaminophen-induced liver injury. *J Biol Chem* **283**, 13565-77.

Harstad, E. B., and Klaassen, C. D. (2002). Tumor necrosis factor-alpha-null mice are not resistant to cadmium chloride-induced hepatotoxicity. *Toxicol Appl Pharmacol* **179**, 155-62.

Hartmann, F., Gruenke, L. D., Craig, J. C., and Bissell, D. M. (1983). Chlorpromazine metabolism in extracts of liver and small intestine from guinea pig and from man. *Drug Metab Dispos* **11**, 244-8.

Hartmann, G., Vassileva, V., and Piquette-Miller, M. (2005). Impact of endotoxin-induced changes in P-glycoprotein expression on disposition of doxorubicin in mice. *Drug Metab Dispos* **33**, 820-8.

Hasegawa, T., Nadai, M., Wang, L., Haghgoo, S., Nabeshima, T., and Kato, N. (1994). Influence of endotoxin and lipid A on the renal handling and accumulation of gentamicin in rats. *Biol Pharm Bull* **17**, 1651-5.

He, K., Talaat, R. E., Pool, W. F., Reily, M. D., Reed, J. E., Bridges, A. J., and Woolf, T. F. (2004). Metabolic activation of troglitazone: identification of a reactive metabolite and mechanisms involved. *Drug Metab Dispos* **32**, 639-46.

He, P., Court, M. H., Greenblatt, D. J., and Von Moltke, L. L. (2005). Genotype-phenotype associations of cytochrome P450 3A4 and 3A5 polymorphism with midazolam clearance in vivo. *Clin Pharmacol Ther* **77**, 373-87.

He, P., Court, M. H., Greenblatt, D. J., and von Moltke, L. L. (2006). Factors influencing midazolam hydroxylation activity in human liver microsomes. *Drug Metab Dispos* **34**, 1198-207.

He, Q., and Sharma, R. P. (2005). Inhibition of tumor necrosis factor alpha signaling by anti-tumor necrosis factor alpha antibodies and pentoxifylline is unable to prevent fumonisin hepatotoxicity in mice. *Toxicon* **46**, 404-13.

Hecht, J. R. (1998). Gastrointestinal toxicity or irinotecan. *Oncology (Williston Park)* **12**, 72-8.

Henderson, N. C., Pollock, K. J., Frew, J., Mackinnon, A. C., Flavell, R. A., Davis, R. J., Sethi, T., and Simpson, K. J. (2007). Critical role of c-jun (NH2) terminal kinase in paracetamol- induced acute liver failure. *Gut* **56**, 982-90.

Hentze, H., Latta, M., Kunstle, G., Dhakshinamoorthy, S., Ng, P. Y., Porter, A. G., and Wendel, A. (2004). Topoisomerase inhibitor camptothecin sensitizes mouse hepatocytes in vitro and in vivo to TNF-mediated apoptosis. *Hepatology* **39**, 1311-20.

Hewett, J. A., Schultze, A. E., VanCise, S., and Roth, R. A. (1992). Neutrophil depletion protects against liver injury from bacterial endotoxin. *Lab Invest* **66**, 347-61.

Higgins, L. M., Frankel, G., Douce, G., Dougan, G., and MacDonald, T. T. (1999). Citrobacter rodentium infection in mice elicits a mucosal Th1 cytokine response and lesions similar to those in murine inflammatory bowel disease. *Infect Immun* **67**, 3031-9.

Higuchi, S., Kobayashi, M., Yoshikawa, Y., Tsuneyama, K., Fukami, T., Nakajima, M., and Yokoi, T. (2011). IL-4 mediates dicloxacillin-induced liver injury in mice. *Toxicol Lett* **200**, 139-45.

Hinson, J. A., Mays, J. B., and Cameron, A. M. (1983). Acetaminophen-induced hepatic glycogen depletion and hyperglycemia in mice. *Biochemical pharmacology* **32**, 1979-88.

Holt, M. P., Cheng, L., and Ju, C. (2008). Identification and characterization of infiltrating macrophages in acetaminophen-induced liver injury. *J Leukoc Biol* **84**, 1410-21.

Holt, M. P., Yin, H., and Ju, C. (2010). Exacerbation of acetaminophen-induced disturbances of liver sinusoidal endothelial cells in the absence of Kupffer cells in mice. *Toxicol Lett* **194**, 34-41.

Hoogerwerf, J. J., de Vos, A. F., Bresser, P., van der Zee, J. S., Pater, J. M., de Boer, A., Tanck, M., Lundell, D. L., Her-Jenh, C., Draing, C., von Aulock, S., and van der Poll, T. (2008). Lung inflammation induced by lipoteichoic acid or lipopolysaccharide in humans. *Am J Respir Crit Care Med* **178**, 34-41.

Horng, T., Barton, G. M., Flavell, R. A., and Medzhitov, R. (2002). The adaptor molecule TIRAP provides signalling specificity for Toll-like receptors. *Nature* **420**, 329-33.

Horng, T., Barton, G. M., and Medzhitov, R. (2001). TIRAP: an adapter molecule in the Toll signaling pathway. *Nat Immunol* **2**, 835-41.

Hu, Z. Y., Yu, Q., Pei, Q., and Guo, C. (2010). Dose-dependent association between UGT1A1*28 genotype and irinotecan-induced neutropenia: low doses also increase risk. *Clin Cancer Res* **16**, 3832-42.

Hunter, E. B., Johnston, P. E., Tanner, G., Pinson, C. W., and Awad, J. A. (1999). Bromfenac (Duract)-associated hepatic failure requiring liver transplantation. *The American journal of gastroenterology* **94**, 2299-301.

Hussaini, S. H., and Farrington, E. A. (2007). Idiosyncratic drug-induced liver injury: an overview. *Expert opinion on drug safety* **6**, 673-84.

Ikeda, T. (2011). Drug-induced idiosyncratic hepatotoxicity: prevention strategy developed after the troglitazone case. *Drug Metab Pharmacokinet* **26**, 60-70.

Imaeda, A. B., Watanabe, A., Sohail, M. A., Mahmood, S., Mohamadnejad, M., Sutterwala, F. S., Flavell, R. A., and Mehal, W. Z. (2009). Acetaminophen-induced hepatotoxicity in mice is dependent on Tlr9 and the Nalp3 inflammasome. *J Clin Invest* **119**, 305-14.

Ip, Y. T., and Davis, R. J. (1998). Signal transduction by the c-Jun N-terminal kinase (JNK)--from inflammation to development. *Current opinion in cell biology* **10**, 205-19.

Ishak, K. G., and Irey, N. S. (1972). Hepatic injury associated with the phenothiazines. Clinicopathologic and follow-up study of 36 patients. *Archives of pathology* **93**, 283-304.

Ishida, Y., Kondo, T., Tsuneyama, K., Lu, P., Takayasu, T., and Mukaida, N. (2004). The pathogenic roles of tumor necrosis factor receptor p55 in acetaminophen-induced liver injury in mice. *J Leukoc Biol* **75**, 59-67.

Ishikawa, M., Ohzeki, R., Takayanagi, Y., and Sasaki, K. (1990a). Potentiation of cisplatin lethality by bacterial lipopolysaccharide pretreatment in mice. *Res Commun Chem Pathol Pharmacol* **70**, 375-8.

Ishikawa, M., Tanno, K., Sasaki, M., Takayanagi, Y., and Sasaki, K. (1990b). Antidotal effect of lipopolysaccharide against acetaminophen-induced mortality in mice. *Pharmacol Toxicol* **67**, 387-91.

Ishikawa, M., Tanno, K., Takayanagi, Y., and Sasaki, K. (1990c). Prevention of acetaminophen-induced hepatotoxicity by endotoxin in mice. *Res Commun Chem Pathol Pharmacol* **69**, 111-4.

James, L. P., Lamps, L. W., McCullough, S., and Hinson, J. A. (2003a). Interleukin 6 and hepatocyte regeneration in acetaminophen toxicity in the mouse. *Biochem Biophys Res Commun* **309**, 857-63.

James, L. P., McCullough, S. S., Lamps, L. W., and Hinson, J. A. (2003b). Effect of N-acetylcysteine on acetaminophen toxicity in mice: relationship to reactive nitrogen and cytokine formation. *Toxicol Sci* **75**, 458-67.

Jernas, M., Olsson, B., Arner, P., Jacobson, P., Sjostrom, L., Walley, A., Froguel, P., McTernan, P. G., Hoffstedt, J., and Carlsson, L. M. (2009). Regulation of carboxylesterase 1 (CES1) in human adipose tissue. *Biochem Biophys Res Commun* **383**, 63-7.

Jones, A. E., Brown, K. C., Werner, R. E., Gotzkowsky, K., Gaedigk, A., Blake, M., Hein, D. W., van der Horst, C., and Kashuba, A. D. (2010). Variability in drug metabolizing enzyme activity in HIV-infected patients. *European journal of clinical pharmacology* **66**, 475-85.

Jover, R., Bort, R., Gomez-Lechon, M. J., and Castell, J. V. (2002). Down-regulation of human CYP3A4 by the inflammatory signal interleukin-6: molecular mechanism and transcription factors involved. *Faseb J* **16**, 1799-801.

Ju, C., Reilly, T. P., Bourdi, M., Radonovich, M. F., Brady, J. N., George, J. W., and Pohl, L. R. (2002). Protective role of Kupffer cells in acetaminophen-induced hepatic injury in mice. *Chem Res Toxicol* **15**, 1504-13.

Kacevska, M., Downes, M. R., Sharma, R., Evans, R. M., Clarke, S. J., Liddle, C., and Robertson, G. R. (2011). Extrahepatic cancer suppresses nuclear receptor-regulated drug metabolism. *Clin Cancer Res* **17**, 3170-80.

Kagan, J. C., and Medzhitov, R. (2006). Phosphoinositide-mediated adaptor recruitment controls Toll-like receptor signaling. *Cell* **125**, 943-55.

Kaisho, T., Takeuchi, O., Kawai, T., Hoshino, K., and Akira, S. (2001). Endotoxin-induced maturation of MyD88-deficient dendritic cells. *J Immunol* **166**, 5688-94.

Kakimi, K., Guidotti, L. G., Koezuka, Y., and Chisari, F. V. (2000). Natural killer T cell activation inhibits hepatitis B virus replication in vivo. *J Exp Med* **192**, 921-30.

Kakuda, T. N. (2000). Pharmacology of nucleoside and nucleotide reverse transcriptase inhibitor-induced mitochondrial toxicity. *Clin Ther* **22**, 685-708.

Kaneda, N., Nagata, H., Furuta, T., and Yokokura, T. (1990). Metabolism and pharmacokinetics of the camptothecin analogue CPT-11 in the mouse. *Cancer Res* **50**, 1715-20.

Kaplowitz, N. (2005). Idiosyncratic drug hepatotoxicity. *Nat Rev Drug Discov* **4**, 489-99.

Kaplowitz, N., Aw, T. Y., Simon, F. R., and Stolz, A. (1986). Drug-induced hepatotoxicity. *Ann Intern Med* **104**, 826-39.

Kaplowitz, N., Shinohara, M., Liu, Z. X., and Han, D. (2008). How to protect against acetaminophen: don't ask for JUNK. *Gastroenterology* **135**, 1047-51.

Kato, R. (1977). Drug metabolism under pathological and abnormal physiological states in animals and man. *Xenobiotica; the fate of foreign compounds in biological systems* **7**, 25-92.

Kato, R., Frontino, G., and Vassanellip (1963). Decreased activities of liver microsomal drug-metabolizing enzymes in the rats bearing Walker carcinosarcoma. *Experientia* **19**, 31-2.

Kato, R., Takanaka, A., and Oshima, T. (1968). Drug metabolism in tumor-bearing rats. II. In vivo metabolisms and effects of drugs in tumor-bearing rats. *Jpn J Pharmacol* **18**, 245-54.

Kawai, T., Adachi, O., Ogawa, T., Takeda, K., and Akira, S. (1999). Unresponsiveness of MyD88-deficient mice to endotoxin. *Immunity* **11**, 115-22.

Kayama, F., Yoshida, T., Elwell, M. R., and Luster, M. I. (1995). Role of tumor necrosis factor-alpha in cadmium-induced hepatotoxicity. *Toxicol Appl Pharmacol* **131**, 224-34.

Kikuchi, R., McCown, M., Olson, P., Tateno, C., Morikawa, Y., Katoh, Y., Bourdet, D. L., Monshouwer, M., and Fretland, A. J. (2010). Effect of hepatitis C virus infection on the mRNA expression of drug transporters and cytochrome p450 enzymes in chimeric mice with humanized liver. *Drug metabolism and disposition: the biological fate of chemicals* **38**, 1954-61.

Kinloch, R. D., Lee, C. M., van Rooijen, N., and Morgan, E. T. (2011). Selective role for tumor necrosis factor-alpha, but not interleukin-1 or Kupffer cells, in down-regulation of CYP3A11 and CYP3A25 in livers of mice infected with a noninvasive intestinal pathogen. *Biochem Pharmacol* **82**, 312-21.

Kleiner, D. E., Brunt, E. M., Van Natta, M., Behling, C., Contos, M. J., Cummings, O. W., Ferrell, L. D., Liu, Y. C., Torbenson, M. S., Unalp-Arida, A., Yeh, M., McCullough, A. J., and Sanyal, A. J. (2005). Design and validation of a histological scoring system for nonalcoholic fatty liver disease. *Hepatology* **41**, 1313-21.

Klotz, U., McHorse, T. S., Wilkinson, G. R., and Schenker, S. (1974). The effect of cirrhosis on the disposition and elimination of meperidine in man. *Clin Pharmacol Ther* **16**, 667-75.

Kohlroser, J., Mathai, J., Reichheld, J., Banner, B. F., and Bonkovsky, H. L. (2000). Hepatotoxicity due to troglitazone: report of two cases and review of adverse events

reported to the United States Food and Drug Administration. *The American journal of gastroenterology* **95**, 272-6.

Kotegawa, T., Laurijssens, B. E., Von Moltke, L. L., Cotreau, M. M., Perloff, M. D., Venkatakrishnan, K., Warrington, J. S., Granda, B. W., Harmatz, J. S., and Greenblatt, D. J. (2002). In vitro, pharmacokinetic, and pharmacodynamic interactions of ketoconazole and midazolam in the rat. *J Pharmacol Exp Ther* **302**, 1228-37.

Kovari, H., Ledergerber, B., Battegay, M., Rauch, A., Hirschel, B., Foguena, A. K., Vernazza, P., Bernasconi, E., Mueller, N. J., and Weber, R. (2010). Incidence and risk factors for chronic elevation of alanine aminotransferase levels in HIV-infected persons without hepatitis b or c virus co-infection. *Clin Infect Dis* **50**, 502-11.

Kraemer, M. J., Furukawa, C. T., Koup, J. R., Shapiro, G. G., Pierson, W. E., and Bierman, C. W. (1982). Altered theophylline clearance during an influenza B outbreak. *Pediatrics* **69**, 476-80.

Lang, C., Meier, Y., Stieger, B., Beuers, U., Lang, T., Kerb, R., Kullak-Ublick, G. A., Meier, P. J., and Pauli-Magnus, C. (2007). Mutations and polymorphisms in the bile salt export pump and the multidrug resistance protein 3 associated with drug-induced liver injury. *Pharmacogenet Genomics* **17**, 47-60.

Larson, A. M., Polson, J., Fontana, R. J., Davern, T. J., Lalani, E., Hynan, L. S., Reisch, J. S., Schiodt, F. V., Ostapowicz, G., Shakil, A. O., Lee, W. M., and Acute Liver Failure Study, G. (2005). Acetaminophen-induced acute liver failure: results of a United States multicenter, prospective study. *Hepatology* **42**, 1364-72.

Laskin, D. L., Pilaro, A. M., and Ji, S. (1986). Potential role of activated macrophages in acetaminophen hepatotoxicity. II. Mechanism of macrophage accumulation and activation. *Toxicol Appl Pharmacol* **86**, 216-26.

Lasser, K. E., Allen, P. D., Woolhandler, S. J., Himmelstein, D. U., Wolfe, S. M., and Bor, D. H. (2002). Timing of new black box warnings and withdrawals for prescription medications. *JAMA* **287**, 2215-20.

Le, H. T., Boquet, M. P., Clark, E. A., Callahan, S. M., and Croyle, M. A. (2006). Renal pathophysiology after systemic administration of recombinant adenovirus: changes in renal cytochromes P450 based on vector dose. *Hum Gene Ther* **17**, 1095-111.

Lee, B. L., Wong, D., Benowitz, N. L., and Sullam, P. M. (1993). Altered patterns of drug metabolism in patients with acquired immunodeficiency syndrome. *Clin Pharmacol Ther* **53**, 529-35.

Lee, C. C., Avalos, A. M., and Ploegh, H. L. (2012). Accessory molecules for Toll-like receptors and their function. *Nat Rev Immunol* **12**, 168-79.

Lee, J. S., Wang, J., Martin, M., Germer, S., Kenwright, A., Benayed, R., Spleiss, O., Platt, A., Pilson, R., Hemmings, A., Weinblatt, M. E., Kaplowitz, N., and Krasnow, J. (2011). Genetic variation in UGT1A1 typical of Gilbert syndrome is associated with unconjugated hyperbilirubinemia in patients receiving tocilizumab. *Pharmacogenet Genomics* **21**, 365-74.

Lee, W. M. (2003). Acute liver failure in the United States. *Semin Liver Dis* **23**, 217-26.

Leemans, J. C., Vervoordeldonk, M. J., Florquin, S., van Kessel, K. P., and van der Poll, T. (2002). Differential role of interleukin-6 in lung inflammation induced by lipoteichoic acid and peptidoglycan from Staphylococcus aureus. *Am J Respir Crit Care Med* **165**, 1445-50.

Leiro-Fernandez, V., Valverde, D., Vazquez-Gallardo, R., Constenla, L., and Fernandez-Villar, A. (2010). Genetic variations of NAT2 and CYP2E1 and isoniazid hepatotoxicity in a diverse population. *Pharmacogenomics* **11**, 1205-6; author reply 1207-8.

Lewis, J. H., Mullick, F., Ishak, K. G., Ranard, R. C., Ragsdale, B., Perse, R. M., Rusnock, E. J., Wolke, A., Benjamin, S. B., Seeff, L. B., and et al. (1990). Histopathologic analysis of suspected amiodarone hepatotoxicity. *Hum Pathol* **21**, 59-67.

Li, A. P. (2002). A review of the common properties of drugs with idiosyncratic hepatotoxicity and the "multiple determinant hypothesis" for the manifestation of idiosyncratic drug toxicity. *Chem Biol Interact* **142**, 7-23.

Lin, A. (2003). Activation of the JNK signaling pathway: breaking the brake on apoptosis. *Bioessays* **25**, 17-24.

Liu, J., Sendelbach, L. E., Parkinson, A., and Klaassen, C. D. (2000). Endotoxin pretreatment protects against the hepatotoxicity of acetaminophen and carbon tetrachloride: role of cytochrome P450 suppression. *Toxicology* **147**, 167-76.

Liu, S., Gallo, D. J., Green, A. M., Williams, D. L., Gong, X., Shapiro, R. A., Gambotto, A. A., Humphris, E. L., Vodovotz, Y., and Billiar, T. R. (2002). Role of toll-like

receptors in changes in gene expression and NF-kappa B activation in mouse hepatocytes stimulated with lipopolysaccharide. *Infect Immun* **70**, 3433-42.

Liu, Z. X., Govindarajan, S., and Kaplowitz, N. (2004). Innate immune system plays a critical role in determining the progression and severity of acetaminophen hepatotoxicity. *Gastroenterology* **127**, 1760-74.

Lu, C. Y., Li, C. C., Liu, K. L., Lii, C. K., and Chen, H. W. (2009). Docosahexaenoic acid downregulates phenobarbital-induced cytochrome P450 2B1 gene expression in rat primary hepatocytes via the c-Jun NH2-terminal kinase mitogen-activated protein kinase pathway. *Mol Nutr Food Res* **53**, 341-8.

Lu, J., Jones, A. D., Harkema, J. R., Roth, R. A., and Ganey, P. E. (2012). Amiodarone Exposure During Modest Inflammation Induces Idiosyncrasy-like Liver Injury in Rats: Role of Tumor Necrosis Factor-alpha. *Toxicol Sci* **125**, 126-33.

Lucena, M. I., Garcia-Martin, E., Andrade, R. J., Martinez, C., Stephens, C., Ruiz, J. D., Ulzurrun, E., Fernandez, M. C., Romero-Gomez, M., Castiella, A., Planas, R., Duran, J. A., De Dios, A. M., Guarner, C., Soriano, G., Borraz, Y., and Agundez, J. A. (2010). Mitochondrial superoxide dismutase and glutathione peroxidase in idiosyncratic drug-induced liver injury. *Hepatology* **52**, 303-12.

Luyendyk, J. P., Maddox, J. F., Cosma, G. N., Ganey, P. E., Cockerell, G. L., and Roth, R. A. (2003). Ranitidine treatment during a modest inflammatory response precipitates idiosyncrasy-like liver injury in rats. *The Journal of pharmacology and experimental therapeutics* **307**, 9-16.

Luyendyk, J. P., Shores, K. C., Ganey, P. E., and Roth, R. A. (2002). Bacterial lipopolysaccharide exposure alters aflatoxin B(1) hepatotoxicity: benchmark dose analysis for markers of liver injury. *Toxicol Sci* **68**, 220-5.

Macher, E., and Chase, M. W. (1969). Studies on the sensitization of animals with simple chemical compounds. XI. The fate of labeled picryl chloride and dinitrochlorobenzene after sensitizing injections. *J Exp Med* **129**, 81-102.

Maddox, J. F., Amuzie, C. J., Li, M., Newport, S. W., Sparkenbaugh, E., Cuff, C. F., Pestka, J. J., Cantor, G. H., Roth, R. A., and Ganey, P. E. (2010). Bacterial- and viral-induced inflammation increases sensitivity to acetaminophen hepatotoxicity. *Journal of toxicology and environmental health* **73**, 58-73.

Maddox, J. F., Luyendyk, J. P., Cosma, G. N., Breau, A. P., Bible, R. H., Jr., Harrigan, G. G., Goodacre, R., Ganey, P. E., Cantor, G. H., Cockerell, G. L., and Roth, R. A. (2006). Metabonomic evaluation of idiosyncrasy-like liver injury in rats cotreated with ranitidine and lipopolysaccharide. *Toxicology and applied pharmacology* **212**, 35-44.

Mandema, J. W., Tuk, B., van Steveninck, A. L., Breimer, D. D., Cohen, A. F., and Danhof, M. (1992). Pharmacokinetic-pharmacodynamic modeling of the central nervous system effects of midazolam and its main metabolite alpha-hydroxymidazolam in healthy volunteers. *Clin Pharmacol Ther* **51**, 715-28.

Manian, A. A., Efron, D. H., and Goldberg, M. E. (1965). A comparative pharmacological study of a series of monohydroxylated and methoxylated chlorpromazine derivatives. *Life Sci* **4**, 2425-38.

Maniratanachote, R., Shibata, A., Kaneko, S., Yamamori, I., Wakasugi, T., Sawazaki, T., Katoh, K., Tokudome, S., Nakajima, M., and Yokoi, T. (2005). Detection of autoantibody to aldolase B in sera from patients with troglitazone-induced liver dysfunction. *Toxicology* **216**, 15-23.

Mannering, G. J., and Deloria, L. B. (1986). The pharmacology and toxicology of the interferons: an overview. *Annu Rev Pharmacol Toxicol* **26**, 455-515.

Margalit, M., Shibolet, O., Klein, A., Elinav, E., Alper, R., Thalenfeld, B., Engelhardt, D., Rabbani, E., and Ilan, Y. (2005). Suppression of hepatocellular carcinoma by transplantation of ex-vivo immune-modulated NKT lymphocytes. *Int J Cancer* **115**, 443-9.

Marshall, T., Shult, P., and Busse, W. W. (1988). Release of lysosomal enzyme beta-glucuronidase from isolated human eosinophils. *J Allergy Clin Immunol* **82**, 550-5.

Martin, G. S., Mannino, D. M., Eaton, S., and Moss, M. (2003). The epidemiology of sepsis in the United States from 1979 through 2000. *N Engl J Med* **348**, 1546-54.

Masson, M. J., Carpenter, L. D., Graf, M. L., and Pohl, L. R. (2008). Pathogenic role of natural killer T and natural killer cells in acetaminophen-induced liver injury in mice is dependent on the presence of dimethyl sulfoxide. *Hepatology* **48**, 889-97.

Masubuchi, Y., Bourdi, M., Reilly, T. P., Graf, M. L., George, J. W., and Pohl, L. R. (2003). Role of interleukin-6 in hepatic heat shock protein expression and protection against acetaminophen-induced liver disease. *Biochem Biophys Res Commun* **304**, 207-12.

Matuskova, Z., Tunkova, A., Anzenbacherova, E., Zidek, Z., Tlaskalova-Hogenova, H., and Anzenbacher, P. (2009). Influence of probiotics on rat liver biotransformation enzymes. *Neuro Endocrinol Lett* **30 Suppl 1**, 41-5.

Mayo, P. R., Skeith, K., Russell, A. S., and Jamali, F. (2000). Decreased dromotropic response to verapamil despite pronounced increased drug concentration in rheumatoid arthritis. *Br J Clin Pharmacol* **50**, 605-13.

McBurney, R. N., Hines, W. M., Von Tungeln, L. S., Schnackenberg, L. K., Beger, R. D., Moland, C. L., Han, T., Fuscoe, J. C., Chang, C. W., Chen, J. J., Su, Z., Fan, X. H., Tong, W., Booth, S. A., Balasubramanian, R., Courchesne, P. L., Campbell, J. M., Graber, A., Guo, Y., Juhasz, P. J., Li, T. Y., Lynch, M. D., Morel, N. M., Plasterer, T. N., Takach, E. J., Zeng, C., and Beland, F. A. (2009). The liver toxicity biomarker study: phase I design and preliminary results. *Toxicol Pathol* **37**, 52-64.

McGill, M. R., Sharpe, M. R., Williams, C. D., Taha, M., Curry, S. C., and Jaeschke, H. (2012). The mechanism underlying acetaminophen-induced hepatotoxicity in humans and mice involves mitochondrial damage and nuclear DNA fragmentation. *J Clin Invest* **122**, 1574-83.

McKay, L. I., and Cidlowski, J. A. (1999). Molecular control of immune/inflammatory responses: interactions between nuclear factor-kappa B and steroid receptor-signaling pathways. *Endocr Rev* **20**, 435-59.

McKenzie, R., Fried, M. W., Sallie, R., Conjeevaram, H., Di Bisceglie, A. M., Park, Y., Savarese, B., Kleiner, D., Tsokos, M., Luciano, C., and et al. (1995). Hepatic failure and lactic acidosis due to fialuridine (FIAU), an investigational nucleoside analogue for chronic hepatitis B. *N Engl J Med* **333**, 1099-105.

Medzhitov, R., and Janeway, C. A., Jr. (1997). Innate immunity: the virtues of a nonclonal system of recognition. *Cell* **91**, 295-8.

Milosevic, N., Schawalder, H., and Maier, P. (1999). Kupffer cell-mediated differential down-regulation of cytochrome P450 metabolism in rat hepatocytes. *Eur J Pharmacol* **368**, 75-87.

Mingatto, F. E., dos Santos, A. C., Rodrigues, T., Pigoso, A. A., Uyemura, S. A., and Curti, C. (2000). Effects of nimesulide and its reduced metabolite on mitochondria. *Br J Pharmacol* **131**, 1154-60.

Mitchell, J. R., Zimmerman, H. J., Ishak, K. G., Thorgeirsson, U. P., Timbrell, J. A., Snodgrass, W. R., and Nelson, S. D. (1976). Isoniazid liver injury: clinical spectrum, pathology, and probable pathogenesis. *Ann Intern Med* **84**, 181-92.

Modric, S., Webb, A. I., and Derendorf, H. (1998). Pharmacokinetics and pharmacodynamics of tilmicosin in sheep and cattle. *J Vet Pharmacol Ther* **21**, 444-52.

Monshouwer, M., Witkamp, R. F., Nijmeijer, S. M., Pijpers, A., Verheijden, J. H., and Van Miert, A. S. (1995). Selective effects of a bacterial infection (Actinobacillus pleuropneumoniae) on the hepatic clearances of caffeine, antipyrine, paracetamol, and indocyanine green in the pig. *Xenobiotica* **25**, 491-9.

Monshouwer, M., Witkamp, R. F., Nijmeijer, S. M., Van Leengoed, L. A., Vernooy, H. C., Verheijden, J. H., and Van Miert, A. S. (1996a). A lipopolysaccharide-induced acute phase response in the pig is associated with a decrease in hepatic cytochrome P450-mediated drug metabolism. *J Vet Pharmacol Ther* **19**, 382-88.

Monshouwer, M., Witkamp, R. F., Nujmeijer, S. M., Van Amsterdam, J. G., and Van Miert, A. S. (1996b). Suppression of cytochrome P450- and UDP glucuronosyl transferase-dependent enzyme activities by proinflammatory cytokines and possible role of nitric oxide in primary cultures of pig hepatocytes. *Toxicol Appl Pharmacol* **137**, 237-44.

Morgan, E. T. (1989). Suppression of constitutive cytochrome P-450 gene expression in livers of rats undergoing an acute phase response to endotoxin. *Mol Pharmacol* **36**, 699-707.

Morgan, E. T. (1997). Regulation of cytochromes P450 during inflammation and infection. *Drug Metab Rev* **29**, 1129-88.

Moriguchi, T., Toyoshima, F., Masuyama, N., Hanafusa, H., Gotoh, Y., and Nishida, E. (1997). A novel SAPK/JNK kinase, MKK7, stimulated by TNFalpha and cellular stresses. *EMBO J* **16**, 7045-53.

Morris-Stiff, G., Tan, Y. M., and Vauthey, J. N. (2008). Hepatic complications following preoperative chemotherapy with oxaliplatin or irinotecan for hepatic colorectal metastases. *Eur J Surg Oncol* **34**, 609-14.

Morris, S. M., Jr., and Billiar, T. R. (1994). New insights into the regulation of inducible nitric oxide synthesis. *Am J Physiol* **266**, E829-39.

Mullock, B. M., Hall, D. E., Shaw, L. J., and Hinton, R. H. (1983). Immune responses to chlorpromazine in rats. Detection and relation to hepatotoxicity. *Biochemical pharmacology* **32**, 2733-8.

Muntane-Relat, J., Ourlin, J. C., Domergue, J., and Maurel, P. (1995). Differential effects of cytokines on the inducible expression of CYP1A1, CYP1A2, and CYP3A4 in human hepatocytes in primary culture. *Hepatology* **22**, 1143-53.

Murphy, E. J., Davern, T. J., Shakil, A. O., Shick, L., Masharani, U., Chow, H., Freise, C., Lee, W. M., and Bass, N. M. (2000). Troglitazone-induced fulminant hepatic failure. Acute Liver Failure Study Group. *Dig Dis Sci* **45**, 549-53.

Nagai, H., Matsumaru, K., Feng, G., and Kaplowitz, N. (2002). Reduced glutathione depletion causes necrosis and sensitization to tumor necrosis factor-alpha-induced apoptosis in cultured mouse hepatocytes. *Hepatology* **36**, 55-64.

Nakagawa, H., Maeda, S., Hikiba, Y., Ohmae, T., Shibata, W., Yanai, A., Sakamoto, K., Ogura, K., Noguchi, T., Karin, M., Ichijo, H., and Omata, M. (2008). Deletion of apoptosis signal-regulating kinase 1 attenuates acetaminophen-induced liver injury by inhibiting c-Jun N-terminal kinase activation. *Gastroenterology* **135**, 1311-21.

Nebert, D. W., and Russell, D. W. (2002). Clinical importance of the cytochromes P450. *Lancet* **360**, 1155-62.

Nguyen, C., Rose, N. R., and Njoku, D. B. (2008). Trifluoroacetylated IgG4 antibodies in a child with idiosyncratic acute liver failure after first exposure to halothane. *J Pediatr Gastroenterol Nutr* **47**, 199-202.

Nies, A. T., Koepsell, H., Winter, S., Burk, O., Klein, K., Kerb, R., Zanger, U. M., Keppler, D., Schwab, M., and Schaeffeler, E. (2009). Expression of organic cation transporters OCT1 (SLC22A1) and OCT3 (SLC22A3) is affected by genetic factors and cholestasis in human liver. *Hepatology* **50**, 1227-40.

Niisato, N., Post, M., Van Driessche, W., and Marunaka, Y. (1999). Cell swelling activates stress-activated protein kinases, p38 MAP kinase and JNK, in renal epithelial A6 cells. *Biochem Biophys Res Commun* **266**, 547-50.

Njoku, D. B. (2010). Suppressive and pro-inflammatory roles for IL-4 in the pathogenesis of experimental drug-induced liver injury: a review. *Expert Opin Drug Metab Toxicol* **6**, 519-31.

Ohtsu, T., Sasaki, Y., Igarashi, T., Murayama, T., Kobayashi, Y., and Tobinai, K. (1998). Unexpected hepatotoxicities in patients with non-Hodgkin's lymphoma treated with irinotecan (CPT-11) and etoposide. *Jpn J Clin Oncol* **28**, 502-6.

Ong, J. P., and Younossi, Z. M. (2007). Epidemiology and natural history of NAFLD and NASH. *Clin Liver Dis* **11**, 1-16, vii.

Pacitto, S. R., Uetrecht, J. P., Boutros, P. C., and Popovic, M. (2007). Changes in gene expression induced by tienilic Acid and sulfamethoxazole: testing the danger hypothesis. *J Immunotoxicol* **4**, 253-66.

Palkama, V. J., Ahonen, J., Neuvonen, P. J., and Olkkola, K. T. (1999). Effect of saquinavir on the pharmacokinetics and pharmacodynamics of oral and intravenous midazolam. *Clin Pharmacol Ther* **66**, 33-9.

Park, B. K., Coleman, J. W., and Kitteringham, N. R. (1987). Drug disposition and drug hypersensitivity. *Biochem Pharmacol* **36**, 581-90.

Park, B. K., Kitteringham, N. R., Maggs, J. L., Pirmohamed, M., and Williams, D. P. (2005). The role of metabolic activation in drug-induced hepatotoxicity. *Annu Rev Pharmacol Toxicol* **45**, 177-202.

Park, W. B., Kim, W., Lee, K. L., Yim, J. J., Kim, M., Jung, Y. J., Kim, N. J., Kim, D. H., Kim, Y. J., Yoon, J. H., Oh, M. D., and Lee, H. S. (2010). Antituberculosis drug-induced liver injury in chronic hepatitis and cirrhosis. *The Journal of infection* **61**, 323-9.

Pascussi, J. M., Dvorak, Z., Gerbal-Chaloin, S., Assenat, E., Maurel, P., and Vilarem, M. J. (2003). Pathophysiological factors affecting CAR gene expression. *Drug Metab Rev* **35**, 255-68.

Pauli-Magnus, C., and Meier, P. J. (2006). Hepatobiliary transporters and drug-induced cholestasis. *Hepatology* **44**, 778-87.

Perloff, M. D., von Moltke, L. L., Court, M. H., Kotegawa, T., Shader, R. I., and Greenblatt, D. J. (2000). Midazolam and triazolam biotransformation in mouse and human liver microsomes: relative contribution of CYP3A and CYP2C isoforms. *J Pharmacol Exp Ther* **292**, 618-28.

Perloff, M. D., Von Moltke, L. L., and Greenblatt, D. J. (2003). Differential metabolism of midazolam in mouse liver and intestine microsomes: a comparison of cytochrome P450 activity and expression. *Xenobiotica* **33**, 365-77.

Pilgrim, C. H., Thomson, B. N., Banting, S., Phillips, W. A., and Michael, M. (2012). The developing clinical problem of chemotherapy-induced hepatic injury. *ANZ J Surg* **82**, 23-9.

Pinder, M., Bellomo, R., and Lipman, J. (2002). Pharmacological principles of antibiotic prescription in the critically ill. *Anaesth Intensive Care* **30**, 134-44.

Pirmohamed, M., James, S., Meakin, S., Green, C., Scott, A. K., Walley, T. J., Farrar, K., Park, B. K., and Breckenridge, A. M. (2004). Adverse drug reactions as cause of admission to hospital: prospective analysis of 18 820 patients. *BMJ* **329**, 15-9.

Polli, J. W., Wring, S. A., Humphreys, J. E., Huang, L., Morgan, J. B., Webster, L. O., and Serabjit-Singh, C. S. (2001). Rational use of in vitro P-glycoprotein assays in drug discovery. *J Pharmacol Exp Ther* **299**, 620-8.

Poolsup, N., Li Wan Po, A., and Knight, T. L. (2000). Pharmacogenetics and psychopharmacotherapy. *Journal of clinical pharmacy and therapeutics* **25**, 197-220.

Ramadori, G., Van Damme, J., Rieder, H., and Meyer zum Buschenfelde, K. H. (1988). Interleukin 6, the third mediator of acute-phase reaction, modulates hepatic protein synthesis in human and mouse. Comparison with interleukin 1 beta and tumor necrosis factor-alpha. *Eur J Immunol* **18**, 1259-64.

Read, A. E., Harrison, C. V., and Sherlovk, S. (1961). Chronic chlorpromazine jaundice: with particular reference to its relationship to primary biliary cirrhosis. *The American journal of medicine* **31**, 249-58.

Reed, M. D., Rodarte, A., Blumer, J. L., Khoo, K. C., Akbari, B., Pou, S., Pharmd, Kearns, G. L., and Pediatric Pharmacology Research Unit, N. (2001). The single-dose pharmacokinetics of midazolam and its primary metabolite in pediatric patients after oral and intravenous administration. *J Clin Pharmacol* **41**, 1359-69.

Regazzi, M., Maserati, R., Villani, P., Cusato, M., Zucchi, P., Briganti, E., Roda, R., Sacchelli, L., Gatti, F., Delle Foglie, P., Nardini, G., Fabris, P., Mori, F., Castelli, P., and Testa, L. (2005). Clinical pharmacokinetics of nelfinavir and its metabolite M8 in human immunodeficiency virus (HIV)-positive and HIV-hepatitis C virus-coinfected subjects. *Antimicrobial agents and chemotherapy* **49**, 643-9.

Renehan, A. G., Tyson, M., Egger, M., Heller, R. F., and Zwahlen, M. (2008). Body-mass index and incidence of cancer: a systematic review and meta-analysis of prospective observational studies. *Lancet* **371**, 569-78.

Renton, K. W. (1981). Depression of hepatic cytochrome P-450-dependent mixed function oxidases during infection with encephalomyocarditis virus. *Biochem Pharmacol* **30**, 2333-6.

Renton, K. W., and Nicholson, T. E. (2000). Hepatic and central nervous system cytochrome P450 are down-regulated during lipopolysaccharide-evoked localized inflammation in brain. *J Pharmacol Exp Ther* **294**, 524-30.

Richardson, T. A., and Morgan, E. T. (2005). Hepatic cytochrome P450 gene regulation during endotoxin-induced inflammation in nuclear receptor knockout mice. *J Pharmacol Exp Ther* **314**, 703-9.

Richardson, T. A., Sherman, M., Kalman, D., and Morgan, E. T. (2006). Expression of UDP-glucuronosyltransferase isoform mRNAs during inflammation and infection in mouse liver and kidney. *Drug Metab Dispos* **34**, 351-3.

Rivero, A., Mira, J. A., and Pineda, J. A. (2007). Liver toxicity induced by non-nucleoside reverse transcriptase inhibitors. *The Journal of antimicrobial chemotherapy* **59**, 342-6.

Ros, E., Small, D. M., and Carey, M. C. (1979). Effects of chlorpromazine hydrochloride on bile salt synthesis, bile formation and biliary lipid secretion in the rhesus monkey: a model for chlorpromazine-induced cholestasis. *Eur J Clin Invest* **9**, 29-41.

Roth, R. A., and Ganey, P. E. (2010). Intrinsic versus idiosyncratic drug-induced hepatotoxicity--two villains or one? *J Pharmacol Exp Ther* **332**, 692-7.

Roth, R. A., Harkema, J. R., Pestka, J. P., and Ganey, P. E. (1997). Is exposure to bacterial endotoxin a determinant of susceptibility to intoxication from xenobiotic agents? *Toxicology and applied pharmacology* **147**, 300-11.

Roth, R. A., Luyendyk, J. P., Maddox, J. F., and Ganey, P. E. (2003). Inflammation and drug idiosyncrasy--is there a connection? *J Pharmacol Exp Ther* **307**, 1-8.

Roulston, A., Reinhard, C., Amiri, P., and Williams, L. T. (1998). Early activation of c-Jun N-terminal kinase and p38 kinase regulate cell survival in response to tumor necrosis factor alpha. *The Journal of biological chemistry* **273**, 10232-9.

Ruot, B., Breuille, D., Rambourdin, F., Bayle, G., Capitan, P., and Obled, C. (2000). Synthesis rate of plasma albumin is a good indicator of liver albumin synthesis in sepsis. *Am J Physiol Endocrinol Metab* **279**, E244-51.

Saif, M. W. (2009). Secondary hepatic resection as a therapeutic goal in advanced colorectal cancer. *World J Gastroenterol* **15**, 3855-64.

Saini, S. P., Zhang, B., Niu, Y., Jiang, M., Gao, J., Zhai, Y., Hoon Lee, J., Uppal, H., Tian, H., Tortorici, M. A., Poloyac, S. M., Qin, W., Venkataramanan, R., and Xie, W. (2011). Activation of liver X receptor increases acetaminophen clearance and prevents its toxicity in mice. *Hepatology* **54**, 2208-17.

Sallie, R. W., McKenzie, T., Reed, W. D., Quinlan, M. F., and Shilkin, K. B. (1991). Diclofenac hepatitis. *Aust N Z J Med* **21**, 251-5.

Samorajski, T., Ordy, J. M., and Rolsten, C. (1965). Prenatal chlorpromazine effects on liver enzymes, glycogen, and ultrastructure in mice offspring. *The American journal of pathology* **47**, 803-31.

Scheele, J., Stang, R., Altendorf-Hofmann, A., and Paul, M. (1995). Resection of colorectal liver metastases. *World J Surg* **19**, 59-71.

Schleuning, M. J., Duggan, A., and Reem, G. H. (1989). Inhibition by chlorpromazine of lymphokine-specific mRNA expression in human thymocytes. *European journal of immunology* **19**, 1491-5.

Schnare, M., Holt, A. C., Takeda, K., Akira, S., and Medzhitov, R. (2000). Recognition of CpG DNA is mediated by signaling pathways dependent on the adaptor protein MyD88. *Curr Biol* **10**, 1139-42.

Schoene, B., Fleischmann, R. A., Remmer, H., and von Oldershausen, H. F. (1972). Determination of drug metabolizing enzymes in needle biopsies of human liver. *Eur J Clin Pharmacol* **4**, 65-73.

Scott, M. J., and Billiar, T. R. (2008). Beta2-integrin-induced p38 MAPK activation is a key mediator in the CD14/TLR4/MD2-dependent uptake of lipopolysaccharide by hepatocytes. *J Biol Chem* **283**, 29433-46.

Scott, M. J., Liu, S., Shapiro, R. A., Vodovotz, Y., and Billiar, T. R. (2009). Endotoxin uptake in mouse liver is blocked by endotoxin pretreatment through a suppressor of cytokine signaling-1-dependent mechanism. *Hepatology* **49**, 1695-708.

Seki, E., and Brenner, D. A. (2008). Toll-like receptors and adaptor molecules in liver disease: update. *Hepatology* **48**, 322-35.

Sermsappasuk, P., Abdelrahman, O., and Weiss, M. (2008). Cardiac pharmacokinetics and inotropic response of verapamil in rats with endotoxemia. *J Pharm Sci* **97**, 2798-804.

Servoss, J. C., Kitch, D. W., Andersen, J. W., Reisler, R. B., Chung, R. T., and Robbins, G. K. (2006). Predictors of antiretroviral-related hepatotoxicity in the adult AIDS Clinical Trial Group (1989-1999). *Journal of acquired immune deficiency syndromes (1999)* **43**, 320-3.

Sewer, M. B., Koop, D. R., and Morgan, E. T. (1996). Endotoxemia in rats is associated with induction of the P4504A subfamily and suppression of several other forms of cytochrome P450. *Drug Metab Dispos* **24**, 401-7.

Sewer, M. B., Koop, D. R., and Morgan, E. T. (1997). Differential inductive and suppressive effects of endotoxin and particulate irritants on hepatic and renal cytochrome P-450 expression. *J Pharmacol Exp Ther* **280**, 1445-54.

Sewer, M. B., and Morgan, E. T. (1997). Nitric oxide-independent suppression of P450 2C11 expression by interleukin-1beta and endotoxin in primary rat hepatocytes. *Biochem Pharmacol* **54**, 729-37.

Shan, W., Palkar, P. S., Murray, I. A., McDevitt, E. I., Kennett, M. J., Kang, B. H., Isom, H. C., Perdew, G. H., Gonzalez, F. J., and Peters, J. M. (2008). Ligand activation of peroxisome proliferator-activated receptor beta/delta (PPARbeta/delta) attenuates carbon tetrachloride hepatotoxicity by downregulating proinflammatory gene expression. *Toxicol Sci* **105**, 418-28.

Sharma, R. P., Bhandari, N., He, Q., Riley, R. T., and Voss, K. A. (2001). Decreased fumonisin hepatotoxicity in mice with a targeted deletion of tumor necrosis factor receptor 1. *Toxicology* **159**, 69-79.

Sharma, R. P., He, Q., Meredith, F. I., Riley, R. T., and Voss, K. A. (2002). Paradoxical role of tumor necrosis factor alpha in fumonisin-induced hepatotoxicity in mice. *Toxicology* **180**, 221-32.

Shaw, P. J., Beggs, K. M., Sparkenbaugh, E. M., Dugan, C. M., Ganey, P. E., and Roth, R. A. (2009a). Trovafloxacin enhances TNF-induced inflammatory stress and cell death signaling and reduces TNF clearance in a murine model of idiosyncratic hepatotoxicity. *Toxicol Sci* **111**, 288-301.

Shaw, P. J., Ditewig, A. C., Waring, J. F., Liguori, M. J., Blomme, E. A., Ganey, P. E., and Roth, R. A. (2009b). Coexposure of mice to trovafloxacin and lipopolysaccharide, a model of idiosyncratic hepatotoxicity, results in a unique gene expression profile and interferon gamma-dependent liver injury. *Toxicol Sci* **107**, 270-80.

Shaw, P. J., Fullerton, A. M., Scott, M. A., Ganey, P. E., and Roth, R. A. (2009c). The role of the hemostatic system in murine liver injury induced by coexposure to lipopolysaccharide and trovafloxacin, a drug with idiosyncratic liability. *Toxicology and applied pharmacology* **236**, 293-300.

Shaw, P. J., Ganey, P. E., and Roth, R. A. (2009d). Trovafloxacin enhances the inflammatory response to a Gram-negative or a Gram-positive bacterial stimulus, resulting in neutrophil-dependent liver injury in mice. *The Journal of pharmacology and experimental therapeutics* **330**, 72-8.

Shaw, P. J., Ganey, P. E., and Roth, R. A. (2009e). Tumor necrosis factor alpha is a proximal mediator of synergistic hepatotoxicity from trovafloxacin/lipopolysaccharide coexposure. *J Pharmacol Exp Ther* **328**, 62-8.

Shaw, P. J., Ganey, P. E., and Roth, R. A. (2010). Idiosyncratic drug-induced liver injury and the role of inflammatory stress with an emphasis on an animal model of trovafloxacin hepatotoxicity. *Toxicol Sci* **118**, 7-18.

Shaw, P. J., Hopfensperger, M. J., Ganey, P. E., and Roth, R. A. (2007). Lipopolysaccharide and trovafloxacin coexposure in mice causes idiosyncrasy-like liver injury dependent on tumor necrosis factor-alpha. *Toxicol Sci* **100**, 259-66.

Shedlofsky, S. I., Israel, B. C., McClain, C. J., Hill, D. B., and Blouin, R. A. (1994). Endotoxin administration to humans inhibits hepatic cytochrome P450-mediated drug metabolism. *J Clin Invest* **94**, 2209-14.

Shenton, J. M., Teranishi, M., Abu-Asab, M. S., Yager, J. A., and Uetrecht, J. P. (2003). Characterization of a potential animal model of an idiosyncratic drug reaction: nevirapine-induced skin rash in the rat. *Chem Res Toxicol* **16**, 1078-89.

Shimada, T., Gillam, E. M., Sandhu, P., Guo, Z., Tukey, R. H., and Guengerich, F. P. (1994). Activation of procarcinogens by human cytochrome P450 enzymes expressed in Escherichia coli. Simplified bacterial systems for genotoxicity assays. *Carcinogenesis* **15**, 2523-9.

Shimamoto, Y., Kitamura, H., Hoshi, H., Kazusaka, A., Funae, Y., Imaoka, S., Saito, M., and Fujita, S. (1998). Differential alterations in levels of hepatic microsomal cytochrome P450 isozymes following intracerebroventricular injection of bacterial lipopolysaccharide in rats. *Arch Toxicol* **72**, 492-8.

Shimoi, K., Saka, N., Nozawa, R., Sato, M., Amano, I., Nakayama, T., and Kinae, N. (2001). Deglucuronidation of a flavonoid, luteolin monoglucuronide, during inflammation. *Drug Metab Dispos* **29**, 1521-4.

Siddiqui, H. H., Malhotra, N. K., Bhatia, B., and Subramanian, R. (1979). Factors affecting blood glucose and liver glycogen in chlorpromazine-treated mice subjected to simulated altitudes. *The Indian journal of medical research* **70**, 833-40.

Siewert, E., Bort, R., Kluge, R., Heinrich, P. C., Castell, J., and Jover, R. (2000). Hepatic cytochrome P450 down-regulation during aseptic inflammation in the mouse is interleukin 6 dependent. *Hepatology* **32**, 49-55.

Singh, G., and Renton, K. W. (1981). Interferon-mediated depression of cytochrome P-450-dependent drug biotransformation. *Mol Pharmacol* **20**, 681-4.

Singh, G., and Renton, K. W. (1984). Inhibition of the synthesis of hepatic cytochrome P-450 by the interferon-inducing agent poly rI.rCi. *Canadian journal of physiology and pharmacology* **62**, 379-83.

Singh, R., and Czaja, M. J. (2007). Regulation of hepatocyte apoptosis by oxidative stress. *Journal of gastroenterology and hepatology* **22 Suppl 1**, S45-8.

Smith, D. A., and Schmid, E. F. (2006). Drug withdrawals and the lessons within. *Curr Opin Drug Discov Devel* **9**, 38-46.

Sonne, J., Dossing, M., Loft, S., and Andreasen, P. B. (1985). Antipyrine clearance in pneumonia. *Clin Pharmacol Ther* **37**, 701-4.

Sotsuka, T., Sasaki, Y., Hirai, S., Yamagishi, F., and Ueno, K. (2011). Association of isoniazid-metabolizing enzyme genotypes and isoniazid-induced hepatotoxicity in tuberculosis patients. *In Vivo* **25**, 803-12.

Sparreboom, A., de Jonge, M. J., de Bruijn, P., Brouwer, E., Nooter, K., Loos, W. J., van Alphen, R. J., Mathijssen, R. H., Stoter, G., and Verweij, J. (1998). Irinotecan (CPT-11) metabolism and disposition in cancer patients. *Clin Cancer Res* **4**, 2747-54.

Sriskandan, S., and Cohen, J. (1999). Gram-positive sepsis. Mechanisms and differences from gram-negative sepsis. *Infect Dis Clin North Am* **13**, 397-412.

Sulkowski, M. S., Thomas, D. L., Chaisson, R. E., and Moore, R. D. (2000). Elevated liver enzymes following initiation of antiretroviral therapy. *Jama* **283**, 2526-7.

Sulkowski, M. S., Thomas, D. L., Mehta, S. H., Chaisson, R. E., and Moore, R. D. (2002). Hepatotoxicity associated with nevirapine or efavirenz-containing antiretroviral therapy: role of hepatitis C and B infections. *Hepatology* **35**, 182-9.

Sun, F., Chen, Y., Xiang, Y., and Zhan, S. (2008). Drug-metabolising enzyme polymorphisms and predisposition to anti-tuberculosis drug-induced liver injury: a meta-analysis. *Int J Tuberc Lung Dis* **12**, 994-1002.

Swantek, J. L., Cobb, M. H., and Geppert, T. D. (1997). Jun N-terminal kinase/stress-activated protein kinase (JNK/SAPK) is required for lipopolysaccharide stimulation of tumor necrosis factor alpha (TNF-alpha) translation: glucocorticoids inhibit TNF-alpha translation by blocking JNK/SAPK. *Mol Cell Biol* **17**, 6274-82.

Swart, E. L., de Jongh, J., Zuideveld, K. P., Danhof, M., Thijs, L. G., and Strack van Schijndel, R. J. (2005). Population pharmacokinetics of lorazepam and midazolam and their metabolites in intensive care patients on continuous venovenous hemofiltration. *Am J Kidney Dis* **45**, 360-71.

Synold, T. W., Dussault, I., and Forman, B. M. (2001). The orphan nuclear receptor SXR coordinately regulates drug metabolism and efflux. *Nat Med* **7**, 584-90.

Takasuna, K., Hagiwara, T., Hirohashi, M., Kato, M., Nomura, M., Nagai, E., Yokoi, T., and Kamataki, T. (1996). Involvement of beta-glucuronidase in intestinal microflora in the intestinal toxicity of the antitumor camptothecin derivative irinotecan hydrochloride (CPT-11) in rats. *Cancer Res* **56**, 3752-7.

Takeuchi, O., Hoshino, K., Kawai, T., Sanjo, H., Takada, H., Ogawa, T., Takeda, K., and Akira, S. (1999). Differential roles of TLR2 and TLR4 in recognition of gram-negative and gram-positive bacterial cell wall components. *Immunity* **11**, 443-51.

Takeuchi, O., Kaufmann, A., Grote, K., Kawai, T., Hoshino, K., Morr, M., Muhlradt, P. F., and Akira, S. (2000). Cutting edge: preferentially the R-stereoisomer of the mycoplasmal lipopeptide macrophage-activating lipopeptide-2 activates immune cells through a toll-like receptor 2- and MyD88-dependent signaling pathway. *J Immunol* **164**, 554-7.

Tang, L. J., Tian, F. Z., and Gao, X. M. (2002). Hepatocellular glycogen in alleviation of liver ischemia-reperfusion injury. *Hepatobiliary Pancreat Dis Int* **1**, 532-5.

Tapner, M., Liddle, C., Goodwin, B., George, J., and Farrell, G. C. (1996). Interferon gamma down-regulates cytochrome P450 3A genes in primary cultures of well-differentiated rat hepatocytes. *Hepatology* **24**, 367-73.

Temple, R. J., and Himmel, M. H. (2002). Safety of newly approved drugs: implications for prescribing. *JAMA* **287**, 2273-5.

Teng, S., and Piquette-Miller, M. (2007). Hepatoprotective role of PXR activation and MRP3 in cholic acid-induced cholestasis. *Br J Pharmacol* **151**, 367-76.

Tett, S., Moore, S., and Ray, J. (1995). Pharmacokinetics and bioavailability of fluconazole in two groups of males with human immunodeficiency virus (HIV) infection compared with those in a group of males without HIV infection. *Antimicrobial agents and chemotherapy* **39**, 1835-41.

Thummel, K. E., O'Shea, D., Paine, M. F., Shen, D. D., Kunze, K. L., Perkins, J. D., and Wilkinson, G. R. (1996). Oral first-pass elimination of midazolam involves both gastrointestinal and hepatic CYP3A-mediated metabolism. *Clin Pharmacol Ther* **59**, 491-502.

Thummel, K. E., Shen, D. D., Podoll, T. D., Kunze, K. L., Trager, W. F., Bacchi, C. E., Marsh, C. L., McVicar, J. P., Barr, D. M., Perkins, J. D., and et al. (1994). Use of midazolam as a human cytochrome P450 3A probe: II. Characterization of inter- and intraindividual hepatic CYP3A variability after liver transplantation. *J Pharmacol Exp Ther* **271**, 557-66.

Tournade, H., Pelletier, L., Pasquier, R., Vial, M. C., Mandet, C., and Druet, P. (1990). D-penicillamine-induced autoimmunity in Brown-Norway rats. Similarities with HgCl2-induced autoimmunity. *J Immunol* **144**, 2985-91.

Tukov, F. F., Luyendyk, J. P., Ganey, P. E., and Roth, R. A. (2007). The role of tumor necrosis factor alpha in lipopolysaccharide/ranitidine-induced inflammatory liver injury. *Toxicol Sci* **100**, 267-80.

Tukov, F. F., Maddox, J. F., Amacher, D. E., Bobrowski, W. F., Roth, R. A., and Ganey, P. E. (2006). Modeling inflammation-drug interactions in vitro: a rat Kupffer cell-hepatocyte coculture system. *Toxicol In Vitro* **20**, 1488-99.

Uetrecht, J. (2003). Screening for the potential of a drug candidate to cause idiosyncratic drug reactions. *Drug discovery today* **8**, 832-7.

Uetrecht, J. P. (1999). New concepts in immunology relevant to idiosyncratic drug reactions: the "danger hypothesis" and innate immune system. *Chem Res Toxicol* **12**, 387-95.

van Waterschoot, R. A., van Herwaarden, A. E., Lagas, J. S., Sparidans, R. W., Wagenaar, E., van der Kruijssen, C. M., Goldstein, J. A., Zeldin, D. C., Beijnen, J. H., and Schinkel, A. H. (2008). Midazolam metabolism in cytochrome P450 3A knockout mice can be attributed to up-regulated CYP2C enzymes. *Mol Pharmacol* **73**, 1029-36.

Vauthey, J. N., Pawlik, T. M., Ribero, D., Wu, T. T., Zorzi, D., Hoff, P. M., Xiong, H. Q., Eng, C., Lauwers, G. Y., Mino-Kenudson, M., Risio, M., Muratore, A., Capussotti, L., Curley, S. A., and Abdalla, E. K. (2006). Chemotherapy regimen predicts steatohepatitis and an increase in 90-day mortality after surgery for hepatic colorectal metastases. *J Clin Oncol* **24**, 2065-72.

Veronese, L., Rautaureau, J., Sadler, B. M., Gillotin, C., Petite, J. P., Pillegand, B., Delvaux, M., Masliah, C., Fosse, S., Lou, Y., and Stein, D. S. (2000). Single-dose pharmacokinetics of amprenavir, a human immunodeficiency virus type 1 protease inhibitor, in subjects with normal or impaired hepatic function. *Antimicrobial agents and chemotherapy* **44**, 821-6.

Vial, T., Goubier, C., Bergeret, A., Cabrera, F., Evreux, J. C., and Descotes, J. (1991). Side effects of ranitidine. *Drug Saf* **6**, 94-117.

von Moltke, L. L., Greenblatt, D. J., Schmider, J., Duan, S. X., Wright, C. E., Harmatz, J. S., and Shader, R. I. (1996). Midazolam hydroxylation by human liver microsomes in vitro: inhibition by fluoxetine, norfluoxetine, and by azole antifungal agents. *J Clin Pharmacol* **36**, 783-91.

Vrzal, R., Daujat-Chavanieu, M., Pascussi, J. M., Ulrichova, J., Maurel, P., and Dvorak, Z. (2008). Microtubules-interfering agents restrict aryl hydrocarbon receptor-mediated CYP1A2 induction in primary cultures of human hepatocytes via c-jun-N-terminal kinase and glucocorticoid receptor. *Eur J Pharmacol* **581**, 244-54.

Walgren, J. L., Mitchell, M. D., and Thompson, D. C. (2005). Role of metabolism in drug-induced idiosyncratic hepatotoxicity. *Crit Rev Toxicol* **35**, 325-61.

Wang, T., Yu, H. T., Wang, W., Pan, Y. Y., He, L. X., and Wang, Z. Y. (2010). Genetic polymorphisms of cytochrome P450 and glutathione S-transferase associated with antituberculosis drug-induced hepatotoxicity in Chinese tuberculosis patients. *J Int Med Res* **38**, 977-86.

Wang, X., Wu, D., Yang, L., and Cederbaum, A. I. (2011). Hepatotoxicity mediated by pyrazole (cytochrome P450 2E1) plus tumor necrosis factor alpha treatment occurs in c-Jun N-terminal kinase 2-/- but not in c-Jun N-terminal kinase 1-/- mice. *Hepatology* **54**, 1753-66.

Wang, X. Y., Li, W. Q., Lu, J., Li, N., and Li, J. S. (2005). [Mechanism of reduction of albumin expression induced by lipopolysaccharide in rat hepatocytes]. *Chin Med J (Engl)* **118**, 1695-702.

Wang, Y., Singh, R., Lefkowitch, J. H., Rigoli, R. M., and Czaja, M. J. (2006). Tumor necrosis factor-induced toxic liver injury results from JNK2-dependent activation of caspase-8 and the mitochondrial death pathway. *J Biol Chem* **281**, 15258-67.

Waring, J. F., and Anderson, M. G. (2005). Idiosyncratic toxicity: mechanistic insights gained from analysis of prior compounds. *Curr Opin Drug Discov Devel* **8**, 59-65.

Waring, J. F., Liguori, M. J., Luyendyk, J. P., Maddox, J. F., Ganey, P. E., Stachlewitz, R. F., North, C., Blomme, E. A., and Roth, R. A. (2006). Microarray analysis of lipopolysaccharide potentiation of trovafloxacin-induced liver injury in rats suggests a role for proinflammatory chemokines and neutrophils. *J Pharmacol Exp Ther* **316**, 1080-7.

Warren, G. W., Poloyac, S. M., Gary, D. S., Mattson, M. P., and Blouin, R. A. (1999). Hepatic cytochrome P-450 expression in tumor necrosis factor-alpha receptor (p55/p75) knockout mice after endotoxin administration. *J Pharmacol Exp Ther* **288**, 945-50.

Warren, G. W., van Ess, P. J., Watson, A. M., Mattson, M. P., and Blouin, R. A. (2001). Cytochrome P450 and antioxidant activity in interleukin-6 knockout mice after induction of the acute-phase response. *J Interferon Cytokine Res* **21**, 821-6.

Warrington, J. S., Poku, J. W., von Moltke, L. L., Shader, R. I., Harmatz, J. S., and Greenblatt, D. J. (2000). Effects of age on in vitro midazolam biotransformation in male CD-1 mouse liver microsomes. *J Pharmacol Exp Ther* **292**, 1024-31.

Watkins, P. B. (2005). Idiosyncratic liver injury: challenges and approaches. *Toxicol Pathol* **33**, 1-5.

Watson, R. G., Olomu, A., Clements, D., Waring, R. H., Mitchell, S., and Elias, E. (1988). A proposed mechanism for chlorpromazine jaundice--defective hepatic sulphoxidation combined with rapid hydroxylation. *Journal of hepatology* **7**, 72-8.

Weber, R., Sabin, C. A., Friis-Moller, N., Reiss, P., El-Sadr, W. M., Kirk, O., Dabis, F., Law, M. G., Pradier, C., De Wit, S., Akerlund, B., Calvo, G., Monforte, A., Rickenbach, M., Ledergerber, B., Phillips, A. N., and Lundgren, J. D. (2006). Liver-related deaths in persons infected with the human immunodeficiency virus: the D:A:D study. *Archives of internal medicine* **166**, 1632-41.

Weekes, J., Lam, A. K., Sebesan, S., and Ho, Y. H. (2009). Irinotecan therapy and molecular targets in colorectal cancer: a systemic review. *World J Gastroenterol* **15**, 3597-602.

Whitmarsh, A. J., and Davis, R. J. (1996). Transcription factor AP-1 regulation by mitogen-activated protein kinase signal transduction pathways. *Journal of molecular medicine (Berlin, Germany)* **74**, 589-607.

Wichterman, K. A., Baue, A. E., and Chaudry, I. H. (1980). Sepsis and septic shock--a review of laboratory models and a proposal. *J Surg Res* **29**, 189-201.

Wilkinson, G. R. (1997). The effects of diet, aging and disease-states on presystemic elimination and oral drug bioavailability in humans. *Adv Drug Deliv Rev* **27**, 129-159.

Wonganan, P., Zamboni, W. C., Strychor, S., Dekker, J. D., and Croyle, M. A. (2009). Drug-virus interaction: effect of administration of recombinant adenoviruses on the pharmacokinetics of docetaxel in a rat model. *Cancer Gene Ther* **16**, 405-14.

Wright, K., and Morgan, E. T. (1990). Transcriptional and post-transcriptional suppression of P450IIC11 and P450IIC12 by inflammation. *FEBS letters* **271**, 59-61.

Wyles, D. L., and Gerber, J. G. (2005). Antiretroviral drug pharmacokinetics in hepatitis with hepatic dysfunction. *Clin Infect Dis* **40**, 174-81.

Xiao, C., and Ghosh, S. (2005). NF-kappaB, an evolutionarily conserved mediator of immune and inflammatory responses. *Adv Exp Med Biol* **560**, 41-5.

Xu, D. X., Wei, W., Sun, M. F., Wu, C. Y., Wang, J. P., Wei, L. Z., and Zhou, C. F. (2004). Kupffer cells and reactive oxygen species partially mediate lipopolysaccharide-induced downregulation of nuclear receptor pregnane x receptor and its target gene CYP3a in mouse liver. *Free Radic Biol Med* **37**, 10-22.

Xu, G., Zhang, W., Ma, M. K., and McLeod, H. L. (2002). Human carboxylesterase 2 is commonly expressed in tumor tissue and is correlated with activation of irinotecan. *Clin Cancer Res* **8**, 2605-11.

Xu, J., Kulkarni, S. R., Li, L., and Slitt, A. L. (2012). UDP-glucuronosyltransferase expression in mouse liver is increased in obesity- and fasting-induced steatosis. *Drug Metab Dispos* **40**, 259-66.

Yee, S. B., Bourdi, M., Masson, M. J., and Pohl, L. R. (2007). Hepatoprotective role of endogenous interleukin-13 in a murine model of acetaminophen-induced liver disease. *Chem Res Toxicol* **20**, 734-44.

Yee, S. B., Ganey, P. E., and Roth, R. A. (2003a). The role of Kupffer cells and TNF-alpha in monocrotaline and bacterial lipopolysaccharide-induced liver injury. *Toxicol Sci* **71**, 124-32.

Yee, S. B., Hanumegowda, U. M., Hotchkiss, J. A., Ganey, P. E., and Roth, R. A. (2003b). Role of neutrophils in the synergistic liver injury from monocrotaline and bacterial lipopolysaccharide exposure. *Toxicol Sci* **72**, 43-56.

Yee, S. B., Harkema, J. R., Ganey, P. E., and Roth, R. A. (2003c). The coagulation system contributes to synergistic liver injury from exposure to monocrotaline and bacterial lipopolysaccharide. *Toxicol Sci* **74**, 457-69.

Yee, S. B., Kinser, S., Hill, D. A., Barton, C. C., Hotchkiss, J. A., Harkema, J. R., Ganey, P. E., and Roth, R. A. (2000). Synergistic hepatotoxicity from coexposure to bacterial endotoxin and the pyrrolizidine alkaloid monocrotaline. *Toxicol Appl Pharmacol* **166**, 173-85.

Yeung, P. K., Hubbard, J. W., Korchinski, E. D., and Midha, K. K. (1993). Pharmacokinetics of chlorpromazine and key metabolites. *Eur J Clin Pharmacol* **45**, 563-9.

Yohe, H. C., O'Hara, K. A., Hunt, J. A., Kitzmiller, T. J., Wood, S. G., Bement, J. L., Bement, W. J., Szakacs, J. G., Wrighton, S. A., Jacobs, J. M., Kostrubsky, V., Sinclair, P. R., and Sinclair, J. F. (2006). Involvement of Toll-like receptor 4 in acetaminophen hepatotoxicity. *Am J Physiol Gastrointest Liver Physiol* **290**, G1269-79.

Yoshii, K., Kobayashi, K., Tsumuji, M., Tani, M., Shimada, N., and Chiba, K. (2000). Identification of human cytochrome P450 isoforms involved in the 7-hydroxylation of chlorpromazine by human liver microsomes. *Life Sci* **67**, 175-84.

You, Q., Cheng, L., Reilly, T. P., Wegmann, D., and Ju, C. (2006). Role of neutrophils in a mouse model of halothane-induced liver injury. *Hepatology* **44**, 1421-31.

Yu, R., Lei, W., Mandlekar, S., Weber, M. J., Der, C. J., Wu, J., and Kong, A. N. (1999). Role of a mitogen-activated protein kinase pathway in the induction of phase II detoxifying enzymes by chemicals. *J Biol Chem* **274**, 27545-52.

Zhu, B., Bush, D., Doss, G. A., Vincent, S., Franklin, R. B., and Xu, S. (2008). Characterization of 1'-hydroxymidazolam glucuronidation in human liver microsomes. *Drug Metab Dispos* **36**, 331-8.

Ziegler, W. H., Schalch, E., Leishman, B., and Eckert, M. (1983). Comparison of the effects of intravenously administered midazolam, triazolam and their hydroxy metabolites. *Br J Clin Pharmacol* **16 Suppl 1**, 63S-69S.

Zimmerman, H. J. (1993). Hepatotoxicity. *Dis Mon* **39**, 675-787.

Zinetti, M., Galli, G., Demitri, M. T., Fantuzzi, G., Minto, M., Ghezzi, P., Alzani, R., Cozzi, E., and Fratelli, M. (1995). Chlorpromazine inhibits tumour necrosis factor synthesis and cytotoxicity in vitro. *Immunology* **86**, 416-21.

Zorzi, D., Laurent, A., Pawlik, T. M., Lauwers, G. Y., Vauthey, J. N., and Abdalla, E. K. (2007). Chemotherapy-associated hepatotoxicity and surgery for colorectal liver metastases. *Br J Surg* **94**, 274-86.

Zou, W., Beggs, K. M., Sparkenbaugh, E. M., Jones, A. D., Younis, H. S., Roth, R. A., and Ganey, P. E. (2009a). Sulindac metabolism and synergy with tumor necrosis factor-

alpha in a drug-inflammation interaction model of idiosyncratic liver injury. *J Pharmacol Exp Ther* **331**, 114-21.

Zou, W., Devi, S. S., Sparkenbaugh, E., Younis, H. S., Roth, R. A., and Ganey, P. E. (2009b). Hepatotoxic interaction of sulindac with lipopolysaccharide: role of the hemostatic system. *Toxicol Sci* **108**, 184-93.

Zou, W., Roth, R. A., Younis, H. S., Malle, E., and Ganey, P. E. (2011). Neutrophil-cytokine interactions in a rat model of sulindac-induced idiosyncratic liver injury. *Toxicology* **290**, 278-85.